(4+3)-CYCLOADDITION CHEMISTRY OF OXIDOPYRIDINIUM IONS AND RELATED STUDY

A Dissertation

presented to

the Faculty of the Graduate School

at the University of Missouri-Columbia

In Partial Fulfillment

of the Requirements for the Degree

Doctor of Philosophy

---

by

CHENCHENG FU

Dr. Michael Harmata, Dissertation Supervisor

JULY 2019

The undersigned, appointed by the dean of the Graduate School, have examined the dissertation entitled

(4+3)-CYCLOADDITION CHEMISTRY OF OXIDOPYRIDINIUM IONS

AND RELATED STUDY

Presented by Chencheng Fu,

a candidate for the degree of Doctor of Philosophy,

and hereby certify that, in their opinion, it is worthy of acceptance.

_____

Professor Michael Harmata

_____

Professor Susan Z. Lever

_____

Professor Steven W. Keller

_____

Professor Peter A. Tipton

Dedicated to my parents

Min Chen

and

Xianwen Fu

ACKNOWLEDGEMENTS

I would like to extend my sincere gratitude to the people who have supported me during my time at the University of Missouri.

Foremost, I would like to thank my advisor, professor Michael Harmata, for his motivation, advice and support throughout my time here. His guidance helped me in all the time of research and writing of this thesis. I could not have imagined having a better advisor and mentor for my Ph.D study. I would also like to thank my committee members: Dr. Susan Lever, Dr. Steven Keller and Dr. Peter Tipton for their helpful advice and comments.

I would like to thank Dr. Wei Wycoff and Dr. Shaokai Jiang for the NMR training and assistant, Dr. Charles Barnes and Dr. Steven Kelley for their work on X-ray crystallography. My sincere thanks to Jerry Brightwell for his administrative help.

I want to thank the Harmata group members, past and present, and to all my fellow chemists in the MU Chemistry department. Addition, I am grateful for the help of Zhiyu Yang, Andrew Romisch and Le Zhang for taking time to proofread my dissertation.

I would also thank my undergraduate professors at Western China School of Pharmacy in Sichuan University for all their teachings, knowledge, and drive during my time there. To my friends and family, thank you for your love, support and interest in my research.

TABLE OF CONTENTS

LIST OF FIGURES

LIST OF SCHEMES

LIST OF TABLES

LIST OF ABBREVIATIONS

BHT	butylated hydroxytoluene
Cy	cyclohexyl
DBU	1,8-diazabicyclo[5.4.0]undec-7-ene
DCM	dichloromethane
DIBAL	diisobutylaluminium hydride
DMF	*N*,*N*-dimethylformamide
EtOAc	ethyl acetate
LAH	lithium aluminium hydride
MeCN	acetonitrile
OTf	trifluoromethanesulfonyl
$Pd(OAc)_2$	palladium(II) acetate
TEA	triethylamine
TEMPO	2,2,6,6-tetramethylpiperidine-1-oxyl
TFA	trifluoroacetic acid
THF	tetrahydrofuran
TMS	trimethylsilyl
p-TsOH	*para*-toluenesulfonic acid

(4+3)-CYCLOADDITION CHEMISTRY OF OXIDOPYRIDINIUM IONS AND RELATED STUDY AND DIHYDROFURANONES

Chencheng Fu

Dr. Michael Harmata, Dissertation Supervisor

ABSTRACT

The (4+3)-cycloaddition reaction is a cycloaddition between a 4-atom species and a 3-atom species to form a seven-membered ring. This reaction results in the formation of seven-membered rings. Our research expanded the scope of (4+3)-cycloaddition reaction by using the oxidopyridinium species as the dienophile – the 3-atom species. By adding an electron-withdrawing functional group to the starting material, we were be able to get good to excellent product yield. The process provides rapid access to bicyclic nitrogenous structures resembling natural alkaloids.

[2+2]-Photocycloaddition is a cycloaddition between two olefins to form a cyclobutane ring. The intramolecular [2+2]-cycloaddition of nitrogen-substituted alkenes can be employed to make complicated alkaloids. Our previous work made the 7-azabicyclo[4.3.1]deca-3,8-diene skeleton, which is a nice substrate for the cycloaddition. Under UV radiation, the heteroatom-substituted unsaturated ester undergoes intramolecular [2+2]-cycloaddition with the cyclic alkene to make a cage-like ketone in good to excellent yield, giving rise to a rigid tropane-like alkaloid skeleton. The scope and mechanism of the photochemical reaction will be discussed.

CHAPTER 1

OXIDOPYRIDINIUM IONS IN (4+3)-CYCLOADDITION REACTIONS

1.1 Introduction

Cycloaddition reactions are highly efficient and straightforward means to generate molecular complexity. For example, the Diels-Alder reaction between dienes and dienophiles is the most extensively used method to build six-membered rings. Other commonly used transformations in synthesis are (3+2)-cycloaddition reactions to make five-membered rings and [2+2]-photochemical cycloadditions to make four-membered rings.

Since seven-membered carboxylic rings exist in a wide range of bioactive pharmaceuticals and natural compounds (Figure 1),[1-4] the (4+3)-cycloaddition reaction between

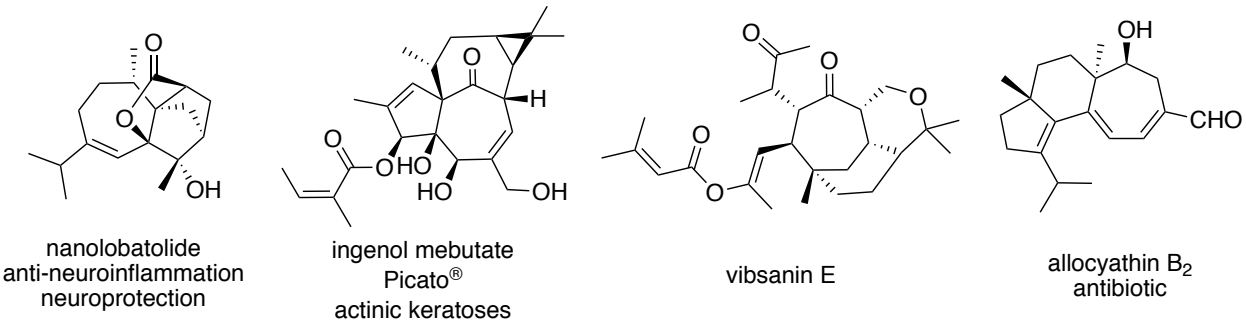

Figure 1. Selective bioactive pharmaceuticals and natural compounds bearing a seven-membered ring.

allylic cations and dienes in building seven-membered carboxylic rings is a synthetic process that is currently of great interest. However, the formation of seven-membered rings is generally more challenging compared with five- or six-membered rings due to the increased ring strain and increased entropic demands due to ring closure. The angle strain, conformational strain, and transannular strain contribute to the ring strain. The magnitude of such strains has been evaluated

by Allinger and coworkers[5] on the basis of force-field calculations (Table 1). As the chain gets longer, the entropy would be further reduced when the chain terminals coming close to each other in order for the reaction to occur in both cyclization and cycloaddition reaction.[6]

Table 1. Experimental strain energy of cycloalkanes.

ring size	total ring stain (kcal/mol)
3	27.6
4	26.2
5	6.5
6	0.0
7	6.3
8	9.6

The (4+3)-cycloaddition reaction is the reaction between an electron-deficient three-atom (2π) system and an electron-rich four-atom (4π) system to form a seven-membered ring. It is symmetry-allowed according to Woodward-Hoffmann rules.[7] The general process of this reaction is shown below (Figure 2). The 4π moiety is usually a diene, and the 2π moiety is

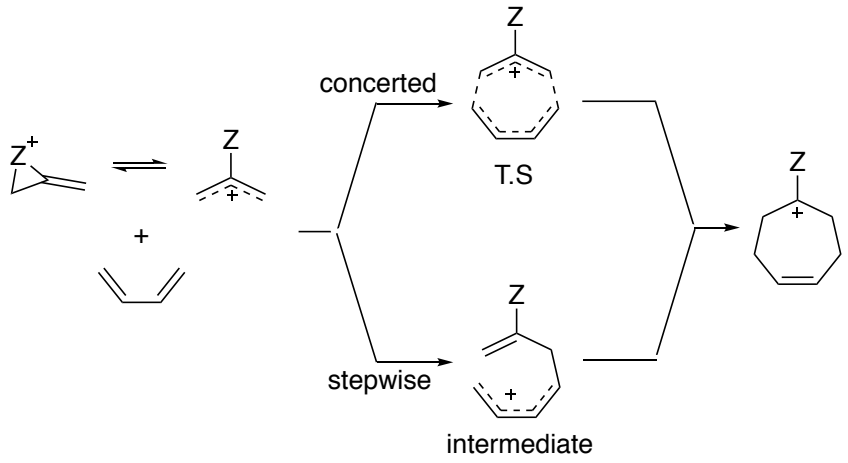

Figure 2. Mechanism of the (4+3)-cycloaddition reaction.

allylic cation. The substituent Z on the central carbon of the allylic moiety is believed to be crucial for stabilizing the positive charge generated in the product.[8-9] Typically, it is an oxygen-bearing functional group that results in the formation of a cycloheptenone, or a silylated methyl group, which leads to a methylene cycloheptene as the cycloadduct (Figure 3). The theoretical study of Cramer and co-workers suggested that both stepwise and concerted

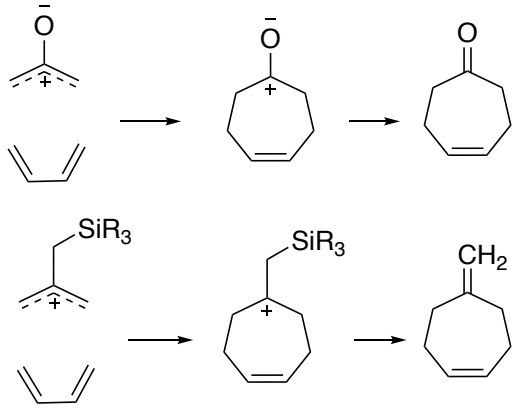

Figure 3. Typical functional groups on dienophiles in (4+3)-cycloadditions.

mechanisms were possible pathways.[10-11] The actual mechanism of the reaction is controlled by the reactivity of the allylic cation.[9] In general, the activation energy of the pericyclic pathway is lower than the stepwise pathway. Thus, the pericyclic pathway is the preferred mechanism only when a planar delocalized allyl cation is formed properly. But when Z is too nucleophilic, it tends to react with the terminal carbon cation to form a cyclic valence tautomer and completely loses the allyl resonance, resulting in a stepwise mechanism to form the product. Moreover, the more electrophilic cations, caused by more covalent oxygen-catalyst bonds, would also give access to a stepwise cycloaddition due to a greater mismatch in reactivity with dienes.[9]

1.2 Methods to generate allylic cations

The design of allylic cations with appropriate reactivity is the most challenging part in expanding the scope of (4+3)-cycloaddition reaction. Considerable efforts have been made to generate the oxyallyl cation species. Several useful methods are listed below (Figure 4).

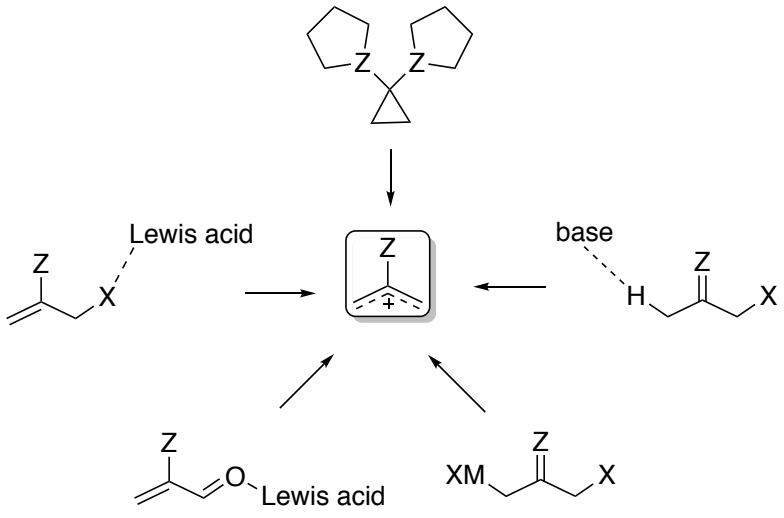

Figure 4. Overview of allylic cation generation in (4+3)-cycloaddition reactions.

The first (4+3)-cycloaddition reaction was reported in 1962 by Fort and co-workers (Scheme 1).[12] Deprotonation of α-haloketones **1** with base produced an reactive intermediate **2**, which was trapped by furan to yield 1-methyl-2,4-diphenyl-8-oxabicyclo[3.2.1]oct-6-en-3-one **3** as a mixture of diastereomers. Even though the reaction yield was only 18% after 4 days stirring at room temperature, it laid the foundation for the study of (4+3)-cycloadditions.

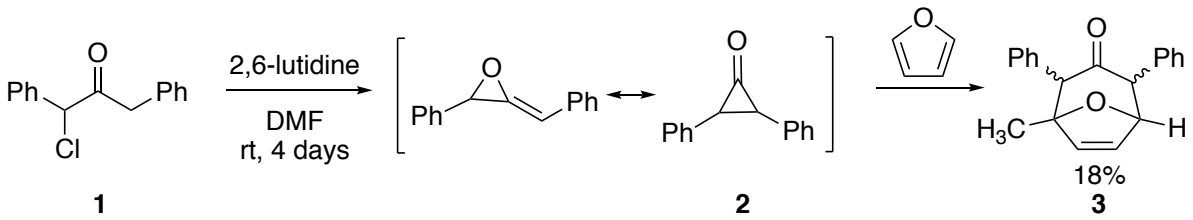

1 **2** **3**

Scheme 1. Generation of oxallylic cation with α-haloketone and base.

Ten years later, the field of (4+3)-cycloaddition methodology underwent a rapid expansion especially with respect to the generation of allylic cations under mild conditions. In 1973, Hoffman and co-workers reported the generation of reactive allyl cations through the use of silver salts as Lewis acids (Scheme 2).[13] The 2-methoxyallyl cation **5** was generated from 2-methoxyallyl bromide **4** and silver trifluoroacetate in the presence of sodium carbonate. The allylic cation was trapped with arenes through a (4+3)-cycloaddition reaction. The compensation of the loss of aromaticity in cycloaddition is the formation of bicyclo[3.2.2]nona-6,8-dien-3-one **7**.

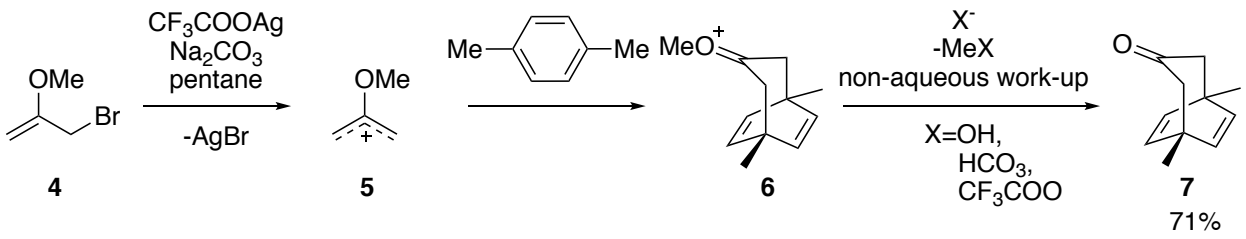

Scheme 2. Generation of allyl cations promoted by allyl halides and Lewis acids.

In 1980, Hoffman and coworkers demonstrated the acid-catalyzed (4+3)-cycloaddition reaction between an allylic alcohol and cyclopentadiene (Scheme 3).[14] The tertiary alcohol **8** served as a precursor of an allylic cation. In the presence of 50 mol % of *p*-toluenesulfonic acid, the allylic cation **9** formed and reacted with cyclopentadiene to give the bridged cycloheptenyl cation **10**, which was attacked by water to deliver secondary alcohol **11** in 37% yield.

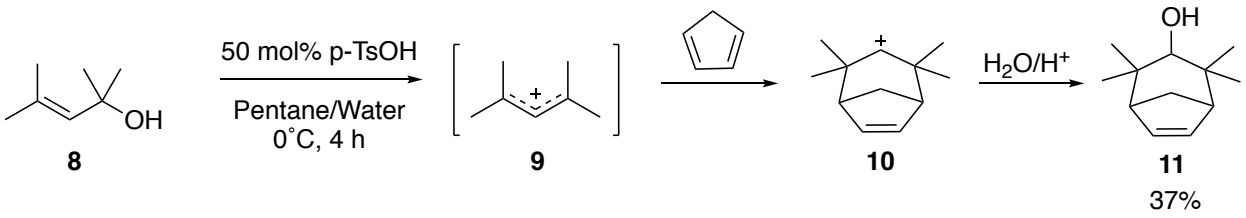

Scheme 3. Generation of allylic cation from an allylic alcohol.

Shortly thereafter, Hoffmann's group followed up with a report of the (4+3)-cycloaddition reaction of allyl cation generated from reductive dehalogenation (Scheme 4).[15] The insertion of zinc/copper couple into one of the carbon-bromide bonds in the presence of chlorotrimethylsilane made a silyl enol ether **13**. The other bromide was removed with the assistance of the newly formed zinc halide, resulting in a carbocation via an S_N1-like conversion. The allylic cation **14** then reacted with the nucleophilic anthracene to give oxopropanoanthracene **15** in 71% yield.

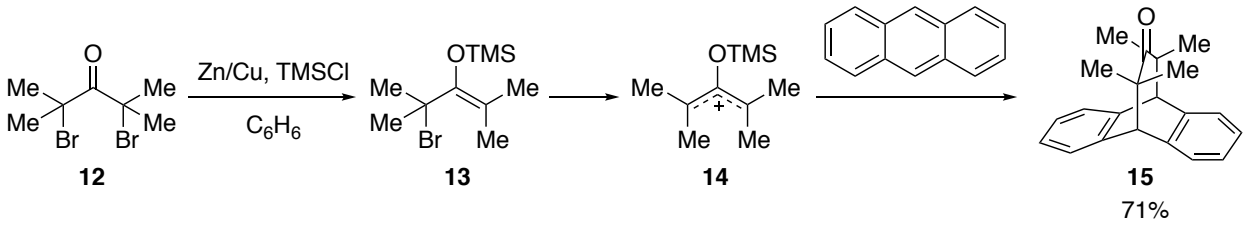

Scheme 4. Generation of allylic cation with α,α'-dihaloketones and a reducing agent.

The generation of allylic cations from cyclopropanones is of theoretical interest. However, due to the inaccessibility and difficult handling, the preparation of these small-ring compounds is impractical.[9] Instead, masked cyclopropenone derivatives such as allene oxide and bicyclic aminals are more frequently employed. The following example was reported in 1974 by Schmid and cowokers (Scheme 5).[16] In this case, the allylic cation precursor – bicyclic aminal **16** was used to produce cyclic amino allyl cation **19** through its electrophilic valence tautomer **18**. The cyclic amino allyl cation **19** was trapped with nucleophilic furan to give oxatricyclo[4.3.1.1^{2,5}]undec-3-en-10-one **20** as cycloadduct. The bicyclic aminals are very useful because they can be easily purified and stored.

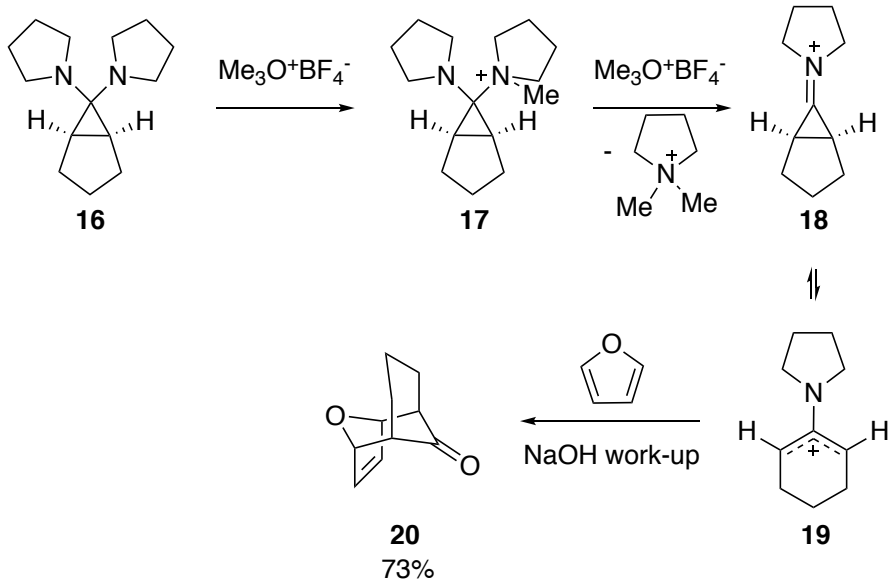

Scheme 5. Generation of an allylic cation from cyclopropenone derivatives.

1.3. Transition state conformations in concerted (4+3)-cycloaddition reactions

In one sense, the concerted (4+3)-cycloaddition is a homologue of Diels Alder reaction, since both reactions share the same electron count. For this reason, the (4+3)-cycloaddition reaction retains continual interest in the synthetic community for its potential ability to introduce regio- and stereoselectivity into the product. In general, (4+3)-cycloadditions tend to be less stereoselective than Diels-Alder reactions. The *endo* transition state of (4+3)-cycloaddition reaction has the diene part overlapping with the oxyallyl oxygen, which makes the conformation more compact. The *exo* transition state has the diene part pointing out away from the oxyallyl oxygen, making the conformation more extended. Some factors do have an impact on the configuration of transition states. For example, the dipole minimization favors the compact mode (*endo* T.S.) for highly charged oxygen, while unstable and electrophilic allyllic cations would prefer an extended transition state (*exo* T.S.). The different possible configurations of the allylic cation make the stereoselectivity of (4+3)-cycloaddition even more complicated. Three configurations are possible for acyclic cations: the U form, the sickle form and the W form. Both

conformations of the allylic intermediate and the transition state should be considered when trying to draw the mechanism in detail.[17]

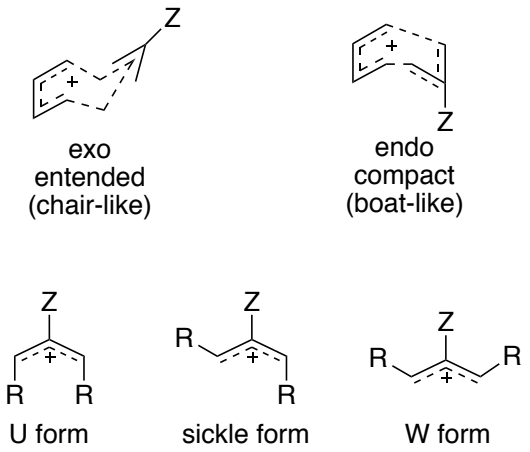

Figure 5. Transition state analysis of concerted (4+3)-cycloaddition reaction.

1.4 ß-Oxidoaziniums in (4+3)-cycloaddition reactions

The ß-oxidoaziniums are very active species that are known to react with a wide variety of π-systems to give cycloadducts.[18] Both the experimental results and the FMO theory calculations[19] showed mono-olefins and acetylenes reacted with the betaines across the 2,6-positions, while dienes reacted with the betaines across both 2,6- and 2,4-positions. Ketenes reacted with the betaines across its O,C2- or O,C4-positions, and fulvenes reacted across the 2,6-positions. In addition, the thermal dimers between 2,6- and 2,4-positions are also observed in nitrogen heteroaromatic betaines (Figure 6).[19]

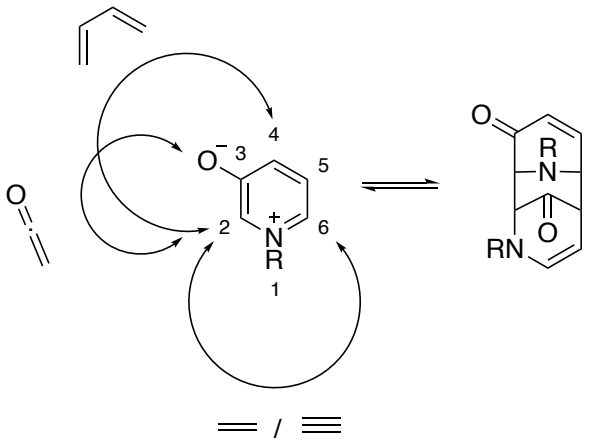

Figure 6. Reactivity of oxidopyridinium ions.

The use of oxidopyridinium ions as dienophiles in (4+3)-cycloaddition reactions was firstly demonstrated by Katritzky. Three examples[19-20] are shown below. These examples in Scheme 6

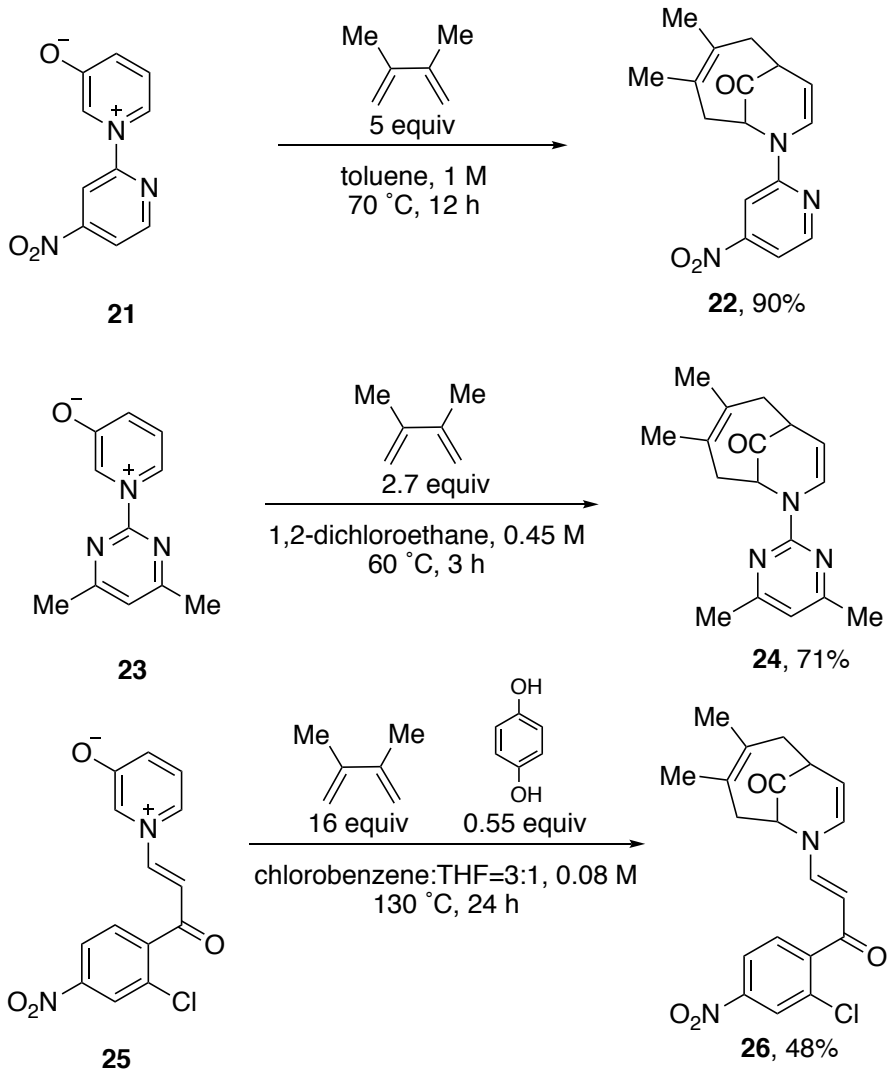

Scheme 6. (4+3)-cycloaddition reactions of *N*-aryl- and *N*-alkenyl-substituted oxidopyridinium ions.

represent reactions between the dienes and 2,4-positions of the aryl- and alkenyl-substituted oxidopyridinium ions to give (4+3)-cycloadducts. As the cycloaddition progresses, the nascent lone pair on the nitrogen atom can be stabilized by the aryl- or alkenyl- substituents, providing at least part of the driving force for the process. From an FMO perspective, the cycloaddition to 3-oxidopyridinium across 2,6-positions is ruled by dipolarophile LUMO and betaine HOMO, while the cycloaddition across 2,4-positions is controlled by the diene HOMO and betaine

LUMO. Adding strong electron-withdrawing group to the betaine and electron-donating group to the diene could reverse the electron demand and consequently facilitate the (4+3)-cycloaddition.

1,3-Dienes can also react as 2π-electron components across the 2- and 6-positions of the betaine. Besides the electronic factor mentioned above, the pathway of the reaction is also controlled by other factors such as temperature and steric hinderance. The reaction between pyridyl-substituted oxidopyridinium **21** and cyclopentadiene gave only one product **28,** which was derived from the (2+3)-cycloadduct **27** when being heated at 140 ˚C (Scheme 7). However, this reaction gave a mixture of both (2+3)-cycloadduct **27** and (4+3)-cycloadduct **29** when stirring at rt. This results indicated that the 2,6-adduct is more thermodynamically favored while the 2,4-adduct forms preferentially under conditions of kinetic control[19]. Another decisive factor is the primary steric repulsion caused by the substituents on the dienes. The experiments in

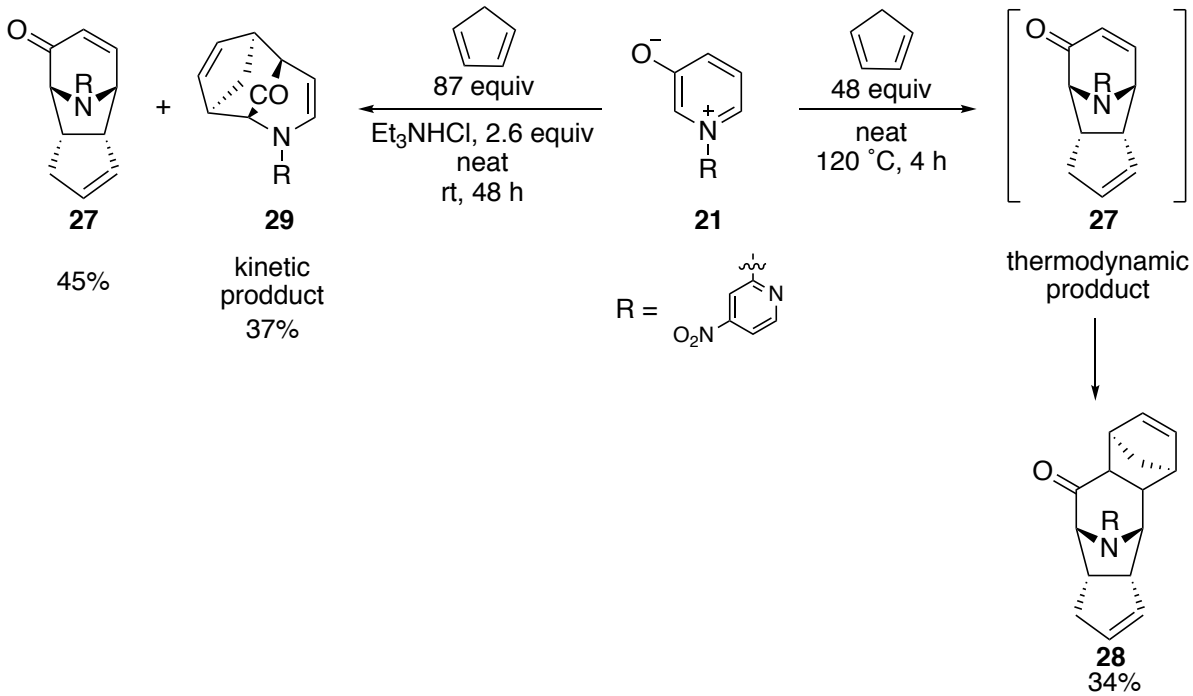

Scheme 7. Kinetic and thermodynamic control of the reactions between oxidopyridinium ions and cyclopentene.

Scheme 8 showed how the steric repulsion from methyl groups affected the orientation of the reaction between pyridyl betaine **21** and different dienes.[19] The reaction between pyridyl betaine **21** and 2,3-dimethylbutadiene yielded predominantly single 2,4-adduct **30**, while the reaction between pyridyl betaine **21** and penta-1,3-diene formed both 2,4-cycloadducts **31** and **32**, as well as 2,6-adduct **33**.

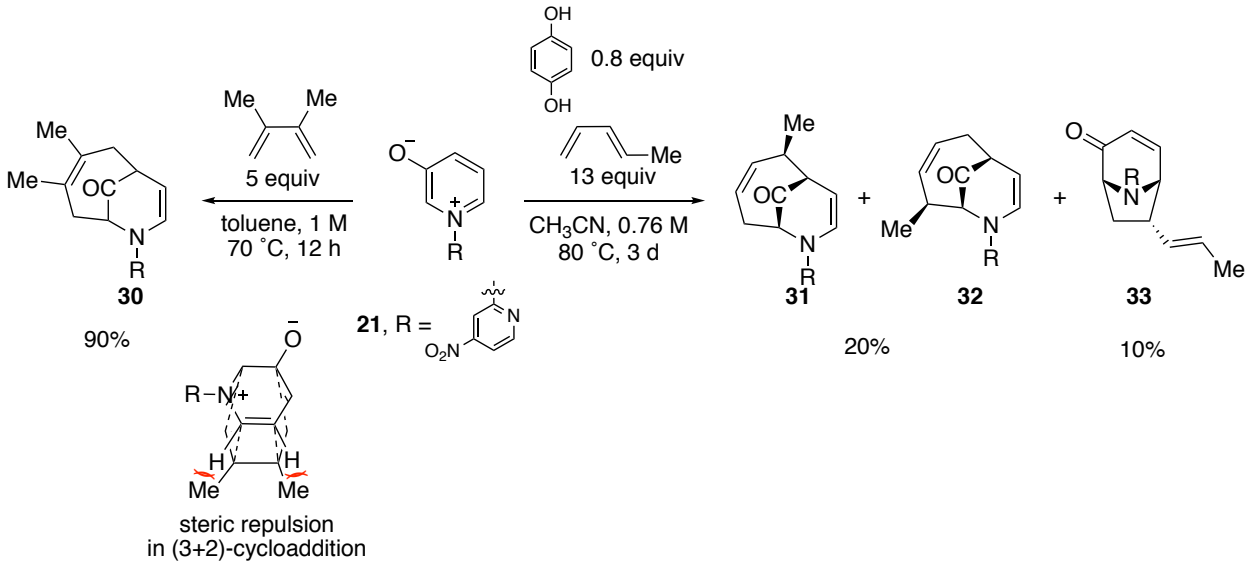

Scheme 8. Steric effects of dienes on the reactivity of oxidopyridinium ions.

It looked like that (4+3)-cycloaddition reactions of oxidopyridinium ions required *N*-aryl or alkenyl substitutions until two exceptional examples were reported. Katritzky and co-workers reported that the reaction of **34** with 2,3-dimethylbutadiene produced (4+3)-cycloadduct **35** in low yield (Scheme 9).[21] A similar reaction was reported by Nye.[22] It was observed that the (4+3)-cycloaddition took place between 1-methylquinolinium-3-olate **36** and dienes. These two examples suggested that the delocalization of the nitrogen lone pair enabled the cycloaddition reaction.

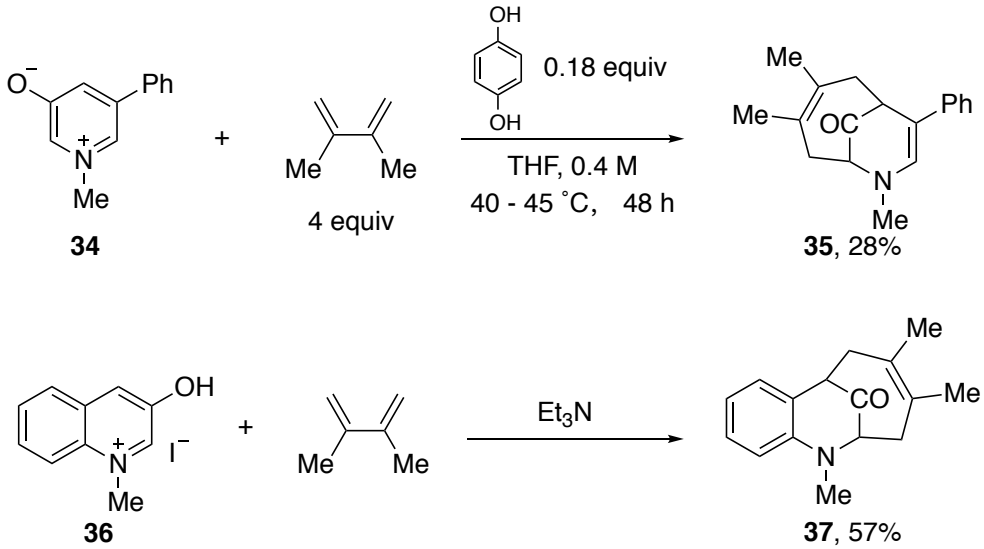

Scheme 9. (4+3)-Cycloaddition reactions of 5-aryl-oxidopyridiniums ions.

The (4+3)-cycloaddition chemistry of a 3-oxidopyrylium ion, the oxygen analogue of 3-oxidopyridinium, has also been explored by Sammes and Street.[23] As shown in Scheme 10, the oxidopyrylium intermediate **39** was prepared in situ from the corresponding pyranulose acetate **38** in the presence of base. This reaction gave both (4+3)-cycloadduct **40** and (3+2)-cycloadduct **41** with the (4+3)-cycloadduct as the major product.

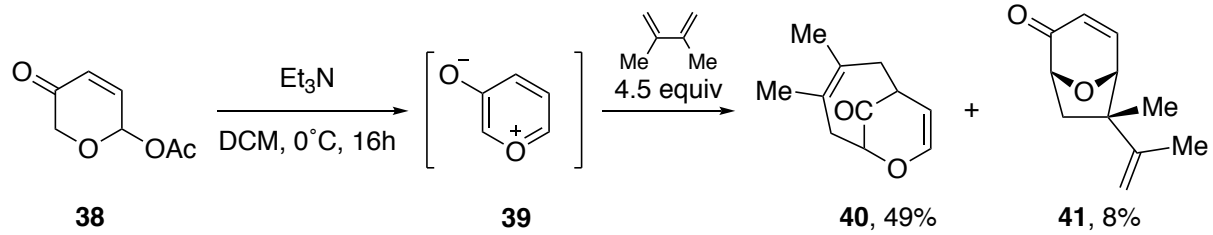

Scheme 10. (4+3)-Cycloaddition reaction of 3-oxidopyrylium ion.

1.5 Application of (4+3)-cycloaddition reaction of oxidopyridinium ion in natural product synthesis

The extensive existence of the 7-azabicyclo[4.3.1]decane ring as the core framework in bioactive natural products aroused our interests in this synthetic area. Examples of natural products[24-28] that contain the 7-azabicyclo[4.3.1]decane ring system are shown in Figure 7. The utilization of the (4+3)-cycloaddition reaction between oxidopyridinium ion and dienes would provide a convenient way to construct the azabicyclodecane ring from simple starting materials. Variation of substituents on dienes and on the nitrogen of the pyridinium ion can provide complexity in the cycloaddition product. Meanwhile, several challenges such as the controlling of regio- and stereo-selectivity remain to be solved before turning this methodology to wide application.

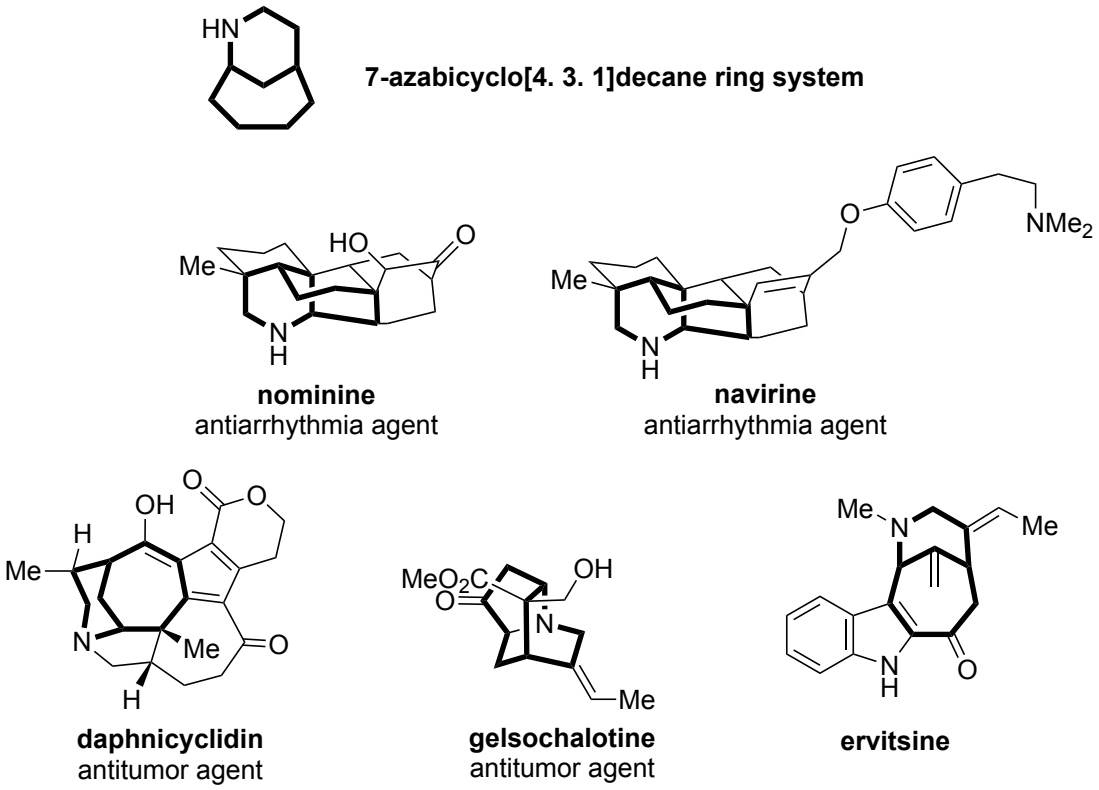

Figure 7. Selected natural products containing the 7-azabicyclo[4.3.1]decane ring system.

The work of Cha and co-workers in Scheme 11 is an example to show how useful the (4+3)-cycloaddition is in the total synthesis of natural products.[29] In this case, the key step is the (4+3)-cycloaddition between the six-membered cyclic oxyallyl **42** and cyclopentadiene to build the central azatricyclodecenone of sarains. This step is diastereoselective, giving only the *endo* cycloadduct.

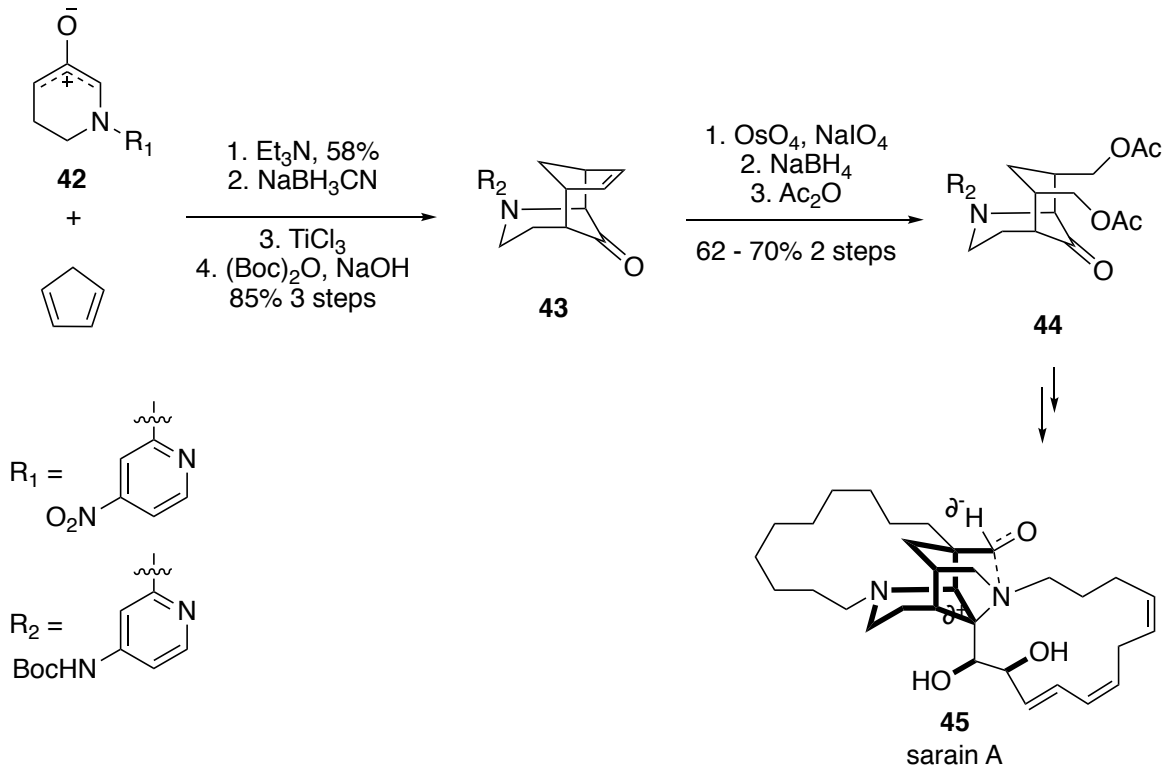

Scheme 11. The utilization of (4+3)-cycloaddition reaction in natural product synthesis.

CHAPTER 2

(4+3)-CYCLOADDITION REACTIONS OF *N*-ALKYL OXIDOPYRIDINIUM IONS

2.1 Discovery

We discussed that the stability of the nascent lone pair on the nitrogen of the cycloadducts is crucial with regard to the reactivity of oxidopyridinium ion when reacting with butadienes. When the lone pair is delocalized by substituents either on the nitrogen or on the C5 position in the dihydropyridinone product, the (4+3)-cycloadduct is formed in greater yield than the (2+3)-cycloadduct (Figure 8).

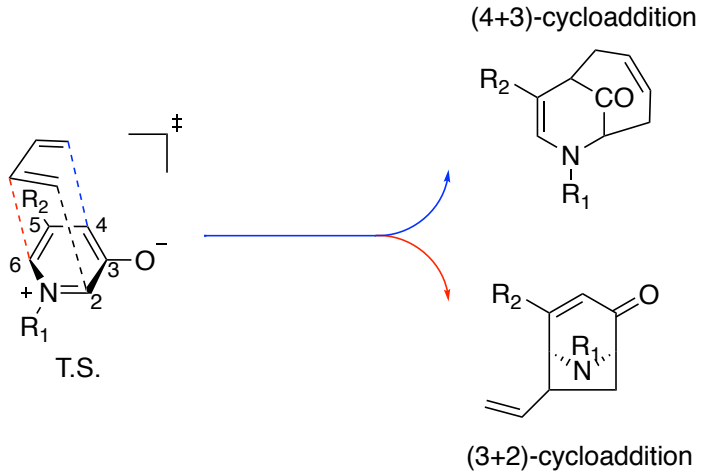

Figure 8. Pathway bifurcation in the cycloaddition of oxidopyridinium ion and butadiene.

Inspired by the work of Katritzky[19] and Nye,[22] together with the commercial availability of methyl 5-hydroxynicotinate **45**, we set out to install an electron-withdrawing methyl ester on the 5-position of an oxidopyridinium ion. The electron-withdrawing group would generally lower LUMO. Consequently, the HOMO-LUMO separation energy is reduced, and the reactivity of the oxidopyridinium is increased.

It was anticipated that simple *N*-alkylation of 5-hydroxynicotinate **45**, followed by deprotonation in the presence of a diene would result in the formation of (4+3)-cycloadducts **46** and **47**. Part of the driving force for the reaction is provided by the formation of a vinylogous carbamate in the product.

The first (4+3)-cycloaddition reaction of 5-(methoxycarbonyl)-1-methylpyridin-1-ium-3-olate **48** with 2,3-dimethylbutadiene was conducted by the former graduate Nestor Lora. *N*-Alkylation of **45** was conducted by treatment with methyl triflate in chlorobenzene or dichloromethane at room temperature for 2 – 3 hours. Removal of solvent and subsequent treatment with 2,3-dimethylbutadiene (10 equiv) in acetonitrile at 85 ˚C for 6 h afforded **46** in 99% yield (Scheme 12). The structure of the compound **46** was confirmed by X-ray crystallographic analysis. The corresponding reaction with 1,3-butadiene produced the parent cycloadduct **47** in 98% yield. In this case, the reaction was conducted in a sealed tube for 24 hours with approximately 30 equivalents of the diene due to the low boiling point of the diene.

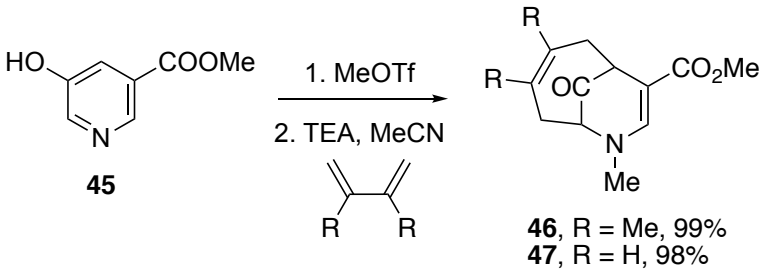

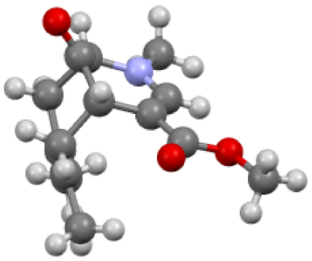

X-ray structure of **46**

Scheme 12. (4+3)-cycloaddition reactions of *N*-alkyl nicotine derivative.

Several possible mechanisms can be envisaged for this (4+3)-cycloaddition. Our collaborator Professor Krenske therefore performed density functional theory calculations to gain insight into the preferred mechanism. The computational procedure consisted of geometry optimizations with M06-2X/6-31G(d),[30] followed by single-point energy calculations with M06-2X/6-311+G(d,p), in which the solvent (acetonitrile) was modeled with the SMD[31] implicit solvent model. The energies of transition states (TSs) and intermediates of various different pathways for the reaction of oxidopyridinium ion **48** with 1,3-butadiene leading to (4+3)-cycloadduct **47** are shown in Figure 9.

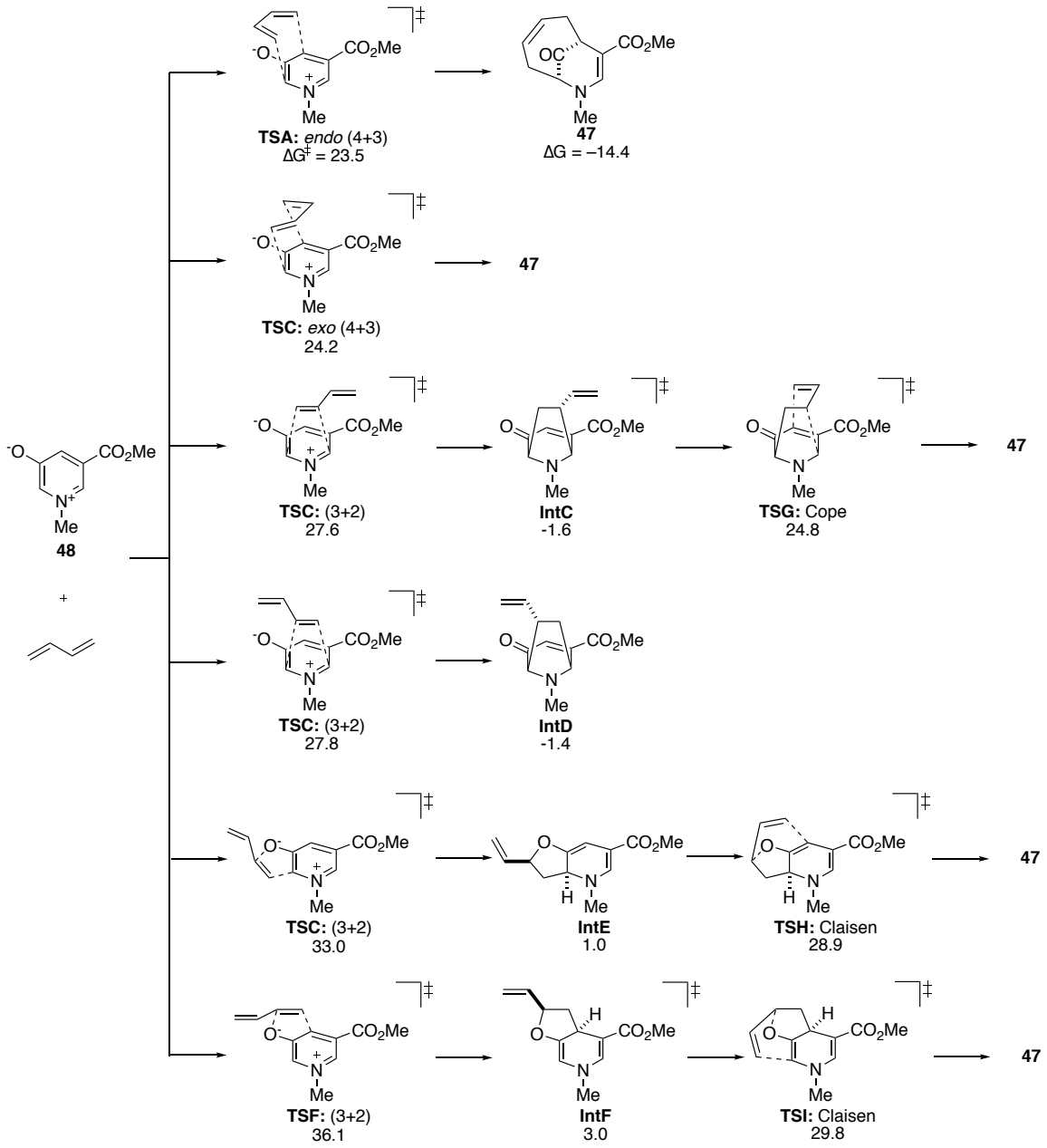

Figure 9. Possible mechanisms for the (4+3)-cycloaddition of oxidopyridinium ion **48** with 1,3-butadiene leading to cycloadduct **47**. The $\Delta G^{\ddagger}$ and ΔG values are in kcal/mol.

The computations predict that the preferred mechanism for the formation of cycloadduct **47** is a concerted (4+3)-cycloaddition across the oxyallyl moiety of the oxidopyridinium ion **48**. The *endo* (4+3)-transition state (TSA) is lower in energy than the *exo* TS (TSB) ($\Delta G^{\ddagger}$ = 23.5 and

24.2 kcal /mol, respectively). We use the oxyanion in **48** as a reference point for *endo* and *exo* descriptors. Overall, the cycloaddition is exergonic by 14.4 kcal/mol. Transition states corresponding to stepwise (4+3)-cycloaddition processes, commencing with the formation of a bond between the diene and either end of the oxyallyl moiety, could not be located. Instead, these TS geometries led to a range of (3+2)-cycloadditions (TSC–TSF). The first of these, a (3+2)-cycloaddition across the CNC moiety (TSC) leads to an intermediate IntC that could be converted into **47** through a Cope rearrangement (TSG). Similarly, (3+2)-cycloadditions onto the two CCO moieties of **47** via TSE and TSF lead to intermediates IntE and IntF, respectively, which can be converted into **47** through Claisen rearrangements (TSH, TSI). All of the pathways involving (3+2) cycloadditions are > 4 kcal/mol higher in energy than the direct formation of **47** via the concerted transition state TSA.

One might expect that an intramolecular proton transfer of **45** would happen slowly allowing the formation of pyridiniumolate that could react directly with the diene to give the secondary vinylogous carbamate **49** as cycloadduct. However, when the reactions between methyl 5-hydroxynicotinate **45** and 2,3-dimethylbutadiene were conducted with the assistance of several Brønsted acids and Lewis acids, no product was observed so far (Table 2). It is still remain unknown if any acids could catalyze this process or not.

Table 2. (4+3)-cycloaddition of oxidopyridinium ion with different Brønsted acids.

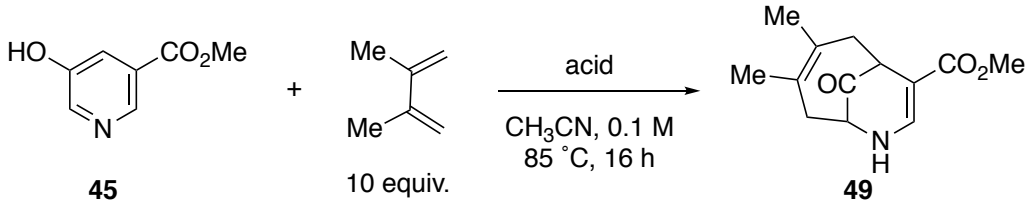

acid	yield (%)
no acid	no reaction
acetic acid	no reaction
TFA	no reaction
benzoic acid	no reaction
AgF	no reaction
AgOTf	no reaction
Ag_2CO_3	no reaction
$Cu(OAc)_2$	no reaction
$Pd(OAc)_2$	no reaction

2.2 Results

2.2.1 (4+3)-Cycloaddition reactions with 2-substituted and 2,3-disubstituted dienes

After our success with the model reaction of an oxidopyridinium ion with 1,3-butadiene, we began to examine other 2-substituted and 2,3-disubstituted dienes. Oxidopyridinium ion **48** reacted smoothly with symmetrical dienes **50** and **51** to give single cycloadducts in good to excellent yields (Table 3, entries 1 and 2). However, reactions with the unsymmetrical dienes **52**

and **53** were not regioselective (Table 3, entries 3 and 4). These results are good from the perspective of diversity-oriented synthesis,[32-36] but better control should be achieved for specific applications.

Table 3: Cycloadducts formed from 2-substituted and 2,3-disubstituted butadienes.

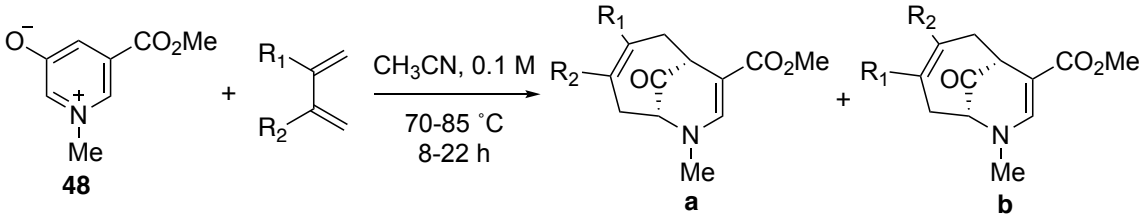

Entry	Diene	Cycloadduct	a/b	Yield (%)
1	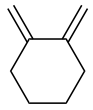 **50**	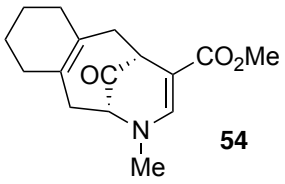 **54**	—	90[a]
2	 **51**	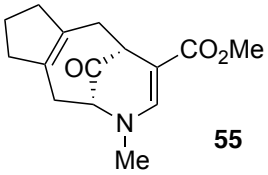 **55**	—	70[a]
3	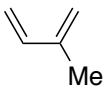 **52**	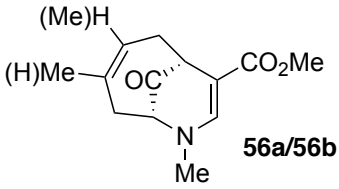 **56a/56b**	1.2 : 1	80[b]
4	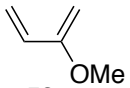 **53**	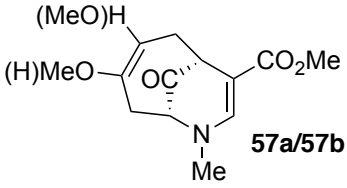 **57a/57b**	1.5 : 1	70[c]

[a] 85 ˚C, 8 h. [b] 70 ˚C, 22 h. [c] 85 ˚C, 17 h.

2.2.2 (4+3)-Cycloaddition reactions with 1-alkyl-substituted and 1,2-alkyl-disubstituted dienes

Dienes with alkyl groups at only one terminal carbon were tested to examine the regioselectivity and stereoselectivity of the (4+3)-cycloaddition (Table 4). The *endo*/*exo* ratio was generally low, approximately 1:1 as evidenced by ^{1}H NMR analysis of crude reaction mixtures. However, the regioselectivity was excellent, 100% in most cases. The structures of the cycloadducts were characterized by single crystal X-ray diffraction. The crystals for the X-ray were grown by recrystallization from ethyl acetate and hexane.

Table 4. Regio- and stereoselectivity of (4+3)-cycloaddition reaction of oxidopyridinium ion **48** with 1-alkyl-substituted and 1,2-alkyl-disubstituted dienes.

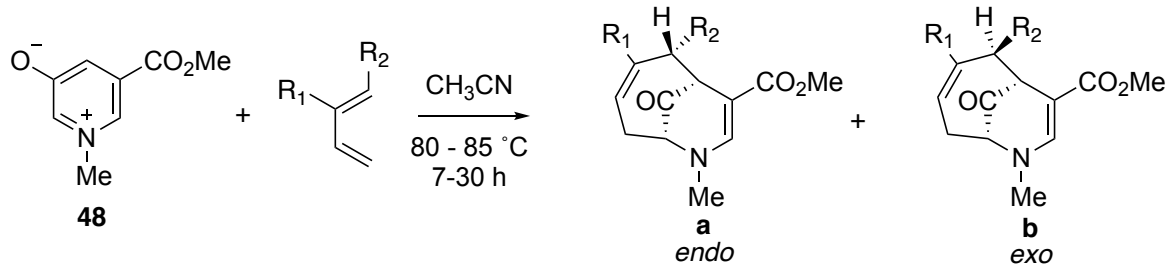

Entry	Diene	Cycloadduct	a/b	Yield (%)
1	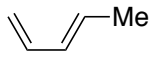 **58**	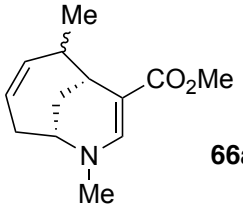 **66a/66b**	1 : 1	70[a]
2	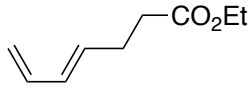 **59**	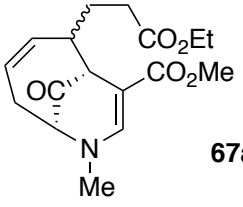 **67a/67b**	1.3 : 1	87[b]

3	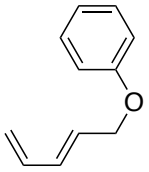 **60**	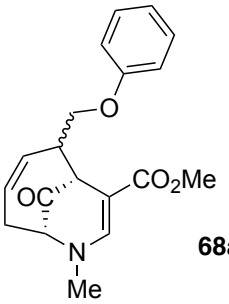 **68a/68b**	1 : 1.3	97[c]
4	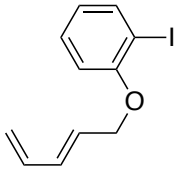 **61**	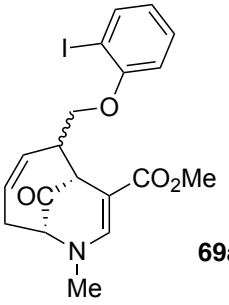 **69a/69b**	1 : 1.4	70[d]
5	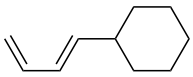 **62**	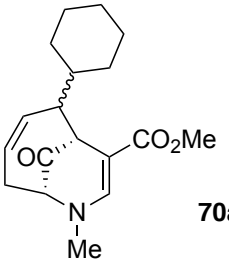 **70a/70b**	1 : 1.6	61[d]
6	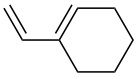 **63**	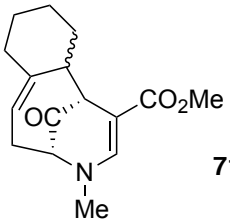 **71a/71b**	1 : 1.7	99[e]
7	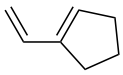 **64**	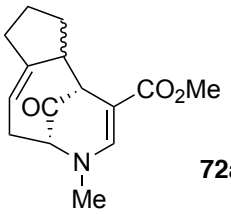 **72a/72b**	1 : 1.5	66[d]
8	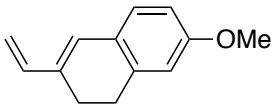 **65**	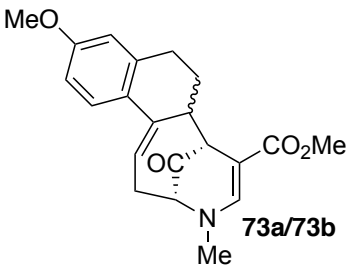 **73a/73b**	1 : 1.7	93[f]

[a] 80˚C, 17 h. [b] 85 ˚C, 7 h. [c] 85 ˚C, 30 h. [d] 85 ˚C, 22 h. [e] 85 ˚C, 20 h. [f] 85 ˚C, 24 h.

DFT calculations of the cycloaddition of **48** with one of 1-substituted dienes **58** are consistent with the observed regioselectivity, predicting that the TSs leading to the observed regioisomer are more than 1 kcal/mol lower in energy than the TSs leading to the alternative regioisomer. The TSs' distances between the diene **58** and the oxidopyridinium **48** show the more electrophilic terminus of the oxyallyl moiety is the iminium carbon atom C2 (Figure 10), and the observed regioselectivity corresponds to the addition of the more electron-rich terminus of the diene to this site.

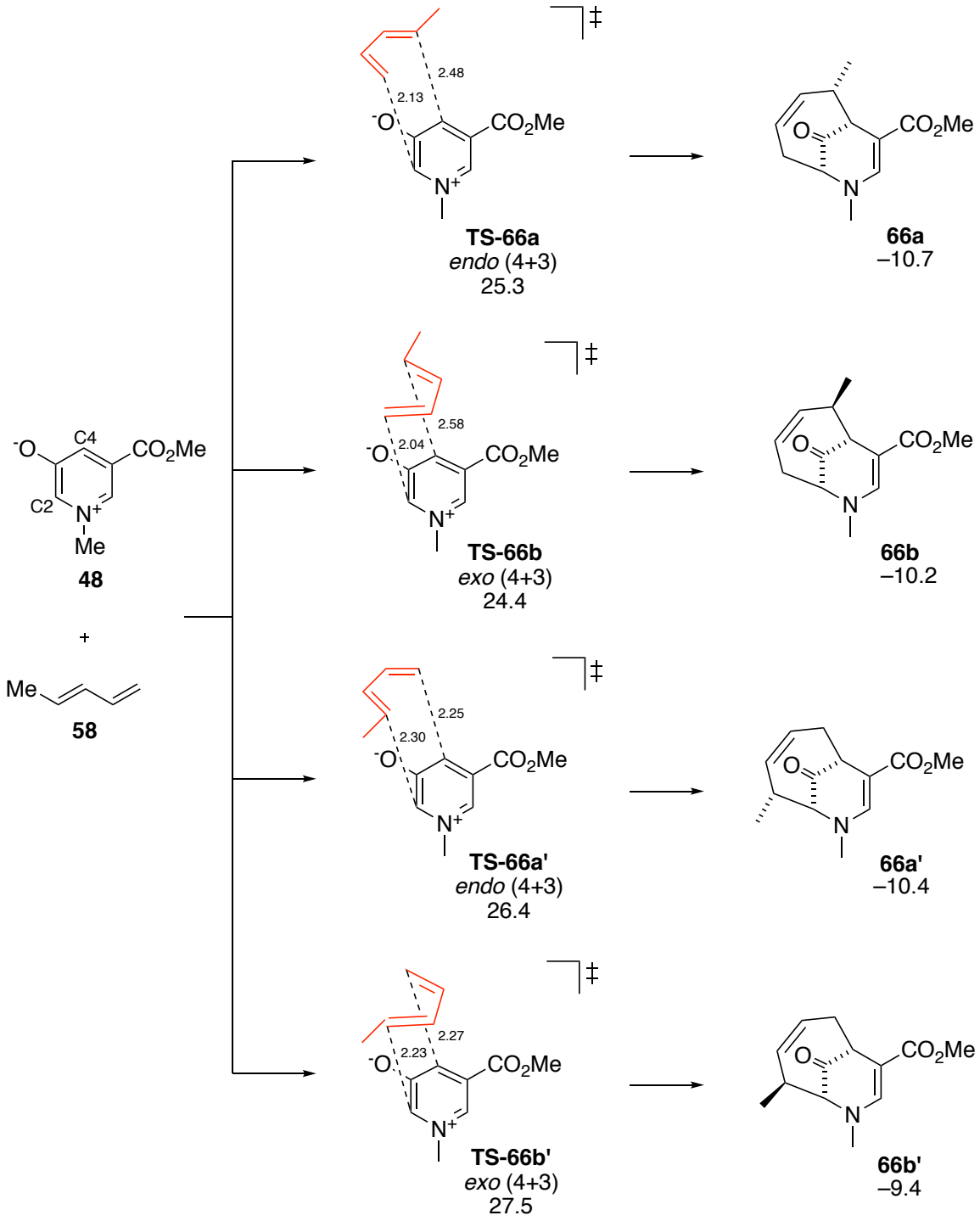

Figure 10. Calculated activation barriers and reaction energies of regio- and stereoisomeric (4+3)-cycloadditions of oxidopyridinium ion **48** with diene **58**. Distances in Å, $\Delta G^{\ddagger}$ and ΔG in kcal/mol.

Another factor that might also influent the regioselective outcome of the reaction is the steric hinderance. The absolute regioselectivity could be attributed to the avoidance of a steric interaction between the terminal substituent on the diene and the methyl group on the nitrogen, which is known as *syn*-pentane interaction.

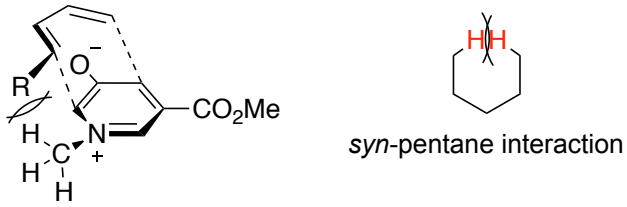

Figure 11. The steric factor in (4+3)-cycloaddition reaction of oxidopyridinium ion and 1-substituted diene.

2.2.3. (4+3)-Cycloaddition reactions with 1-heterosubstituted dienes

The (4+3)-cycloaddition reactions between oxidopyridinium ion **48** and 1-heterosubstituted dienes **74** – **78** were tested next (Table 5). The regioselectivity of reactions turned out to be the same as 1-alkyl-substituted dienes. Both diastereomeric products have allylic substitutions on the same side with the methyl ester. The *endo*/*exo* selectivity is not good in these reactions.

Table 5. Regio- and stereoselectivity of (4+3)-cycloaddition reaction of oxidopyridinium ion **48** with 1-heterosubstituted dienes.

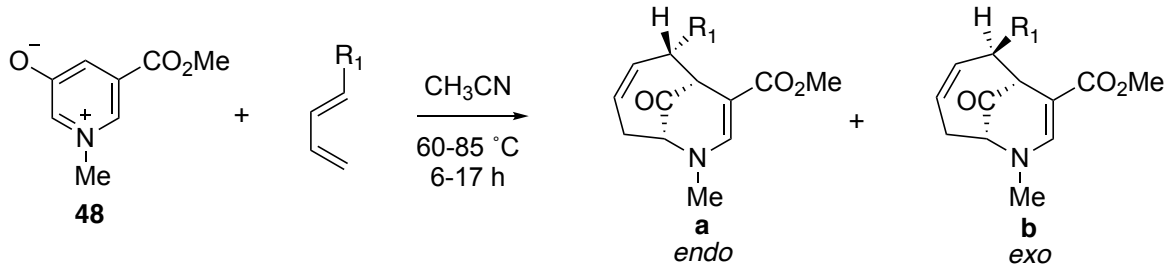

Entry	Diene	Cycloadduct	a/b	Yield (%)
1	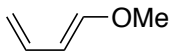 **74**	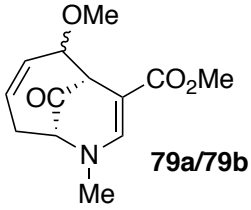 **79a/79b**	1 : 1	69[a]
2	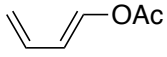 **45**	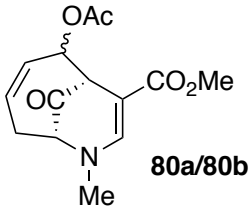 **80a/80b**	1 : 1	60[b]
3	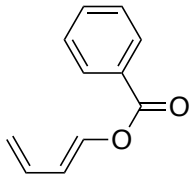 **76**	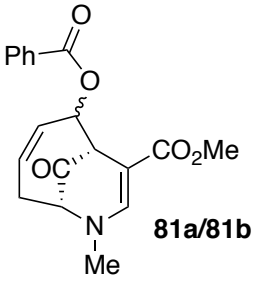 **81a/81b**	1.6 : 1	90[c]
4	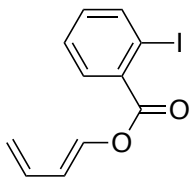 **77**	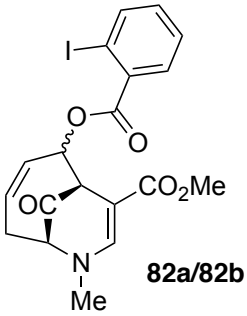 **82a/82b**	1 : 1	86[c]

[a] 80˚C, 17 h. [b] 80 ˚C, 14 h. [c] 85 ˚C, 17 h.

2.2.4. (4+3)-Cycloaddition reactions with 1-aryl-substituted dienes

It is interesting that when 1-phenyl-1,3-butadiene **84** was tested in this reaction, two regioisomeric *endo* products, **86a** and **86b**, were observed. The structures of both isomers were characterized by X-ray crystallography. Similar results were observed in the case with diene **85** (Table 6). We hypothesize the planar geometry of the aryl substituents relieves the steric hindrance previously mentioned, which allows the formation of the other regioisomer as the minor product. Although a mixture of regioisomers was found in the reaction, the major regioisomer was the one with allylic substituent on the other side of *N*-methyl group. These results were still agreed with the *syn*-pentane interaction mentioned before.

Table 6. Regio- and stereoselectivity of (4+3)-cycloaddition reaction of oxidopyridinium ion **48** with 1-aryl-substituted dienes.

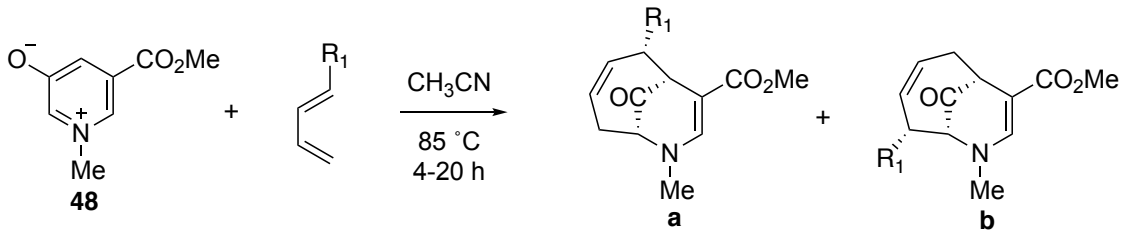

Entry	Diene	Cycloadduct	a/b	Yield (%)
1	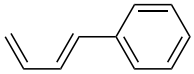 **84**	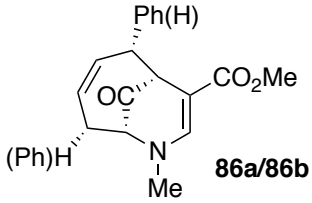 **86a/86b**	10 : 1	86[a]
2	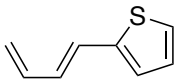 **85**	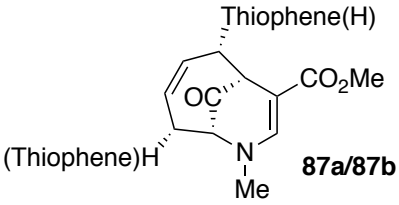 **87a/87b**	3 : 1	49[b]

[a] 4 h. [b] 20 h.

DFT calculations predict that the cycloadditions of **48** with **84** leading to **86a** and **86b** have ΔG = -6.9 and -6.5kcal/mol, respectively, thus making these cycloadditions less exergonic than those of butadiene (-14.4 kcal/mol) or 1-methylbutadiene (-10 kcal/mol). The calculations also predict that the cycloadduct should also furnish **86a'** with ΔG = 7.0 kcal/mol. The reason why **86a'** was not detected during the reversible cycloaddition reactions is not yet fully understood but may relate to the instability of **86a'** under the reaction conditions.

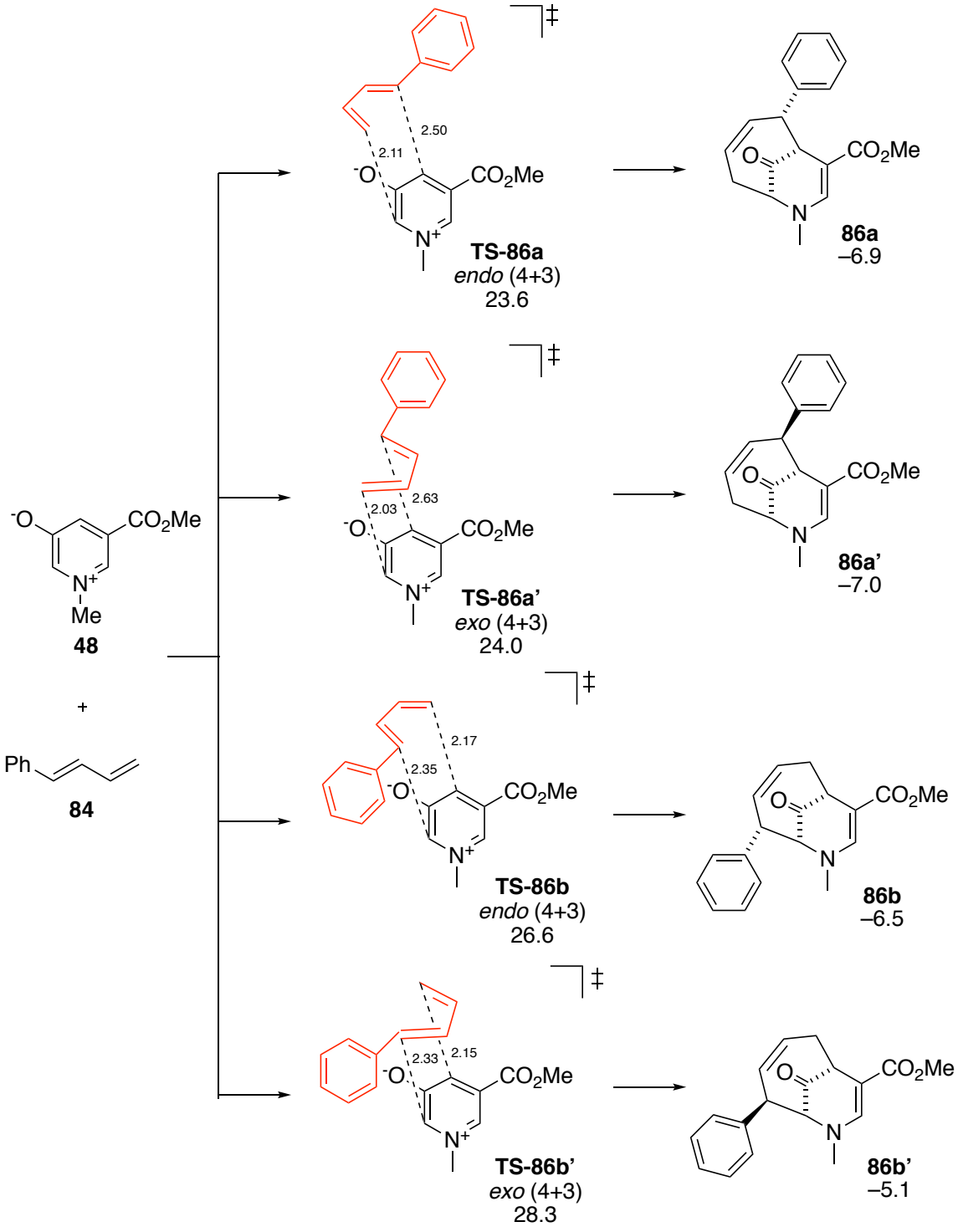

Figure 12. Calculated activation barriers and reaction energies of regio- and stereoisomeric (4+3)-cycloadditions of oxidopyridinium ion **48** with diene **84** (istances in Å, $\Delta G^{\ddagger}$ and ΔG in kcal/mol).

2.3 Mechanistic study

From the data obtained so far, a few questions were raised: 1) what is the reversibility of this reaction? 2) what factors would influence the composition of two regioisomers under the reaction conditions?

2.3.1. Reversibility of (4+3)-cycloaddition reactions of oxidopyridinium ion

The following reactions were conducted in order to elucidate the reversibility of the reaction. When the regioisomers **86a** and **86b** were heated under the original reaction condition individually, both **86a** and **86b** converged to nearly the same ratio of regioisomers (Scheme 13, entry A). The results indicated the reversibility of the cycloaddition process. Concerned that too much triflic acid might have been added to the reaction mixtures, we prepared triethylammonium triflate separately and conducted the experiment with one equivalent of the ammonium salt and two equivalents of triethylamine in the reaction mixture (Scheme 13, entry B). The isomeric ratio of the product mixture was essentially the same. However, we did note the yield of recovered **86a** and **86b** was rather low, which suggested these cycloadducts are not stable upon the heating under the standard reaction condition. Interestingly, when either **86a** or **86b** was heated under the conditions mentioned above with presence of excess 2,3-dimethylbutadienes, only cycloadduct **46** was obtained in 76% and 67% yield, respectively (Scheme 13, entry C). Finally, when cycloadduct **71** was heated under the same condition (Scheme 13, entry D), only the starting material was recovered with 87 % yield, thus revealing its stability relative to **86a** and **86b**.

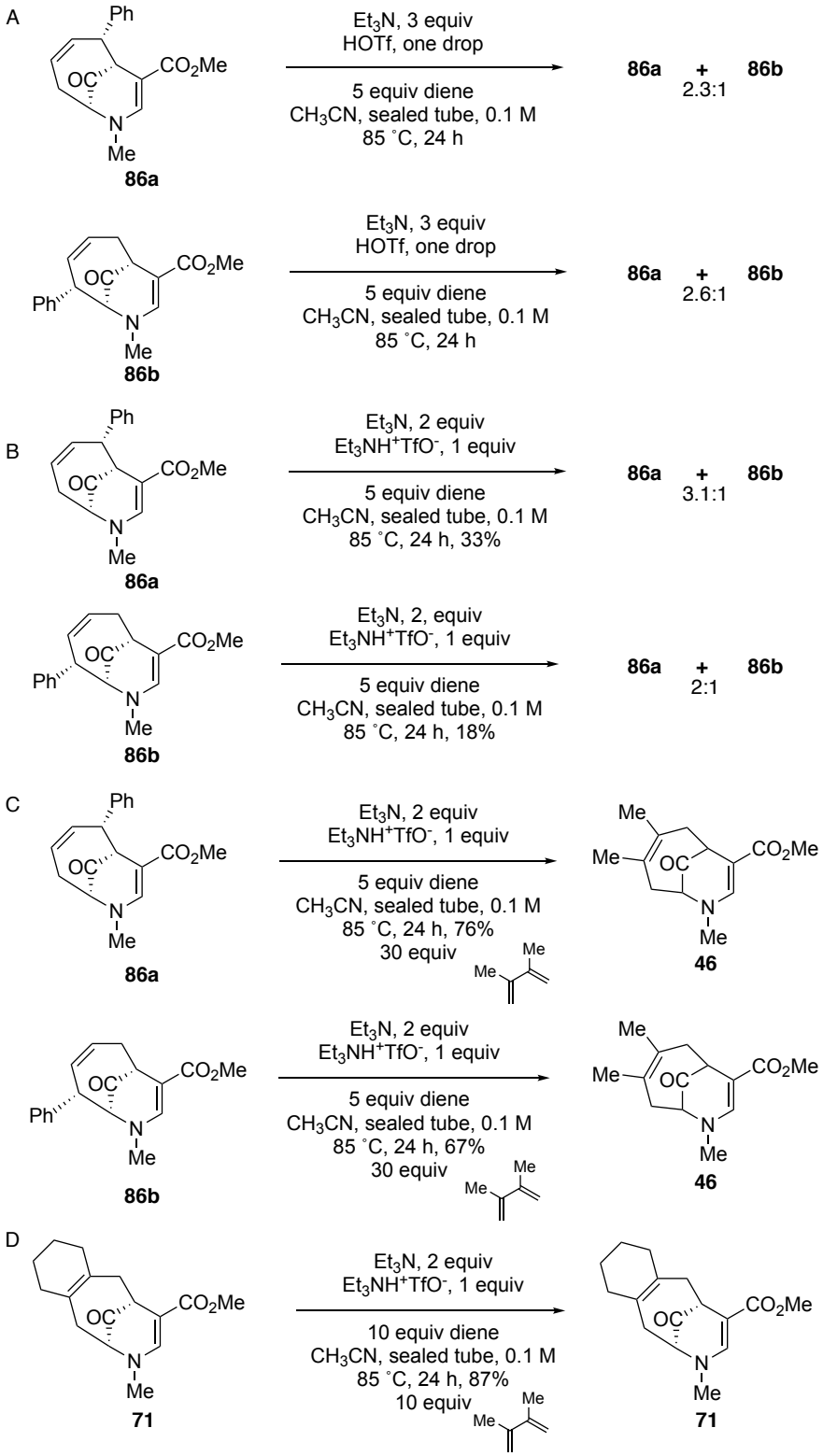

Scheme 13. Experiments examining the reversibility of cycloaddition reaction and thermal stability of aryl- and alkyl-substituted cycloadduct.

2.3.2. Thermodynamic vs. kinetic control of (4+3)-cycloaddition reactions of oxidopyridinium ions

In order to figure out if this reaction is controlled by thermodynamic or kinetic control, two reactions were run for 48 hours. The yield of each isomer at different points of time was determined individually. Figure 13 shows the individual yield of the two products as a function of reaction time. This set of data was obtained from two parallel experiments in which the reaction between diene **84** and oxidopyridinium ion **48** was carried out under typical reaction conditions in sealed tubes. At the time points shown, the reaction mixture was cooled, and an aliquot was removed. ^{1}H NMR analysis of the aliquot gave the regioisomer ratio (**86a**/**86b**) in the crude reaction mixture, and the yield at that time point was determined after flash chromatographic purification of the aliquot and is based on the volume of the aliquot removed from the reaction mixture. The experiments were repeated. The calculated yields are prone to error, but generally suggest that yields a decrease over time after 4 h for this particular process, thus possibly reflecting decomposition of the cycloadducts at different rates. Hypothetically, faster decomposition of **86a** compared to **86b** would account for both the decrease in yield and the apparent decrease in regiomeric ratio at long reaction time. It looked like **86a** was both kinetic and thermodynamic product.

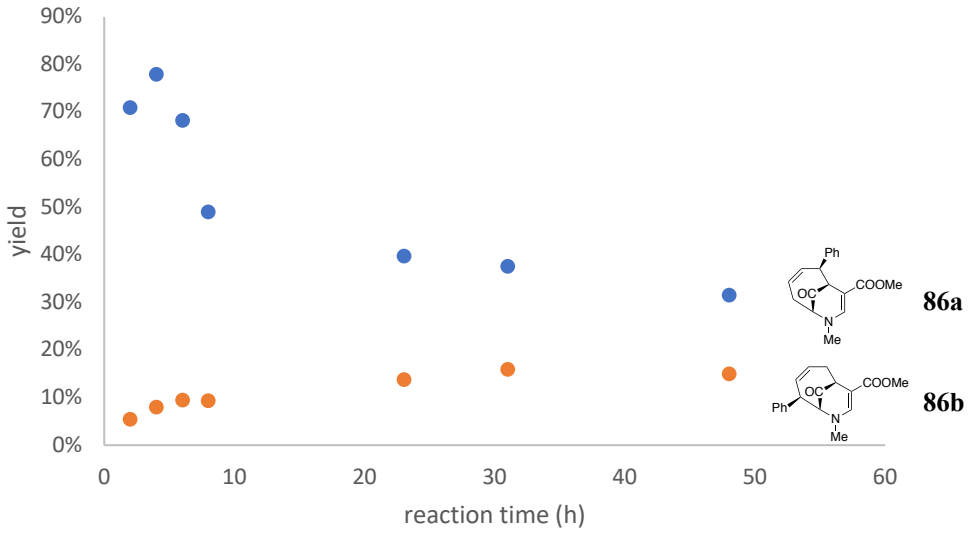

reaction time (h)	Yield of **86a** (%)	yield of **86b** (%)
2	71 [a]	5 [a]
4	78 [a]	8 [a]
6	68 [a]	9 [a]
8	49 [a]	9 [a]
23	40 [b]	14 [b]
31	38 [b]	16 [b]
48	32 [b]	15 [b]

a. average of three experiements. b. average of two experiments.

Figure 13. The yield of two isomeric cycloadducts as a function of reaction time.

2.4 Modifications

2.4.1 Reducing the equivalents of diene use

Several aspects of this reaction need to be improved before its extensive use in synthesis. The most obvious problem of this reaction is the large dose of dienes. While some dienes can be

recovered from the reaction mixture, it is still a huge waste of start material, especially because dienes can be expensive and difficult to synthesize. The idea of this optimization is to lower the amount of the diene while keeping the related concentration of the diene as the same. The best result we obtained for model reaction between **88** and **63** was to use 2.5 equivalents of the dienes with a concentration of 0.8 M (as for the pyridinium salt) giving 86% yield in the reaction with vinyl cyclohexene (Table 7).

Table 7. Optimization study of the equivalent of diene in (4+3)-cycloaddition reaction.

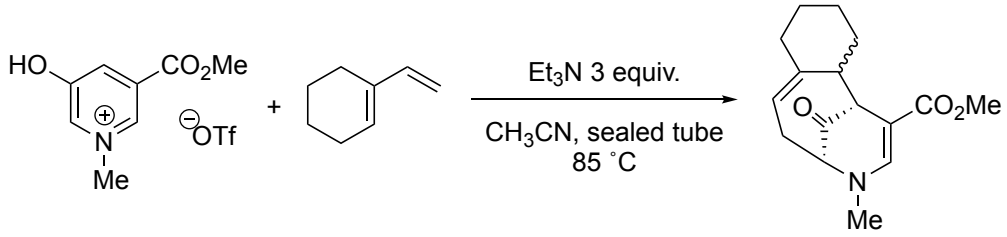

88 **63** **71a/71b**
endo:exo=1:1.7

diene equiv.	concentration(salt)	concentration(diene)	Yield (%)
10	0.1	1	99[a]
5	0.2	1	99[b]
2.5	**0.4**	**1**	**86[b]**
1.75	0.57	1	76[b]
1.25	0.8	1	55[b]

a. yield is an average of 5 experiments. b. yield is the average of 2 experiments.

2.4.2 1,4-Disubstituted dienes in (4+3)-cycloaddition reactions of oxidopyridinium ions

Several 1,4-disubstituted dienes were tested for the cycloaddition and failed under normal conditions. The DFT prediction shows the pathway involving 1,4-disubstituted diene **89** is more than 2.4 to 4.0 kcal/mol higher in energy and less exergonic than the ones with 1-substituents (Figure 14). The steric hindrance raises the activation energy of this reaction and perhaps lowers

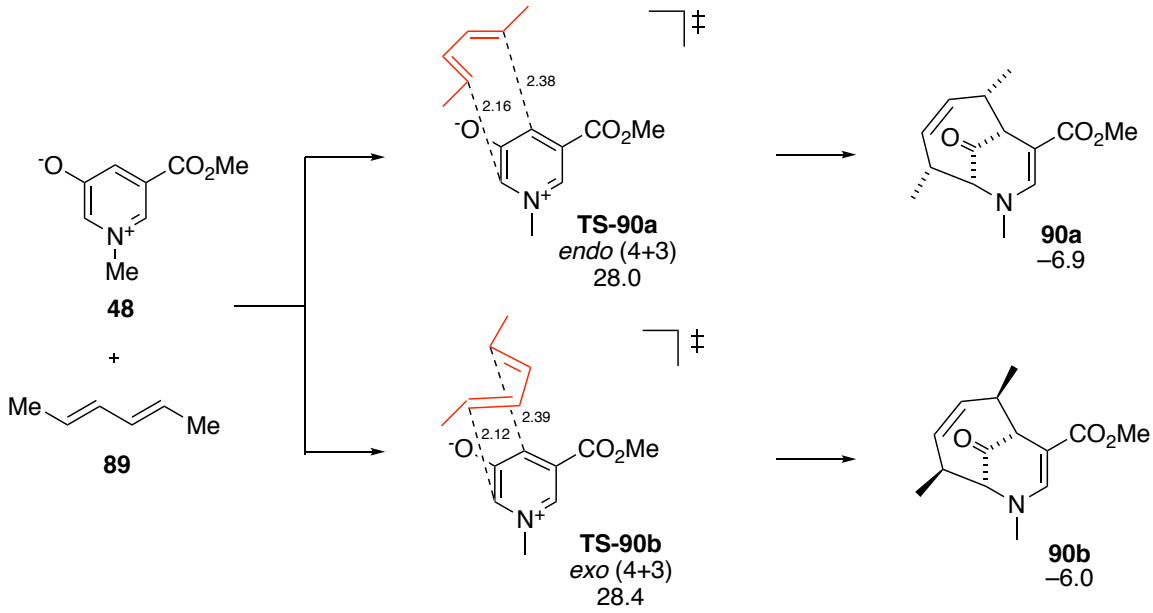

Figure 14. Calculated activation barriers and reaction energies of regio- and stereoisomeric (4+3)-cycloadditions of oxidopyridinium ion **48** with diene **89** (distances in Å, $\Delta G^{\ddagger}$ and ΔG in kcal/mol).

the stability of the cycloadduct. In order to expand the scope of this reaction, our next target was to develop reaction conditions to allow for this unfavored reaction. After some trials with different reaction conditions, we successfully made the mixture of regio- and stereoisomers as cycloadducts by simply increasing the solvent concentration and reaction time (Table 8). Most of the cycloadducts (**94 -96**) were separated by column chromatography and the structure of isomers were determined by NMR and X-ray analysis. For example, for reaction in entry 1, **94a**

and **94d** was isolated through flash column chromatography of 30%- 50% ethyl acetate/hexane followed by a second flash column chromatography of 1% -2% methanol/dicholoromethane. The structures of both were determined by X-ray analysis. The crystals of hemiacetal **94a** were grown by slow evaporation of methanol solution at rt. The crystals of **94d** was grown via recrystallization from 30% ethyl acetate and hexane. Since only the *endo* isomers can form the hemiacetal, the determination of the structures of **94b** and **94c** could be solved by ^{1}H NMR. In the case in entry 2, only **95d** afforded crystals to run X-ray analysis. The structure of acetate esters **95a**, **95b** and **95c** were determined by comparing the ^{1}H spectra of the hydrolyzed alcohol products with the ^{1}H spectra of **94a**, **94b**, **94c** and **94d**. It is worth mentioning that the reaction between oxidopyridinium **48** and diene bearing thiophenol gave only two *endo* regio-isomers (Table 8, entry 3). The structures of both regio-isomers **96a** and **96c** were confirmed by X-ray crystallography. This result is very similar as the reactions with aryl-substituted dienes.

Table 8. Regio- and stereoselectivity of (4+3)-cycloaddition reactions of oxidopyridinium ion **48** with 1,4-disubstituted dienes.

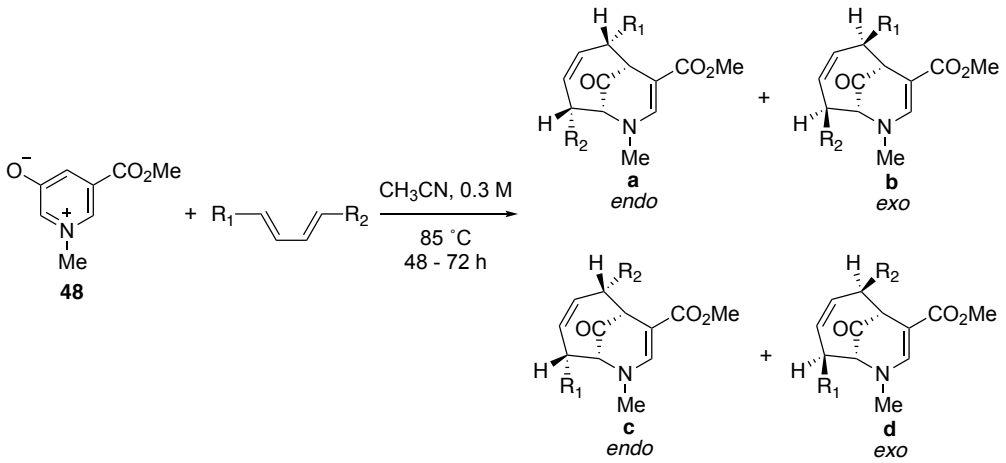

Entry	Diene	Cycloadduct	a:b:c:d	Yield (%)
1	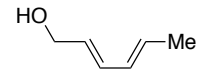 **91**	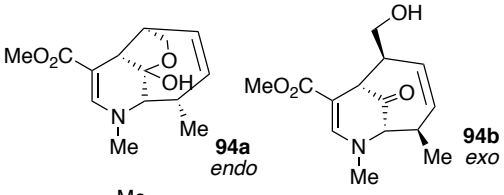 **94a** *endo*; **94b** *exo*; **94c** *endo*; **94d** *exo*	2.4 :1 : 2.5 : 2.5	86[a]
2	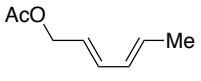 **92**	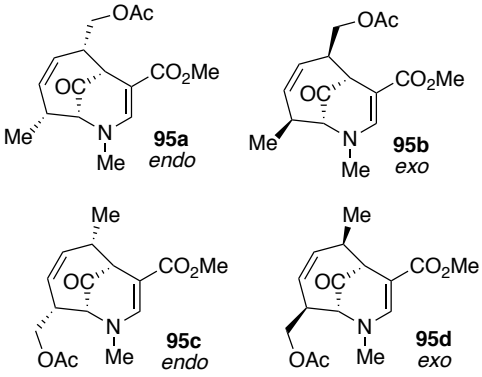 **95a** *endo*; **95b** *exo*; **95c** *endo*; **95d** *exo*	2.6 : 1.4 : 4.5 : 1	63[a]
3	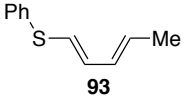 **93**	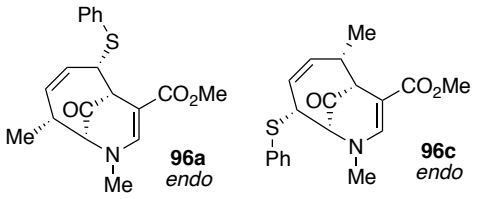 **96a** *endo*; **96c** *endo*	3 : N/A:1 : N/A	41[b]

[a] 72 h. [b] 48 h.

2.4.3. Base effects on (4+3)-cycloaddition of oxidopyridinium ion

The base is an important participant in cycloadditions involving the oxidopyridinium ion. Bases of different categories were screened in order to expand the scope of this reaction. Since we started with triethylamine, amines with different hybridization and substitutions were initially tested. Nonconjugated alkylamines, (+)-cinchonine and diisopropylamine, gave the best yields, followed by the amidine, DBU, giving a moderate yield. Heterocyclic aromatic amine, pyridine, and arylamine, dimethylaniline, provided the lowest yield (Table 9).

Table 9. (4+3)-cycloaddition of oxidopyridinium ion with different amine bases.

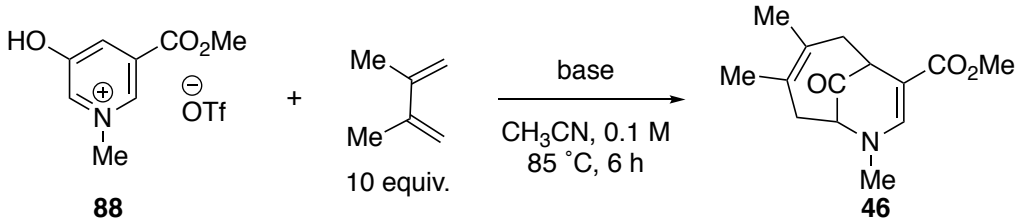

base	yield (%)	pKa
N,*N*-dimethylaniline[a]	7[g]	5.20[e]
pyridine[a]	17[g]	5.21[e]
triethylamine[a]	33[g]	10.75[e]
1,8-Diazabicyclo[5.4.0]undec-7-ene[a]	40[g]	12[f]
diisopropylamine[a]	63[g]	11.05[e]
(+)-cinchonine[a]	78[g]	11[f]
triethylamine[b]	99[g]	10.75[e]
triethylamine[c]	99[g]	10.75[e]

a. a. 1 equiv. b. 2 equiv. c. 3 equiv. d. 0.25 equiv. e. Evan's pKa table. f. estimate pKa value. g. yield is based on one experiment.

As an alternative to amines, an array of carboxylate bases was screened. Among all the tested aliphatic carboxylate bases, sodium acetate provided the product with the highest yield. Weaker aryl substituted carboxylates were also tested. For most aryl carboxylate bases, in general, the reaction yields rise along with the rising pKa of the acids, except sodium 4-nitrobenzoate provided a super low yield. Since most reactions are conducted only for one time, errors could happen. Sodium benzoate gave the best product yield among all the screened carboxylates.

Table 10. (4+3)-cycloaddition of oxidopyridinium ion with different carboxylate bases.

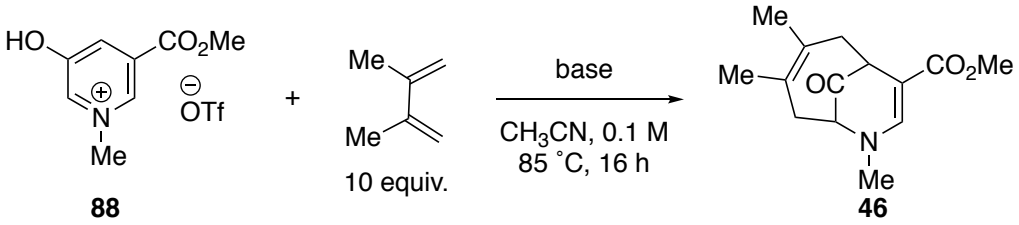

base	yield (%)	pKa
sodium tartrate	7[e, g]	2.98[37]
potassium L-tartrate monobasic	13[g]	2.98[37]
sodium succinate	60[g]	4.16[38]
sodium acetate	93[g]	4.76[f]
sodium 4-nitrobenzoate[a]	2[g]	3.44[f]
sodium 2-hydroxybenzoate[a]	18[h]	2.98[39]
sodium 2-bromobenzoate[a]	26[h]	2.85[40]
sodium 3,5-bis(trifluoromethyl)benzoate[a]	43[g]	3.34[41]

sodium [1,1'-biphenyl]-2,2'-dicarboxylate[a]	74[g]	3.20[42]
sodium benzoate[a]	99[h]	4.2[f]
sodium benzoate[b]	33[g]	4.2[f]
sodium benzoate[c]	17[g]	4.2[f]
sodium benzoate[d]	13[g]	4.2[f]

a. 1 equiv. b. 0.75 equiv. c. 0.5 equiv. d. 0.25 equiv. e. 6 h.
f. Evan's pKa table. g. yield is based on one experiment. h. yield is the average of two experiments.

Several selective inorganic sodium, potassium and cesium bases were tested. Those inorganic bases worked well in acetonitrile with the product being obtained in high yields.

Table 11. (4+3)-cycloaddition of oxidopyridinium ion with different inorganic bases.

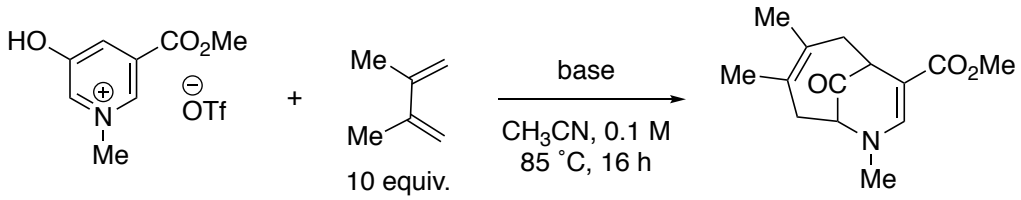

base	yield (%)	pKa
$NaHCO_3$[a]	82[b]	6.35
K_2CO_3[a]	99[c]	10.33
$CsCO_3$[a]	99[c]	10.33
K_2HPO_4[a]	99[c]	7.2
K_3PO_4[a]	99[c]	12.4

b. 1 equiv. b. yield is the average of two experiments. c. yield is based on one experiment.

2.4.4. Organocatalysis in (4+3)-cycloaddition reactions of 3-formyl-5-hydroxy-1-methylpyridin-1-ium ions

Another area of focus in this study was the facial selectivity of this reaction. Many approaches to develop asymmetric (4+3)-cycloaddition reactions have been developed. Among those, the uses of chiral Lewis acid or chiral auxiliary are promising.[43-44] In 2003, our group reported the first asymmetric, catalytic (4+3)-cycloaddition reaction between dienal **97** and 2,5-dimethylfuran **99** in the presence of amine **98** to give 100 in 64% yield (Scheme 14).[44] Inspired by that, we wanted to bind the C5 functional group with a chiral auxiliary that can selectively

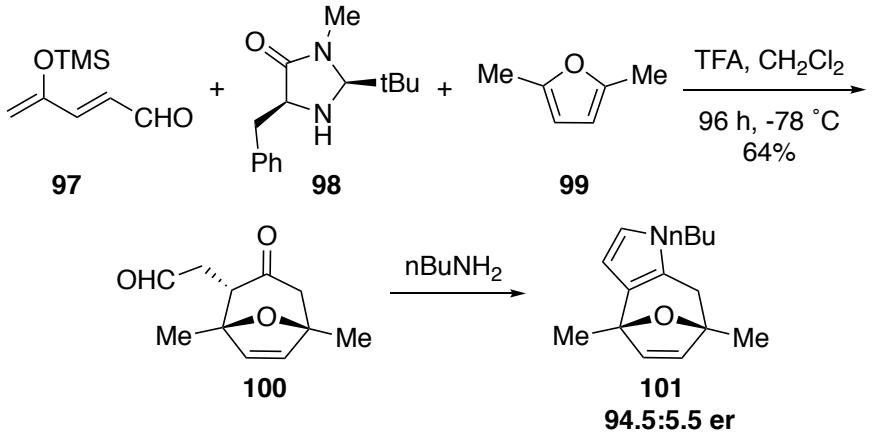

Scheme 14. The first asymmetric, catalytic (4+3)-cycloaddition reaction

block one face of the oxidopyridinium ion once it was installed. This protocol required us to convert the methyl ester to an aldehyde. Reducing the nicotinate ethyl ester **102** with DIBAL-H[45] or LAH[46] afforded an alcohol **103**. The oxidation of alcohol **103** to the corresponding aldehyde **104** is tricky. Several approaches were tried such as Swern oxidation,[47] Dess-Martin oxidation,[48] radical oxidation with TEMPO and $NaBrO_3$,[49] and Ru/O_2 oxidation.[50] But none of those worked. The main problem in the oxidation reaction was the low solubility of the alcohol. This problem

was solved by the treatment of **103** with 7 equivalents of MnO_2 in acetonitrile,[51] resulting in a complete conversion to the aldehyde **104**. Although the actually yield was affected by the strong absorbance of the manganese dioxide particle, we successfully isolated the corresponding aldehyde by filtration through Celite®. The alkylation was achieved quantitatively by stirring the pyridine derivative **104** with methyl triflate in dichloromethane at ambient temperature. Upon

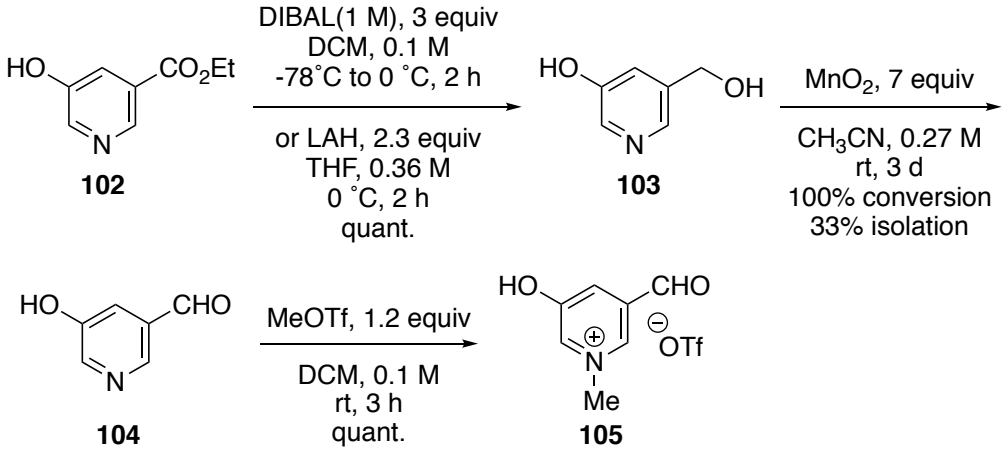

Scheme 15. Synthesis of 3-formyl-5-hydroxy-1-methylpyridin-1-ium trifluoromethanesulfonate.

attaining the pyridinium salt **105**, we reacted it with 2,3-dimethylbutadiene under the standard reaction conditions. It turned out that even though the 3-formyl-5-hydroxy-1-methylpyridinium salt **105** was equipped with a better electron-withdrawing group compared with ester, the reaction rate was slower and there was still starting material remained upon working up after 7 h. The (4+3)-cycloaddition of the aldehyde species in 10% presence of the chiral amine, (2*S*,5*S*)-5-

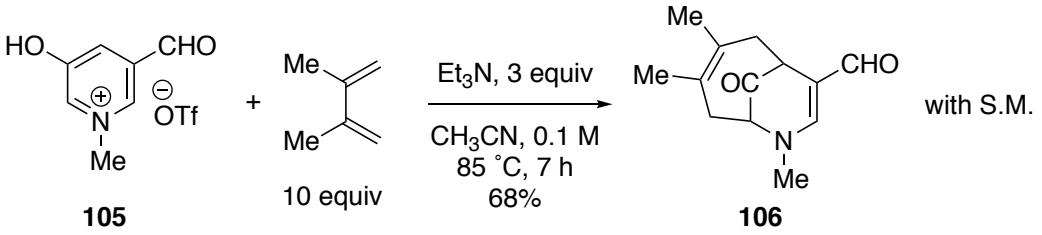

Scheme 16. (4+3)-cycloaddition of 3-formyl-5-hydroxy-1-methylpyridin-1-iumion.

benzyl-2-(*tert*-butyl)-3-methylimidazolidin-4-one **98**, was tested as well (Scheme 16). The reaction took place at rt with the help of amine catalyst. The TLC monitor showed that after 17 h, the conversion stopped, and 48% of the corresponding product **106** was isolated after flash column chromatography. A chiral HPLC hasn't been run yet for the product so that the ee ratio is unknown for this reaction.

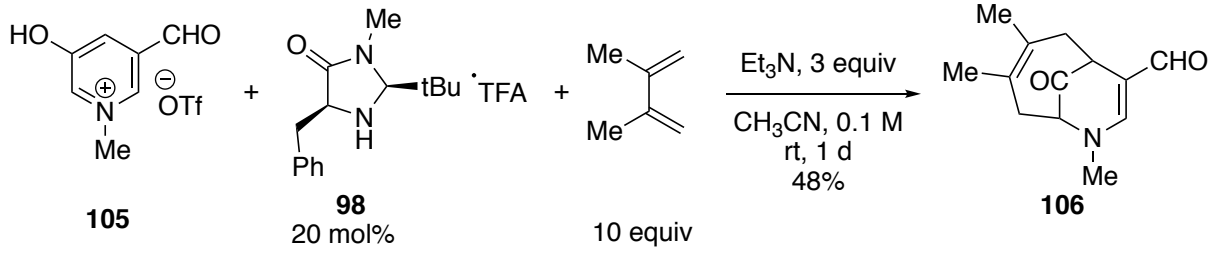

Scheme 17. Chiral amine catalyzed (4+3)-cycloaddition of 3-formyl-5-hydroxy-1-methylpyridin-1-ium.

2.4.5. Exploration of the cation effect on (4+3)-cycloaddition reactions of oxidopyridinium ions

This (4+3)-cycloadditions were considered as the reactions simply between the dienes and the 1-methyl-3-pyridiniumolate **48** generated by deprotonation. However, since the base used in the reaction is not very basic compared with the 1-methyl-3-pyridiniumolate **48**, the

reversibility of deprotonation was another issue. DFT calculations show that the formation of a hydrogen bond to R_3NH^+ raises the barrier of the reaction by 1.8 kcal/mol, but protonation of the oxidopyridinium oxygen lowers the (4+3)-cycloaddition energy barrier by 1.4 kcal/mol. This result suggests that deprotonation of the hydroxyl group by trimethylamine may increase the

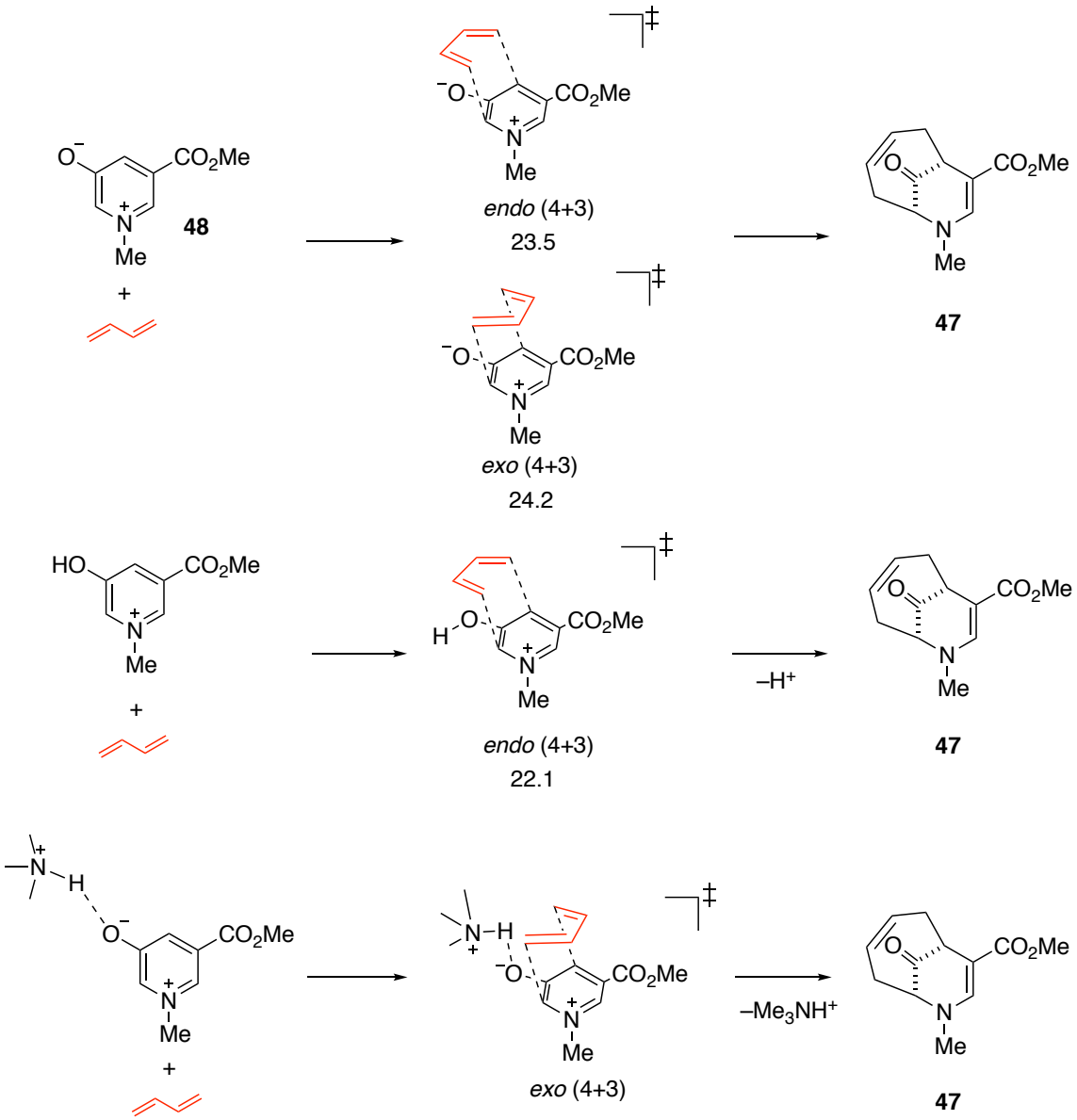

Figure 15. Calculated activation barriers of H^+ and Me_3NH^+ catalyzed (4+3)-cycloadditions of oxidopyridinium ion **48** with 1,3-butadiene. Distances in Å and $\Delta G^{\ddagger}$ in kcal/mol. $\Delta G^{\ddagger}$ and ΔG values (kcal/mol) were computed with M06- 2X/6-311+G(d,p)//M06-2X/6-31G(d) in SMD implicit acetonitrile.

energy demand for the cycloaddition. To verify the hypothesis, a set of reactions were conducted to figure out how well the cycloadditions go with different cations. At different temperatures, pyridinium triflate salt **88** was treated with triethylamine to get the triethylammonium catalyzed yield. The sodium cation catalyzed reactions are conducted by using sodium pyridinium triflate salt generated from pyridinium triflate and sodium hydroxide. The inner salt was also prepared to eliminate the interference from the hydrogen. We tried to make the inner salt by deprotonating the hydroxyl group on the pyridinium ion separately via Amberlyst® A-21 (free base) resin. The X-ray analysis showed that after recrystallization, only half of the molecules were deprotonated. The data in Figure 16 showed that the ammonium-catalyzed reaction gave the highest yield, followed by the sodium catalyzed one. The half-deprotonated mixture gave the lowest yield. The result suggested that the triethylammonium cation might be a better catalyst than the sodium cation. All the yields are from one experiment.

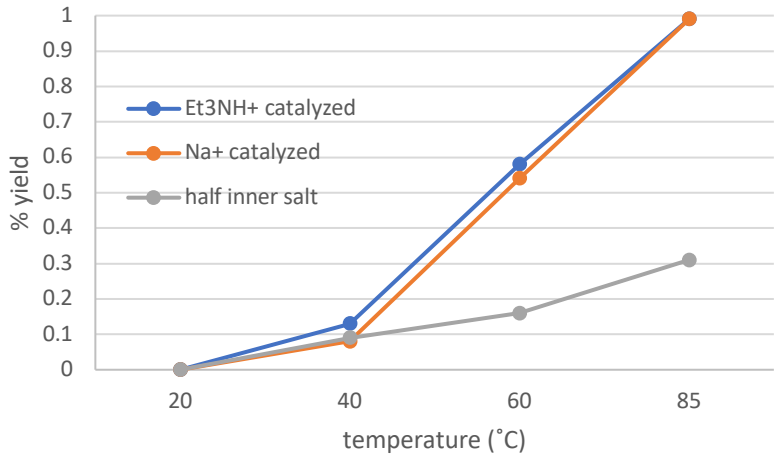

Figure 16. The effect of alkali metal and ammonium catalyst in (4+3)-cycloaddition reaction.

In order to figure out how the alkali cations affect the reactions, the experiments with different benzoate salts was carried out (Figure 17). The yields from PhCOOLi and PhCOOK are average of two experiments and yields from PhCOONa and PhCOOCs are based on one experiment. The result showed that the reaction with less Lewis acidic metals afforded a higher yield of product.

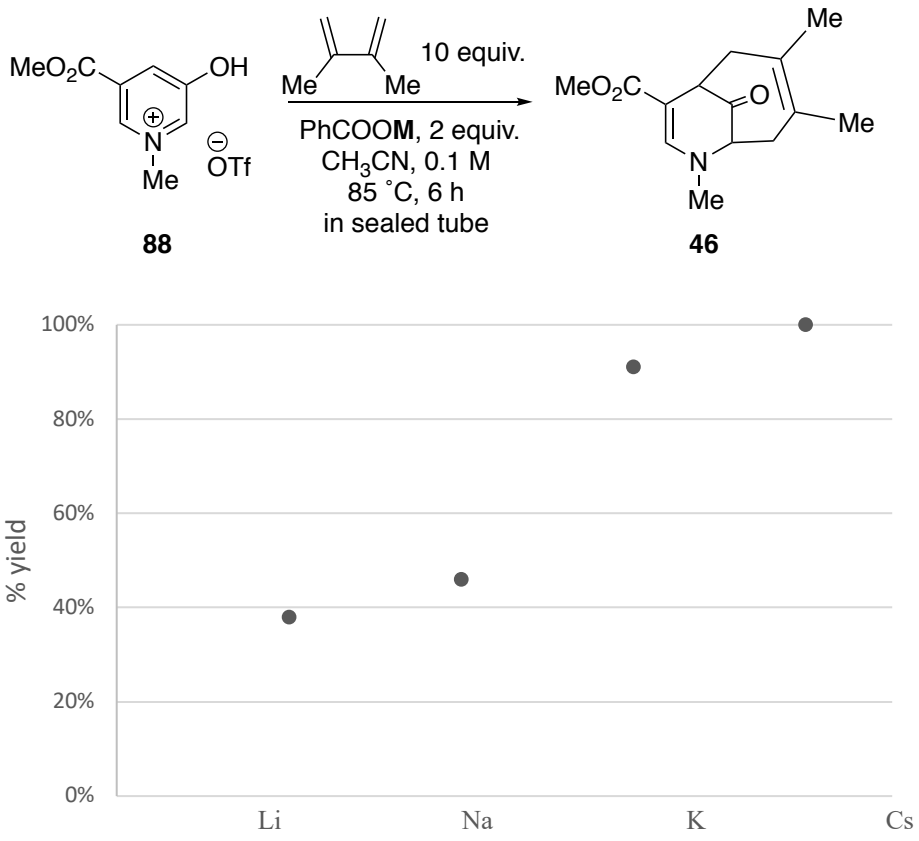

Figure 17. The metal counterion effect in (4+3)-cycloaddition reaction of oxidopyridinium ion.

Since the conjugate acid of the amine base may participate in the cycloaddition as a Lewis acid. With several chiral amines at hand, it was worthwhile to test them in the (4+3)-cycloaddition in order to know if protonated chiral amines could selectively control the approach of the dienes to the oxidopyridinium ions. Chiral amines, (-)-sparteine, (+)-cinchonine, and chiral

imidazolidinone (**98**), were tested both in stoichiometric and catalytic amounts. Analytical high-performance liquid chromatography (HPLC) was conducted to get the enantiomeric ratio of products. The AD column was used as stationary phase (flow 6 mL/min). The mixture of isopropanol and hexane was used as mobile phase (0-5 min, 2.5%; 50-20 min, 3%; 20-30 min, 3.5%, 30-50 min, 4%) to separate the enantiomeric products. Unfortunately, no stereoselectivity was evident in the product when reacted with the bases mentioned. The failures might be caused by the low facial selectivity of the catalyst binding to the substrates. The single hydrogen bond can freely rotate causing no fixed conformation for the diene to attack.

Table 12. Chiral amine catalyzed (4+3)-cycloadditions of oxidopyridinium ion.

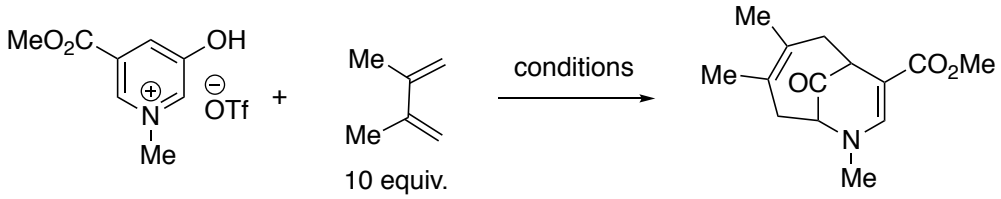

base	adductive	solvent	temperature (˚C)	yield (%)
(-)-sparteine[a]	-	CH_3CN[e]	85	99[g,h]
(-)-sparteine[a]	-	CH_3CN[e]	rt	7[i,h]
(+)-cinchonine[a]	-	CH_3CN/MeOH[f]	rt	27[j,h]
K_2HPO_4[b]	cat.[c]/water[d]	CH_3CN[e]	rt	13[k,h]

a. 3 equiv. b. 5 equiv. c. 5 mol %. d. 4 equiv. e. 0.1 M. f. 2:1, g. 12 h.
h. racemic products. i. 7 d. j. 9 d. k. 6 d.

2.4.6. Supramolecule assistant of (4+3)-cycloaddition of oxidopyridinium ion

Another potential way to introduce facial selectivity to the cycloaddition is to use a chiral supramolecule – cyclodextrin. The hydrophobic cavity of the cyclodextrin cone is ready to

encapsulate the nonpolar reactants while keeping the polar water molecules outside.[52] The reactants in the host could interact with each other without interference from solvent. The hydrophobic effect and van der Waals interaction are the primary factors[53-55] that contribute to the host-guest interaction of a cyclodextrin and the reactants.

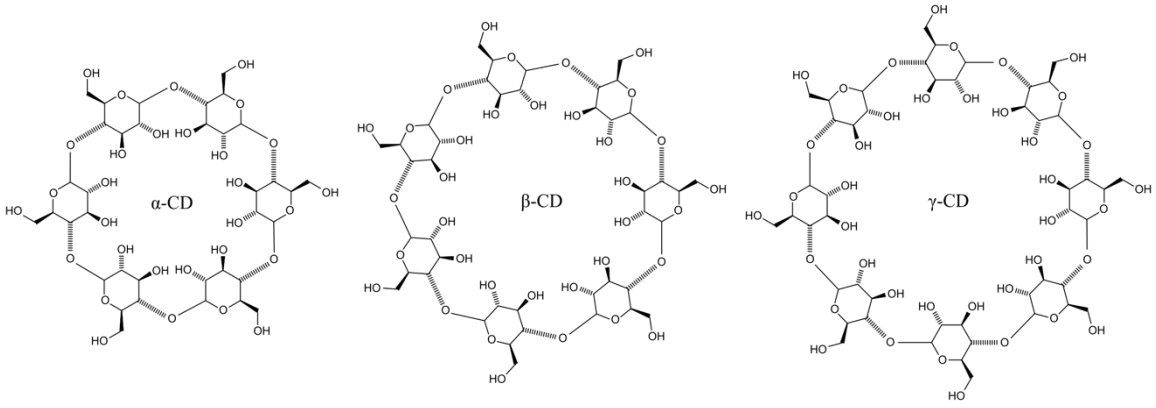

Figure 18. The structures of α-, β-, and γ-cyclodextrins.

Since the supramolecule-catalyzed reactions are usually carried out in aqueous solution,[56] control experiments between oxidopyridinium **88** and 2,3-dimethylbutadiene were run (Table 11). The reaction with the nonpolar base, triethylamine, showed that it was not compatible with the aqueous condition. Alternatively, water-soluble sodium benzoate was then used in this reaction (Table 11, entry 2). Sodium benzoate was allowed when the reaction was conducted in the aqueous solution to give 20% yield. When we switched the solvent from water to brine (Table 11, entry 3), the yield of the bimolecular cycloaddition reaction increased from 20% to 54%. The reaction was worked up by the addition of 10% NaOH aqueous solution and extracted with dichloromethane. The acceleration of the reaction rate with the increasing polarity of the solvent media supported the hydrophobic acceleration of the (4+3)-cycloaddition reactions. The reaction was faster when 20 mol % of the α-cyclodextrin (Table 11, entry 4) was added to the

reaction, but slower with 20 mol % of β-cyclodextrin (Table 11, entry 5). When increasing the loading of the host from 0.2 to 1.1 equivalent (Table 11, entry 5, 7), the yields were almost the same. The results were unexpected because the cavity (4.7 and 5.3 Å[57]) of α-cyclodextrin is too

Table 13. Cyclodextrin catalyzed (4+3)-cycloadditions of oxidopyridinium ion.

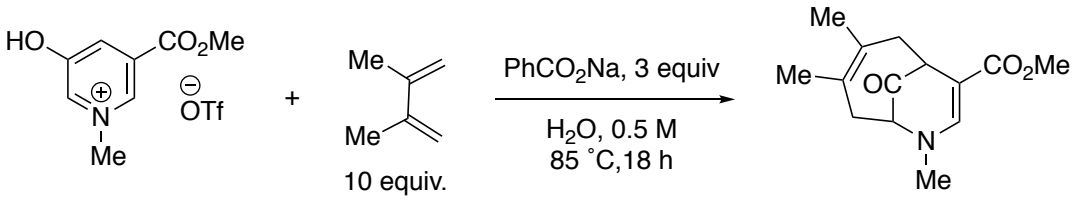

entry	host	equivalent	yield (%)
1	--	--	no reaction[a]
2	--	--	20
3	--	--	54[b]
4	α-cyclodextrin	0.2	39
5	α-cyclodextrin	1.1	35
6	β-cyclodextrin	0.2	15
7	β-cyclodextrin	1.1	4

a. Et_3N as base, 0.1 M. b. brine as solvent.

small to allow the diene and dienophile enter at the same time and probably can't promote the reaction rate through hydrophobic effect.[58] The abnormal increase in yields might suggest that another type of catalysis took place, such as Brønsted acid catalysis from the hydroxyl groups of cyclodextrin. The inhibition by β-cyclodextrin might come from the ineffective extraction.

Dichloromethane is not an ideal molecule for the displacement of the products from the inclusion complex. The solvent molecules that have high association constants with β-cyclodextrin are alcohols like methanol[59]and cyclohexanol.[60]

2.4.7. Intramolecular (4+3)-cycloaddition of oxidopyridinium ions

Another approach to the control of regioselectivity in this cycloaddition reactions is the use of an intramolecular reaction. Our first attempt shows below was quite promising (Scheme 18). Treatment of **102**[61] with the triflate **107**[62] afforded the salt **108.**[63] When salt **108** was treated with TEA in acetonitrile at 85 ˚C, the cycloadducts **109a** and **109b** were obtained in a total yield of 84 % with a ratio of 1:2. If the tether between diene and dienophile could be removed, this process would allow the acquisition of cycloadducts formally derived from an intermolecular cycloaddition but not currently available directly from this reaction. Thus, this process offers a powerful alternative to the intermolecular process.

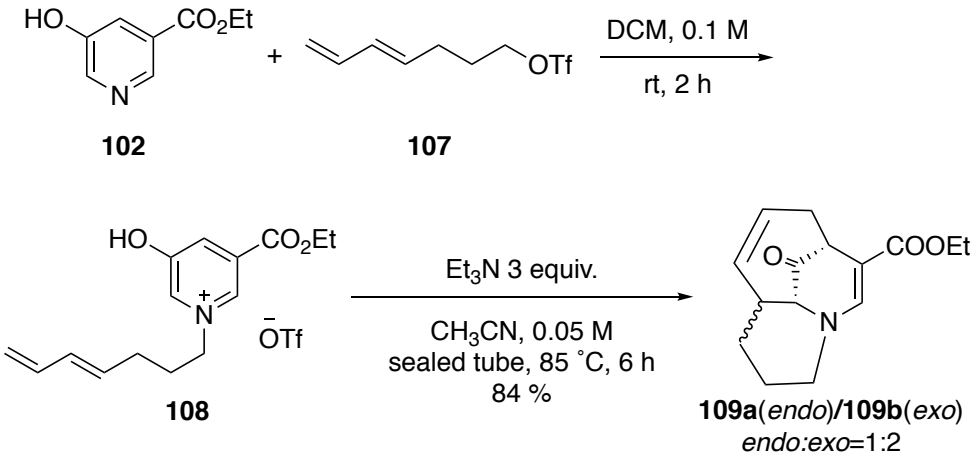

Scheme 18. The intramolecular (4+3)-cycloaddition of an oxidopyridinium ion.

2.4.8. Intramolecular Heck coupling of 7-azabicyclo[4.3.1]decane derivatives

One interesting extension of this reaction is the fast synthesis of a tetracyclic ring system from a (4+3)-cycloadduct via intramolecular cross-coupling. The Pd-mediated-cross coupling of an aryl or vinyl halide or triflate with an alkene is a current topic of interest.[64] The intramolecular Heck reaction provides a powerful and rapid way to add the complexity of a molecule. We wanted to enable Heck coupling by introducing aryl iodide component on the 4π unit. The initial idea was to add an iodide on the *ortho* position of the benzoate on the (4+3)-cycloadduct **81a**/**81b**. The resulting diastereomeric cycloadducts **82a**/**82b** were treated with 10 mol % of a palladium catalyst and 2 equivalents of base. However, an E2' reaction instead of the desired

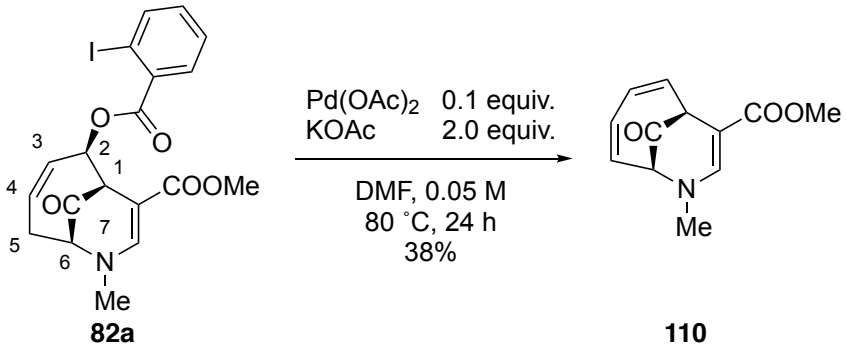

Scheme 19. Elimination reaction under Heck condition.

Heck reaction took place under such reaction conditions. The reason for the failure of this reaction is that the ester tethered intermediate prefers the undesired conformer **111** over the desired conformer **113** by 5–6 kcal/mol, with a rotation barrier of 10–13 kcal/mol, resulting the inefficient cyclization of ester-tethered compounds. Under basic conditions, even if the oxidative addition happened to form the palladium intermediate,[65] the elimination reaction is preferred because the unfavored conformation dominated. To solve the problem, ether linker was introduced to replace the ester. The ether tether has a rotation barrier as low as 3–5 kcal/mol.

Thus, it is would not only prevent the elimination reaction, but also make it easier for the palladium–aryl intermediate to find its olefin partner and complete a cyclization reaction.

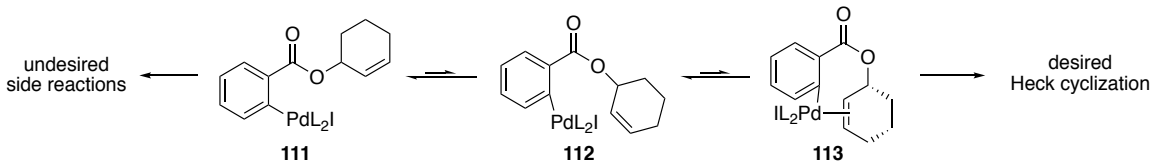

Figure 19. Proposed unproductive intermediate, with favored conformer **113** and unfavored conformers **111** and **112**.

The addition of vinyl magnesium bromide to acrolein (**114**) resulted the divinyl carbinol **115**, which was then converted to chloropentadiene **116** in the presence of concentrated HCl. The reaction of 2-iodophenol **117** with the chloropentadiene **116** gave (*E*)-1-iodo-2-(penta-2,4-dien-1-yloxy)benzene (**118**) in 26% yield for three steps (Scheme 20).[66] Once the iodophenyl group was installed, the (4+3)-cycloaddition was performed to yield diastereometric mixture of

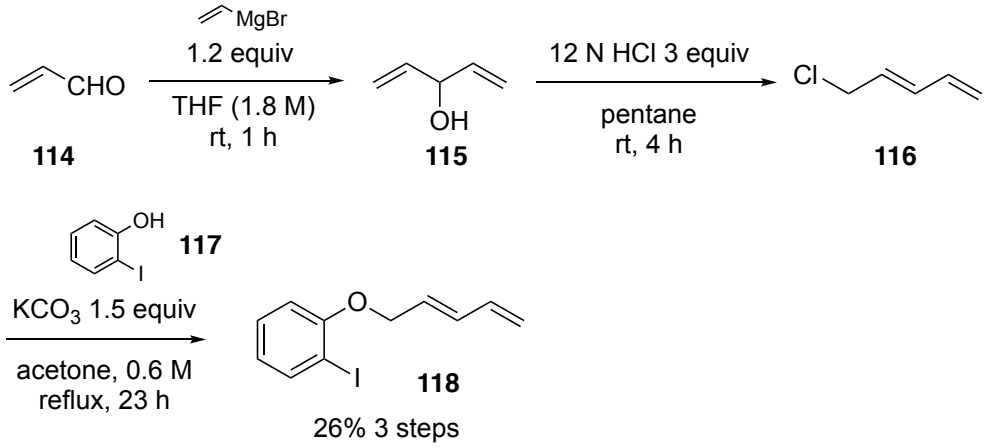

Scheme 20. Synthesis of (*E*)-1-iodo-2-(penta-2,4-dien-1-yloxy)benzene.

cycloadducts **119a/119b**, which were not separable (Scheme 21). Treatment of the mixture with a palladium catalyst successfully gave the coupling products (**120**) from both diastereomeric starting materials.

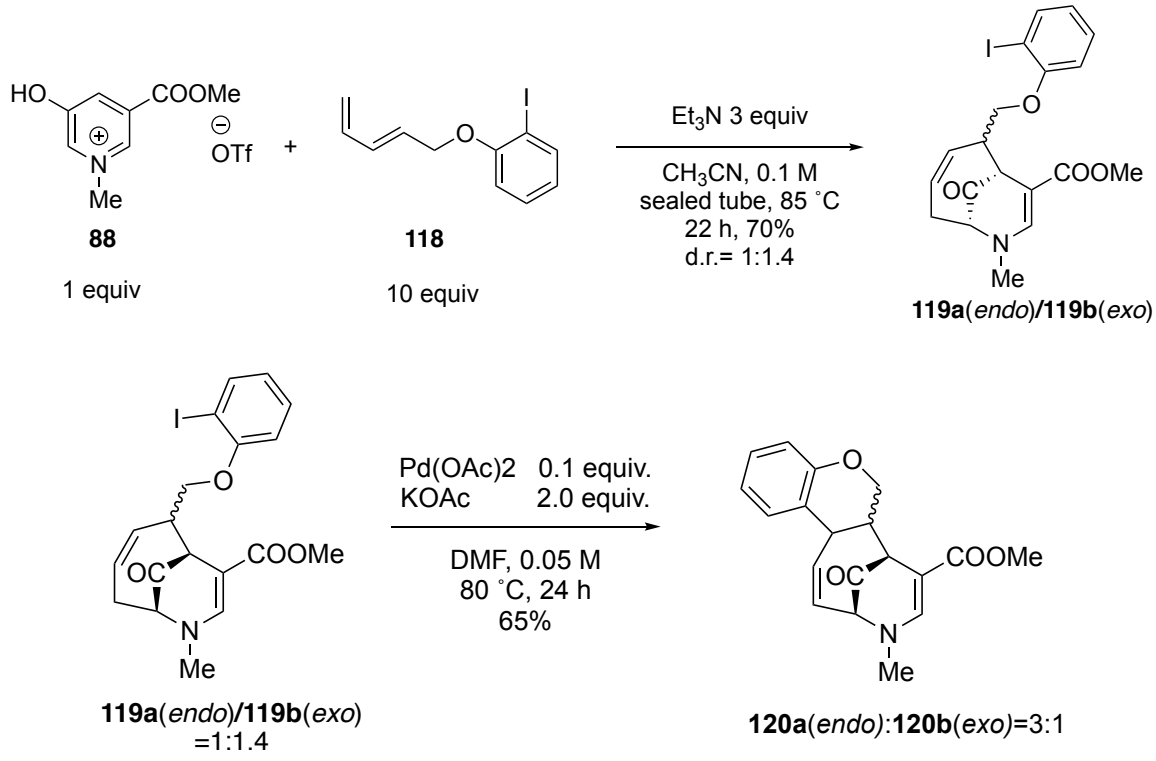

Scheme 21. (4+3)-cycloaddition with iodobenzoate diene **118** and Intramolecular Heck reaction of ether tethered 7-azabicyclo[4.3.1]decane derivatives **120a** and **120b.**

2.5. Conclusions

We showed that *N*-alkyl oxidopyridinium ions substituted with an electron-withdrawing group at the 5-position are competent dienophiles in (4+3) cycloaddition reactions with a variety of dienes. These reactions lead to a rapid increase in molecular complexity to afford cycloadducts that contain the 7-azabicyclo[4.3.1]decane ring skeleton, which is a substructure of a number of bioactive alkaloids. The reactions are often completely regioselective, though

generally not *endo*/*exo* selective. We also described the first example of an intramolecular version of this process, a reaction that may solve certain problems in regiochemical control in the corresponding intermolecular reaction. In the end, we expanded the scope of (4+3)-cycloadditions of oxidopyridinium ions and worked to optimize these processes.

CHAPTER 3

SYNTHESIS OF RIGID TROPANE-LIKE ALKALOID BY PHOTO-MEDIATED [2+2]-CYCLOADDITION REACTION

3.1. Introduction

Tropane alkaloids belong to the world's oldest plant medicines and have a long history in the folk medicine of various ethnic groups. These compounds have a broad range of pharmacological applications including analgesic, anticholinergic, and stimulant (Figure 20).[67] However, due to their strong addictive properties and toxicity[68], many tropane alkaloids isolated from plants are not approved for medicinal application. Modifications on the structure and convenient synthetic access are needed in order to take advantage of the beneficial therapeutic effects of these tropane alkaloids.

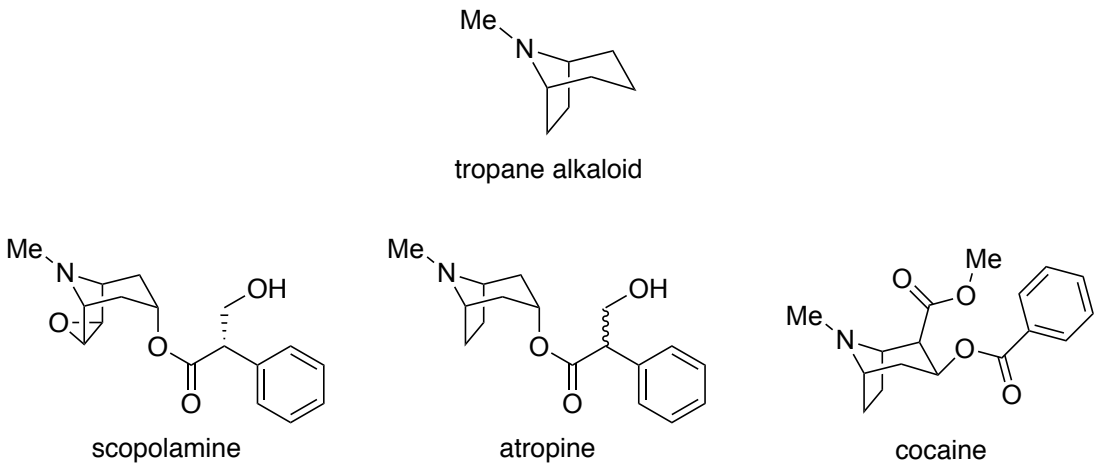

Figure 20. The structure of several important tropane alkaloids.

3.2. Background

Cycloaddition reactions are a highly efficient and straightforward means to obtain carbocyclic organic compounds. The intramolecular [2+2]-cycloaddition reaction is one of the

most frequently used photochemical reactions that provides synthetic approaches to structural systems incorporating cyclobutanes. Although other ways such as reduction of cyclobutene[69] and reductive dehalogenation of 1,4-dihalobutane[70] exist to make cyclobutane ring, the [2+2]-photocyclization is the most robust and frequently used methods to provide these ring system.

In 1964, Eaton and Cole achieved their landmark synthesis of hydrocarbon cubane. In their method, the homocubanone **122**, obtained through intramolecular [2+2]-cycloaddition from Diels-Alder cycloadduct **121**, was the key intermediate in their synthetic route (Scheme 22).[71]

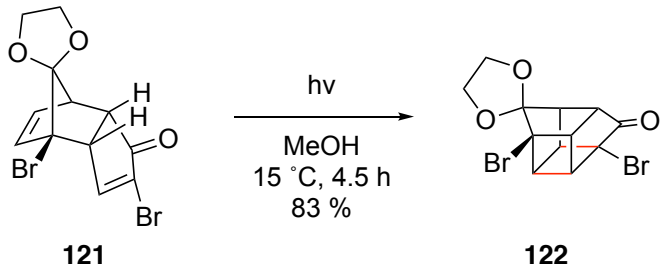

121 **122**

Scheme 22. The synthesis of a homocubanone via intramolecular [2+2]-photocycloaddition reaction from Diels-Alder adduct.

More recently, Riera's group reported the [2+2]-photocycloaddition of Pauson-Khand adducts **123** to make the homocubanone **124** (Scheme 23).[72]

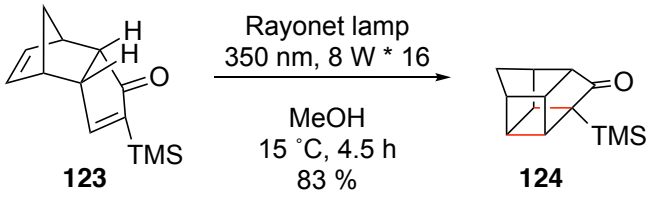

123 **124**

Scheme 23. The synthesis of a homocubanone **124** via intramolecular [2+2]-photocycloaddition reaction from Pauson-Khand adduct.

Winkler and coworkers added to this body of work in 1988. In this work, they achieved the synthesis of azabicyclooctanones **126** via intramolecular [2+2]-photocycloaddition between the olefin and vinylogous amides **125** (Scheme 24).[73-74]

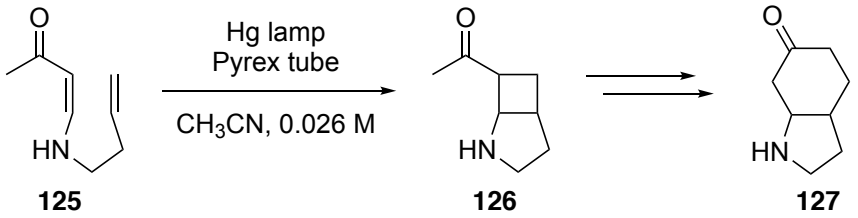

Scheme 24. Intramolecular [2+2]-photocycloaddition between dioxanone and vinylogous amide.

This method of synthesizing nitrogen-containing ring systems was successfully utilized in the total synthesis of the cores several bioactive alkaloids, such as mesembrine[74], vindorosine[75], and manzamine A (Scheme 25).[76]

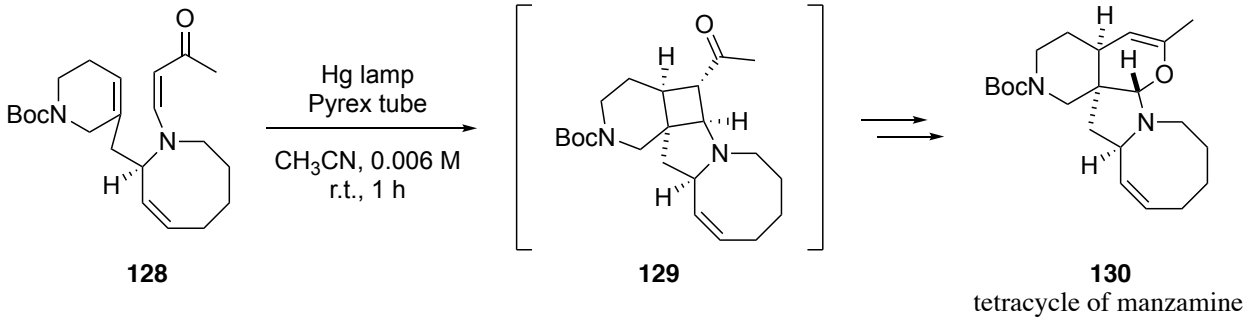

Scheme 25. Synthesis the tetracycle of manzamine via intramolecular [2+2]-cycloaddition. reaction.

3.3. The discovery of a brand-new polycyclic tropane-like alkaloid derivatives

In the context of expanding the chemistry of (4+3)-cycloadducts, we found one interesting conversion via photolysis. When the (4+3)-cycloadduct **46** was irradiated under

mercury-vapor lamp, a new product is observed. The reaction mixture was purified by flash chromatography to obtain the pure product as a colorless oil. The ^{1}H spectrum of the isolated product revealed the disappearance of the downfield vinylic proton previously assigned to the vinylogues carbamate. The two methyl singlet peaks at 1.36 ppm and 1.19 ppm showed that the two vicinal methyl groups were still connected to tertiary carbons. The methyl singlet peak at 3.76 ppm in ^{1}H NMR, along with the peak at 171.1 ppm in ^{13}C NMR indicated the retention of the methyl ester. The data collectively suggested an intramolecular [2+2]-cycloaddition between the alkene on the vinylogue carbamate and the alkene on the cycloheptanone ring might take place under UV irradiation.

In the cycloadduct (Figure 21), H1 forms a doublet due to long-range W-type coupling (1.9 Hz) with the H4. The splitting pattern of H4 can be clarified by homonuclear decoupling experiment (see experimental). The double irradiation at the frequency of H1 caused the H4 to collapse to doublet of triplets, which was caused by H5 for $^{3}J_{cis}$ coupling (11.5 Hz), and long-range W-type coupling (0.9 Hz) with H3. H3 also couples with H8 through $^{3}J_{cis}$ coupling (6.5 Hz). The NOE data (Figure 21) validated our hypothesis of the intramolecular [2+2]-photocycloaddition. Thus, a highly congested, tetracyclic tropane alkaloid derivative, methyl 9-methyl-10-oxo-9-azatetracyclo[4.3.1.03,8.04,7]decane-7-carboxylate, was generated by photolysis.

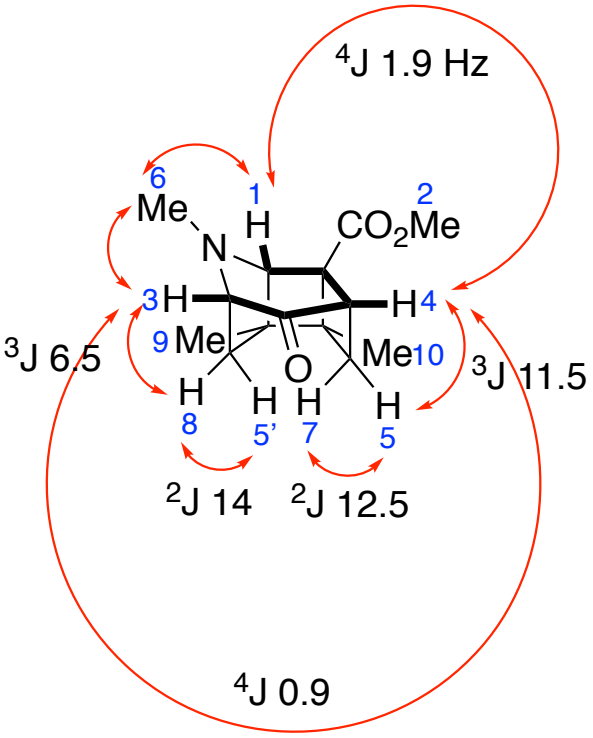

Figure 21. NOE correlations for compound **131**.

3.4. Solvent effects on the [2+2]-photocycloaddition reactions

After getting [2+2]-cycloadduct in the photolysis trial, we set off to optimize the reaction conditions by examining the solvent effects on the reaction rate and the results are summarized in Table 14. Among all the solvents that were screened, chloroform was the only solvent that failed to yield the anticipated product since the starting material decomposed shortly under this reaction conditions. The best conversion that was observed in the model reaction is 96% when using acetonitrile as the solvent. We also observed a decrease of the product yield from 96% to 76% with additional irradiation for just half an hour, suggesting that the [2+2]-cycloadduct did decompose under extended irradiation.

Table 14. Solvent effects.

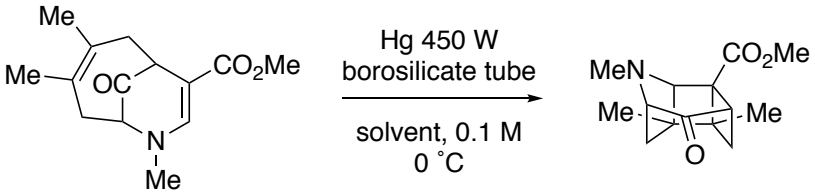

46 **131**

entry	solvents	Yield (%)
1	toluene	90[a]
2	dichloromethane	84[a]
3	chloroform	decomposed[b]
4	ethyl acetate	74[b]
5	methanol	66[b]
6	acetonitrile	79[a]
7	acetonitrile	96[c]
8	acetonitrile	76[d]

a. 2 h. b. 1.5 h. c. 2.5 h. d. 3 h.

3.5. Results

3.5.1. Intramolecular [2+2]-photocyclization of alkyl- and hetero substituted 7-azabicyclo[4.3.1]deca-3,8-dien-10-one

The scope of substrates for intramolecular [2+2]-cycloaddition reaction was studied next. The parent starting material **47** gave the corresponding cycloadduct **132** in 85% yield after 2 h (Figure 22). Starting materials bearing alkyl- and heterosubstitents as R_1 were tested as well. It turned out that both the *endo* and *exo* isomers of starting materials in this category were able to generate products in good yields.

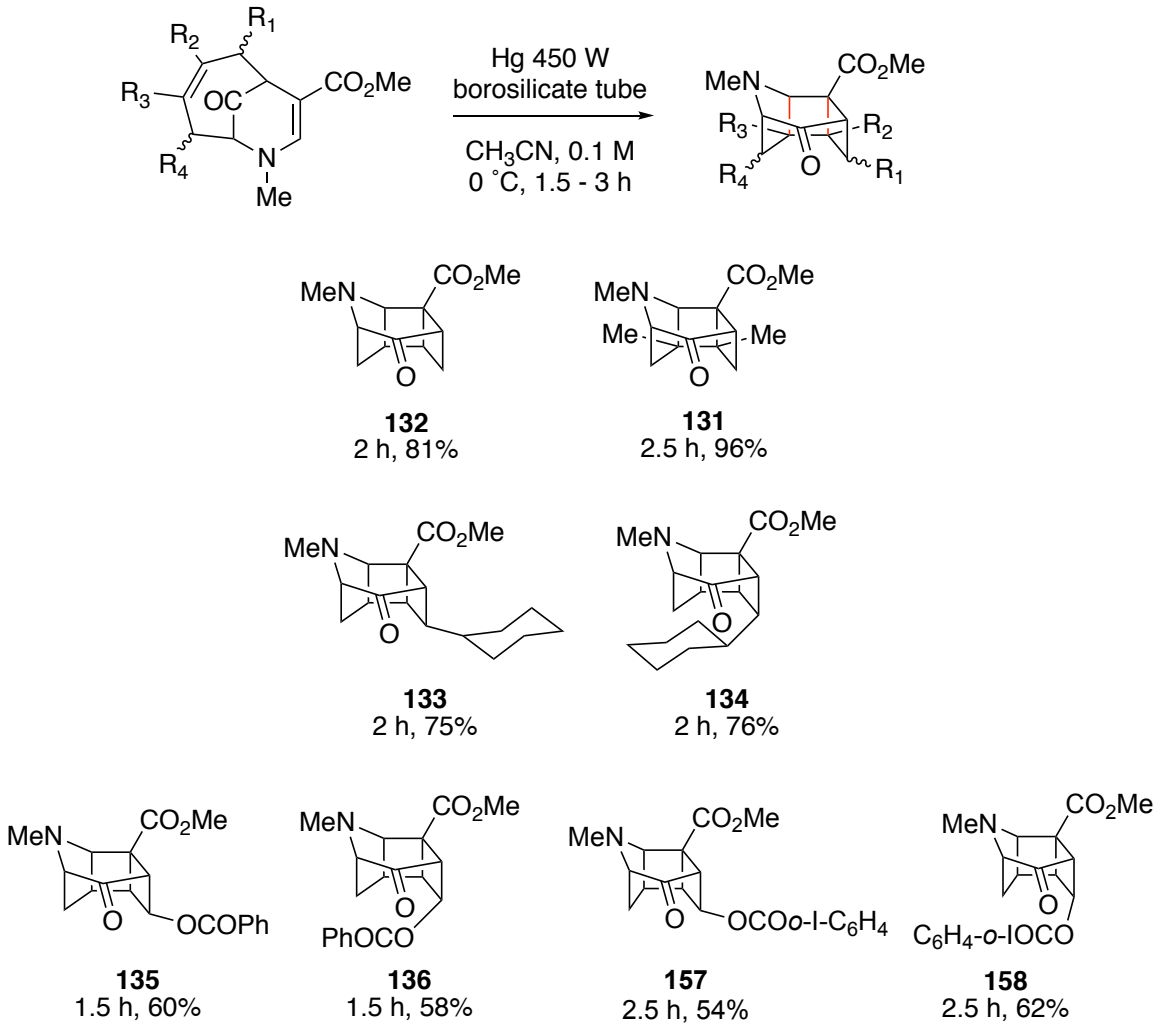

Figure 22. Results of intramolecular [2+2]-photocycloaddition.

3.5.2. Intramolecular [2+2]-photocyclization of ring fused 7-azabicyclo[4.3.1]deca-3,8-dien-10-one

In contrast, starting material with a fused ring moiety on the R_1 and R_2 positions gave different results (Figure 23). The corresponding [2+2]-cycloadducts were observed only from the *exo* isomers of starting materials, while no conversion was observed from the *endo* isomers. A possible reason for this is the large strain caused by the extra fused ring prevents the formation of the highly congested cuban-like compound.

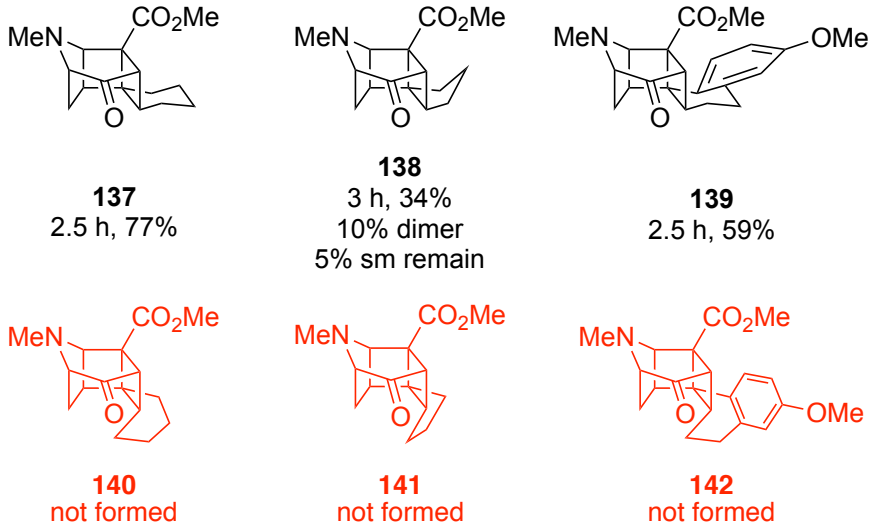

Figure 23. Results of intramolecular [2+2]-photocycloaddition.

3.5.3. Intramolecular [2+2]-photocyclization of aryl-substituted 7-azabicyclo[4.3.1]deca-3,8-dien-10-one

More interestingly, divergent products were observed when the aryl-substituted starting materials were tested. Instead of forming [2+2]-cycloadduct, the irradiation of 1-phenyl substituted starting material **86a** under a mercury lamp led to a rearranged product **143** (Scheme 26). The structure of this rearranged product was confirmed by X-ray diffraction on singlecrystal grown from ethyl acetate/hexane. No product observed in the photolysis of regioisomer **86b**. Similarly, the starting material **87a** bearing thiophene group gave both rearranged product **144** and [2+2]-cycloadduct **145** in 14% (4 h 40 min) and 48% (2 h) yields respectively. The regioisomer **87b** did give [2+2]-cycloadduct **146**, but no rearranged product.

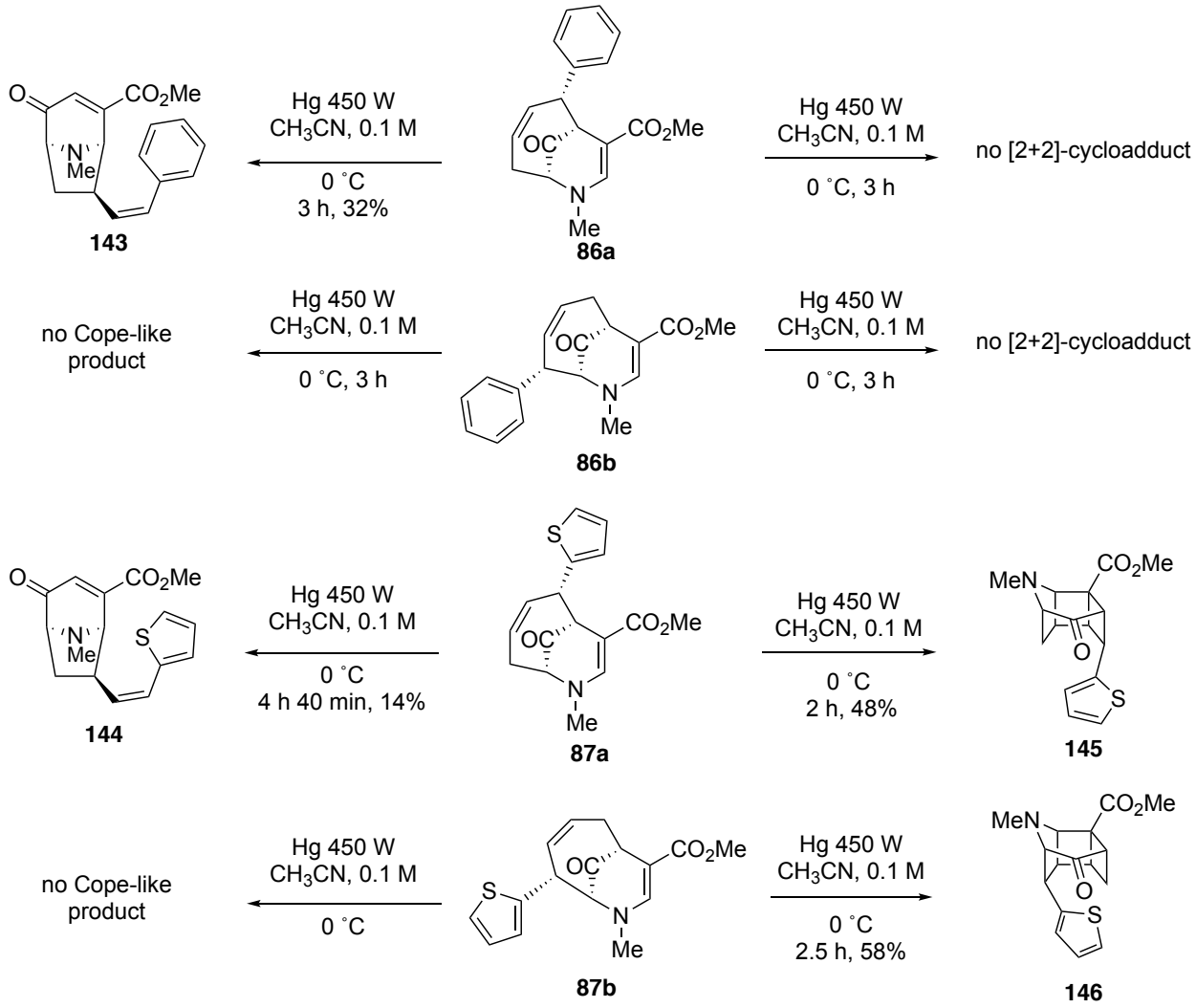

Scheme 26. Divergent products found in photolysis of aryl-substituted diene starting material.

3.5.4. Proposed mechanism

A simple connectivity analysis reveals that the 1,5-diene moiety in the starting material could undergo Cope rearrangement-like conversion to give the rearranged product (Scheme 27).

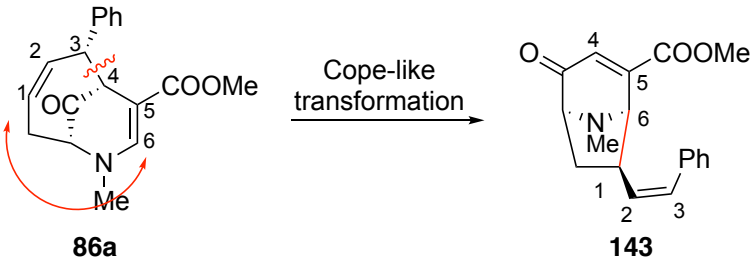

Scheme 27. Connection analysis between **86a** and **143**.

This type of rearrangement was observed upon the irradiation of Pauson–Khand cycloadducts in the work of Riera and coworkers (Scheme 28).[72] They rationalized this transformation by a diradical mechanism. The C-C bond between γ-carbon of the enone and the bridgehead carbon of **147** cleaved into bis-allyl diradicals in intermediate **148**. After bond rotation, a new bond between the carbons on the opposite sides was formed to close the ring.

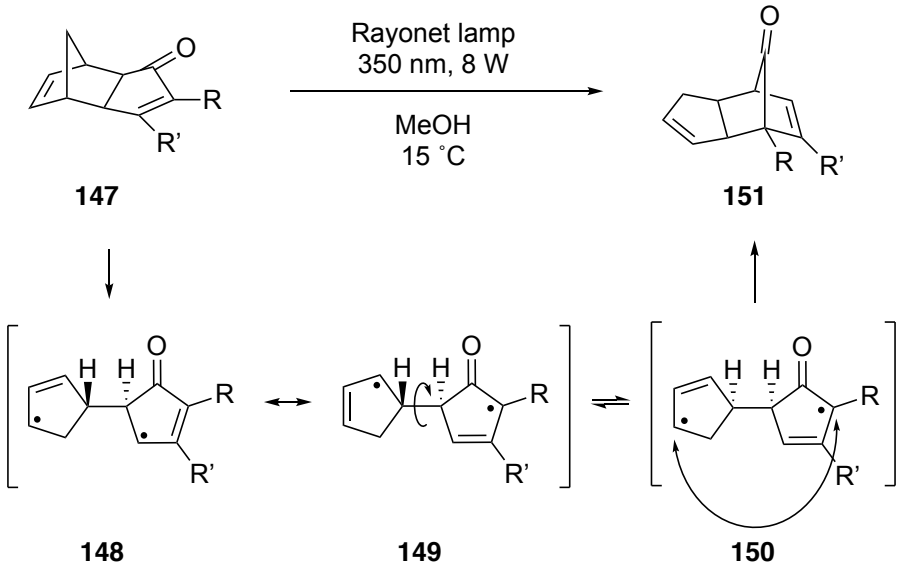

Scheme 28. Proposed diradical mechanism for the formation of **151**.

Enlightened by this, we proposed a mechanism for the observed Cope rearrangement-like product (Scheme 29). The C-C bond between C3 and C4 of **86a** cleaved into bis-allylic radicals.

The aryl group on C3 of **152** could help to stabilize the radical and facilitate the formation of the rearranged product. This could explain why only the regioisomers bearing the aryl group on the same side with the methyl ester yielded the rearrangement products, while the other regio-isomers didn't. At this stage, the single bond rotation between C2 and C4 is also under consideration. The rate of bond rotation competes with the rate of ring closure. The retained

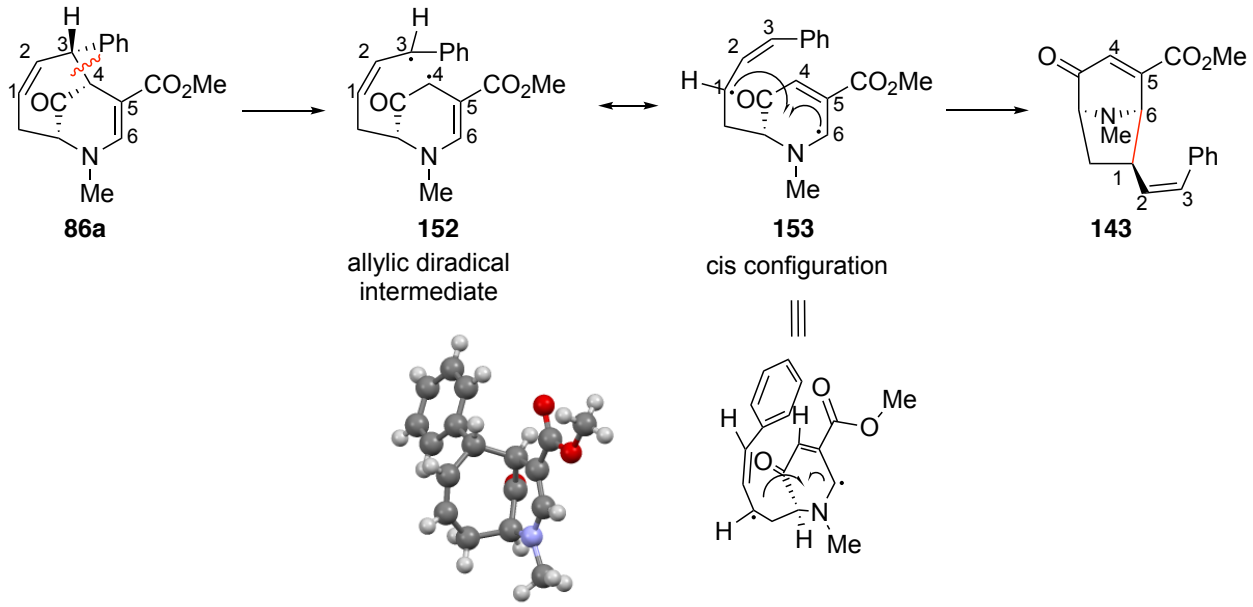

Scheme 29. Proposed mechanism for the forming of compound **143**.

stereochemical configuration of the product indicates that the ring closes before the single bond rotation, giving only Z conformer as the product **143**.

3.6 An application of intramolecular [2+2]-photocycloaddition

With the goal of making bioactive tropane-like alkaloids using this methodology, we decided to synthesize a cocaine analogue via this reaction. Compared with tropane alkaloid, the

parent core of the [2+2]-cycloadduct has two more carbons which makes the structure less flexible by forming two cyclobutane rings (Figure 23).

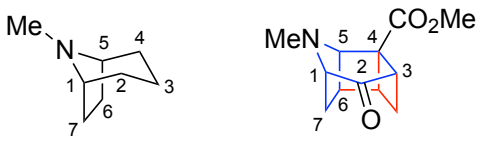

Figure 24. Comparison between tropane core with methyl 9-methyl-10-oxo-9-azatetracyclo[4.3.1.03,8.04,7]decane-7-carboxylate core.

The initial strategy to synthesis a cocaine analogue was to functionalize C3 position with a benzoate ester (compound **154**). The intermediate **155** of this protocol requires the fuctionalization of oxidopyridinium ion **156**. In order to simplify the synthesis and take the advantage of the developed [2+2]-cycloaddition reaction, we decided to move the benzoate substitution to the nearby C8 instead (compound **135**). The C8 functionalized target compound can be obtained from the photolysis of (4+3)-cycloadduct **81**, which was synthesized from the (*E*)-buta-1,3-dien-1-yl benzoate **76** (Figure 24).

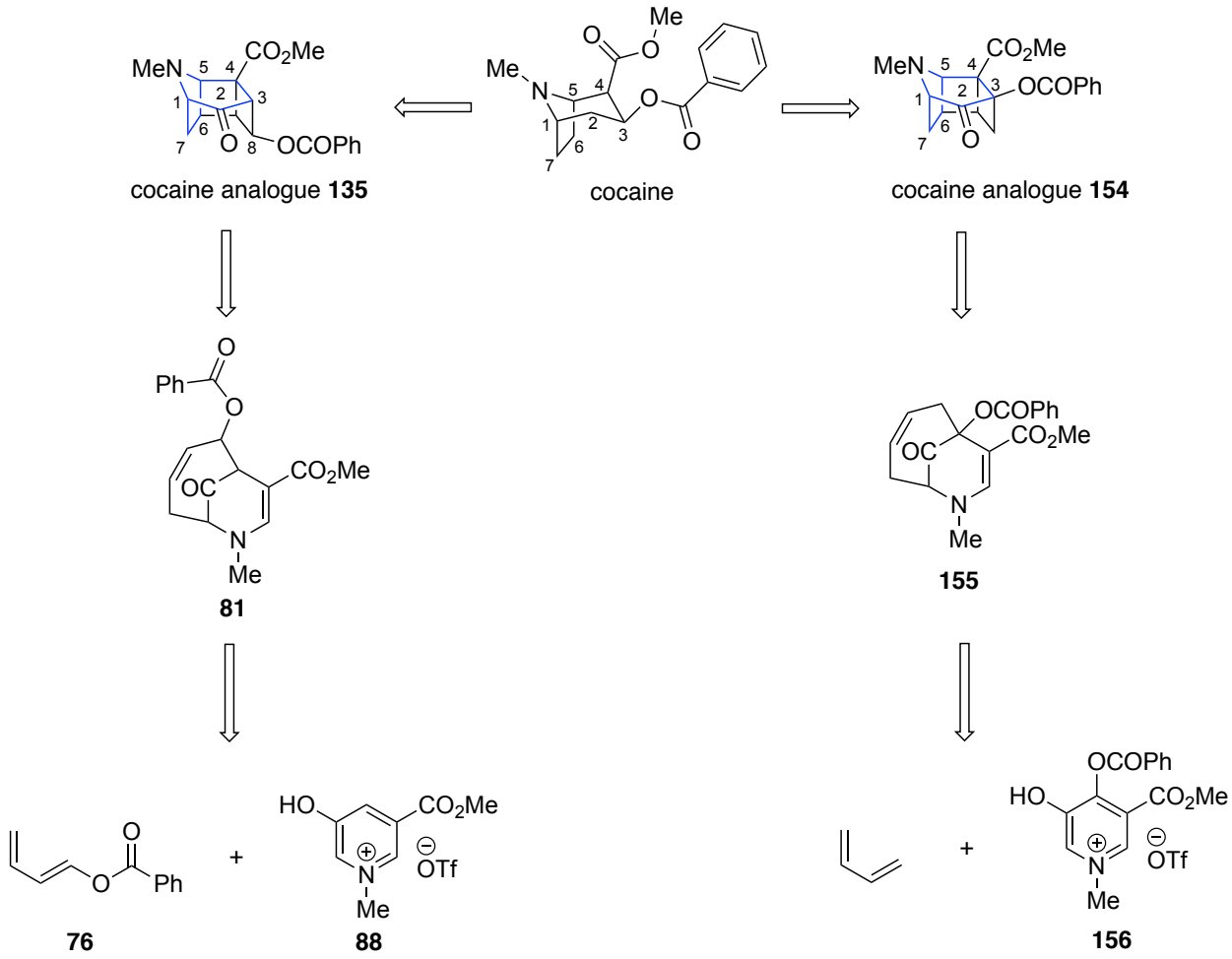

Figure 25. Retro synthetic analysis of cocaine analogues.

The synthesis began with the preparation of (*E*)-buta-1,3-dien-1-yl benzoate **76** via O-alkylation of crotonaldehyde.[77] The oxidopyridinium salt **88** reacted with 10 equivalents of the diene **76** in the presence of triethylamine at 85 ˚C, giving the mixture of diastereomers **81a/81b** with a total yield of 90% after 17 h. The designed *exo* isomer **81b** was isolated and irradiated under mercury lamp, yielding the benzoate tropane-like alkaloid **135**. The overlapping of crystal structures of cocaine (blue) and target compound, a nice overlap was observed despite our analogue **135** has two extra carbons (Scheme 25).

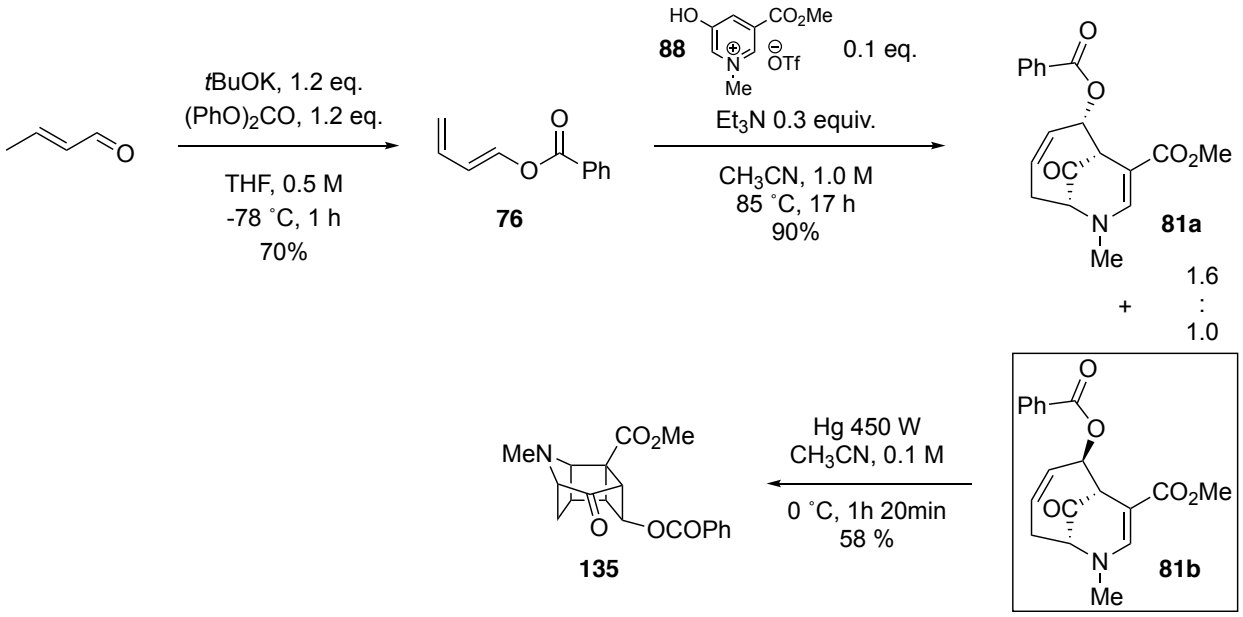

Scheme 30. Synthesis of rigid cocaine analogue.

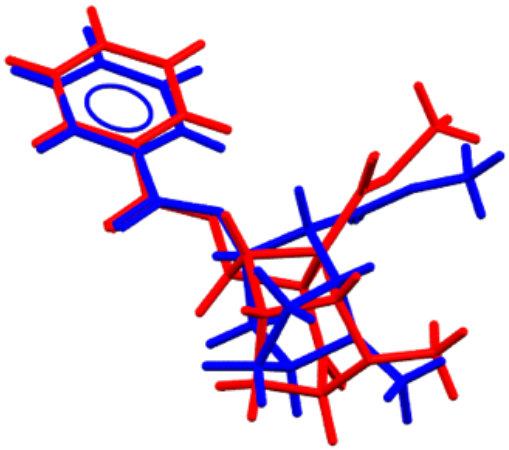

Figure 26. The overlay between crystal structures of cocaine (blue) and its analogue (red).

Compound **135** (red) and its diastereomer **136** (blue) was then evaluated as a probe for the dopamine transporter (DAT) in rat striatum with the help of Prof. Lever (Figure 27). The method used the radioactive dopamine inhibitor -- ^{125}I RTI-121 -- as a competitor to obtain the specific binding number of the tested compounds.[78] The tested concentrations of both

compounds ranges from 3.16 nM to 100,000 nM. The IC_{50} for active (-)-isomer of cocaine should be about 100 nM, while the inctive isomer is about 22,000 nM. Compound **135** has the IC_{50} of 93,440 nM and compound **136** has the IC_{50} of 271,000 nM. Even though the isomer we predicted had higher affinity, both compounds in general have very low interaction with the DAT.

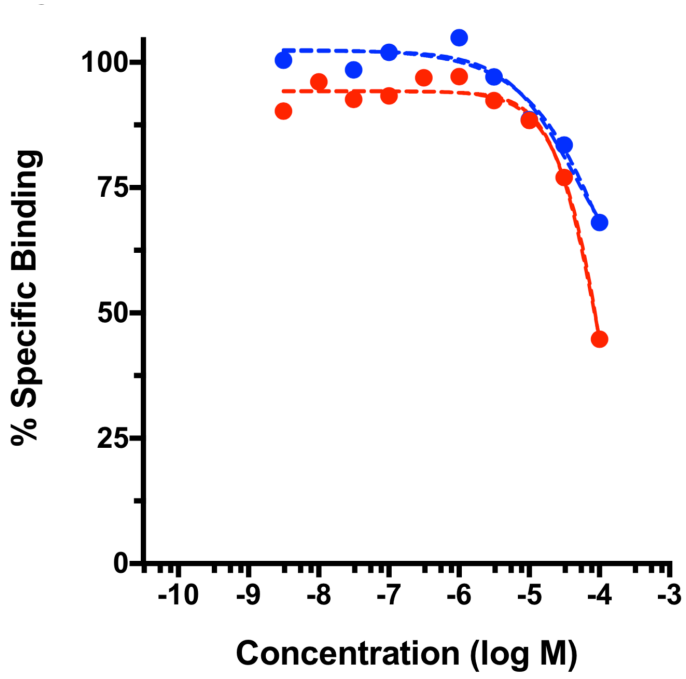

compound	IC_{50} (nM)
cocaine active isomer	100
cocaine inactive isomer	22,000
135	93,440
136	271,000

Figure 27. DAT assay results of compound **135** and **136** vs. ^{125}I RTI-121 in Rat Striatum.

3.7 Conclusions

We developed the intramolecular [2+2]-photocycloaddition reaction of (4+3)-cycloadduct to make a rigid tropane-like alkaloid. Among the photolysis reactions, formal Cope rearrangement products were observed in the photolysis of aryl-substituted starting material. In the end, we utilized the protocol of (4+3)-cycloaddition combined with intramolecular [2+2]-cycloadditions to make rigid tropane-like alkaloids derivatives.

CHAPTER 4

EXPERIMENTAL SECTION

4.1 General information

All reactions were carried out in oven-dried glassware under an argon atmosphere. Tetrahydrofuran was ordered from Sigma Aldrich and was distilled under a nitrogen atmosphere over sodium metal with benzophenone ketyl as an indicator. Dichloromethane was ordered from Sigma Aldrich and was distilled under a nitrogen atmosphere over calcium hydride. Analytical thin layer chromatography was performed on silica gel plates with UV indicator. Flash chromatography was carried out using 230-400 mesh silica gel with HPLC grade solvents. ^{1}H NMR spectra were recorded on either a Bruker DRX-500 (500 MHz) or a DRX-600 (600 MHz) spectrometer with chemical shifts reported in δ ppm with tetramethylsilane as an internal reference (s = singlet, d = doublet, t = triplet, m = multiplet, dd = doublet of doublets, etc). ^{13}C NMR spectra were obtained on the same instruments at 125 and 150 MHz, respectively, in $CDCl_3$ solution with $CDCl_3$ (77.16 ppm) as an internal reference. Melting points were determined with a Fisher-Johns melting point apparatus and are uncorrected. Infrared spectra were recorded on a Perkin Elmer 1600 series FT-IR spectrometer. High-resolution mass spectra were performed by College of Science Major Instrumentation Center, Old Dominion University, on a Bruker 12 Tesla APEX - Qe FTICR-MS with an Apollo II ion source.

4.2. (4+3)-Cycloaddition reactions of N-alkyl oxidopyridinium ions

4.2.1 General preparation procedure of methyl 7-methyl-10-oxo-7-azabicyclo[4.3.1]deca-3,8-diene-9-carboxylates

Methyl trifluoromethanesulfonate (1.72 mL, 15.7 mmol) was added to a suspension of methyl 5-hydroxynicotinate (**45** ; 2.0 g, 13.1 mmol) in dichloromethane (130 ml, 0.1 M), and the mixture was stirred for 3 h at ambient temperature under argon. After completion, the precipitate was filtered off and rinsed with pentane to give a white solid (2.7 g, 94 %). The resulting N-methyl oxidopyridinium salt (100 mg, 0.20 mmol) was dissolved in acetonitrile (2 mL, 0.1m) and treated with excess diene (2.0 mmol, 10 equiv), followed by triethylamine (90 mL, 0.60 mmol, 3 equiv). The reaction mixture was heated at 85 ˚C in a sealed tube for 4–24 h and quenched with 10% HCl solution. The aqueous solution was extracted with dichloromethane (3 * 5 mL), dried over Na_2SO_4, and concentrated under reduced pressure. The crude mixture was purified by column chromatography (5–50% EtOAc/hexanes) to give the product.

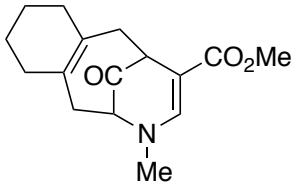

methyl 3-methyl-12-oxo-2,3,6,7,8,9,10,11-octahydro-1*H*-2,6-methanobenzo[*d*]azonine-5-carboxylate (54). Colorless oil (8 h, 17 mg, 90% yield); ^{1}H NMR (600 MHz, $CDCl_3$) δ 7.32 (s, 1H), 3.66 (s, 3H), 3.62 (dd, J = 7.2, 3.0 Hz, 1H), 3.47 (ddd, J = 6.6, 2.4, 1.8 Hz, 1H), 2.96 (s, 3H), 2.52 (ddd, J = 27.6, 15.6, 7.2 Hz, 2H), 2.26 (d, J = 15.6 Hz, 1H), 2.16 (d, J = 14.4 Hz, 1H), 2.09 (d, J = 17.4 Hz, 1H), 2.01-1.97 (m, 2H), 1.75 (d, J = 16.8 Hz, 1H), 1.55-1.53 (m, 1H); ^{13}C NMR (150 MHz, $CDCl_3$) δ 207.0, 167.7, 146.9, 134.1, 127.6, 92.2, 66.3, 50.7, 45.7, 40.4, 37.2,

35.9, 34.1, 34.0, 23.2, 23.0; IR (CH_2Cl_2): ν_{max} 2961, 2926, 2851, 1619, 1264, 908, 727 cm^{-1}; HRMS calcd for $(C_{16}H_{21}NO_3)Na^+$: 298.1414, found: 298.1411.

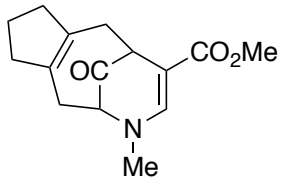

methyl 3-methyl-11-oxo-1,2,3,6,7,8,9,10-octahydro-2,6-methanocyclopenta[*d*]azonine-5-carboxylate (55). Colorless oil (8h, 23 mg, 72% yield); ^1H NMR (600 MHz, $CDCl_3$) δ 7.34 (s, 1H), 3.72 (ddd, J = 7.2, 2.4 Hz, 1H), 3.67 (s, 3H), 3.51 (dt, J = 4.2, 3.0 Hz, 1H), 2.92 (s, 3H), 2.74 (dd, J = 16.2, 4.8 Hz, 1H), 2.68 (dd, J = 16.2, 4.8 Hz, 1H), 2.45-2.37 (m, 3H), 2.28-2.26 (m, 1H), 2.21-2.17 (m, 1H), 1.80-1.68 (m, 3H); ^{13}C NMR (150 MHz, $CDCl_3$) δ 207.3, 167.7, 146.8, 136.7, 130.4, 92.7, 66.5, 50.7, 45.3, 41.3, 40.9, 39.9, 32.5, 30.5, 21.1; IR (CH_2Cl_2): ν_{max} 2950, 2833, 1719, 1678, 1625, 1625 cm^{-1}; HRMS calcd for $(C_{15}H_{19}NO_3)Na^+$: 284.1257, found: 284.1255.

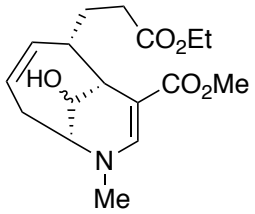

methyl (1R,2S,6S)-2-(3-ethoxy-3-oxopropyl)-10-hydroxy-7-methyl-7-azabicyclo[4.3.1]deca-3,8-diene-9-carboxylate (67a'). 7 h, 45 mg, 38% yield for the **67a**; ^1H NMR (500 MHz, $CDCl_3$): δ 7.28 (s, 1H), 5.57 (ddd, J = 11.0, 7.5, 2.5 Hz, 1H), 5.43 (ddd, J = 11.5, 8.5, 2.5 Hz, 1H), 4.43 (t, J = 5.5 Hz, 1H), 4.13 (q, J = 7.0 Hz, 2H), 3.61 (s, 3H), 3.40 (t, J = 5.0 Hz, 1H), 3.25 (s, 3H), 3.08 (t, J = 2.5 Hz, 1H), 2.94 (s, 3H), 2.84 (dd, J = 16.5, 2.5 Hz, 1H), 2.58 (dddd, J = 10.5, 7.5, 3.0 Hz, 1H), 2.48 q, J = 7.0 Hz, 2H), 2.38 (ddd, J = 13.5, 8.5, 5.0 Hz, 1H), 2.17 (dddd,

J = 15.0, 8.0, 1.0 Hz, 1H), 1.96 (dddd, J = 14.5, 2.5 Hz, 1H), 1.25 (t, J = 7.0 Hz, 3H); ^{13}C NMR (125 MHz, $CDCl_3$): 175.3, 168.1, 147.4, 135.3, 124.2, 95.3, 71.7, 60.5, 58.1, 50.4, 44.2, 40.7, 36.6, 33.6, 29.7, 24.9, 14.2; IR (CH_2Cl_2): ν_{max} 3417, 3055, 2979, 1724, 1672, 1614, 1415, 1264, 1170, 1065, 986 cm^{-1}; HRMS calcd for $(C_{17}H_{25}NO_5)H^+$: 324.1805, found: 324.1804.

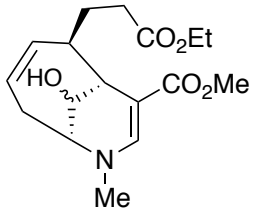

methyl (1R,2R,6S)-2-(3-ethoxy-3-oxopropyl)-10-hydroxy-7-methyl-7-azabicyclo[4.3.1]deca-3,8-diene-9-carboxylate (67b'). 7 h, 35 mg, 49% yield for **67b**; ^{1}H NMR (500 MHz, $CDCl_3$): δ 7.36 (s, 1H), 5.57- 5.52 (m, 1H), 5.26 (ddd, J = 10.0, 3.0 Hz, 1H), 4.24 (t, J = 5.0 Hz, 1H), 4.13 (q, J = 7.5 Hz, 2H), 3.62 (s, 3H), 3.27 (t, J = 6.0 Hz, 1H), 3.07- 3.04 (m, 2H), 2.92 (s, 3H), 2.86 (d, J = 16 Hz, 1H), 2.58- 2.44 (m, 3H), 2.37 (s, 1H), 2.91 (ddd, J = 15.5, 8.5, 6.5 Hz, 1H), 1.67 (dddd, J = 22.0, 14.5, 8.5 Hz, 1H), 1.77 (dddd, J = 21.5, 15.5, 7.5 Hz, 1H), 1.26 (t, J = 7 Hz, 3H); ^{13}C NMR (125 MHz, $CDCl_3$): 174.3, 168.8, 148.8, 139.4, 125.0, 93.0, 69.5, 60.3, 56.8, 50.4, 40.6, 36.8, 35.3, 32.6, 30.0, 22.9, 14.2; IR (CH_2Cl_2): ν_{max} 3434, 3049, 2979, 1724, 1666, 1608, 1433, 1404, 1264, 1176, 1059, 896 cm^{-1}; HRMS calcd for $(C_{17}H_{25}NO_5)H^+$: 324.1805, found: 324.1804.

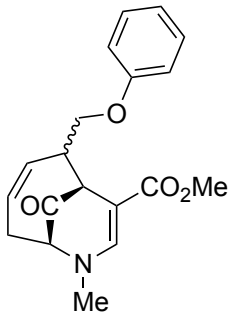

methyl (1*S*,6*S*)-7-methyl-10-oxo-2-(phenoxymethyl)-7-azabicyclo[4.3.1]deca-3,8-diene-9-carboxylate (68a/68b). 30 h, 100 mg, 97% yield; ^{13}C NMR (500 MHz, $CDCl_3$): 205.8, 205.4, 168.2, 167.5, 158.9, 158.7, 148.5, 147.4, 135.6, 132.9, 129.53, 129.47, 126.0, 125.6, 212.0, 120.9, 114.8, 114.6, 93.2, 90.6, 70.3, 68.7, 66.2, 66.0, 50.93, 50.87, 47.8, 47.1, 43.3, 41.4, 39.82, 39.78, 28.8, 27.7; IR (CH_2Cl_2): ν_{max} 3056, 2980, 1726, 1681, 1627, 1416, 1249, 903, 679 cm^{-1}.

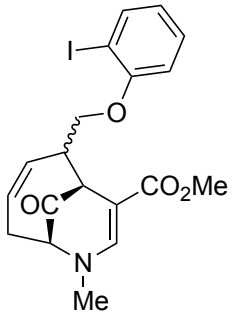

methyl (1S,6S)-2-((2-iodophenoxy)methyl)-7-methyl-10-oxo-7-azabicyclo[4.3.1]deca-3,8-diene-9-carboxylate (69a/69b). Yellow solid (22 h, 100 mg, 70% yield); ^{1}H NMR (500 MHz, $CDCl_3$): δ 7.77 – 7.74 (m, 2H), 7.418 (s, 1H), 7.415 (s, 1H), 7.30 – 7.24 (m, 2H), 6.84 (ddd, J = 8.3, 1.2 Hz, 1H), 6.78 (ddd, J = 8.3, 1.2 Hz, 1H), 6.70 (dddd, J = 13.6, 8.9, 6.0, 1.4 Hz, 2H), 5.97 (ddd, J = 11.7, 7.9, 2.7 Hz, 1H), 5.92 – 5.83 (m, 2H), 5.78 (ddd, J = 11.5, 8.4, 2.4 Hz, 1H), 4.26 (dd, J = 9.2, 6.8 Hz, 1H), 4.06 (t, J = 9.1 Hz, 1H), 3.91 (dd, J = 9.1, 7.6 Hz, 1H), 3.87 (t, J = 3.2 Hz, 1H), 3.84 (s, 1H), 3.77 (dd, J = 9.1, 7.4 Hz, 1H), 3.74 – 3.71 (m, 2H), 3.69 (s, 3H), 3.47 (s, 3H), 3.43 – 3.38 (m, 1H), 2.93 (s, 3H), 2.93 – 2.86 (m, 1H), 2.91 (s, 3H), 2.79 – 2.72 (m, 2H), 2.20 – 2.15 (m, 2H); ^{13}C NMR (500 MHz, $CDCl_3$): 205.6, 205.4, 168.2, 167.6, 157.4, 157.2, 148.7, 147.4, 139.5, 139.4, 135.3, 132.7, 129.6, 129.5, 125.9, 125.5, 122.74, 122.69, 112.32, 112.26, 93.1, 90.4, 86.72, 86.65, 71.5, 69.4, 66.2, 65.9, 51.0, 50.8, 47.6, 46.5, 43.1, 41.2, 39.83, 39.81, 29.8, 28.8, 27.8; IR (CH_2Cl_2) ν_{max} = 3056, 3007, 2993, 1721, 1676, 1622, 1164, 1074, 1016 cm^{-1}; HRMS calcd for $(C_{19}H_{20}INO_4)Na^+$: 476.0329, found: 476.0326.

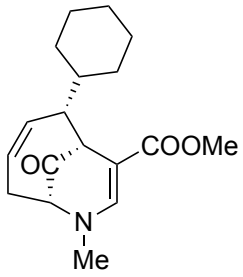

methyl (1*R*,2*S*,6*R*)-2-cyclohexyl-7-methyl-10-oxo-7-azabicyclo[4.3.1]deca-3,8-diene-9-carboxylate (70a). 22 h, 20 mg, 23% yield; ^{1}H NMR (500 MHz, $CDCl_3$): δ 7.35 (s, 1H), 5.86 (ddd, J = 15,0, 8.3, 2.8 Hz, 1H), 5.66 (dddd, J = 15.3, 8.5, 3.2, 0.6 Hz, 1H), 3.78 (t, J = 3.4 Hz, 1H), 3.66 (s, 3H), 3.62 (ddd, J = 4.9, 2.0 Hz, 1H), 2.91 (s, 3H), 2.68 (ddd, J = 16.4, 8.6, 5.8 Hz, 1H), 2.58 (ddd, J = 10.1, 8.5, 4.2 Hz, 1H), 2.23 (d, J = 12.7 Hz, 1H), 2.10 (dq, J = 16.3, 3,0 Hz, 1H), 1.75 – 1.72 (m, 2H), 1.66 – 1.60 (m, 2H), 1.33 -1.12 (m, 4H), 1.10 – 0.94 (m, 2H); ^{13}C NMR (500 MHz, $CDCl_3$): 206.3, 167.7, 147.4, 137.5, 123.0, 94.2, 66.2, 50.8, 47.7, 46.3, 40.1, 39.7, 32.2, 31.4, 27.1, 26.6, 26.4, 26.0; IR (CH_2Cl_2): ν_{max} 3035, 2965, 1694, 1648, 1617, 1263, 945, 899, 740 cm^{-1}; HRMS calcd for $(C_{18}H_{25}NO_3)Na^+$: 326.1727, found: 326.1727.

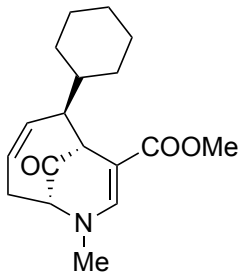

methyl (1*R*,2*R*,6*R*)-2-cyclohexyl-7-methyl-10-oxo-7-azabicyclo[4.3.1]deca-3,8-diene-9-carboxylate (70b). 22 h, 19 mg, 38% yield; ^{1}H NMR (500 MHz, $CDCl_3$): δ 7.38 (s, 1H), 5.84 (dddd, J = 10.7, 6.8, 4.6, 1.9 Hz, 1H), 5.75 (ddd, J = 11.1, 5.1, 2.5 Hz, 1H), 3.86 (d, J = 2.3 Hz, 1H), 3.66 (s, 3H), 3.65 (d, J = 2.3 Hz, 1H), 2.90 (s, 3H), 2.82 (dddd, J = 15.1, 8.4, 6.8, 0.9 Hz, 1H), 2.48 (dsextet, J = 12.6, 2.6 Hz, 1H), 2.10 (d, J = 15.5 Hz, 1H), 1.87 – 1.83 (m, 2H), 1.77 –

1.64 (m, 4H), 1.52 (qt, J = 10.8, 3.2 Hz, 1H), 1.36 -1.14 (m, 4H), 1.00 (dddd, J = 23.3, 14.2, 12.4, 3.5 Hz, 1H), 0.79 (dddd, J = 24.0, 14.4, 12.5, 3.2, Hz, 1H); ^{13}C NMR (500 MHz, $CDCl_3$): δ 207.2, 168.3, 148.5, 139.6, 124.3, 91.8, 66.6, 50.8, 50.1, 47.4, 39.8, 39.7, 32.6, 31.6, 28.1, 26.7, 26.6, 26.4; IR (CH_2Cl_2): ν_{max} 3065, 2961, 1708, 1649, 1627, 1273, 1169, 966, 944, 751 cm^{-1}; HRMS calcd for $(C_{18}H_{25}NO_3)Na^+$: 326.1727, found: 326.1727.

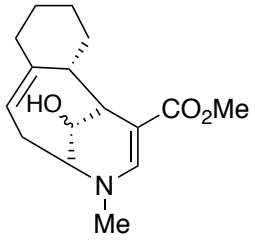

methyl (1*S*,5*R*,11a*S*)-4-methyl-12-oxo-4,5,6,8,9,10,11,11a-octahydro-1*H*-1,5-methanobenzo[*e*]azonine-2-carboxylate (71a'). Colorless solid, mp = 165-166℃ (20 h, 136 mg, 37% for **71a**); ^{1}H NMR (500 MHz, $CDCl_3$) δ 7.31 (s, 1H), 5.13 (d, J = 6.0 Hz, 1H), 4.39 (q, J = 5.5 Hz, 1H), 3.65 (s, 3H), 3.44 (d, J = 2.5 Hz, 1H), 2.98 (t, J = 2.0 Hz, 1H), 2.97 (s, 3H), 2.64 (ddddd, J = 8.0, 2.0 Hz, 1H), 2.46 (d, J = 13.5 Hz, 2H), 2.42 (ddd, J = 18.0, 7.0, 3.0 Hz, 1H), 2.10 (d, J = 12.0 Hz, 1H), 2.01-1.97 (m, 1H), 1.93 (t, J = 13.0 Hz, 3H), 1.80 (d, J = 12.0 Hz, 1H), 1.74 (dd, J = 22.5, 5.5 Hz, 1H)); ^{13}C NMR (125 MHz, $CDCl_3$) δ 168.4, 146.1, 145.2, 114.5, 95.7, 71.4, 59.0, 50.4, 48.9, 42.3, 41.0, 40.8, 38.6, 30.6, 28.6, 26.2; IR (CH_2Cl_2): ν_{max} 3423, 3048, 2984, 2862, 1425, 1257, 912, 891 cm^{-1}; HRMS calcd for $(C_{16}H_{23}NO_3)Na^+$: 300.1570 , found: 300.1569.

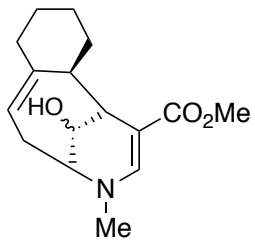

methyl (1*S*,5*S*,11a*R*)-4-methyl-12-oxo-4,5,6,8,9,10,11,11a-octahydro-1*H*-1,5-methanobenzo[*e*]azonine-2-carboxylate (71b'). Colorless solid, mp = 186-189℃ (20 h, 229 mg, 62% yield for **71b**) ^{1}H NMR (500 MHz, $CDCl_3$) δ 7.35 (s, 1H), 5.24 (ddd, J = 6.5, 4.5, 2.0 Hz, 1H), 4.18 (t, J = 5.0 Hz, 1H), 3.64 (s, 3H), 3.22 (t, J = 5.5 Hz, 1H), 3.10 (dd, J=12.0, 5.5 Hz, 1H), 2.91 (dt, J = 16.0, 3.5, 1H), 2.87 (s, 3H), 2.29 (s, 1H), 2.21 (ddd, J = 15.0, 8.0, 6.0 Hz, 1H), 1.95-1.80 (m, 3H), 1.69-1.57 (m, 2H), 1.49-1.35 (m, 2H), 1.30 - 1.22 (m, 1H); ^{13}C NMR (125 MHz, $CDCl_3$) δ 169.2, 148.4, 148.3, 116.3, 93.0, 70.0, 56.9, 50.4, 40.5, 39.2, 37.8, 31.0, 27.4, 22.9, 21.2, 21.1; IR (CH_2Cl_2): ν_{max} 3387, 2932, 2902, 2859, 1653, 1602, 1433, 1334, 1175, 1059 cm^{-1}; HRMS calcd for $(C_{16}H_{23}NO_3)Na^+$: 300.1570, found: 300.1569.

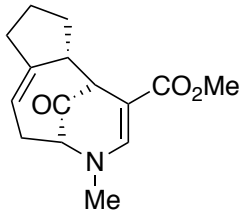

methyl (1*S*,5*R*,10a*S*)-4-methyl-11-oxo-1,4,5,6,8,9,10,10a-octahydro-1,5-methanocyclopenta[*e*]azonine-2-carboxylate (72a). Colorless oil (22 h, 79 mg, 26% yield); ^{1}H NMR (600 MHz, $CDCl_3$) δ 7.31 (s, 1H), 5.59 (dddd, J = 10.2, 2.4 Hz, 1H), 3.72 (s, 3H), 3.45 (td, J = 8.4, 2.4, 0.6 Hz, 1H), 3.15 (t, J = 2.4 Hz, 1H), 2.99 (s, 3H), 2.76 (ddd, J = 13.2, 7.8 Hz, 1H), 2.53 (t, J = 7.8 Hz, 1H), 2.35 (ddd, J =12.6, 5.4 Hz, 1H), 2.29-2.26 (m, 2H), 2.23-2.18 (m, 1H), 1.83-1.78 (m, 1H), 1.76-1.70 (m, 1H), 1.55-1.48 (m, 1H); ^{13}C NMR (150 MHz, $CDCl_3$) δ 204.8, 167.4, 153.0, 144.0, 114.9, 98.3, 66.7, 51.2, 50.9, 48.7, 40.7, 37.1, 34.1, 28.9, 25.3; IR (CH_2Cl_2): νmax 3052, 2958, 2925, 2852, 1728, 1683, 1610, 1438 cm^{-1}; HRMS calcd for $(C_{15}H_{19}NO_3)Na^+$: 284.1257, found: 284.1258.

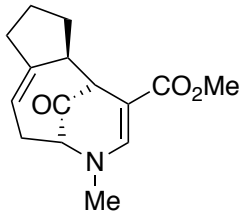

methyl (1*S*,5*R*,10a*R*)-4-methyl-11-oxo-1,4,5,6,8,9,10,10a-octahydro-1,5-methanocyclopenta[*e*]azonine-2-carboxylate (72b). Colorless solid, mp = 104- 108 ˚C (22 h, 122 mg, 40% yield); ^{1}H NMR (600 MHz, $CDCl_3$) δ 7.41 (s, 1H), 5.55 (dd, J = 5.4, 2.4 Hz, 1H), 3.65 (s, 3H), 3.63 (dd, J = 3.0 Hz, 1H), 2.85 (s, 3H), 2.79 (ddd, J = 16.2, 9.0, 6.6 Hz, 1H), , 2.40 (dddd, J = 7.8, 2.4 Hz, 1H), 2.34-2.30 (m, 1H), 2.25-2.16 (m, 1H), 2.02-1.97 (m, 1H), 1.90-1.84 (m, 1H), 1.64-1.59 (m, 1H), 1.47-1.39 (m, 1H); ^{13}C NMR (150 MHz, $CDCl_3$) δ 206.7, 168.6, 151.3, 148.0, 113.1, 90.8, 66.2, 50.7, 49.0, 47.3, 39.5, 36.6, 32.1, 30.4, 25.6; IR (CH_2Cl_2): ν_{max} 3052, 2958, 2925, 2852, 1728, 1683, 1610, 1438 cm^{-1}; HRMS calcd for $(C_{15}H_{19}NO_3)Na^+$: 284.1257, found: 284.1258.

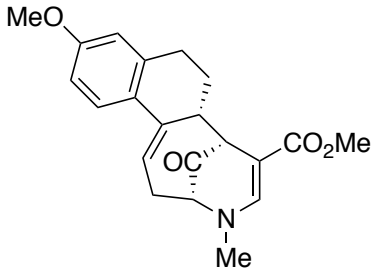

methyl (3*R*,7*R*,7a*R*)-11-methoxy-4-methyl-14-oxo-3,4,7,7a,8,9-hexahydro-2*H*-3,7-methanonaphtho[1,2-*e*]azonine-6-carboxylate (73a). 14 h, 43 mg, 34% yield; ^{1}H NMR (600 MHz, $CDCl_3$): δ 7.40 (s, 1H), 7.37 (d, J = 8.4 Hz, 1H), 6.69 (dd, J = 9.0, 3.0 Hz, 1H), 6.63 (d, J = 2.4 Hz, 1H), 6.11 (ddd, J = 8.4, 7.2, 2.4 Hz, 1H), 3.78 (s, 3H), 3.71 (s, 3H), 3.60 (ddd, J = 10.8, 6.6, 3.4 Hz, 1H), 2.30 (ddd, J = 14.4, 8.4 Hz, 1H), 2.87 – 2.83 (m, 2H), 2.57 (ddd, J = 15.6, 7.8, 3.6 Hz, 1H), 2.45 (ddd, J = 13.2, 6.0 Hz, 1H); ^{13}C NMR (150 MHz, $CDCl_3$): δ 206.9, 167.6,

158.9, 145.0, 142.0, 139.8, 128.0, 125.2, 117.4, 112.7, 112.6, 96.7, 65.8, 55.2, 50.9, 50.6, 44.5, 40.6, 29.5, 28.8, 28.1; IR ($CDCl_3$): ν_{max} 3049, 2921, 2845, 1730, 1684, 1608, 1491, 1433, 1258 cm^{-1}; HRMS calcd for $(C_{21}H_{23}NO_4)Na^+$: 376.1519, found: 376.1516.

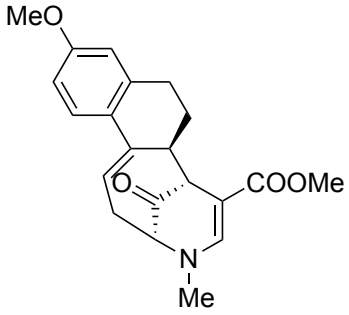

methyl (3S,7R,7aS)-11-methoxy-4-methyl-14-oxo-3,4,7,7a,8,9-hexahydro-2H-3,7-methanonaphtho[1,2-e]azonine-6-carboxylate (73b). 14 h, 72 mg, 59% yield; ^1H NMR (600 MHz, $CDCl_3$): δ 7.34 (s, 1H), 7.29 (d, J = 8.6 Hz, 1H), 6.70 (dd, J = 8.5, 2.5 Hz, 1H), 6.60 (d, J = 2.2 Hz, 1H), 6.07 (ddd, J = 8.7, 4.1, 2.3 Hz, 1H), 3.67 – 3.66 (m, 2H), 3.51 (s, 3H), 3.03 (ddd, J = 15.8, 8.2, 7.0 Hz, 1H), 2.92 (s, 3H), 2.65 (dd, J = 11.5, 6.0 Hz, 1H), 2.61 (dt, J = 14.8, 3.4 Hz, 1H), 2.43 (td, J = 14.6, 2.7 Hz, 1H), 2.25 (dd, J = 16.0, 4.3 Hz, 1H), 2.16 (dddd, J = 12.8, 6.2, 3.2 Hz, 1H), 1.88 (qd, J = 13.3, 3.0 Hz, 1H); ^{13}C NMR (150 MHz, $CDCl_3$): δ 205.9, 168.0, 158.8, 148.0, 143.3, 140.7, 130.4, 126.1, 118.0, 112.5, 112.1, 91.1, 65.4, 55.2, 51.3, 50.6, 44.7, 39.6, 30.2, 29.4, 29.2; IR (CH_2Cl_2): ν_{max} 3052, 2993, 2953, 1721, 1685, 1613, 1425, 903, 741, 710 cm^{-1}; HRMS calcd for for $(C_{19}H_{19}NO_5)Na^+$: 364.1155, found: 364.1155.

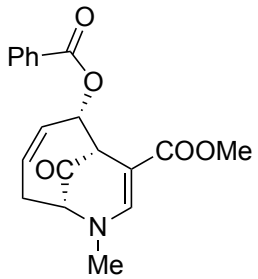

methyl (1*S*,2*S*,6*R*)-2-(benzoyloxy)-7-methyl-10-oxo-7-azabicyclo[4.3.1]deca-3,8-diene-9-carboxylate (81a). Colorless solid, mp = 117- 178 ˚C (17 h, 135 mg, 35% yield); ^{1}H NMR (500 MHz, $CDCl_3$): δ 7.98 (dd, J = 8.4, 1.3 Hz, 2H), 7.54 (tt, J= 7.4, 1.3 Hz, 1H), 7.43 (s, 1H), 7.42 (dd, J = 8.0, 7.4 Hz, 2H), 6.22 (ddd, J =11.8, 7.4, 3.0 Hz, 1H), 5.98 (ddd, J = 11.9, 8.7, 3.4 Hz, 1H), 5.71 (dd, J = 7.2, 5.9 Hz, 1H), 3.77 – 3.76 (m, 1H), 3.71 (s, 3H), 2.99 (s, 3H), 2.81 (ddd, J = 16.4, 8.7, 6.1 Hz, 1H), 2.39 (dddd, J = 16.4, 4.8, 3.2 Hz, 1H); ^{13}C NMR (125 MHz, $CDCl_3$): 202.6, 167.3, 165.4, 148.8, 133.2, 132.0, 130.0, 129.9, 129.8, 128.6, 89.9, 67.5, 66.7, 51.2, 49.2, 40.0, 27.2; IR (CH_2Cl_2): ν_{max} 3065, 2953, 1726, 1685, 1631, 1267, 1168, 742, 778 cm^{-1}; HRMS calcd for $(C_{19}H_{19}NO_5)Na^+$: 364.1155, found: 364.1153.

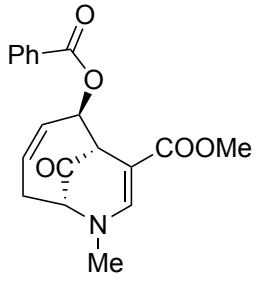

methyl (1*S*,2*R*,6*R*)-2-(benzoyloxy)-7-methyl-10-oxo-7-azabicyclo[4.3.1]deca-3,8-diene-9-carboxylate (81b). Yellow solid, mp = 135- 136 ˚C (17 h, 194 mg, 55% yield); ^{1}H NMR (500 MHz, $CDCl_3$): δ 8.07 (dd, J = 8.3, 1.2 Hz, 2H), 7.56 (tt, J= 7.4, 1.3 Hz, 1H), 7.43 (s, 1H), 7.44 (dd, J = 7.9, 7.4 Hz, 2H), 5.86 (dddd, J =12.5, 4.3, 3.4, 2.6 Hz, 1H), 5.78 (dddd, J = 11.7, 8.4, 2.9 Hz, 1H), 5.51 (dddd, J = 11.4, 6.1, 2.5 Hz, 1H), 4.23 (ddd, J = 4.0, 2.9, 1.5 Hz, 1H), 3.77 – 3.75 (m, 1H), 3.23 (s, 3H), 2.94 (s, 3H), 2.94 (ddd, J = 15.5, 8.3, 6.1 Hz, 1H), 2.39 (dddd, J = 16.4, 5.0, 2.7 Hz, 1H); ^{13}C NMR (125 MHz, $CDCl_3$): 202.5, 168.2, 165.6, 148.4, 135.3, 133.2, 130.2, 129.9, 128.4, 123.6, 90.5, 73.3, 66.4, 50.8, 49.6, 39.8, 29.5; IR (CH_2Cl_2): ν_{max} 3052, 3002, 1726, 1685, 1609, 1425, 1281, 1263, 1164, 894, 764 cm^{-1}; HRMS calcd for $(C_{19}H_{19}NO_5)Na^+$: 364.1155, found: 364.1156.

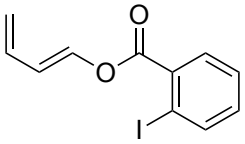

(*E*)-buta-1,3-dien-1-yl 2-iodobenzoate (77). Crotonaldehyde (1.0 g, 14.3 mmol, 1 equiv.) in THF (10ml) was added dropwise to a stirred solution of *t*BuOK (10 ml, 1.6 M in THF, 1.17 equiv.) at -78 ˚C over 10 min. The mixture was stirred for 15 min. Then a solution of 2-iodobenzoyl chloride (4.45 g, 16.7 mmol, 1.17 equiv.) in THF (10 ml) was added and the reaction was stirred for 1 h. After the reaction was completed (TLC), it was quenched by saturated NH_4Cl solution, extracted with DCM, and concentrated under vacuum. The compound **77** was purified via column chromatograph with 61% yield (2.466 g) as yellow oil. ^{1}H NMR (500 MHz, $CDCl_3$): 8.04 (dd, J = 8.0, 1.1 Hz, 1H), 7.91, (dd, J = 7.8, 1.7 Hz, 1H), 7.63 (dd, J = 12.3, 0.4 Hz, 1H), 7.44 (td, J = 7.6, 1.2 Hz, 1H), 7.20 (td, J = 7.9, 1.7 Hz, 1H), 6.36 (ddd, J = 16.8, 10.5 Hz, 1H), 6.24 (t, J = 12.3 Hz, 1H), 5.28 (dt, J = 16.8, 0.7 Hz, 1H), 5.16 (dt, J = 10.2, 0.7 Hz, 1H); ^{13}C NMR (125 MHz, $CDCl_3$) 163.1, 141.9, 138.9, 133.5, 132.1, 131.7, 131.6, 128.1, 118.0, 117.3, 94.8; IR (CH_2Cl_2): ν_{max} 3061, 2993, 2935, 2858, 1726, 1420, 1285, 1249, 1137, 899, 719, 791 cm^{-1}; HRMS calcd for $(C_{11}H_9IO_2)_2Na^+$: 622.9187, found: 622.9190.

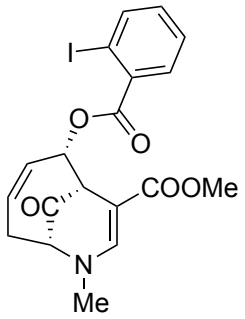

methyl (1*S*,2*S*,6*R*)-2-((2-iodobenzoyl)oxy)-7-methyl-10-oxo-7-azabicyclo[4.3.1]deca-3,8-diene-9-carboxylate (82a). 17 h, 95 mg, 49% yield; ^{1}H NMR (500 MHz, $CDCl_3$): δ 7.98 (dd, J = 8.0, 1.0 Hz, 1H), 7.80 (dd, J = 7.8, 1.7 Hz, 1H), 7.43 (s, 1H), 7.40 (td, J = 7.6, 1.1 Hz, 1H),

7.14 (td, J = 7.9, 1.8 Hz, 1H), 6.22 (ddd, J = 11.8, 7.4, 3.0 Hz, 1H), 6.01 (ddd, J = 11.9, 8.6, 3.2 Hz, 1H), 5.75 (dd, J = 7.4, 5.8 Hz, 1H), 3.96 (dd, J = 5.6, 2.8 Hz, 1H), 3.75 – 3.74 (m, 1H), 3.71 (s, 3H), 2.99 (s, 3H), 2.81 (ddd, J = 16.5, 8.7, 6.1 Hz, 1H), 2.39 (dddd, J = 16.6, 4.7, 3.0 Hz, 1H); ^{13}C NMR (125 MHz, $CDCl_3$): δ 202.5, 167.2, 165.0, 148.8, 141.6, 134.0, 133.0, 131.6, 131.3, 130.5, 128.2, 94.5, 89.7, 68.1, 66.6, 51.2, 49.0, 40.0, 27.2; IR (CH_2Cl_2): ν_{max} 3061, 2984, 1730, 1699, 1663, 1420, 1272, 894, 760, 728 cm^{-1}; HRMS: calcd for $(C_{19}H_{18}INO_5)Na^+$: 490.0122, found: 490.0122.

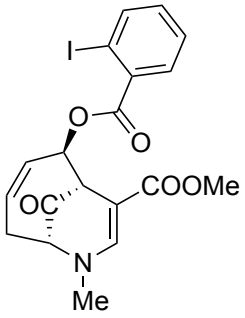

methyl (1*S*,2*R*,6*R*)-2-((2-iodobenzoyl)oxy)-7-methyl-10-oxo-7-azabicyclo[4.3.1]deca-3,8-diene-9-carboxylate (82b). (17 h, 95 mg, 49% yield)^{1}H NMR (500 MHz, $CDCl_3$): δ 8.04 (dd, J = 8.0, 1.1 Hz, 1H), 8.00 (dd, J = 7.9, 1.7 Hz, 1H), 7.50 (s, 1H), 7.42 (td, J = 7.8, 1.2 Hz, 1H), 7.17 (td, J = 7.7, 1.8 Hz, 1H), 5.92 (dddd, J = 12.5, 3.2, 2.6 Hz, 1H), 5.80 (dddd, J = 11.7, 8.4, 2.9 Hz, 1H), 5.52 (ddd, J = 8.7, 6.0, 2.6 Hz, 1H), 4.25 (ddd, J = 4.9, 3.9, 1.5 Hz, 1H), 3.78 – 3.76 (m, 1H), 3.37 (s, 3H), 2.98 – 2.92 (m, 4H), 2.20 (dddd, J = 16.1, 7.8, 5.1, 2.3 Hz, 1H); ^{13}C NMR (125 MHz, $CDCl_3$): δ 202.2, 168.0, 164.8, 148.4, 141.8, 135.0, 133.7, 133.1, 132.1, 128.0, 123.7, 94.9, 90.3, 74.2, 66.3, 50.9, 49.6, 39.8, 29.4; IR (CH_2Cl_2): ν_{max} 3070, 3034, 1703, 1649, 1604, 1258, 746 cm^{-1}; HRMS calcd for $(C_{19}H_{18}INO_5)Na^+$: 490.0122, found: 490.0122.

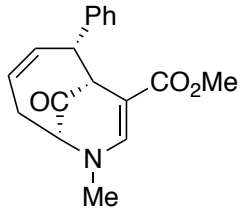

(1R,2S,6R)-methyl 7-methyl-10-oxo-2-phenyl-7-azabicyclo[4.3.1]deca-3,8-diene-9-carboxylate (86a). Yellow solid, mp = 134-138 ˚C (4 h , 112 mg, 78% yield); ^{1}H NMR (500 MHz, $CDCl_3$) δ 7.43 (s, 1H), 7.30 (t, J = 7.8 Hz, 2H), 7.23-7.21 (m, 3H), 5.59 (ddddd, J = 12.0, 7.2, 2.4 Hz, 2H), 4.23 (dd, J = 6.6, 3.6 Hz, 1H), 3.75 (s, 3H), 3.74 (t, J = 3.0 Hz, 1H), 3.68 (ddd, J = 7.2, 2.4 Hz, 1H), 2.98 (s, 3H), 2.81 (ddd, J = 16.8, 7.8, 5.4 Hz, 1H), 2.36 (dq, J = 16.8, 2.4 Hz, 1H); ^{13}C NMR (125Hz, $CDCl_3$) δ 203.6, 167.5, 146.9, 138.9, 133.8, 128.4, 127.8, 126.8, 125.4, 93.8, 65.6, 53.0, 50.8, 48.1, 39.7, 27.7; IR (CH_2Cl_2): ν_{max} 3031, 2921, 2847, 1715, 1674, 1634, 1442, 1266, 1155, 1078, 906, 743 cm^{-1} ; HRMS calcd for $(C_{18}H_{19}NO_3)Na^+$: 320.1257, found: 320.1258.

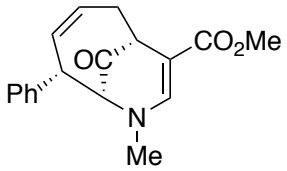

(1R,5S,6R)-methyl 7-methyl-10-oxo-5-phenyl-7-azabicyclo[4.3.1]deca-3,8-diene-9-carboxylate (86b). Yellow solid, mp = 125- 127 ˚C (4 h, 12 mg, 8% yield); ^{1}H NMR (500 MHz, $CDCl_3$) δ 7.41 (s, 1H), 7.32 (t, J = 7.0 Hz, 2H), 7.25 (t, J = 7.5 Hz, 1H), 7.14 (d, J = 7.5 Hz, 2H), 5.96 (ddddd, J = 12.0, 8.0, 2.5 Hz, 2H), 4.14 (dd, J = 7.0, 4.5 Hz, 1H), 3.82 (t, J = 3.5 Hz, 1H), 3.68 (s, 3H), 3.48 (q, J = 4.0 Hz, 1H), 3.11 (s, 3H), 2.81 (ddd, J = 16.0, 8.0, 4.0 Hz, 1H), 2.36 (dq, J = 16.0, 3.0 Hz, 1H); ^{13}C NMR (125Hz, $CDCl_3$) δ 203.6, 167.3, 146.1, 136.5, 131.3, 128.8, 128.7, 128.0, 127.3, 94.2, 73.3, 50.7, 45.0, 44.4, 40.4, 30.1; IR (CH_2Cl_2): ν_{max} 3031, 2921, 2847,

1715, 1674, 1634, 1442, 1266, 1155, 1078, 906, 743 cm^{-1}; HRMS calcd for $(C_{18}H_{19}NO_3)Na^+$: 320.1257, found: 320.1258.

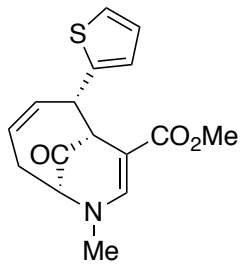

methyl (1*R*,2*S*,6*R*)-7-methyl-10-oxo-2-(thiophen-2-yl)-7-azabicyclo[4.3.1]deca-3,8-diene-9-carboxylate (87a). Yellow solid, mp = 125- 126 ˚C (20 h, 72 mg, 38% yield); ^{1}H NMR (500 MHz, $CDCl_3$): δ 7.40 (s, 1H), 7.14 (dd, J = 5.1, 1.1 Hz, 1H), 6.91 (dd, J = 5.1, 3.6 Hz, 1H), 6.88 (dt, J = 3.5, 1.2 Hz, 1H), 6.09 (ddd, J = 15.01, 8.2, 2.8 Hz, 1H), 5.90 (ddd, J = 14.8, 8.5, 2.7 Hz, 1H), 4.44 (dd, J = 8.1, 4.1 Hz, 1H), 3.85 (t, J = 3.2 Hz, 1H), 3.71 (s, 3H), 3.65 (ddd, J = 7.8, 2.5 Hz, 1H), 2.93 (s, 3H), 2.76 (ddd, J = 16.8, 8.4, 5.6 Hz, 1H), 2.35 (dq, J = 16.8, 2.5 Hz, 1H); ^{13}C NMR (125 MHz, $CDCl_3$): δ 203.5, 167.5, 147.5, 142.9, 14.5, 127.0, 126.0, 125.1, 124.2, 93.2, 65.8, 53.4, 51.0, 42.7, 39.8, 27.0; IR (CH_2Cl_2): ν_{max} 3061, 2989, 1717, 1676, 1627, 1443, 1420, 1272, 1169, 903, 737, 706 cm^{-1}; HRMS calcd for $(C_{16}H_{17}NO_3S)Na^+$: 326.0821 found: 326.0821.

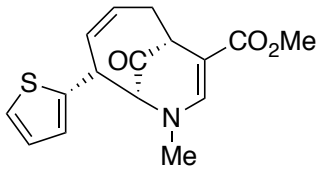

methyl (1*R*,5*R*,6*S*)-7-methyl-10-oxo-5-(thiophen-2-yl)-7-azabicyclo[4.3.1]deca-3,8-diene-9-carboxylate (87b). Yellow solid, mp = 147- 148 ˚C (20 h, 21 mg, 11% yield); ^{1}H NMR (500 MHz, $CDCl_3$): δ 7.37 (s, 1H), 7.19 (dd, J = 5.2, 1.1 Hz, 1H), 6.93 (dd, J = 5.1, 3.6 Hz, 1H), 6.81 (dt, J = 3.6, 1.1 Hz, 1H), 6.07 – 5.95 (m, 2H), 4.38 (dd, J = 7.5, 4.9 Hz, 1H), 3.93 (dd, J = 4.1, 3.0

Hz, 1H), 3.67 (s, 3H), 3.47 (q, J = 3.8 Hz, 1H), 3.08 (s, 3H), 2.78 (ddd, J = 16.3, 8.4, 4.7 Hz, 1H), 2.35 (dq, J = 16.5, 2.9 Hz, 1H); ^{13}C NMR (125 MHz, $CDCl_3$): δ 203.6, 167.3, 146.4, 140.1, 132.0, 129.2, 127.2, 125.8, 125.0, 94.5, 73.3, 50.9, 44.8, 40.6, 39.8, 29.4; IR (CH_2Cl_2): ν_{max} 3052, 2984, 2948, 1721, 1685, 1636, 1438, 1420, 1272, 1164, 894 cm^{-1}; HRMS: calcd for $(C_{16}H_{17}NO_3S)Na^+$: 326.0821 found: 326.0821.

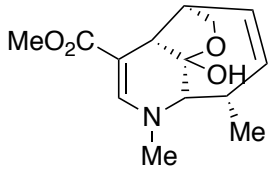

methyl (3*R*,8*S*)-7a-hydroxy-4,8-dimethyl-2,3,3a,4,7,7a-hexahydro-3,7-prop[1]enofuro[3,2-*b*]pyridine-6-carboxylate (94a). Colorless solid, mp = 160 -161 ˚C (72 h, 159 mg, 25% yield); ^{1}H NMR (500 MHz, $CDCl_3$): δ 7.29 (s, 1H), 5.73 (dd, J = 12.2, 7.6 Hz, 1H), 5.56 (dd, J = 12.2, 8.5 Hz, 1H), 4.25 (dd, J = 8.1, 4.8 Hz, 1H), 3.72 (d, J = 8.0 Hz, 1H), 3.66 (s, 1H), 3.56 (dd, J = 6.1, 1.9 Hz, 1H), 3.50 (s, 1H), 3.02 (ddd, J = 8.2, 5.9, 4.9 Hz, 1H), 2.95 (s, 3H), 2.94- 2.93 (m, 1H), 2.48 (dquin, J = 7.4, 1.5 Hz, 1H), 1.26 (d, J = 7.5 Hz, 3H); ^{13}C NMR (500 MHz, $CDCl_3$): 168.6, 145.0, 138.7, 124.3, 104.2, 98.8, 70.7, 66.2, 50.8, 44.8, 41.5, 39.7, 39.6, 22.4; IR (CH_2Cl_2): ν_{max} 3056, 2989, 1636, 1425, 1254, 921, 773 cm^{-1}; HRMS: calcd for $(C_{14}H_{19}NO_4)H^+$: 266.1388, found: 266.1391.

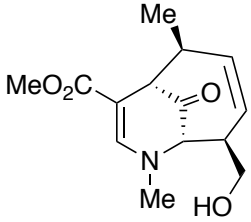

methyl (2*R*,5*S*)-5-(hydroxymethyl)-2,7-dimethyl-10-oxo-7-azabicyclo[4.3.1]deca-3,8-diene-9-carboxylate (94d). Colorless solid, mp = 157- 158 ˚C (72 h, 166 mg, 26% yield); ^{1}H NMR (500 MHz, $CDCl_3$): δ 7.36 (s, 1H), 5.60 (dddd, J = 11.3, 4.0, 2.5, 0.7 Hz, 1H), 5.41 (dddd, J =

11.4, 4.0, 2.5, 0.7 Hz, 1H), 4.02 (ddd, J = 11.1, 7.1, 4.4 Hz, 1H), 3.99 (ddd, J = 2.4, 1.2 Hz, 1H), 3.79 (ddd, J = 10.6, 10.0, 6.8 Hz, 1H), 3.66 (s, 3H), 3.49 (t, J = 2.0 Hz, 1H), 3.00 (s, 3H), 2.42-2.40 (m, 2H), 1.78- 1.73 (m, 1H), 1.29 (d, J = 7.3 Hz, 3H); ^{13}C NMR (500 MHz, CDCl3): 207.2, 168.3, 148.9, 140.3, 127.1, 92.1, 67.2, 64.4, 52.3, 50.9, 45.7, 43.2, 38.6, 21.5; IR (CH_2Cl_2): ν_{max} 3061, 2984, 1699, 1622, 1429, 1285, 903, 787 cm^{-1}; HRMS: calcd for $(C_{14}H_{19}NO_4)Na^+$: 288.1206, found: 288.1208.

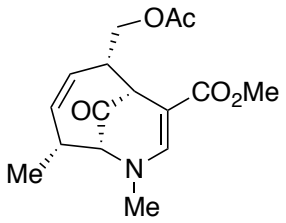

methyl (1R,2S,5R,6R)-2-(acetoxymethyl)-5,7-dimethyl-10-oxo-7-azabicyclo[4.3.1]deca-3,8-diene-9-carboxylate (95a). (72 h, 50 mg, 17% yield); ^{1}H NMR (500 MHz, $CDCl_3$): δ 7.39 (s, 1H), 5.77 (dd, J = 12.9, 7.3 Hz, 1H), 5.58 (dd, J = 12.9, 7.4 Hz, 1H), 4.13 (dd, J = 11.1, 5.3 Hz, 1H), 3.68 (dd, J = 11.1, 9.1 Hz, 1H), 3.66 (s, 3H), 3.61 (dt, J = 3.1, 0.7 Hz, 1H), 3.49 (dt, J = 3.4, 0.9 Hz, 1H), 3.03- 2.99 (m, 1H), 2.99 (s, 3H), 2.81 (dddd, J = 25.5, 14.4, 7.1, 3.8 Hz, 1H), 2.10 (s, 3H), 1.03 (d, J = 7.3 Hz, 3H); ^{13}C NMR (500 MHz, $CDCl_3$): 203.8, 171.1, 167.4, 146.6, 134.5, 128.0, 93.5, 71.6, 65.0, 50.9, 45.5, 40.7, 40.5, 33.1, 21.1, 19.2; IR (CH_2Cl_2): ν_{max} 3061, 2984, 1636, 1276, 1258, 760, 733, 701 cm^{-1}; HRMS: calcd for $(C_{16}H_{21}NO_5)Na^+$: 330.1312, found: 330.1315.

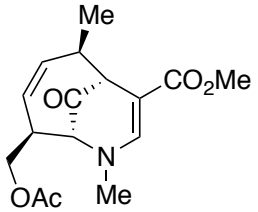

methyl (1*R*,2*R*,5*S*,6*R*)-5-(acetoxymethyl)-2,7-dimethyl-10-oxo-7-azabicyclo[4.3.1]deca-3,8-diene-9-carboxylate (95d). (72h, 19 mg, 7% yield); ^{1}H NMR (500 MHz, $CDCl_3$): δ 7.35 (s, 1H),

5.62 (dddd, J = 11.3, 4.1, 2.5, 0.6 Hz, 1H), 5.45 (dddd, J = 11.3, 4.3, 2.6, 0.9 Hz, 1H), 4.42 (dd, J = 11.2, 7.4 Hz, 1H), 4.22 (dd, J = 11.2, 9.3 Hz, 1H), 3.75 (ddd, J = 2.3, 1.2 Hz, 1H), 3.66 (s, 3H), 3.49 (t, J = 2.3 Hz, 1H), 2.96 (s, 3H), 2.62- 2.59 (m, 1H), 2.44- 2.40 (m, 1H), 2.12 (s, 3H), 1.30 (d, J = 7.3 Hz, 3H); ^{13}C NMR (500 MHz, $CDCl_3$): 206.2, 170.0, 168.1, 148.7, 140.7, 126.5, 92.6, 68.1, 65.4, 52.1, 50.9, 43.3, 42.3, 38.4, 21.5, 21.0; IR (CH_2Cl_2): ν_{max} 3052, 2984, 1622, 1272, 1258, 755, 728, 710 cm^{-1}; HRMS: calcd for $(C_{16}H_{21}NO_5)Na^+$: 330.1312, found: 330.1315.

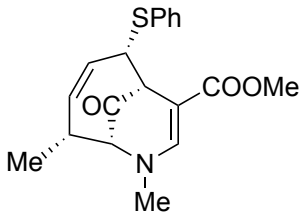

methyl (1*R*,2*S*,5*R*,6*R*)-5,7-dimethyl-10-oxo-2-(phenylthio)-7-azabicyclo[4.3.1]deca-3,8-diene-9-carboxylate (96a). (48 h, 67 mg, 31% yield); ^{1}H NMR (500 MHz, $CDCl_3$): δ 7.60 (d, J = 7.1 Hz, 2H), 7.37 (s, H), 7.35 (tt, J = 7.5, 1.8 Hz, 2H), 7.25 (dddd, J = 7.4, 7.1, 1.8 Hz, 1H), 5.87 (dd, J = 5.1, 2.6 Hz, 2H), 4.27 (ddd, J = 6.6, 4.3 Hz, 1H), 3.59- 3.58 (m, 4H), 3.51 (dd, J = 4.1, 3.1 Hz, 1H), 2.96 (s, 3H), 2.89- 2.82 (m, 1H), 1.17 (d, J = 7.3 Hz, 3H); ^{13}C NMR (500 MHz, $CDCl_3$): 201.9, 167.1, 147.3, 134.5, 133.4, 131.8, 128.9, 128.0, 127.1, 92.2, 71.4, 50.6, 47.6, 40.3, 32.4, 18.5; IR (CH_2Cl_2): ν_{max} 3065, 2957, 2926, 2876, 1735, 1734.8, 1470, 1371, 1249, 1047, 899, 683 cm^{-1}; HRMS: calcd for $(C_{19}H_{21}NO_3S)Na^+$: 366.1134, found: 366.1132.

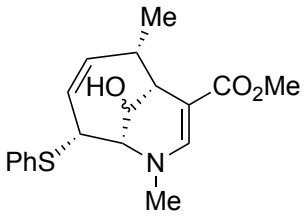

methyl (1*R*,2*S*,5*R*,6*S*)-10-hydroxy-2,7-dimethyl-5-(phenylthio)-7-azabicyclo[4.3.1]deca-3,8-diene-9-carboxylate (96c`). Colorless solid, mp = 130 -132 ˚C (48 h, 22 mg, 10% yield for **96c**);

^{1}H NMR (600 MHz, $CDCl_3$): δ 7.57 – 7.55 (m, 2H), 7.39 – 7.33 (m, 3H), 7.17 (s, 1H), 5.78 (dd, J = 12.2, 7.3 Hz, 1H), 5.65 (dd, J = 12.2, 6.9 Hz, 1H), 4.54 (ddd, J = 7.8, 5.3 Hz, 1H), 4.14 (dd, J = 6.9, 3.3 Hz, 1H), 3.76 (d, J = 7.9 Hz, 1H), 3.64 (s, 3H), 3.63 (dd, J = 3.3, 1.8 Hz, 1H), 3.14 (ddd, J = 5.4, 2.6 Hz, 1H), 2.93 (quintet of d, J = 7.5, 2.5 Hz, 1H), 2.78 (s, 3H), 1.44 (d, J = 7.6 Hz, 3H); ^{13}C NMR (150 MHz, $CDCl_3$): 168.0, 145.5, 139.5, 134.1, 132.7, 129.5, 128.4, 122.7, 97.8, 75.4, 59.6, 50.6, 48.4, 40.8, 39.9, 38.7, 23.3; IR (CH_2Cl_2): ν_{max} 3398, 3061, 3011, 2993, 1676, 1627, 921, 733, 652 cm^{-1}; HRMS: calcd for $(C_{19}H_{23}NO_{3S})Na^{+}$: 368.1291, found: 368.1288.

4.2.2 Intramolecular (4+3)-cycloaddition reactions of N-alkyl oxidopyridinium ions

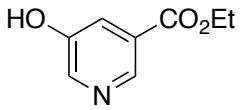

ethyl 5-hydroxynicotinate (102). To a mixture of 5-hydroxynicotinic acid (5 g, 35.9 mmol) in ethanol (20 ml, 342.5 mmol) was added concentrated sulfuric acid (2 ml, 36.8 mmol). The reaction turned clear brown after adding the sulfuric acid. The reaction was then stirred and refluxed at 80° C for 24 h. The solution was cooled to room temperature and neutralized with sodium bicarbonate saturated solution to pH 8 and was extracted with EtOAc. The solution was dried over Na_2SO_4 and the solvent was evaporated to yield ethyl 5-hydroxynicotinate **102** (209 mg, 87%). White solid, mp = 137-139 ℃; ^{1}H NMR (500 MHz, $CDCl_3$) δ 8.78 (d, J = 4.5 Hz, 1H), 8.44 (t, J = 2.5 Hz, 1H), 7.86 (ddd, J = 7.5, 1.5 Hz, 1H), 4.42 (q, J = 7.0 Hz, 2H), 1.65 (s, 1H), 1.41 (t, J = 7.0 Hz, 3H); ^{13}C NMR (500 MHz, $CDCl_3$) δ 165.1, 154.1, 141.3, 140.6, 127.9, 124.9, 61.8, 14.2; IR (CH_2Cl_2): ν_{max} 3014, 2991, 2921, 1719, 1584, 1444, 1299, 1211, 1100, 1024 cm^{-1}; HRMS calcd for $(C_8H_9NO_3)Na^{+}$: 190.0475, found: not observed.

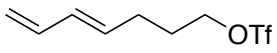

(*E*)-hepta-4,6-dien-1-yl trifluoromethanesulfonate (107). The (E)-hepta-4,6-dien-1-ol (250 mg, 2.2 mmol, 1.0 equiv) was dissolved in dry dichloromethane (7.3 ml, 0.3 M) in an oven-dried round bottom flask, 2,6-lutidine (0.22 mL, 2.5 mmol, 1.1 eq.) was added at -78 ˚C. A solution of trifluoromethanesulfonic anhydride (0.4 mL, 2.3 mmol, 1.05 eq.) was added dropwise to the reaction mixture. After the reaction complete, the dry-ice bath was removed from the reaction and the reaction mixture was quenched by water. The aqueous solution was extracted with dichloromethane (3 * 10 mL), dried over Na_2SO_4 and the solvent was evaporated at rt. The crude organic residue was then eluted (dichloromethane on silica gel) quickly to afford the pure trifluoromethanesulfonate ester **107** (0.209 mg, quantitative yield). Colorless liquid; ^{1}H NMR (600 MHz, $CDCl_3$): δ 6.31 (ddd, J = 16.8, 10.2 Hz, 1H), 6.13-6.09 (m, 1H), 5.63 (ddd, J= 22.2, 7.2 Hz, 1H), 5.15 (dt, J = 16.8, 0.6 Hz, 1H), 5.03 (dt, J = 10.2, 0.6 Hz, 1H), 4.55 (t, J = 6.6 Hz, 2H), 2.25 (q, J = 7.2 Hz, 2H), 1.94 (quintet, J = 6.6 Hz 2H); ^{13}C NMR (600 MHz, $CDCl_3$): δ 136.5, 133.0, 131.4, 116.3, 76.7, 28.7, 27.9; IR (CH_2Cl_2): ν_{max} 3434, 3084, 3037, 3002, 2973, 2845, 1649, 1415, 1240, 1205, 1147, 995, 908, 738 cm^{-1}.

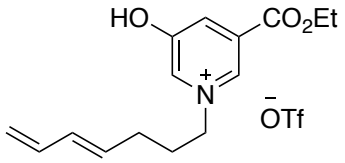

(*Z*)-3-(ethoxycarbonyl)-1-(hepta-4,6-dien-1-yl)-5-hydroxypyridin-1-ium trifluoromethanesulfonate (108). To the solution of **102** (131 mg, 0.86 mmol, 1 equiv) in dichloromethane(8.6 mL, 0.1 M), **107** (0.209g, 0.86 mmol, 1 equiv) was added. The reaction mixture was stirred at rt for 2 h. The resultant mixture was concentrated and extracted with MeOH/hexane to give the pyridinium triflate **108** (0.34 mg, quantitative yield). The crude product was directly used for the next step without further purifications. Ionic liquid; ^{1}H NMR

(500 MHz, MeOD) δ 9.00 (t, J = 1.5 Hz, 1H), 8.68 (dd, J = 2.5, 1.5 Hz, 1H), 8.33 (dd, J = 2.5, 1.0 Hz, 1H), 6.28 (dddd, J = 20.5, 10.0 Hz, 1H), 6.11 (dd, J = 15.0, 10.5 Hz, 1H), 5.68 (ddd, J = 14.0, 6.5 Hz, 1H), 5.10 (ddd, J = 17.0, 1.0, 0.5 Hz, 1H), 4.98 (ddd, J = 10.5, 1.0, 0.5 Hz, 1H), 4.63 (t, J = 7.5 Hz, 2H), 4.49 (q, J = 7.5 Hz, 2H), 2.25 (q, J = 7.0 Hz, 2H), 1.44 (t, J = 7.0 Hz, 3H); ^{13}C NMR (500 MHz, MeOD) δ 162.8, 159.2, 138.0, 137.8, 137.2, 134.0, 133.2, 133.0, 132.1, 125.5, 123.1, 120.5, 118.0, 116.4, 64.2, 63.1, 30.1, 24.2, 14.4; IR (film): ν_{max} 3014, 2839, 1736, 1654, 1596, 1514, 1421, 1211, 1024, 925, 773, 663 cm^{-1}; HRMS calcd for ($C_{15}H_{20}NO_3$): 262.1438, found: 262.1433.

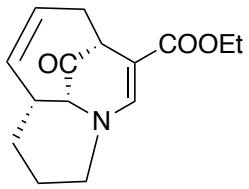

ethyl (4a*S*,8*S*,9a*S*)-9-oxo-2,3,4,4a,7,8,9,9a-octahydro-1,8-ethenocyclohepta[*b*]pyridine-10-carboxylate (109a). A sealed tube (ca. 40 mL capacity) was charged with the pyridinium salt (200 mg, 0.49 mmol), TEA (0.13 mL, 1.46 mmol, 3 equiv), and acetonitrile (9.8 mL, 0.05 M). The tube was then sealed with a threaded Teflon cap. The reaction mixture was heated in an oil bath at 85 ˚C for 6 h and then allowed to cool to rt. The reaction mixture was quenched by addition of 10% HCl solution. The aqueous solution was extracted with dichloromethane (3 * 10 mL), dried over Na_2SO_4, and concentrated under reduced pressure. The crude mixture was purified by column chromatography (20–30% EtOAc/hexanes) to give the **109a** and **109b** (*endo*: *exo* = 1: 2, in total 0.107 g, 84%). Colorless solid, mp = 75-80 ˚C; ^{1}H NMR (500 MHz, $CDCl_3$) δ 7.43 (s, 1H), 5.79-5.77 (m, 1H), 4.23-4.14 (m, 2H), 3.55-3.48 (m, 2H), 3.31-3.25 (m, 1H), 3.17 (ddd, J = 9.0, 1.5, 1.0 Hz, 1H), 3.06-2.99 (m, 1H), 2.67-2.63 (m, 1H), 2.22-2.18 (m, 1H), 2.15-2.10 (m, 1H), 1.79-1.71 (m, 1H), 1.29 (t, J = 7.0 Hz, 3H); ^{13}C NMR (125 MHz, $CDCl_3$) δ 204.3,

166.9, 144.6, 133.0, 130.3, 102.7 , 72.8, 59.7, 53.0, 43.3, 41.3, 32.8, 28.8, 26.5, 14.5; IR (CH_2Cl_2): ν_{max} 3055, 2979, 2938, 2851, 1724, 1678, 1421, 1258, 1135, 896 cm^{-1}; HRMS calcd for $(C_{15}H_{19}NO_3)Na^+$: 284.1257, found: 284.1258.

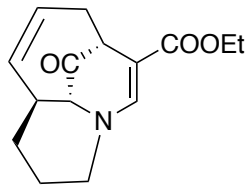

ethyl (4a*S*,8*R*,9a*R*)-9-oxo-2,3,4,4a,7,8,9,9a-octahydro-1,8-ethenocyclohepta[*b*]pyridine-10-carboxylate (109b). mp = 84- 96 ˚C; ^1H NMR (500 MHz, $CDCl_3$) δ 7.40 (s, 1H), 5.78 (dddd, J = 15.5, 5.5, 3.0 Hz, 1H), 5.43 (dddd, J= 4.5, 1.5 H), 4.16-4.07 (m, 2H), 3.77 (dt, J = 4.5, 1.5 Hz, 1H), 3.56 (q, J = 4.0, 1.0 Hz, 1H), 3.47-3.44 (m, 1H), 3.21 (dt, J = 15.5, 3.0, 1H), 2.79 (ddd, J = 16.5, 8.5, 4.0 Hz, 1H), 2.45 (s, 1H), 2.17 (dddd, J = 10.0, 3.5, Hz, 1H), 2.09-2.05 (m, 1H), 1.91-1.76 (m, 1H), 1.61- 1.58 (m, 1H), 1.25 (t, J = 7.5 Hz, 3H); ^{13}C NMR (125 MHz, $CDCl_3$) δ 206.7, 167.4, 145.3, 131.7, 130.4, 93.2 , 67.3, 59.2, 53.0, 44.9, 36.5, 32.5, 32.1, 21.9, 14.6; IR (CH_2Cl_2): ν_{max} 3052, 2987, 2921, 2848, 1712, 1667, 1618, 1597, 1438, 1417, 1266, 1168, 894 cm^{-1}; HRMS calcd for $(C_{15}H_{19}NO_3)Na^+$: 284.1257, found: 284.1258.

4.2.3 Intramolecular Heck coupling of 7-azabicyclo[4.3.1]decane derivatives

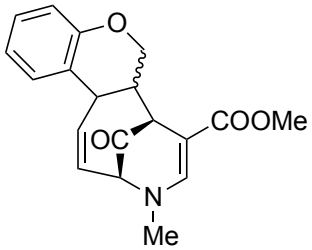

methyl (3S,7S)-4-methyl-14-oxo-3,4,7,7a,8,13b-hexahydro-3,7-methanochromeno[3,4-e]azonine-6-carboxylate (120a/120b). To a mixture of $Pd(OAc)_2$ (3mg, 0.0132 mmol, 0.1 equiv), KOAc (26mg, 0.264 mmol, 2 equiv), and 4 Å molecular sieves in DMF (3 mL 0.05 M), the diastereomers **119a/119b** (60mg, 0.132 mmol, 1 equiv) was added. The reaction mixture was stirred at 80 ˚C for 24 h. When the reaction was complete, water was added, and the mixture was extracted with DCM. The combined organic layer was dryied over anhydrous Na_2SO_4 and concentrated. The residue was purified and purified by chromatography to give **120a and 120b** as an inseparable colorless oil (24h, 28 mg, 65% yield); ^{1}H NMR (600 MHz, $CDCl_3$): Major product δ 7.76 (s, 1H), 7.15 – 7.09 (m, 2H), 6.93 (td, J = 7.5, 1.2 Hz, 1H), 6.80 (dd, J = 8.2, 1.1 Hz, 1 H), 6.28 (dd, J = 10.8, 4.8 Hz, 1H), 5.97 (ddd, J = 10.7, 7.9, 2.7 Hz, 1H), 4.33 (dt, J = 11.0, 3.5 Hz, 1H), 4.22 (dd, J = 11.4, 3.6 Hz, 1H), 3.90 - 3.84 (m, 1H), 3.75 (t, J = 2.5 Hz, 1H), 3.66 (s, 3H), 3.61 (t, J = 11.5 Hz, 1H), 3.05 (s, 3H), 2.66 (tdd, J = 11.4, 3.5, 2.5 Hz, 1H); minor product δ 7.62 (s, 1H), 7.15 – 7.09 (m, 1H), 7.02 (dd, J = 7.6, 1.5 Hz, 1H), 6.87 (td, J = 7.4, 1.1 Hz, 1H), 6.81 (dd, J = 8.1, 0.9 Hz, 1H), 5.97 – 5.94 (m, 1H), 5.89 (ddd, J = 11.0, 7.8, 3.0 Hz, 1H), 4.30 (ddd, J = 11.1, 3.1, 2.1 Hz, 1H), 3.94 (s, 1H), 3.90 – 3.84 (m, 2H), 3.66 (s, 3H), 3.61 – 3.60 (m, 1H), 3.03 (s, 3H), 2.81, dddd, J = 11.4, 7.3, 3.5 Hz, 1H); ^{13}C NMR (150 MHz, $CDCl_3$): major product 201.1, 167.9, 154.8, 149.6, 145.7, 143.2, 128.9, 127.8, 124.5, 121.5, 117.1, 89.1, 69.9, 65.2, 51.1, 49.3, 45.4, 40.5, 34.6; minor compound 199.6, 167.3, 153.7, 147.0, 129.4, 128.5, 126.8, 125.7, 122.7, 120.7, 117.0, 91.5, 66.9, 65.7, 51.1, 48.2, 40.7, 38.9, 37.1; IR (CH_2Cl_2) ν_{max} = 3011, 2984, 1730, 1685, 1622, 1492, 1280, 912, 777, 724, 656 cm^{-1}; HRMS calcd for $(C_{19}H_{19}NO_4)Na^+$: 348.1206, found: 348.1206.

4.3. [2+2]-Cycloaddition reactions of methyl 7-methyl-10-oxo-7-azabicyclo[4.3.1]deca-3,8-diene-9-carboxylates

4.3.1 General preparation procedure of methyl 7-methyl-10-oxo-7-azabicyclo[4.3.1]deca-3,8-diene-9-carboxylates(131, 142, 145 and 146) and methyl (1R,5S,7S)-8-methyl-4-oxo-7-vinyl-8-azabicyclo[3.2.1]oct-2-ene-2-carboxylates(143 and 144).

A solution of vinylogous amide (200 mg, 0.80 mmol) in acetonitrile (8 ml) in a borosilicate tube was irradiated (450-watt Hanovia medium pressure mercury lamp) in iced water bath under open air. TLC analysis (50% EtOAc-hexanes) indicated the complete consumption of starting material. Evaporation of volatiles gave a brown oil. The resulting brown residue was purified by column chromatography (30-70% EtOAc-hexanes) to give cycloadduct.

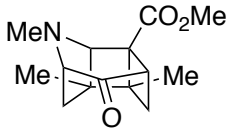

methyl 3,4,9-trimethyl-10-oxo-9-azatetracyclo[4.3.1.03,8.04,7]decane-7-carboxylate (131).
Colorless oil (2.5 h, 48 mg, 96% yield); ^{1}H NMR (800 MHz, $CDCl_3$): δ 3.80 (d, J = 0.9 Hz, 1H), 3.76 (s, 3H), 3.49 (dd, J = 6.5, 1.9 Hz, 1H), 3.23 (dtd, J = 11.5, 1.9, 1.0 Hz, 1H), 2.383 (d, J = 14.0 Hz, 1H), 2.379 (dd, J = 12.3, 11.5 Hz, 1H), 2.32 (s, 3H), 2.30 (dd, J = 12.5, 2.0 Hz, 1H), 1.96 (dd, J = 14.0, 6.5 Hz, 1H), 1.36 (s, 3H), 1.19 (s,3H); ^{13}C NMR (500 MHz, $CDCl_3$): δ 211.1, 171.1, 72.7, 67.2, 52.7, 51.9, 46.4, 45.5, 42.9, 37.6, 34.7, 34.4, 22.2, 18.7; IR (CH_2Cl_2): ν_{max} 3052, 2980, 2948, 1717, 1438, 1272, 1029, 890, 697 cm^{-1}; HRMS calcd for $(C_{14}H_{19}NO_3)H^+$:250.1438, found: 250.1438.

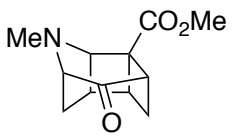

methyl 9-methyl-10-oxo-9-azatetracyclo[4.3.1.0^{3,8}.0^{4,7}]decane-7-carboxylate (132). Colorless oil (2 h, 26 mg, 81% yield); ^{1}H NMR (500 MHz, $CDCl_3$): δ 4.19 (d, J = 7.5 Hz, 1H), 3.75 (s, 3H), 3.53 (dd, J = 5.8, 1.5 Hz, 1H), 3.36 (q, J = 7.7 Hz, 1H), 3.26 (dsextet, J = 11.2, 1.7 Hz, 1H), 3.05 (td, J = 7.1, 3.1 Hz, 1H), 2.82 (ddd, J = 12.5, 11.2, 6.8 Hz, 1H), 2.37 (s, 3H), 2.30 (d, J = 14.0 Hz, 1H), 2.23 (ddd, J = 14.1, 8.4, 6.1 Hz, 1H), 2.02, (dd, J = 12.6, 1.8 Hz, 1H); ^{13}C NMR (500 MHz, $CDCl_3$): δ 210.7, 172.2, 72.0, 63.1, 52.5, 52.3, 46.1, 36.1, 35.6, 34.9, 28.0, 26.3; IR (CH_2Cl_2): ν_{max} 3056, 2957, 2845, 2800, 1726, 1456, 1443, 1321, 1267, 1227, 1074, 1034, 908, 733 cm^{-1}; HRMS calcd for ($C_{12}H_{15}NO_3$)Na^+: 244.0944, found: 244.0943.

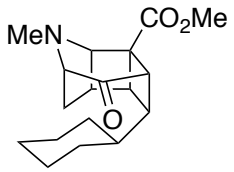

methyl 5-cyclohexyl-9-methyl-10-oxo-9-azatetracyclo[4.3.1.0^{3,8}.0^{4,7}]decane-7-carboxylate (134). 2 h, 27 mg, 75% yield; ^{1}H NMR (500 MHz, $CDCl_3$): δ 4.17 (d, J = 7.4 Hz, 1H), 3.74 (s, 3H), 3.51 (dd, J = 5.9, 1.5 Hz, 1H), 3.39 (d, J = 10.4 Hz, 1H), 3.28 (q, J = 7.9 Hz, 1H), 3.04 (ddd, J = 7.6, 6.7, 3.4 Hz, 1H), 2.30 (td, J = 11.0, 6.6, Hz, 1H), 2.39 (s, 3H), 2.30 (d, J = 14.0 Hz, 1H), 2.08 (ddd, J = 14.5, 8.7, 6.0 Hz, 1H), 1.82 (dsextet, J = 12.8, 1.5 Hz, 1H), 1.68 (dt, J = 12.8, 3.2 Hz, 1H), 1.62 (d, J = 11.0 Hz, 2H), 1.52 (dsextet, J = 13.0, 1.5 Hz, 1H), 1.33 (qt, J = 11.3, 2.6 Hz, 1H), 1.12 (septet, J = 10.9, 3.31 Hz, 3H), 0.76 (qd, J = 12.3, 3.3 Hz, 1H), 0.67 (qd, J = 11.9, 3.3 Hz, 1H); ^{13}C NMR (500 MHz, $CDCl_3$): δ 210.6, 172.4, 71.9, 61.7, 52.2, 50.4, 48.8, 47.4, 39.6, 38.0, 36.7, 34.9, 31.8, 29.0, 28.9, 26.4, 25.9, 25.5; IR (CH_2Cl_2): ν_{max} 3056, 2980, 2926, 2854, 1708, 1452, 1240, 885, 706 cm^{-1}; HRMS calcd for ($C_{18}H_{25}NO_3$)H^+: 304.1907, found: 304.1907.

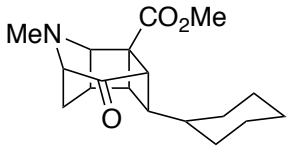

methyl (1*R*,2*S*,6*R*)-2-cyclohexyl-7-methyl-10-oxo-7-azabicyclo[4.3.1]deca-3,8-diene-9-carboxylate (133). 2 h, 45 mg, 76% yield; ^{1}H NMR (500 MHz, $CDCl_3$): δ 4.12 (d, J = 7.4 Hz, 1H), 3.74 (s, 3H), 3.48 (dd, J = 6.1, 1.7 Hz, 1H), 3.40 (q, J = 7.9, 1H), 3.11 (dd, J = 1.7 Hz, 1H), 2.87 (dd, J = 7.7, 3.5 Hz, 1H), 2.38 (s, 3H), 2.29 (d, J = 14.0 Hz, 1`H), 2.18 (ddd, J = 14.1, 8.6, 6.2 Hz, 1H), 1.92 (d, J = 12.8 Hz, 1H), 1.83 (dd, J = 10.3, 1.7 Hz, 1H), 1.75 – 1.65 (m, 4H), 1.37 (qt, J = 11.1, 3.1 Hz, 1H), 1.18 (octet of t, J = 12.2, 3.0 Hz, 1H), 0.78 (qd, J = 12.5, 3.4 Hz, 1H), 0.69 (qd, J = 12.6, 3.4 Hz, 1H); ^{13}C NMR (500 MHz, $CDCl_3$): δ 209.6, 172.7, 71.9, 63.1, 52.3, 51.1, 49.8, 45.6, 39.5, 37.9, 36.3, 34.7, 29.9, 29.7, 28.5, 26.5, 26.0, 25.9; IR (CH_2Cl_2): ν_{max} 3056, 2980, 2930, 2858, 2795, 1717, 1452, 1317, 1267, 1240, 894, 746, 706 cm^{-1}; HRMS calcd for $(C_{18}H_{25}NO_3)Na^+$: 326.1727, found: 326.1727.

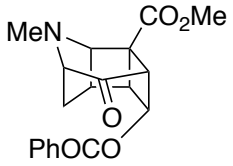

methyl 5-(benzoyloxy)-9-methyl-10-oxo-9-azatetracyclo[4.3.1.0^{3,8}.0^{4,7}]decane-7-carboxylate (136). Colorless solid, mp = 92- 93 ˚C (1.5 h, 30 mg, 60% yield); ^{1}H NMR (500 MHz, $CDCl_3$): δ 7.94 (dd, J = 8.4, 1.3 Hz, 2H), 7.57 (tt, J = 7.5, 1.3 Hz, 1H), 7.45 (dd, J = 8.2, 7.5 Hz, 2H), 5.71 (dd, J = 10.2, 6.5 Hz, 1H), 4.32 (d, J = 7.6 Hz, 1H), 3.78 (s, 3H), 3.71 (ddd, J = 10.3, 3.4, 1.7 Hz, 1H), 3.62 (dd, J = 6.1, 1.6 Hz, 1H), 3.56 (ddd, J = 7.7, 6.7, 3.5, 1H), 3.37 (q, J = 8.0 Hz, 1H), 2.66 (d, J = 13.8 Hz, 1H), 2.46 (s, 3H), 2.17 (ddd, J = 13.8, 9.0, 6.2 Hz, 1H); ^{13}C NMR (125 MHz, $CDCl_3$): δ 206.5, 171.4, 165.1, 133.7, 129.9, 129.2, 128.7, 71.8, 66.3, 61.3, 52.6, 52.2, 45.9, 43.2, 35.3, 35.0, 29.0; IR (CH_2Cl_2): ν_{max} 3052, 2984, 2948, 1730, 1447, 1249, 1119, 1029, 894, 692 cm^{-1}; HRMS calcd for $(C_{19}H_{19}NO_5)Na^+$: 364.1155, found: 364.1155.

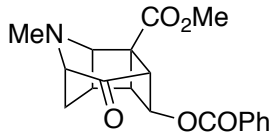

methyl 5-(benzoyloxy)-9-methyl-10-oxo-9-azatetracyclo[4.3.1.0^{3,8}.0^{4,7}]decane-7-carboxylate (135). Colorless solid, mp = 112- 114 ˚C (1 h 20 min, 29 mg, 58% yield); ^{1}H NMR (500 MHz, $CDCl_3$): δ 8.02 (dd, J = 8.4, 1.3 Hz, 2H), 7.58 (tt, J = 7.5, 1.3 Hz, 1H), 7.45 (dd, J = 8.1, 7.6 Hz, 2H), 5.22 (s, 1H), 4.24 (d, J = 7.5 Hz, 1H), 3.76 (s, 3H), 3.58 – 3.50 (m, 3H), 3.14 (dd, J = 8.1, 4.6 Hz, 1H), 2.44 (s, 3H), 2.40 (d, J = 14.4 Hz, 1H), 2.31 (ddd, J = 14.9, 8.9, 6.1 Hz, 1H); ^{13}C NMR (125 MHz, $CDCl_3$): 205.7, 171.4, 165.7, 133.5, 129.8, 129.6, 128.6, 73.1, 71.7, 62.7, 53.8, 52.5, 52.4, 41.4, 35.5, 34.7, 27.6; IR (CH_2Cl_2): ν_{max} 3061, 2989, 1734, 1420, 1272, 1258, 899, 786, 701 cm^{-1}; HRMS calcd for ($C_{19}H_{19}NO_5$)Na^+: 364.1155, found:3 64.1156.

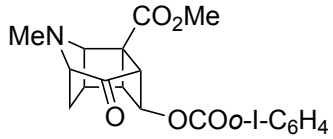

methyl 5-((2-iodobenzoyl)oxy)-9-methyl-10-oxo-9-azatetracyclo[4.3.1.03,8.04,7]decane-7-carboxylate (156). 2.5 h, 32 mg, 62% yield; ^{1}H NMR (500 MHz, $CDCl_3$): δ 8.00 (dd, J = 8.0, 1.0 Hz, 1H), 7.69 (dd, J = 7.8, 1.6 Hz, 1H), 7.40 (td, J = 7.8, 1.0 Hz, 1H), 7.17 (td, J = 7.8, 1.6 Hz, 1H), 5.76 (dd, J = 10.3, 6.6, Hz, 1H), 4.32 (d, J = 7.5 Hz, 1H), 3.78 (s, 3H), 3.71 (dt, J = 10.2, 1.7 Hz, 1H), 3.60 (dd, J = 6.2, 1.6 Hz, 1H), 3.56 (dddd, J = 10.1, 7.6, 6.7, 3.3 Hz, 1H), 3.38 (q, J = 7.7 Hz, 1H), 2.61 (d, J = 13.9 Hz, 1H), 2.46 (s, 3H), 2.16 (ddd, J = 13.8, 9.0, 6.2 Hz, 1H); ^{13}C NMR (125 MHz, $CDCl_3$)**:** δ 206.4, 171.3, 164.7, 141.8, 133.3, 131.2, 128.3, 94.7, 71.8, 66.6, 61.3, 52.6, 52.3, 43.2, 35.3, 35.1, 29.0; IR (CH_2Cl_2): ν_{max} 3061, 2980, 2957, 2849, 2804, 1726, 1438, 1294, 1272, 1240, 1146, 1101, 746, 701 cm^{-1}; HRMS: calcd for ($C_{19}H_{18}INO_5$)Na^+: 490.0122, found: 490.0118.

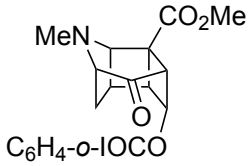

methyl 5-((2-iodobenzoyl)oxy)-9-methyl-10-oxo-9-azatetracyclo[4.3.1.03,8.04,7]decane-7-carboxylate (157). 2.5 h, 26 mg, 54% yield; ^{1}H NMR (500 MHz, $CDCl_3$): δ 8.00 (dd, J = 8.0, 1.1 Hz, 1H), 7.83 (dd, J = 7.8, 1.6 Hz, 1H), 7.42 (td, J = 7.6, 1.2 Hz, 1H), 7.17 (td, J = 7.8, 1.7 Hz, 1H), 5.24 (s, 1H), 4.22 (d, J = 7.5 Hz, 1H), 3.76 (s, 3H), 3.60 (d, J = 4.5 Hz, 1H), 3.56 – 3.51 (m, 2H), 3.20 (dd, J = 8.1, 4.6 Hz, 1H), 2.44 (s, 3H), 2.33 (dd, J = 8.8, 6.1 Hz, 1H), 2.40 (d, J = 14.4 Hz, 1H); ^{13}C NMR (125 MHz, $CDCl_3$): δ 205.3, 171.1, 165.2, 141.5, 133.1, 131.3, 128.0, 94.2, 73.5, 71.5, 62.7, 53.4, 52.4, 41.0, 35.4, 34.6, 27.4; IR (CH_2Cl_2): ν_{max} 3065, 2998, 2997, 2948, 1726, 1267, 1236, 1142, 1101, 728, 701 cm^{-1}; HRMS: calcd for $(C_{19}H_{18}INO_5)Na^+$: 468.0302, found: 468.0299.

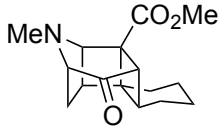

methyl (3b*S*,7a*S*)-1-methyl-3-oxodecahydro-1*H*,3a^{1}*H*-1-aza-2,8-methanocyclobuta[*de*]biphenylene-3a^{1}-carboxylate (137). 2.5 h, 32 mg, 77% yield; ^{1}H NMR (500 MHz, $CDCl_3$): δ 4.21 (dd, J = 7.7, 0.8 Hz, 1H), 3.77 (s, 3H), 3.46 (dd, J = 6.0, 1.5 Hz, 1H), 3.02 (d, J = 1.0 Hz, 1H), 2.86 (t, J = 8.1 Hz, 1H), 2.34 (s, 3H), 2.28 (dd, J = 19.4, 9.7 Hz, 1H), 2.14- 2.10 (m, 1H), 1.66- 1.63 (m, 1H), 1.59- 1.57 (m. 1H), 1.43 (dddd, J = 24.0, 16.8, 10.5, 3.2 Hz, 1H), 1.27- 1.20 (m, 2H), 1.04 (qdd, J = 12.9, 4.1, 2.6 Hz, 1H), 0.90 (qd, J = 13.0, 2.6 Hz, 1H); ^{13}C NMR (500 MHz, $CDCl_3$): 209.9, 172.2, 71.4, 60.9, 52.20, 52.16, 51.49, 46.0, 44.2, 38.8, 34.7, 31.2, 31.0, 27.7, 23.5, 23.3; IR (CH_2Cl_2): ν_{max} 3061, 2989, 1708, 1425, 1254, 894, 773, 692 cm^{-1}; HRMS: calcd for $(C_{16}H_{21}NO_3)H^+$: 276.1594, found: 276.1595.

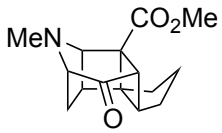

methyl (3a*S*,7b*S*)-5-methyl-8-oxooctahydro-1*H*-4,6-methanocyclopenta[1',4']cyclobuta[1',2':3,4]cyclobuta[1,2-*b*]pyrrole-4a(4b*H*)-carboxylate (138). Yellow oil (3 h, 22 mg, 34% yield); ^{1}H NMR (500 MHz, $CDCl_3$): δ 4.17 (dd. J = 7.5, 0.6 Hz, 1H), 3.74 (s, 3H), 3.50 (dd, J = 6.2, 1.8 Hz, 1H), 3.18 (t, J = 7.8 Hz, 1H), 3.15 (d, J = 0.6 Hz, 1H), 2.48 (dd, J = 9.2, 4.7 Hz, 1H), 2.34 (s, 3H), 2.30 (d, J = 13.7, 1H), 2.23 (ddd, J = 14.3, 8.3, 6.2 Hz, 1H), 2.11 – 2.02 (m, 2H), 176 – 1.66 (m, 2H), 1.65 – 1.57 (m, 1H), 1.51 (dt, J = 13.9, 7.2 Hz, 1H); ^{13}C NMR (500 MHz, $CDCl_3$): δ 210.0, 171.8, 72.0, 61.5, 56.4, 52.1, 50.1, 43.2, 39.2, 34.6, 31.9, 31.3, 30.6, 26.4; IR (CH_2Cl_2): ν_{max} 3043, 2998, 2962, 2867, 2854, 2800, 1712, 1429, 1240, 746 cm^{-1}; HRMS calcd for $(C_{15}H_{19}NO_3)Na^+$: 284.1257, found: 284.1256.

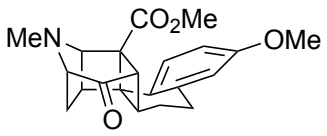

(3b*S*,9b*S*)-7-methoxy-1-methyl-3a^{1}-((methylperoxy)-λ^{2}-methyl)-1,2,3a,3a^{1},3b,4,10,10a-octahydro-3*H*,5*H*-1-aza-2,10-methanobenzo[*a*]cyclobuta[*jk*]biphenylen-3-one (139). Yellow solid, mp = 143- 144 ˚C (2.5 h, 35 mg, 59% yield); ^{1}H NMR (600 MHz, $CDCl_3$): δ 7.34 (d, J = 8.6 Hz, 1H), 6.81 (dd, J = 8.5, 2.5 Hz, 1H), 6.57 (d, J = 2.5 Hz, 1H), 4.54 (dd, J = 7.7, 0.8 Hz, 1H), 3.78 (s, 3H), 3.53 (dd, J = 6.1, 1.7 Hz, 1H), 3.51 (s, 3H), 3.49 (d, J = 8.2 Hz, 1H), 3.17 (d, J = 0.9 Hz, 1H), 2.64 (ddd, J = 12.1, 5.9, 1.5 Hz, 1H), 2.60 (dt, J = 15.9, 3.4 Hz, 1H), 2.52 (ddd, J = 13.1, 3.4 Hz, 1H), 2.42 (d, J = 14.4 Hz, 1H), 2.39 (s, 3H), 2.30 – 2.25 (m, 2H), 1.98 (qd, J = 13.0, 3.8 Hz, 1H); ^{13}C NMR (150 MHz, $CDCl_3$): δ 209.2, 170.5, 158.3, 140.0, 128.5, 127.7, 113.4, 112.8, 71.7, 61.3, 57.2, 55.3, 52.1, 49.5, 47.6, 45.6, 39.9, 35.1, 28.7, 28.6, 28.1; IR

(CH_2Cl_2): ν_{max} 3043, 2962, 2926, 2881, 2854, 1748, 1461, 1371, 1236, 1043, 890, 656 cm^{-1}; HRMS calcd for $(C_{21}H_{23}NO_4)H^+$: 354.1700, found: 354.1700.

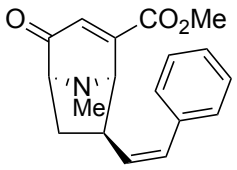

methyl (1*R*,5*S*,7*S*)-8-methyl-4-oxo-7-((*Z*)-styryl)-8-azabicyclo[3.2.1]oct-2-ene-2-carboxylate (143). 3 h, 16 mg, 32% yield; ^1H NMR (500 MHz, $CDCl_3$): δ 7.37 (t, J = 7.4 Hz, 2H), 7.31- 7.27 (m, 3H), 6.83 (dd, J = 1.5, 0.2 Hz, 1H), 6.50 (d, J = 11.4 Hz, 1H), 5.23 (dd, J = 11.3, 10.6 Hz, 1H), 4.28 (d, J = 6.2 Hz, 1H), 3.82 (s, 3H), 3.81- 3.75 (m, 1H), 3.54 (dq, J = 8.1, 1.2 Hz, 1H), 2.71 (ddd, J = 14.0, 9.7, 8.0 Hz, 1H), 2.41 (s, 3H), 1.36 (ddd, J = 14.1, 5.8, 1.0 Hz, 1H); ^{13}C NMR (500 MHz, $CDCl_3$): 200.4, 165.8, 146.9, 136.9, 132.2, 131.1, 130.7, 128.6, 128.5, 127.3, 70.9, 64.9, 52.9, 41.2, 36.3, 33.0; IR (CH_2Cl_2): ν_{max} 3070, 2989, 1730, 1699, 1429, 1285, 903, 706 cm^{-1}; HRMS calcd for $(C_{18}H_{19}NO_3)H^+$: 298.1443, found: 298.1444.

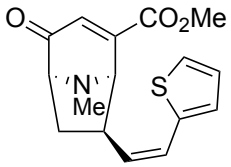

methyl (1*R*,5*S*,7*S*)-8-methyl-4-oxo-7-((*Z*)-2-(thiophen-2-yl)vinyl)-8-azabicyclo[3.2.1]oct-2-ene-2-carboxylate (144). 4.5 h, 3 mg, 14% yield; ^1H NMR (500 MHz, $CDCl_3$): δ 7.13 (d, J = 5.1 Hz, 1H), 6.95 (dd, J = 5.0, 3.5 Hz, 1H), 6.93 (dd, J = 3.5, 1.1 Hz, 1H), 6.65 (s, 1H), 6.60 (d, J =15.6 Hz, 1H), 6.26 (dd, J = 15.0, 8.7 Hz, 1H), 3.98 (s, 1H), 3.87 (s, 3H), 3.62 (d, J = 6.9 Hz, 1H), 2.87 (td, J = 8.8, 3.1 Hz, 1H), 2.48 (s, 3H), 2.27- 2.25 (m, 1H), 1.98 (dd, J = 13.9, 8.9 Hz, 1H); ^{13}C NMR (500 MHz, $CDCl_3$): 200.6, 171.3, 166.0, 146.0, 142.2, 132.7, 129.8,127.4, 125.5, 124.1, 123.7, 70.3, 66.0, 53.0, 47.5, 35.1, 32.5, 31.7, 29.9, 25.4, 22.9, 22.8, 21.2, 20.9, 14.4, 14.3; IR (CH_2Cl_2): ν_{max} 3051, 3015, 2983, 1639, 1612, 1421, 1258, 899, 781 cm^{-1}; HRMS calcd for $(C_{16}H_{17}NO_3)H^+$: 304.1002, found: 304.1001.

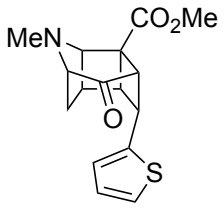

methyl 9-methyl-10-oxo-5-(thiophen-2-yl)-9-azatetracyclo[4.3.1.0^{3,8}.0^{4,7}]decane-7-carboxylate (145). 2 h, 20 mg, 48% yield; ^{1}H NMR (600 MHz, $CDCl_3$): δ 7.15 (dt, J = 5.1, 1.1 Hz, 1H), 6.88 (dd, J = 5.0, 3.6, Hz, 1H), 6.66 (ddd, J = 3.0, 1.7, 1.3 Hz, 1H), 4.47 (dd, J = 10.5, 6.3 Hz, 1H), 4.25 (d, J = 7.1 Hz, 1H), 3.77 (s, 3H), 3.76- 3.74 (m, 1H), 3.46- 3.40 (m, 2H), 3.35 (d, J = 5.5 Hz, 1H), 2.40 (s, 3H), 2.01 (d, J = 14.1 Hz, 1H), 1.91 (ddd, J = 14.4, 6.4, 8.2 Hz, 1H); ^{13}C NMR (150 MHz, $CDCl_3$): 171.7, 171.1, 141.8, 127.1, 124.0, 123.8, 71.3, 62.1, 60.4, 52.3, 51.2, 39.6, 39.2, 36.5, 34.8, 26.9, 14.2; 13C NMR (150 MHz, CDCl3): 171.7, 171.1, 141.8, 127.1, 124.0, 123.8, 71.3, 62.1, 60.4, 52.3, 51.2, 39.6, 39.2, 36.5, 34.8, 26.9, 14.2; IR (CH_2Cl_2): ν_{max} 3056, 2980, 2957, 1726, 1443, 1434, 1263, 903, 741, 701 cm^{-1}; HRMS calcd for $(C_{16}H_{17}NO_3)H^+$: 304.1002, found: 304.1002.

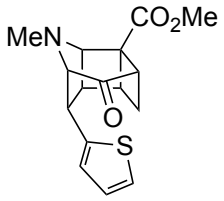

methyl 9-methyl-10-oxo-2-(thiophen-2-yl)-9-azatetracyclo[4.3.1.0^{3,8}.0^{4,7}]decane-7-carboxylate (146). 2.5, 19 mg, 58% yield; ^{1}H NMR (500 MHz, $CDCl_3$): δ 7.16 (dt, J = 5.1, 1.1 Hz, 1H), 6.89 (dd, J = 5.0, 3.5 Hz, 1H), 6.67 (ddd, J = 3.4, 1.7, 1.3 Hz, 1H), 4.47 (dd, J = 10.5, 6.2 Hz, 1H), 4.24 (d, J = 7.1 Hz, 1H), 3.78 (s, 3H), 3.76- 3.73 (m, 1H), 3.47- 3.39 (m, 2H), 3.35 (dd, J = 6.0, 1.6 Hz, 1H), 2.40 (d, J = 14.2 Hz, 1H), 1.90 (ddd, J = 14.6, 8.7, 6.1 Hz, 1H); ^{13}C NMR (500 MHz, $CDCl_3$): 208.8, 171.8, 142.0, 127.3, 124.1, 124.0, 71.5, 62.3, 52.4, 51.3, 50.7,

39.8, 39.3, 36.6, 34.9, 27.0; IR (CH_2Cl_2): ν_{max} 3056, 2989, 2957, 1721, 1442, 1424, 1240, 899, 697 cm^{-1}; HRMS calcd for $(C_{16}H_{17}NO_3)Na^+$: 326.0821, found: 326.0822.

APPENDIX I: COMPUTATIONAL DATA

Computational Methods

Density functional theory calculations were performed in Gaussian 09.[1] The M06-2X functional[2] in conjunction with the 6-31G(d) basis set was used for geometry optimizations. Harmonic frequency calculations confirmed the nature of each stationary point (local minimum or first-order saddle point) and provided thermochemical quantities. For selected transition states, intrinsic reaction coordinate[3] calculations were performed to confirm the identity of the reactants and products. Single-point electronic energies were subsequently calculated with M06-2X in conjunction with the 6-311+G(d,p) basis set, using the SMD implicit solvent model[4] to simulate acetonitrile solution. The M06-2X calculations employed the ultrafine integration grid. Gibbs free energies in acetonitrile were calculated by adding the thermochemical corrections derived from the M06-2X/6-31G(d) frequencies to the M06-2X/6-311+G(d,p) electronic energies and are reported at a standard state of 298.15 K and 1 mol/L.

[1] M. J. Frisch, G. W. Trucks, H. B. Schlegel, G. E. Scuseria, M. A. Robb, J. R. Cheeseman, G. Scalmani, V. Barone, B. Mennucci, G. A. Petersson, H. Nakatsuji, M. Caricato, X. Li, H. P. Hratchian, A. F. Izmaylov, J. Bloino, G. Zheng, J. L. Sonnenberg, M. Hada, M. Ehara, K. Toyota, R. Fukuda, J. Hasegawa, M. Ishida, T. Nakajima, Y. Honda, O. Kitao, H. Nakai, T. Vreven, J. A. Montgomery, Jr., J. E. Peralta, F. Ogliaro, M. Bearpark, J. J. Heyd, E. Brothers, K. N. Kudin, V. N. Staroverov, R. Kobayashi, J. Normand, K. Raghavachari, A. Rendell, J. C. Burant, S. S. Iyengar, J. Tomasi, M. Cossi, N. Rega, J. M. Millam, M. Klene, J. E. Knox, J. B. Cross, V. Bakken, C. Adamo, J. Jaramillo, R. Gomperts, R. E. Stratmann, O. Yazyev, A. J. Austin, R. Cammi, C. Pomelli, J. W. Ochterski, R. L. Martin, K. Morokuma, V. G. Zakrzewski, G. A. Voth, P. Salvador, J. J. Dannenberg, S. Dapprich, A. D. Daniels, O. Farkas, J. B. Foresman, J. V. Ortiz, J. Cioslowski, D. J. Fox, Gaussian 09, Revision A.02, Gaussian, Inc., Wallingford CT, 2009.

[2] a) Y. Zhao, D. G. Truhlar, *Theor. Chem. Acc.* **2008**, *120*, 215–241. b) Y. Zhao, D. G. Truhlar, *Acc. Chem. Res.* **2008**, *41*, 157–167.

[3] a) C. Gonzalez, H. B. Schlegel, *J. Chem. Phys.* **1989**, *90*, 2154–2161. b) C. Gonzalez, H. B. Schlegel, *J. Phys. Chem.* **1990**, *94*, 5523–5527.

[4] A. V. Marenich, C. J. Cramer, D. G. Truhlar, *J. Phys. Chem. B* **2009**, *113*, 6378-6396.

The coordinates of optimized species are given below. Underneath each set of coordinates are listed the following energies:

- M06-2X/6-31G(d) electronic potential energy (E)
- M06-2X/6-31G(d) Gibbs free energy at 298.15 K and 1 mol/L (G)
- Sum of M06-2X/6-311+G(d,p) electronic potential energy and free energy of solvation in SMD acetonitrile at 298.15 K and 1 mol/L (E_{solv})
- Total Gibbs free energy in acetonitrile at the M06-2X/6-311+G(d,p)-SMD(acetonitrile)//M06-2X/6-31G(d) level of theory at 298.15 K and 1 mol/L (G_{solv})

Computed Geometries and Energies

In the following structures, the R group on the oxidopyridinium ion is a CO_2Me group.

Oxidopyridinium ion 48

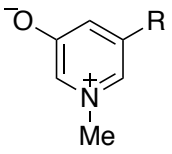

48

C	-0.311916	-0.082208	-0.002268
C	0.141125	1.216898	0.001018
C	1.560436	1.528331	-0.000331
C	2.390911	0.343605	-0.008818
N	1.891651	-0.902434	-0.012258
C	0.574262	-1.164311	-0.009072
O	2.033385	2.667962	0.003101
C	2.841257	-2.024726	0.016925
C	-1.762588	-0.441308	-0.001864
O	-2.170985	-1.579248	-0.005896
O	-2.558846	0.631794	0.004237
C	-3.956662	0.341750	0.005481
H	3.470080	0.439901	-0.011413
H	-0.558608	2.045321	0.004465
H	0.244841	-2.192917	-0.010258
H	3.603202	-1.863351	-0.745793
H	2.306384	-2.950338	-0.188633
H	3.307761	-2.074901	1.001974
H	-4.225110	-0.229318	-0.885660
H	-4.457640	1.307898	0.010852
H	-4.221844	-0.237506	0.892305

0 imaginary frequencies
E = -590.422824
G = -590.291347
E_{solv} = -590.625629
G_{solv} = -590.494153

1,3-Butadiene

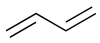

C	0.607553	1.740469	0.000000
C	0.607553	0.405882	0.000000
C	-0.607553	-0.405882	0.000000
C	-0.607553	-1.740469	0.000000
H	1.551836	-0.137433	0.000000
H	-1.551836	0.137433	0.000000
H	1.528802	2.312812	0.000000
H	-1.528802	-2.312812	0.000000
H	-0.322245	2.303592	0.000000
H	0.322245	-2.303592	0.000000

0 imaginary frequencies
E = -155.903553
G = -155.840081
E_{solv} = -155.956255
G_{solv} = -155.892783

TSA

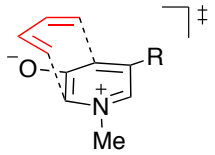

TSA: *endo* (4+3)

$\Delta G^{‡}$ = 23.5

C	0.924789	0.518643	0.268907
C	0.212661	-0.557402	0.845499
C	-1.172436	-0.362415	1.217091
C	-1.795082	0.819648	0.634760
N	-1.032725	1.850433	0.158357
C	0.287339	1.686730	-0.089020
O	-1.860028	-1.199621	1.805327
C	-1.718732	3.052307	-0.303657
C	2.370366	0.443454	-0.047692
O	3.028588	1.354110	-0.498820
O	2.880568	-0.773078	0.209077
C	4.272672	-0.906781	-0.070159
C	-2.565322	-0.213833	-1.195802
C	-2.675933	-1.539940	-0.842118
C	-1.558111	-2.399584	-0.682057
C	-0.266400	-2.011541	-0.931633
H	-2.787883	1.085803	0.978915
H	0.746404	-1.373923	1.315562
H	0.823345	2.509775	-0.544561
H	-2.437687	3.371775	0.452999
H	-0.988928	3.845630	-0.464183
H	-2.246885	2.845888	-1.240253
H	4.850269	-0.199200	0.528501
H	4.529815	-1.931973	0.191028
H	4.468232	-0.716393	-1.127606
H	0.557024	-2.701238	-0.777910
H	-3.464200	0.376650	-1.349553
H	-0.050590	-1.165624	-1.574424
H	-1.677769	0.147915	-1.712252
H	-3.645268	-1.914931	-0.526941
H	-1.734682	-3.360192	-0.207196

1 imaginary frequency

E = -746.319575

G = -746.103252

E_{solv} = -746.565773

G_{solv} = -746.349450

(4+3)-Cycloadduct 47

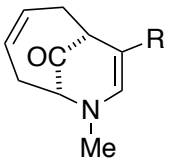

47

ΔG = –14.4

C	-0.774230	0.390533	-0.292189
C	-0.244465	-0.994995	-0.549833
C	1.104044	-0.910346	-1.221332
C	2.068557	0.138958	-0.682690
N	1.408412	1.401630	-0.384550
C	0.067391	1.445328	-0.178839
O	1.482841	-1.705520	-2.050688
C	2.254799	2.486615	0.064412
C	-2.195448	0.647668	-0.072394
O	-2.706355	1.727999	0.142466
O	-2.922172	-0.496499	-0.122796
C	-4.320278	-0.318697	0.076952
C	2.781388	-0.479622	0.550504
C	1.912068	-0.601508	1.777923
C	0.704875	-1.168263	1.858720
C	-0.082226	-1.831701	0.754576
H	2.819004	0.309870	-1.462801
H	-0.902987	-1.556037	-1.218002
H	-0.342399	2.421740	0.067931
H	-1.090745	-2.051087	1.115114
H	0.377364	-2.791744	0.482009
H	3.165783	-1.458714	0.235537
H	3.658050	0.132381	0.785399
H	2.605845	2.339625	1.095358
H	3.126003	2.568398	-0.593347
H	1.696428	3.423787	0.017919
H	-4.734702	0.345365	-0.684909
H	-4.761108	-1.311929	0.000313
H	-4.515509	0.114224	1.060804
H	2.323681	-0.173772	2.689807
H	0.223038	-1.155180	2.834004

0 imaginary frequencies

E = -746.394945

G = -746.172508

E_{solv} = -746.632362

G_{solv} = -746.409925

TSB

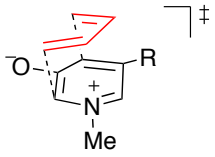

TSB: *exo* (4+3)
24.2

C	-0.759560	0.505882	-0.403156
C	-0.249583	-0.645353	-1.018497
C	1.154282	-0.705393	-1.372540
C	1.969263	0.379441	-0.810620
N	1.383000	1.525569	-0.343600
C	0.071544	1.540486	-0.020620
O	1.693684	-1.643485	-1.967872
C	2.258419	2.563305	0.179789
C	-2.187441	0.649832	-0.032676
O	-2.668681	1.630587	0.489539
O	-2.901678	-0.447953	-0.329586
C	-4.287001	-0.364852	-0.001702

C	2.677631	-0.708993	0.865512
C	1.697459	-0.704531	1.845458
C	0.507404	-1.472537	1.790472
C	0.153723	-2.287335	0.751391
H	2.964555	0.502040	-1.226357
H	-0.914885	-1.380044	-1.456637
H	-0.317551	2.422445	0.473047
H	-0.808938	-2.789457	0.766964
H	0.866070	-2.639786	0.010631
H	2.793098	-1.562617	0.198733
H	3.591565	-0.150259	1.055271
H	2.650536	2.253571	1.156396
H	3.088767	2.720737	-0.510623
H	1.698399	3.492357	0.287873
H	-4.755930	0.463024	-0.537821
H	-4.720845	-1.315814	-0.306242
H	-4.414621	-0.207519	1.071471
H	1.801263	-0.006983	2.674617
H	-0.225919	-1.293590	2.574364

1 imaginary frequency

E = -746.319768

G = -746.103526

E_{solv} = -746.564667

G_{solv} = -746.348425

TSC

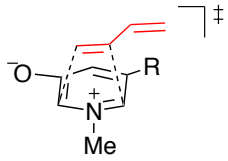

TSC: (3+2)
27.6

C	-0.104519	-1.588322	-0.151297
C	-1.523292	-1.662842	-0.468210
C	-2.313920	-0.542003	0.086700
N	-1.838883	0.147250	1.174220
C	-0.515743	0.424643	1.156440
C	0.360231	-0.534015	0.575900
O	-2.033735	-2.497390	-1.207561
C	-2.731125	1.111006	1.799269
C	1.814559	-0.246421	0.762197
O	2.594787	-1.065624	0.051573
C	3.991534	-0.790590	0.151116
O	2.234595	0.645346	1.461145
C	-1.918188	0.872891	-1.342376
C	-0.768087	1.574155	-0.962771
C	0.509921	1.359991	-1.636950
C	1.584013	2.149546	-1.523796
H	-3.391406	-0.676138	0.050314
H	0.563300	-2.331442	-0.571208
H	-0.128976	1.144909	1.866603
H	-3.694255	0.637697	1.993813
H	-2.297610	1.444173	2.742860
H	-2.874849	1.976013	1.138280
H	4.324482	-0.879250	1.187290
H	4.483978	-1.529916	-0.477870

H	4.197434	0.221758	-0.203985
H	2.499993	1.940897	-2.066270
H	-2.880875	1.364425	-1.216762
H	1.576027	3.030327	-0.887027
H	-1.872167	0.213078	-2.205888
H	-0.871675	2.505853	-0.409008
H	0.561305	0.479977	-2.279282

1 imaginary frequency

E = -746.311981

G = -746.097067

E_{solv} = -746.557812

G_{solv} = -746.342898

IntC

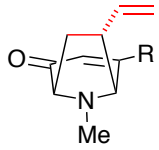

IntC
−1.6

C	0.521228	0.515176	-0.278969
C	0.107847	1.594356	0.399212
C	-1.349311	1.775282	0.645307
C	-2.215977	0.644210	0.108962
N	-1.682482	0.273762	-1.206597
C	-0.478663	-0.470977	-0.833612
O	-1.791032	2.709618	1.277021
C	-2.626474	-0.505713	-1.994367
C	1.963255	0.201916	-0.502571
O	2.346578	-0.740668	-1.153730
O	2.784755	1.073099	0.097970
C	4.174974	0.817148	-0.101453
C	-2.033096	-0.615544	1.017661
C	-0.948190	-1.456572	0.296784
C	0.140260	-1.963786	1.194084
C	0.531095	-3.232553	1.261006
H	-3.247982	0.995142	0.043500
H	0.791169	2.333060	0.804911
H	-0.044597	-0.997421	-1.686063
H	-3.469670	0.134768	-2.266599
H	-2.136275	-0.832029	-2.915577
H	-3.024267	-1.395045	-1.478278
H	4.417999	0.852706	-1.165508
H	4.700256	1.601231	0.440805
H	4.437804	-0.167933	0.289739
H	1.330212	-3.549104	1.923108
H	-2.968887	-1.172842	1.104357
H	0.065548	-4.001397	0.649344
H	-1.730858	-0.337579	2.032718
H	-1.412622	-2.316477	-0.198006
H	0.625440	-1.217472	1.825374

0 imaginary frequencies
E = -746.372354
G = -746.152334
E_{solv} = -746.609461
G_{solv} = -746.389442

TSG

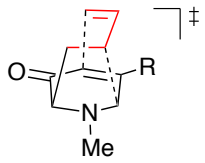

TSG: Cope
24.8

C	-0.593463	0.357197	-0.565925
C	-0.207238	-0.896755	-0.989108
C	1.228989	-1.172913	-1.098197

C	2.152511	-0.109914	-0.508320
N	1.640588	1.228698	-0.680667
C	0.361487	1.317389	-0.190007
O	1.697706	-2.226791	-1.493189
C	2.550318	2.301480	-0.319376
C	-2.000908	0.668472	-0.212676
O	-2.355083	1.674360	0.360498
O	-2.848468	-0.303321	-0.581387
C	-4.215527	-0.057970	-0.257967
C	2.264479	-0.362725	1.061321
C	1.038141	0.077173	1.777269
C	-0.032682	-0.809827	1.988939
C	-0.174687	-2.000218	1.326683
H	3.135248	-0.218272	-0.972371
H	-0.908533	-1.633708	-1.360172
H	3.497043	2.156938	-0.844646
H	2.121927	3.255454	-0.633717
H	2.746531	2.343158	0.762637
H	-4.563071	0.856614	-0.743199
H	-4.766301	-0.922224	-0.625206
H	-4.336946	0.047530	0.822354
H	-1.091898	-2.572724	1.422194
H	3.141074	0.188338	1.412747
H	0.657066	-2.519427	0.862845
H	2.464893	-1.430476	1.194071
H	-0.879635	-0.432611	2.560479
H	0.016322	2.290115	0.147363
H	1.100404	0.968094	2.396102

1 imaginary frequency

E = -746.326794

G = -746.107576

E_{solv} = -746.566585

G_{solv} = -746.347367

TSD

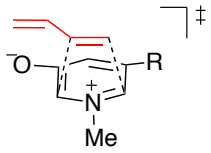

TSD: (3+2)
27.8

C	1.831590	0.582071	-0.996081
N	1.123491	1.654882	-0.587896
C	-0.038571	1.405204	0.110664
C	-0.824857	0.294263	-0.388878
C	-0.234807	-0.713769	-1.071604
C	1.211191	-0.682190	-1.323240
C	1.838623	2.887578	-0.292726
C	-2.249675	0.274179	0.036428
O	-2.946578	-0.725634	-0.515220
C	-4.314147	-0.796468	-0.112403
O	1.852731	-1.644667	-1.745789
O	-2.723109	1.071946	0.814404
C	1.684193	-0.262738	1.449659
C	0.709185	0.678490	1.800818
H	1.037528	1.627518	2.222065

H	2.857369	0.748802	-1.308063
H	-0.792974	-1.579391	-1.411818
H	-0.588629	2.285760	0.427663
H	2.356178	2.805371	0.671536
H	2.568696	3.077197	-1.080145
H	1.129413	3.715339	-0.254301
H	-4.837203	0.122820	-0.383985
H	-4.733433	-1.649880	-0.642025
H	-4.384179	-0.938675	0.968048
C	1.416342	-1.686550	1.415370
H	2.725801	0.044418	1.385817
H	-0.220541	0.315725	2.235780
C	2.278708	-2.610490	0.968025
H	0.421559	-1.994225	1.738623
H	2.024631	-3.664057	0.945991
H	3.260334	-2.331532	0.596740

1 imaginary frequency

E = -746.311695

G = -746.096256

E_{solv} = -746.558129

G_{solv} = -746.342690

IntD

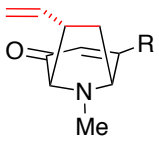

IntD
−1.4

C	0.946852	-0.787532	-1.422728
C	1.747112	0.323033	-0.752630
N	0.926920	1.535558	-0.809062
C	-0.067916	1.261188	0.231988
C	-0.976415	0.165358	-0.273245
C	-0.502621	-0.789288	-1.084647
C	1.689670	2.749556	-0.556509
C	-2.371504	0.166518	0.252194
O	-2.759315	0.942162	1.094817
O	1.450071	-1.636895	-2.124054
O	-3.139593	-0.784137	-0.293263
C	-4.480787	-0.823001	0.194993
C	0.743594	0.719550	1.446134
C	1.965232	0.027919	0.781695
C	2.117303	-1.425967	1.121646
C	3.225590	-1.969892	1.613825
H	1.062372	1.541533	2.092500
H	2.689459	0.438148	-1.292490
H	-1.117658	-1.595964	-1.470000
H	-0.654161	2.151232	0.469564
H	2.225129	2.757220	0.407340
H	2.423343	2.877958	-1.356706
H	1.010246	3.605923	-0.577783
H	-4.982136	0.127118	-0.000671
H	-4.967268	-1.634227	-0.343335
H	-4.486908	-1.012890	1.270375
H	2.883763	0.544115	1.080345
H	0.152722	0.033351	2.058831

```
H     1.244338   -2.056167    0.944454
H     3.289829   -3.029226    1.838989
H     4.112512   -1.370731    1.805732
0 imaginary frequencies
E = -746.371514
G = -746.151808
E_solv = -746.608804
G_solv = -746.389099
```

TSE

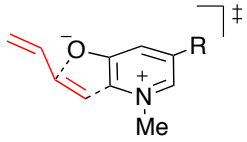

TSE: (3+2)
33.0

```
C    -0.403092    0.583629    0.804270
C     0.883695    0.110107    1.097295
C     1.229291   -1.238020    0.587002
N     0.203480   -2.053105    0.124762
C    -1.005204   -1.541717   -0.202003
C    -1.331221   -0.248054    0.147902
O     1.844597    0.755711    1.576659
C     0.539548   -3.426472   -0.217734
C    -2.706789    0.184125   -0.201870
O    -2.973159    1.430127    0.219455
C    -4.284174    1.897145   -0.088864
O    -3.510473   -0.496367   -0.800429
C     2.401558   -0.753909   -0.799858
C     3.126965    0.367558   -0.357315
C     2.815885    1.707140   -0.792561
C     3.654440    2.747080   -0.684499
H     1.945888   -1.777859    1.203875
H    -0.677892    1.586523    1.108716
H    -1.715815   -2.192058   -0.696735
H     1.098843   -3.877626    0.605515
H    -0.375158   -3.995616   -0.384392
H     1.155231   -3.454915   -1.124136
H    -5.035761    1.254745    0.375067
H    -4.340240    2.907471    0.312923
H    -4.442401    1.901524   -1.169521
H     3.383156    3.735982   -1.036575
H     2.958024   -1.684728   -0.898193
H     4.638054    2.632211   -0.237727
H     1.698958   -0.583841   -1.617428
H     4.034512    0.227363    0.222951
H     1.837120    1.845120   -1.253753
1 imaginary frequency
E = -746.301475
G = -746.087961
E_solv = -746.547874
G_solv = -746.334360
```

IntE

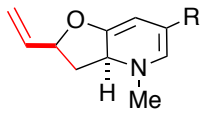

IntE
1.0

C	-0.609668	-0.937976	-0.067633
C	0.655551	-0.565103	-0.262453
C	1.064760	0.864839	-0.513993
N	0.130272	1.770545	0.129098
C	-1.192987	1.416967	0.125920
C	-1.607339	0.131050	-0.003909
O	1.756068	-1.368646	-0.231456
C	0.503356	3.168502	0.087721
C	-3.052279	-0.111935	0.055368
O	-3.345792	-1.429031	-0.011782
C	-4.735328	-1.729484	0.045803
O	-3.911003	0.740598	0.153677
C	2.491556	0.856097	0.040132
C	2.946087	-0.565120	-0.332188
C	3.994505	-1.124624	0.575612
C	5.229196	-1.414879	0.181857
H	1.104941	1.074190	-1.604020
H	-0.891202	-1.969263	0.102556
H	-1.915435	2.211878	0.284286
H	0.665138	3.510977	-0.946092
H	-0.285083	3.771340	0.541423
H	1.427043	3.327176	0.652114
H	-5.264550	-1.256286	-0.784537
H	-4.808412	-2.814268	-0.021406
H	-5.166822	-1.372408	0.983816
H	5.977147	-1.786901	0.873979
H	3.152383	1.618422	-0.377853
H	5.536040	-1.290559	-0.853762
H	2.455400	0.962959	1.130687
H	3.684827	-1.261061	1.610807
H	3.298022	-0.593383	-1.372621

0 imaginary frequencies
E = -746.368284
G = -746.149169
E_{solv} = -746.604430
G_{solv} = -746.385316

TSH

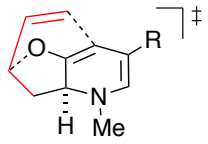

TSH: Claisen
28.9

C	-0.254878	-0.721100	-0.683411
C	1.057213	-0.496499	-1.082075
C	1.783615	0.735733	-0.607529
N	0.914934	1.767249	-0.080225
C	-0.411816	1.573672	0.077725
C	-1.046880	0.404526	-0.233162

O	1.888572	-1.397988	-1.416292
C	1.552536	3.015354	0.281586
C	-2.488105	0.344670	0.018882
O	-2.996580	-0.879388	-0.243132
C	-4.397927	-0.998520	-0.023352
O	-3.174307	1.262117	0.421288
C	2.832848	0.128042	0.445112
C	2.828431	-1.369579	0.320866
C	1.848118	-2.131273	0.986990
C	0.667321	-1.541342	1.369331
H	2.379648	1.158227	-1.425869
H	-0.732839	-1.655477	-0.953593
H	-0.982116	2.411311	0.468284
H	2.272953	2.863454	1.094648
H	2.089183	3.427733	-0.580994
H	0.799866	3.734282	0.608247
H	-4.946037	-0.297668	-0.657094
H	-4.652684	-2.026243	-0.279042
H	-4.641742	-0.789927	1.020904
H	0.615412	-0.491813	1.642276
H	3.828825	0.531955	0.254176
H	-0.172241	-2.142204	1.706454
H	2.527901	0.435064	1.450052
H	1.911568	-3.212972	0.916249
H	3.733433	-1.856506	-0.023817

1 imaginary frequency
E = -746.322863
G = -746.102787
E_{solv} = -746.560950
G_{solv} = -746.340874

TSF

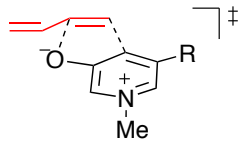

TSF: (3+2)
36.1

C	0.031304	-0.302619	0.637462
C	-1.128593	0.565570	0.929768
C	-1.062197	1.885523	0.476151
N	0.070589	2.410842	-0.092221
C	1.166446	1.656217	-0.295141
C	1.198489	0.337017	0.097736
H	0.206540	-1.076026	1.380970
O	-2.149955	0.032003	1.429277
H	-1.892060	2.565987	0.621925
C	0.068527	3.827107	-0.445862
H	-0.070578	4.432553	0.453208
H	1.019595	4.082709	-0.911760
H	-0.743795	4.031449	-1.147457
H	2.036637	2.133718	-0.728978
C	2.473838	-0.373429	-0.097239
O	3.496158	0.119791	-0.522572
O	2.379679	-1.675073	0.246045
C	3.586563	-2.418416	0.094235

H	3.912181	-2.407148	-0.948186
H	3.352762	-3.432794	0.413849
H	4.377599	-1.991355	0.714445
C	-0.806427	-1.491081	-0.611175
H	-0.702919	-0.954736	-1.552958
H	-0.089966	-2.298343	-0.486446
C	-2.113171	-1.681804	-0.140385
H	-2.301865	-2.401409	0.651215
C	-3.264199	-1.103888	-0.796178
H	-3.057856	-0.307592	-1.511678
C	-4.523625	-1.514490	-0.599106
H	-4.751056	-2.311030	0.103732
H	-5.358119	-1.069888	-1.129937

1 imaginary frequency

E = -746.298357

G = -746.084628

E_{solv} = -746.543146

G_{solv} = -746.329417

IntF

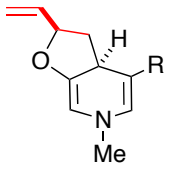

IntF
3.0

C	-0.163345	-0.077491	0.608360
C	-0.824137	1.254891	0.376413
C	-0.180582	2.388969	0.094389
N	1.222807	2.374041	-0.056965
C	1.850371	1.179253	-0.153432
C	1.239278	-0.017924	0.059339
H	-0.157685	-0.308914	1.687377
O	-2.178663	1.129952	0.379515
H	-0.682926	3.326626	-0.107656
C	1.923891	3.634210	-0.178810
H	1.886843	4.198659	0.759373
H	2.967455	3.439912	-0.430327
H	1.479819	4.244519	-0.973071
H	2.901330	1.200073	-0.427224
C	2.066934	-1.208598	-0.114566
O	3.214069	-1.236920	-0.513465
O	1.402366	-2.335889	0.243295
C	2.156840	-3.534658	0.105427
H	2.471162	-3.673551	-0.931544
H	1.494472	-4.341785	0.416730
H	3.046890	-3.503121	0.738067
C	-1.214236	-0.992107	-0.045020
H	-1.082773	-0.991487	-1.133404
H	-1.185544	-2.020770	0.313701
C	-2.520924	-0.276868	0.331410
H	-2.852075	-0.576344	1.334538
C	-3.630954	-0.470401	-0.651321
H	-3.435836	-0.086865	-1.652007
C	-4.770043	-1.090557	-0.364463
H	-4.971406	-1.466974	0.635473

```
H    -5.540113   -1.247720   -1.112382
0 imaginary frequencies
E = -746.367437
G = -746.148828
E_solv = -746.600808
G_solv = -746.382200
```

TSI

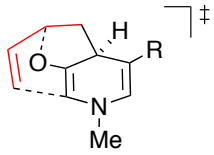

TSI: Claisen
29.8

```
C    -0.127420   -0.678568   -0.755054
C     1.306556   -0.372822   -1.081446
C     1.896942    0.787579   -0.583755
N     1.120811    1.903081   -0.267936
C    -0.209990    1.714658   -0.037839
C    -0.843897    0.533335   -0.242622
H    -0.630706   -1.092676   -1.633755
O     1.992642   -1.413418   -1.334894
H     2.954018    0.967986   -0.743953
C     1.791536    3.121159    0.145369
H     2.518642    3.420669   -0.613982
H     1.054176    3.917349    0.255770
H     2.312984    2.984230    1.101129
H    -0.770827    2.574612    0.315455
C    -2.280885    0.502310    0.056390
O    -2.956340    1.434385    0.439925
O    -2.793937   -0.733707   -0.140158
C    -4.187535   -0.847810    0.130270
H    -4.396937   -0.594477    1.172017
H    -4.446189   -1.886287   -0.072108
H    -4.758381   -0.176092   -0.514745
C     0.028369   -1.904869    0.268833
H    -0.315683   -1.583427    1.255082
H    -0.609728   -2.727972   -0.054107
C     1.472289   -2.325560    0.320310
H     1.727699   -3.327766   -0.006047
C     2.390814   -1.617868    1.120833
H     3.407263   -1.994707    1.185558
C     2.124394   -0.315488    1.479643
H     1.106012    0.031048    1.638368
H     2.896012    0.291526    1.946296
1 imaginary frequency
E = -746.323490
G = -746.103115
E_solv = -746.559853
G_solv = -746.339479
```

Diene 58

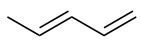

58

```
C     2.463490   -0.217057    0.000179
```

C	1.108909	0.421040	-0.000130
H	2.386283	-1.307722	-0.003197
H	3.040812	0.082928	0.882185
H	3.043951	0.088333	-0.877848
C	-0.049794	-0.245905	-0.000369
C	-1.359191	0.399092	-0.000092
C	-2.518722	-0.262567	0.000235
H	-0.041783	-1.336748	-0.000770
H	1.082053	1.511425	0.000118
H	-2.547416	-1.349210	0.000236
H	-1.360052	1.488848	-0.000130
H	-3.471994	0.254526	0.000469

0 imaginary frequencies
E = -195.201599
G = -195.112443
E_{solv} = -195.265771
G_{solv} = -195.176616

TS-66a

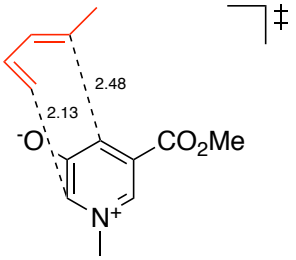

TS-66a
endo (4+3)
25.3

N	1.196436	-1.973676	0.042642
C	1.901635	-0.931334	0.592775
C	-0.127361	-1.862647	-0.210635
C	1.952192	-3.095082	-0.501991
C	-0.836095	-0.767358	0.237706
C	-0.193162	0.289084	0.918312
C	-2.289232	-0.781929	-0.056320
C	1.194212	0.153026	1.279577
O	1.836639	0.967190	1.946792
O	-2.919280	0.308604	0.415669
O	-2.864890	-1.666196	-0.650041
C	-4.323315	0.342182	0.167293
C	2.713094	1.505353	-0.618147
C	1.577047	2.341164	-0.485974
H	-4.678028	1.274832	0.602905
H	-4.812266	-0.514098	0.636520
H	-4.520388	0.316980	-0.906594
H	1.272296	-3.919729	-0.715993
H	2.693783	-3.420712	0.230046
H	2.462691	-2.794514	-1.423289
C	2.650586	0.191200	-1.049321
C	0.301922	1.974854	-0.830117
C	-0.871674	2.902659	-0.696020
H	-1.783118	2.357106	-0.435993
H	-0.686731	3.656966	0.074376
H	-1.060132	3.426332	-1.641952

H	1.817013	-0.133103	-1.671382
H	3.578647	-0.348921	-1.216998
H	0.154545	1.110360	-1.472063
H	3.654396	1.877846	-0.225103
H	1.716065	3.288888	0.029840
H	-0.612404	-2.675530	-0.736124
H	-0.772502	1.059318	1.413798
H	2.882241	-1.190107	0.977330

1 imaginary frequency

E = -785.617345

G = -785.374135

E_{solv} = -785.873661

G_{solv} = -785.630451

66a

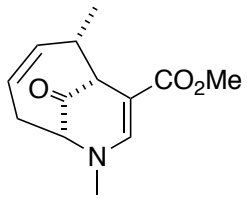

66a
–10.7

N	1.303338	-1.703355	0.288453
C	-0.035459	-1.673189	0.072647
C	-0.830403	-0.592671	0.258162
C	-0.243345	0.747955	0.615280
C	1.086629	0.551118	1.298392
C	2.013767	-0.501259	0.700708
C	-2.260999	-0.775178	0.023720
O	-2.813613	-1.814511	-0.274543
O	-2.944299	0.387575	0.170097
C	-4.348221	0.279048	-0.038238
C	2.106790	-2.792639	-0.224104
O	1.484507	1.256465	2.197984
C	-0.062472	1.667616	-0.632986
C	2.787647	0.168862	-0.461503
C	1.954963	0.463243	-1.686506
C	0.763306	1.065126	-1.750062
C	0.482108	3.048215	-0.240806
H	-0.485602	-2.609999	-0.246588
H	2.732693	-0.769707	1.483237
H	-4.750757	1.279272	0.117524
H	-4.560219	-0.067693	-1.052257
H	-4.787327	-0.426424	0.670768
H	1.504845	-3.703218	-0.252309
H	2.482526	-2.590727	-1.236681
H	2.961482	-2.961820	0.438780
H	-1.080560	1.800137	-1.015779
H	3.620179	-0.484755	-0.741618
H	3.242170	1.083509	-0.058648
H	2.391224	0.138551	-2.629154
H	0.335952	1.181835	-2.744643
H	0.489007	3.715638	-1.107126
H	-0.135551	3.499655	0.541742
H	1.505470	2.979096	0.140268
H	-0.887523	1.286416	1.316788

0 imaginary frequencies
E = -785.689479
G = -785.439764
E_{solv} = -785.937463
G_{solv} = -785.687748

TS-66b

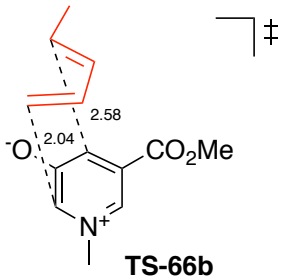

TS-66b
exo (4+3)
24.4

N	1.788388	-1.496897	0.198185
C	2.181833	-0.282910	0.709331
C	0.487147	-1.707766	-0.095889
C	2.802944	-2.317855	-0.443808
C	-0.491062	-0.875952	0.419534
C	-0.164503	0.259920	1.164541
C	-1.888295	-1.209480	0.049842
C	1.219408	0.565391	1.435772
O	1.622329	1.535875	2.085950
O	-2.756717	-0.270646	0.460612
O	-2.223594	-2.195477	-0.567081
C	-4.118236	-0.526653	0.124007
C	2.505777	0.967864	-0.869352
C	1.447514	0.887423	-1.770434
C	0.183497	1.505983	-1.594431
C	-0.205858	2.225098	-0.500321
C	-1.579845	2.814533	-0.375188
H	0.526797	2.547831	0.237536
H	2.571497	1.812023	-0.182921
H	3.468145	0.578740	-1.196244
H	1.570328	0.259003	-2.650460
H	-0.571738	1.295014	-2.351619
H	-1.550084	3.900161	-0.531296
H	-2.266236	2.381717	-1.108823
H	-1.998768	2.647343	0.622080
H	-4.683132	0.318561	0.514022
H	-4.454652	-1.460073	0.580466
H	-4.233670	-0.601894	-0.959461
H	-0.927806	0.824646	1.686154
H	0.231254	-2.592077	-0.666509
H	3.203767	-0.251682	1.076510
H	2.419453	-3.329286	-0.580795
H	3.693196	-2.353345	0.186323
H	3.064854	-1.889997	-1.419734

1 imaginary frequency
E = -785.618312
G = -785.376151
E_{solv} = -785.873967
G_{solv} = -785.631807

66b

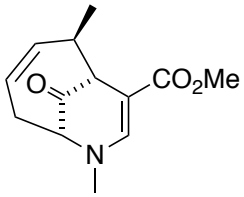

66b
–10.2

N	-1.553618	1.510382	0.112239
C	-0.222749	1.564261	-0.142650
C	0.673681	0.593177	0.161798
C	0.207505	-0.731646	0.708725
C	-1.102303	-0.536921	1.433134
C	-2.141809	0.338896	0.743594
C	2.084394	0.925114	-0.037085
O	2.904771	-0.059392	0.402664
O	2.514601	1.951612	-0.523950
C	-2.466071	2.432037	-0.529215
O	-1.399127	-1.136762	2.441203
C	-0.017994	-1.842879	-0.376298
C	-2.910145	-0.561696	-0.262845
C	-2.112733	-0.881866	-1.500828
C	-0.884106	-1.403299	-1.538415
C	1.318874	-2.369444	-0.901187
H	0.135612	2.489938	-0.586624
H	0.918327	-1.132365	1.436861
H	-2.842611	0.669358	1.518704
H	-1.946089	3.369325	-0.737641
H	-2.859069	2.032917	-1.474805
H	-3.307813	2.641539	0.138784
H	-0.527299	-2.663862	0.150899
H	-2.583828	-0.635241	-2.450153
H	-0.437859	-1.543492	-2.522466
H	1.151173	-3.213771	-1.577414
H	1.849415	-1.588674	-1.454840
H	1.965283	-2.697682	-0.083660
C	4.292819	0.206377	0.235874
H	4.812334	-0.666250	0.630116
H	4.579939	1.105731	0.785328
H	4.531781	0.351469	-0.820332
H	-3.202314	-1.471051	0.278289
H	-3.839785	-0.056878	-0.543676

0 imaginary frequencies
E = -785.688626
G = -785.438935
E_{solv} = -785.936793
G_{solv} = -785.687102

TS-66a'

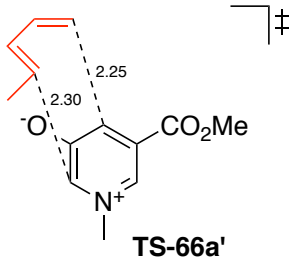

TS-66a'
endo (4+3)
26.4

N	-0.815839	1.766918	0.343631
C	-1.504294	0.699887	0.857261
C	0.492607	1.664970	0.011432
C	-1.546162	2.974202	-0.032690
C	1.197820	0.514948	0.280648
C	0.557404	-0.616758	0.845502
C	2.619860	0.508671	-0.129362
C	-0.795173	-0.468452	1.351797
O	-1.389712	-1.346337	1.980469
O	3.186979	-0.699414	0.037075
O	3.217570	1.461966	-0.577162
C	4.561853	-0.768624	-0.334597
C	-2.406218	-1.695832	-0.594305
C	-1.210139	-2.449758	-0.558883
H	4.870746	-1.793861	-0.137384
H	5.152067	-0.066715	0.258425
H	4.682579	-0.525108	-1.392369
H	-1.909982	2.898562	-1.061888
H	-0.883889	3.836560	0.054246
H	-2.394317	3.103892	0.641385
C	-2.479948	-0.360666	-0.932448
C	0.021845	-1.932315	-0.894293
H	0.963913	2.525948	-0.446514
H	1.153545	-1.415026	1.270652
H	-2.479577	0.920170	1.276578
C	-3.813959	0.334529	-1.033639
H	-1.665954	0.077622	-1.511028
H	-3.303042	-2.166978	-0.197484
H	0.906911	-2.559448	-0.863811
H	0.094426	-1.066614	-1.543865
H	-1.257769	-3.433126	-0.100526
H	-4.539455	-0.125938	-0.356173
H	-4.215572	0.264089	-2.051765
H	-3.755423	1.399021	-0.785482

E = -785.615084
G = -785.371760
E_{solv} = -785.872077
G_{solv} = -785.628754

66a'

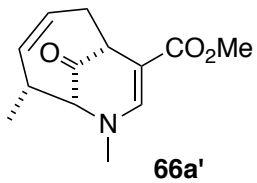

66a'
–10.4

N	-0.990826	1.660473	0.341805
C	0.343607	1.541434	0.128061
C	1.057775	0.399982	0.271302
C	0.374871	-0.902909	0.593911
C	-0.948743	-0.629729	1.267271
C	-1.794972	0.491797	0.678782
C	2.496550	0.481700	0.032383
O	3.088165	-0.735104	0.130700
O	3.126166	1.485617	-0.232654
C	-1.698396	2.844192	-0.099954
O	-1.392298	-1.320555	2.156614
C	0.120256	-1.772925	-0.668002
C	-2.598132	-0.050787	-0.538083
C	-1.739624	-0.364774	-1.743889
C	-0.621071	-1.094354	-1.796019
H	0.862189	2.454444	-0.154186
H	0.970200	-1.500064	1.289723
H	-2.516914	0.778519	1.453230
H	-1.034831	3.708599	-0.028769
H	-2.050733	2.759376	-1.136914
H	-2.562318	3.016856	0.549627
H	-0.410330	-2.682949	-0.355330
H	-3.277401	0.762863	-0.821957
C	-3.470379	-1.250014	-0.140068
H	-2.113870	0.027253	-2.688297
H	-0.176292	-1.224493	-2.780572
H	1.102088	-2.090502	-1.029823
H	-4.137121	-1.514359	-0.964886
H	-2.859153	-2.125230	0.095283
H	-4.077628	-1.020782	0.741357
C	4.495250	-0.727824	-0.084132
H	4.820393	-1.760719	0.034834
H	4.990781	-0.082644	0.644824
H	4.728518	-0.363877	-1.087435

0 imaginary frequencies
E = -785.689124
G = -785.439376
E_{solv} = -785.937030
G_{solv} = -785.687282

TS-66b'

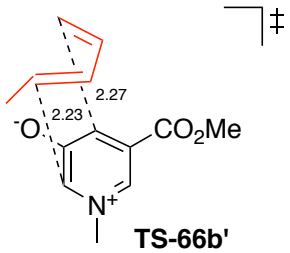

TS-66b'
exo (4+3)
27.5

N	-0.986256	1.537454	0.482412
C	-1.568412	0.426753	1.025628
C	0.310384	1.534625	0.092800
C	-1.867137	2.595040	0.010560
C	1.131714	0.470540	0.382597
C	0.601712	-0.710960	0.945463

C	2.538491	0.589025	-0.055701
C	-0.754904	-0.702519	1.469458
O	-1.260646	-1.632996	2.106132
O	3.225109	-0.552444	0.131532
O	3.032300	1.583354	-0.540097
C	4.593862	-0.495777	-0.263276
C	-2.640102	-0.711259	-0.559837
C	-1.776891	-0.655852	-1.642796
C	-0.528776	-1.307808	-1.723101
C	0.011794	-2.106950	-0.739513
C	-4.015052	-0.096037	-0.645557
H	5.006074	-1.479730	-0.045475
H	5.121035	0.276929	0.300478
H	4.673621	-0.270562	-1.328971
H	1.270502	-1.472624	1.330855
H	0.686233	2.422974	-0.400049
H	-2.516703	0.589100	1.526682
H	-2.296725	2.304349	-0.955659
H	-1.301754	3.520686	-0.101090
H	-2.673057	2.745516	0.731456
H	-4.059129	0.688144	-1.408353
H	-4.345174	0.332065	0.306986
H	-4.751535	-0.861625	-0.916307
H	-2.547083	-1.536550	0.147209
H	-0.607352	-2.592802	0.010859
H	0.992290	-2.545264	-0.900529
H	0.100296	-1.051924	-2.573190
H	-2.041937	0.012905	-2.462666

1 imaginary frequency

E = -785.615281

G = -785.371645

E_{solv} = -785.870609

G_{solv} = -785.626974

66b'

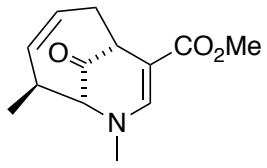

66b'

–9.4

N	-1.131269	1.382873	0.438279
C	0.202018	1.434372	0.193730
C	1.056340	0.386725	0.281305
C	0.543993	-0.995277	0.587395
C	-0.763701	-0.886265	1.333370
C	-1.771929	0.123805	0.793590
C	2.464021	0.648093	-0.005556
O	3.198642	-0.491845	0.029408
O	2.959130	1.727700	-0.258559
C	-1.964564	2.528185	0.132866
O	-1.080497	-1.635112	2.229297
C	0.314746	-1.852455	-0.696063
C	-2.524700	-0.595807	-0.376611
C	-1.700263	-0.629435	-1.642487
C	-0.486230	-1.168385	-1.776928

H	0.596494	2.412053	-0.072547
H	1.235926	-1.543915	1.231442
H	-2.492655	0.312100	1.598213
H	-1.414244	3.446761	0.351773
H	-2.276144	2.551594	-0.919376
H	-2.859663	2.503315	0.761199
H	-0.166878	-2.792579	-0.393309
C	-3.916240	-0.010430	-0.631936
H	-2.148908	-0.151469	-2.512947
H	-0.011526	-1.096773	-2.752856
H	1.303746	-2.108885	-1.084406
H	-2.672341	-1.624524	-0.015806
H	-4.461550	-0.642769	-1.339055
H	-4.498976	0.041704	0.292643
H	-3.864563	0.993263	-1.063017
C	4.585345	-0.310159	-0.234837
H	5.034903	-1.299837	-0.162669
H	5.029527	0.367771	0.497497
H	4.734523	0.108330	-1.232926

0 imaginary frequencies
E = -785.686729
G = -785.437329
E_{solv} = -785.935221
G_{solv} = -785.685822

Diene 84

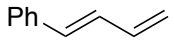

84

C	-0.897131	-0.670731	0.056758
C	-1.967228	0.136517	-0.015531
C	-3.337918	-0.352599	0.018532
C	-4.412965	0.437650	-0.054910
H	-1.843534	1.214529	-0.110231
H	-1.073572	-1.743956	0.135321
H	-4.314285	1.516206	-0.146319
H	-3.465215	-1.430751	0.110002
H	-5.419966	0.036346	-0.026385
C	3.247428	0.390032	-0.032802
C	2.279969	1.393433	0.018123
C	0.930967	1.067583	0.051396
C	0.515317	-0.272167	0.030952
C	1.499237	-1.268373	-0.014019
C	2.851178	-0.943790	-0.047316
H	4.301382	0.648436	-0.057324
H	2.580626	2.436591	0.035840
H	0.193380	1.862610	0.102164
H	1.193158	-2.311470	-0.026115
H	3.594908	-1.733866	-0.084046

0 imaginary frequencies
E = -386.867651
G = -386.730834
E_{solv} = -386.984828
G_{solv} = -386.848011

TS-86a

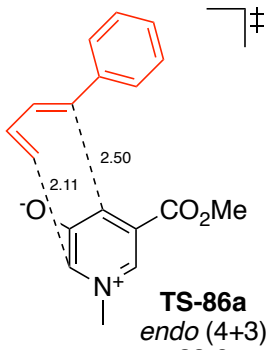

TS-86a
endo (4+3)
23.6

N	-3.115832	0.872294	0.010013
C	-2.956541	-0.400445	0.508577
C	-2.056777	1.698068	-0.147376
C	-4.398936	1.207594	-0.596106
C	-0.823181	1.357100	0.368554
C	-0.625237	0.127109	1.021390
C	0.282046	2.321652	0.139271
C	-1.744823	-0.744126	1.258601
O	-1.686523	-1.816741	1.865941
O	1.420253	1.921986	0.720136
O	0.181573	3.343085	-0.504023
C	2.553216	2.748718	0.471876
C	-1.809604	-2.671590	-0.749307
C	-0.420750	-2.519190	-0.530644
H	3.393415	2.243001	0.944981
H	2.399293	3.742599	0.898687
H	2.722664	2.843580	-0.603419
H	-4.516713	0.678178	-1.547725
H	-4.447076	2.282459	-0.770095
H	-5.205244	0.916100	0.079716
C	-2.637225	-1.639142	-1.166365
C	0.268632	-1.357150	-0.784251
H	-2.215128	-0.804967	-1.726109
H	-3.669894	-1.870778	-1.414019
H	-0.184955	-0.608210	-1.428296
H	-2.262989	-3.609433	-0.443534
H	0.102257	-3.343893	-0.053250
H	-2.218047	2.638966	-0.658721
H	0.300745	-0.073820	1.546669
H	-3.873901	-0.890218	0.817416
C	4.436544	-0.745018	-0.048255
C	3.797841	-0.081736	-1.093870
C	2.441724	-0.286344	-1.324594
C	1.701549	-1.168978	-0.527035
C	2.352279	-1.819904	0.530969
C	3.705880	-1.610965	0.764986
H	5.494341	-0.584731	0.136152
H	4.357092	0.597882	-1.730731
H	1.943475	0.237338	-2.137742
H	1.776735	-2.462699	1.192213
H	4.192499	-2.117962	1.592756

1 imaginary frequency
E = -977.287602
G = -976.995807
E_{solv} = -977.596311

G_{solv} = -977.304516

86a

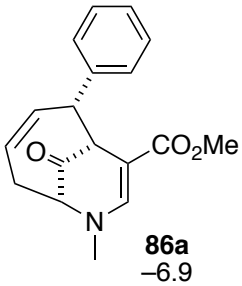

86a
–6.9

N	2.322080	-1.754169	-0.424881
C	2.614450	-0.454379	-0.178084
C	1.733902	0.570959	-0.267518
C	0.276548	0.320525	-0.545686
C	0.108257	-0.995914	-1.262208
C	0.966601	-2.158258	-0.772005
C	2.247441	1.914163	-0.011136
O	3.400269	2.211029	0.226935
O	1.259242	2.844729	-0.058084
C	1.692900	4.180186	0.178205
C	3.238658	-2.804638	-0.035663
O	-0.730638	-1.190436	-2.110390
C	-0.577753	0.333342	0.769632
C	0.216640	-2.817029	0.407287
C	0.149685	-1.984038	1.665172
C	-0.175979	-0.694430	1.804480
H	3.647899	-0.240830	0.083808
H	-0.138670	1.093664	-1.197675
H	1.017213	-2.881079	-1.594356
H	0.800575	4.800793	0.104392
H	2.141796	4.268105	1.170176
H	2.432245	4.480078	-0.567760
H	4.260166	-2.419709	-0.059019
H	3.031400	-3.183600	0.974417
H	3.164895	-3.636908	-0.743078
H	0.698969	-3.773052	0.635824
H	-0.790330	-3.061799	0.043521
H	0.383780	-2.522781	2.581557
H	-0.182287	-0.314187	2.824458
H	-0.358079	1.315666	1.204089
C	-4.773138	0.400129	-0.286267
C	-3.972721	1.529797	-0.448370
C	-2.631800	1.488285	-0.087514
C	-2.064926	0.322772	0.438817
C	-2.874691	-0.799859	0.602092
C	-4.220378	-0.761765	0.240417
H	-5.821538	0.428910	-0.566386
H	-4.395612	2.444272	-0.853159
H	-2.005583	2.370023	-0.212473
H	-2.457262	-1.704872	1.033402
H	-4.837309	-1.645168	0.374828

0 imaginary frequencies
E = -977.349504
G = -977.051500
E_{solv} = -977.651148

G_{solv} = -977.353144

TS-86a'

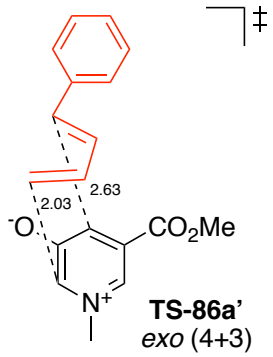

TS-86a'
exo (4+3)
24.0

N	-3.242066	0.452936	0.287900
C	-2.897699	-0.829924	0.648773
C	-2.274126	1.369274	0.077083
C	-4.551012	0.652718	-0.315053
C	-0.994745	1.158095	0.567147
C	-0.646662	-0.032700	1.197946
C	0.013059	2.209250	0.267795
C	-1.619859	-1.086822	1.340204
O	-1.401342	-2.191842	1.849212
O	1.232624	1.857439	0.690593
O	-0.224073	3.243046	-0.315865
C	2.281618	2.763733	0.361863
C	-2.499133	-1.842355	-1.065310
C	-1.688635	-1.080337	-1.906727
C	-0.290686	-0.909358	-1.756880
C	0.455354	-1.431695	-0.735122
H	0.015865	-2.181066	-0.079741
H	-2.067567	-2.659635	-0.487385
H	-3.521099	-2.019941	-1.394674
H	-2.166863	-0.528567	-2.713492
H	0.182305	-0.219747	-2.453085
H	3.193282	2.303050	0.738902
H	2.105993	3.735163	0.829777
H	2.340549	2.893871	-0.721460
H	0.319781	-0.150326	1.673586
H	-2.547779	2.300487	-0.403872
H	-3.730900	-1.456034	0.955348
H	-4.784772	1.717468	-0.332084
H	-5.305510	0.128338	0.273557
H	-4.551504	0.260890	-1.339962
C	4.563957	-0.631382	0.147897
C	3.994985	-0.095336	-1.007430
C	2.666185	-0.351445	-1.321946
C	1.874350	-1.157875	-0.489823
C	2.463181	-1.697146	0.664325
C	3.790101	-1.434553	0.982968
H	5.602421	-0.428462	0.390764
H	4.592315	0.526403	-1.668357
H	2.245298	0.076562	-2.226923
H	1.851877	-2.312525	1.321466
H	4.221694	-1.858472	1.884559

1 imaginary frequency
E = -977.288938
G = -976.996518
E_{solv} = -977.596322
G_{solv} = -977.303903

86a'

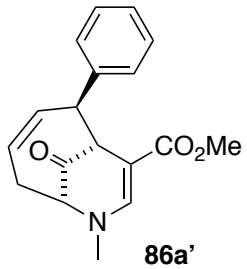

86a'
–7.0

N	-2.794474	1.027680	-0.274975
C	-1.553845	1.569634	-0.368104
C	-0.447115	1.092234	0.249060
C	-0.490084	-0.219812	0.983231
C	-1.888359	-0.482864	1.482507
C	-3.034542	-0.157605	0.532600
C	0.764849	1.915144	0.169905
O	1.730691	1.470757	1.000749
O	0.909407	2.893714	-0.535371
C	-3.839678	1.412055	-1.198215
O	-2.122157	-1.048715	2.526339
C	-0.044388	-1.452293	0.105509
C	-3.273773	-1.426302	-0.321748
C	-2.186437	-1.708429	-1.325379
C	-0.861797	-1.697690	-1.147424
C	1.429246	-1.298026	-0.216527
C	1.853119	-0.574281	-1.334241
C	3.208788	-0.358059	-1.566774
C	4.159738	-0.864611	-0.684214
C	3.745840	-1.587503	0.432194
C	2.389938	-1.800854	0.661226
H	-1.479909	2.484712	-0.950950
H	0.168265	-0.206885	1.855626
H	-3.923670	0.010898	1.151773
H	-3.666069	2.436704	-1.533491
H	-3.874448	0.757646	-2.080356
H	-4.810836	1.371003	-0.693981
H	-0.158767	-2.326283	0.763957
H	-4.230600	-1.322031	-0.843461
H	-3.393904	-2.263244	0.378238
H	-2.535755	-1.966168	-2.323292
H	-0.264378	-1.959146	-2.018415
H	1.116147	-0.152764	-2.013596
H	3.520623	0.212018	-2.436912
H	5.217149	-0.697989	-0.865937
H	4.479921	-1.989753	1.123921
H	2.069638	-2.358882	1.538341
C	2.962543	2.176641	0.918141
H	3.649131	1.649824	1.580023
H	2.832988	3.213993	1.236838

H	3.337998	2.162266	-0.107698

0 imaginary frequencies
E = -977.351475
G = -977.052717
E_{solv} = -977.652022
G_{solv} = -977.353264

TS-86b

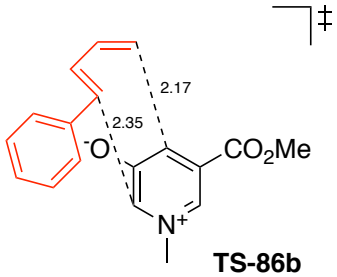

TS-86b
endo (4+3)
26.6

N	-0.111791	-1.447891	0.775530
C	0.364079	-0.223612	1.144689
C	-1.390806	-1.608016	0.357884
C	0.831667	-2.558177	0.652020
C	-2.269547	-0.551576	0.367240
C	-1.837803	0.755636	0.729862
C	-3.639311	-0.834936	-0.114511
C	-0.531192	0.895909	1.353342
O	-0.115985	1.952595	1.836548
O	-4.376761	0.285254	-0.222043
O	-4.062807	-1.933247	-0.398527
C	-5.712398	0.077645	-0.676820
C	1.034439	2.051616	-0.671550
C	-0.268418	2.559153	-0.852639
H	-6.172717	1.063941	-0.704048
H	-6.249727	-0.580487	0.009304
H	-5.709565	-0.375343	-1.670568
H	1.295980	-2.553807	-0.337569
H	0.301947	-3.498565	0.809013
H	1.612466	-2.448028	1.405888
C	1.368413	0.712199	-0.766006
C	-1.360162	1.756367	-1.135856
H	0.718595	0.046232	-1.334406
H	-1.212274	0.798856	-1.624294
H	1.799844	2.745409	-0.333069
H	-0.434517	3.603271	-0.605773
H	-1.695229	-2.598023	0.040897
H	-2.576885	1.506694	0.982579
H	1.330905	-0.214126	1.633611
C	5.374963	-0.685157	-0.166507
C	4.584235	-1.233503	-1.173854
C	3.284130	-0.777784	-1.367837
C	2.750078	0.237066	-0.563526
C	3.551645	0.771582	0.455882
C	4.852220	0.318468	0.647491
H	6.388886	-1.040774	-0.013054
H	4.982972	-2.014529	-1.814387
H	2.674763	-1.197814	-2.165495

H	3.130231	1.529651	1.112759
H	5.457204	0.742917	1.443055
H	-2.333307	2.205674	-1.306800

1 imaginary frequency
E = -977.285762
G = -976.993618
E_{solv} = -977.591855
G_{solv} = -977.299712

86b

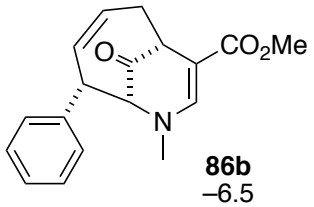

86b
–6.5

N	0.562334	2.046394	0.229760
C	1.826013	1.567924	0.108302
C	2.191783	0.279107	0.299985
C	1.163997	-0.783120	0.586504
C	-0.089603	-0.154917	1.150190
C	-0.550643	1.149702	0.509804
C	3.611870	-0.035297	0.159492
O	4.504263	0.755367	-0.070367
O	3.846160	-1.362746	0.310431
C	5.214174	-1.739166	0.195750
C	0.240600	3.384967	-0.219265
O	-0.767633	-0.686219	1.997951
C	0.782273	-1.595560	-0.676989
C	-1.397026	0.844895	-0.768705
C	-0.611537	0.204153	-1.891217
C	0.279506	-0.792638	-1.853338
C	-2.676295	0.107416	-0.390040
C	-2.861968	-1.252855	-0.630572
C	-4.035513	-1.888522	-0.230468
C	-5.038865	-1.172199	0.412984
C	-4.865827	0.189554	0.651622
C	-3.694392	0.820240	0.250396
H	2.590028	2.301266	-0.137558
H	-1.215202	1.634903	1.234129
H	5.240212	-2.817716	0.346671
H	5.602413	-1.479089	-0.791708
H	5.815978	-1.230756	0.952375
H	1.107733	4.032678	-0.073971
H	-0.043677	3.416484	-1.279722
H	-0.588661	3.779694	0.376497
H	0.033682	-2.345198	-0.384465
H	1.677487	-2.145396	-0.980673
H	-1.714353	1.831454	-1.131156
H	-0.839150	0.609959	-2.875355
H	0.696624	-1.088570	-2.814229
H	-2.092449	-1.814605	-1.150625
H	-4.164076	-2.948698	-0.426018
H	-5.952630	-1.669051	0.723471
H	-5.645477	0.760891	1.145999
H	-3.566802	1.885991	0.432698

H	1.528375	-1.492307	1.334581

0 imaginary frequencies
E = -977.348154
G = -977.050545
E_{solv} = -977.650081
G_{solv} = -977.352472

TS-86b'

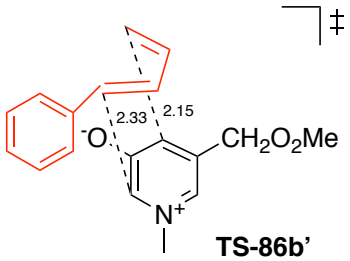

TS-86b'
exo (4+3)
28.3

N	-0.119997	1.231159	-0.917121
C	0.381648	-0.009405	-1.156935
C	-1.414960	1.420437	-0.556250
C	0.832309	2.325097	-0.768736
C	-2.290836	0.366699	-0.506062
C	-1.813772	-0.964605	-0.641353
C	-3.685081	0.683883	-0.137033
C	-0.483124	-1.178419	-1.202519
O	-0.043391	-2.284309	-1.537223
O	-4.420771	-0.426110	0.059750
O	-4.132245	1.802155	-0.008122
C	-5.782078	-0.184226	0.408101
C	1.477470	-0.763177	0.755523
C	0.667264	-0.270857	1.766852
C	-0.642070	-0.717626	2.013900
C	-1.295027	-1.714208	1.300864
H	-0.736754	-2.499809	0.794790
H	1.228483	-1.728031	0.316328
H	1.015255	0.575174	2.357129
H	-1.222911	-0.151620	2.738684
H	-6.237776	-1.166428	0.522643
H	-6.281407	0.383320	-0.380093
H	-5.841829	0.380774	1.340851
H	-2.528144	-1.767458	-0.790959
H	-1.733109	2.437240	-0.360491
H	1.344774	-0.050801	-1.652148
H	1.641371	2.202506	-1.490867
H	1.254451	2.299826	0.241873
H	0.326112	3.275896	-0.938477
H	-2.300721	-1.985118	1.609227
C	5.497281	0.417716	-0.154577
C	4.871988	-0.613925	-0.850524
C	3.570630	-0.983105	-0.529445
C	2.862404	-0.330856	0.491967
C	3.506348	0.704268	1.185113
C	4.807982	1.072418	0.865195
H	6.513843	0.707726	-0.400556
H	5.399210	-1.134995	-1.643791
H	3.076179	-1.785656	-1.073998

H	2.993869	1.222354	1.990944
H	5.290089	1.872444	1.419045

1 imaginary frequency
E = -977.284756
G = -976.991944
E_{solv} = -977.589860
G_{solv} = -977.297048

86b'

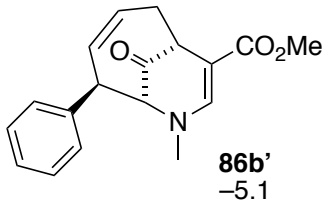

86b'
–5.1

N	0.305504	0.773152	-0.965469
C	-0.953152	1.194318	-0.674437
C	-1.998014	0.389585	-0.371377
C	-1.875630	-1.110782	-0.403651
C	-0.621540	-1.536121	-1.126454
C	0.607705	-0.653805	-0.956043
C	-3.257791	1.048593	-0.025550
O	-4.241122	0.148313	0.223845
O	-3.450522	2.245698	0.032135
C	1.185632	1.638799	-1.736696
O	-0.526254	-2.592706	-1.710081
C	-1.827299	-1.748052	1.008547
C	1.351047	-1.105466	0.343913
C	0.560085	-0.988458	1.632628
C	-0.719135	-1.262839	1.906005
C	2.664459	-0.351185	0.426263
C	3.797018	-0.848944	-0.221513
C	4.985404	-0.124207	-0.236811
C	5.055070	1.113639	0.398207
C	3.931816	1.617915	1.049366
C	2.744867	0.890254	1.063596
H	-1.105861	2.270997	-0.687795
H	-2.722172	-1.558649	-0.932428
H	1.269601	-0.876424	-1.799215
H	1.016383	2.676098	-1.437736
H	2.228242	1.388897	-1.532547
H	0.998733	1.545962	-2.815095
H	-1.754915	-2.837150	0.884643
H	-2.789795	-1.545025	1.485971
H	1.579341	-2.168194	0.174065
H	1.171059	-0.689581	2.482097
H	-1.007851	-1.141720	2.948491
H	3.744084	-1.814052	-0.720991
H	5.857705	-0.528008	-0.741528
H	5.980722	1.680531	0.388357
H	3.978071	2.582568	1.545630
H	1.863595	1.295973	1.553743
C	-5.503309	0.723663	0.544206
H	-6.177512	-0.114347	0.717125
H	-5.862954	1.341971	-0.281341
H	-5.425215	1.346206	1.438445

0 imaginary frequencies

E = -977.349898
G = -977.051780
E_{solv} = -977.648476
G_{solv} = -977.350358

Diene 89

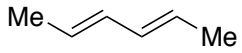

89

C	3.179329	-0.139253	0.000005
C	1.795888	0.434483	-0.000109
H	3.153001	-1.232488	-0.000308
H	3.744271	0.188542	0.880269
H	3.744654	0.189082	-0.879794
C	0.670303	-0.287368	0.000081
C	-0.670303	0.287368	0.000065
C	-1.795888	-0.434482	-0.000125
C	-3.179329	0.139253	0.000012
H	-3.744282	-0.188583	0.880255
H	-3.153002	1.232488	-0.000253
H	-3.744643	-0.189043	-0.879809
H	0.734778	-1.376512	0.000258
H	1.717148	1.522235	-0.000221
H	-1.717147	-1.522234	-0.000215
H	-0.734777	1.376512	0.000247

E = -234.499371
G = -234.384025
E_{solv} = -234.574742
G_{solv} = -234.459396

TS-90a

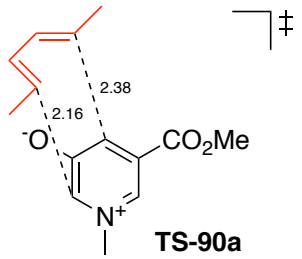

TS-90a
endo (4+3)
28.0

N	0.964870	-1.880645	0.166146
C	1.614505	-0.832033	0.778092
C	-0.346428	-1.806362	-0.157108
C	1.749499	-3.009154	-0.323367
C	-1.109814	-0.728371	0.233061
C	-0.520330	0.364334	0.911787
C	-2.546414	-0.797744	-0.120716
C	0.833850	0.239025	1.397608
O	1.394291	1.066418	2.119213
O	-3.239517	0.263260	0.331680
O	-3.063225	-1.702588	-0.737800
C	-4.632759	0.239990	0.028564
C	2.478149	1.639800	-0.337812
C	1.276451	2.377863	-0.362986
H	-5.042744	1.154680	0.453612

H	-5.103629	-0.638393	0.474946
H	-4.787112	0.212497	-1.052306
H	2.153374	-2.796049	-1.318290
H	1.113834	-3.894049	-0.373913
H	2.574277	-3.198559	0.366182
C	2.608884	0.323018	-0.758425
C	0.073687	1.886661	-0.816254
C	-1.163388	2.737540	-0.890309
H	-2.069334	2.143075	-0.745329
H	-1.141163	3.522776	-0.128618
H	-1.238226	3.223179	-1.871424
H	1.885394	-0.053671	-1.483176
C	3.983628	-0.300819	-0.821838
H	0.077117	1.000493	-1.446537
H	3.328184	2.094077	0.166621
H	1.279590	3.347957	0.129553
H	-0.778741	-2.640008	-0.696637
H	-1.143864	1.125344	1.367291
H	2.559818	-1.086018	1.246732
H	3.958481	-1.391504	-0.737278
H	4.612304	0.080571	-0.011044
H	4.478839	-0.061096	-1.769937

1 imaginary frequency

E = -824.912220

G = -824.642027

E_{solv} = -825.179162

G_{solv} = -824.908970

90a

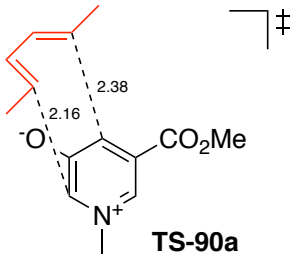

TS-90a

endo (4+3)

28.0

N	-0.909889	1.894668	0.235082
C	0.418924	1.739361	0.025504
C	1.108595	0.591625	0.223883
C	0.407028	-0.680778	0.620690
C	-0.920495	-0.361934	1.264601
C	-1.738412	0.769944	0.652675
C	2.550336	0.639886	-0.007398
O	3.193378	1.615960	-0.337262
O	3.130261	-0.571167	0.187741
C	4.539432	-0.591478	-0.011776
C	-1.587716	3.099195	-0.196697
O	-1.394656	-1.024402	2.161274
C	0.190870	-1.631106	-0.589982
C	-2.597809	0.212083	-0.508863
C	-1.809387	-0.357461	-1.667943
C	-0.694607	-1.096369	-1.694720
C	-0.290675	-3.017852	-0.140594
H	0.956344	2.626097	-0.301287

H	-2.422410	1.119162	1.436409
H	4.853295	-1.616273	0.183228
H	4.786647	-0.301354	-1.035571
H	5.033616	0.098990	0.675459
H	-0.892271	3.939904	-0.150574
H	-1.972476	3.021972	-1.221972
H	-2.426208	3.307465	0.475645
H	1.192351	-1.752507	-1.019458
H	-3.154035	1.075688	-0.896783
C	-3.642636	-0.793284	-0.003936
H	-2.275776	-0.172757	-2.635241
H	-0.382219	-1.426221	-2.685332
H	-0.398411	-3.685583	-1.000483
H	0.426852	-3.463544	0.555337
H	-1.257594	-2.957087	0.366483
H	0.993873	-1.233501	1.360977
H	-4.291640	-1.102391	-0.827917
H	-4.265127	-0.348838	0.779423
H	-3.168139	-1.686023	0.409386

0 imaginary frequencies

E = -824.982971

G = -824.706154

E_{solv} = -825.241336

G_{solv} = -824.964520

TS-90b

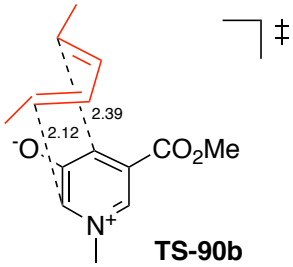

TS-90b
exo (4+3)
28.4

N	1.270945	-1.673163	0.304360
C	1.761149	-0.561291	0.943763
C	-0.024545	-1.736622	-0.080337
C	2.229064	-2.586132	-0.299091
C	-0.939956	-0.807771	0.362126
C	-0.527634	0.309808	1.112215
C	-2.336301	-0.999315	-0.087557
C	0.840383	0.390240	1.578534
O	1.277884	1.272965	2.325254
O	-3.136933	0.008566	0.303426
O	-2.732365	-1.938962	-0.740928
C	-4.496390	-0.114514	-0.106526
C	2.592117	0.788148	-0.459829
C	1.677636	0.842363	-1.509780
C	0.413706	1.462232	-1.469026
C	-0.132670	2.121689	-0.390406
C	-1.483207	2.776943	-0.485066
H	0.508341	2.455630	0.424208
H	2.515004	1.539822	0.328058
C	3.999656	0.301778	-0.723175
H	1.929133	0.295470	-2.419229

H	-0.229455	1.309588	-2.335729
H	-1.376570	3.823154	-0.798809
H	-2.120087	2.267349	-1.214142
H	-2.004190	2.779047	0.476044
H	-5.002833	0.769099	0.278801
H	-4.938387	-1.023857	0.306428
H	-4.563200	-0.153525	-1.196068
H	-1.260698	0.938474	1.604295
H	-0.326223	-2.580368	-0.689190
H	2.722172	-0.697171	1.430515
H	1.759950	-3.558495	-0.454111
H	3.088866	-2.700045	0.363842
H	2.566997	-2.183252	-1.261352
H	4.037625	-0.378596	-1.580083
H	4.439238	-0.209253	0.140011
H	4.650977	1.153174	-0.951093

1 imaginary frequency

E = -824.912636

G = -824.642582

E_{solv} = -825.178338

G_{solv} = -824.908285

90b

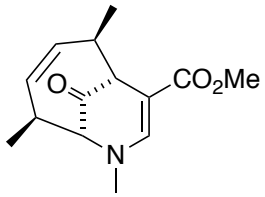

90b

–6.0

N	-1.271422	1.517914	0.134436
C	0.055136	1.561938	-0.140540
C	0.952293	0.586334	0.147652
C	0.485732	-0.723084	0.729795
C	-0.789791	-0.480228	1.500991
C	-1.854630	0.366704	0.809150
C	2.359417	0.902337	-0.093174
O	3.181611	-0.088636	0.329119
O	2.786510	1.921340	-0.598384
C	-2.157379	2.522616	-0.415799
O	-1.042662	-1.021163	2.553437
C	0.204973	-1.843495	-0.334392
C	-2.649420	-0.611278	-0.123176
C	-1.892287	-0.866222	-1.403177
C	-0.662751	-1.378027	-1.484614
C	1.515273	-2.420312	-0.871895
H	0.411397	2.483063	-0.595639
H	1.214778	-1.123385	1.439785
H	-2.533783	0.725075	1.592074
H	-1.628179	3.476752	-0.479058
H	-2.516858	2.257549	-1.418712
H	-3.021458	2.647673	0.243679
H	-0.325070	-2.640217	0.209835
C	-4.083349	-0.147669	-0.391748
H	-2.718999	-1.547354	0.450093
H	-2.392130	-0.568489	-2.324670
H	-0.218981	-1.472564	-2.474971

H	1.310409	-3.262677	-1.540282
H	2.065693	-1.661520	-1.436409
H	2.160232	-2.765576	-0.060027
H	-4.635788	-0.934054	-0.914899
H	-4.115068	0.747443	-1.019050
H	-4.609083	0.068952	0.542980
C	4.567293	0.163590	0.126188
H	5.088614	-0.712222	0.510935
H	4.876469	1.062345	0.664571
H	4.781025	0.302253	-0.936243

0 imaginary frequencies
E = -824.980589
G = -824.703941
E_{solv} = -825.239758
G_{solv} = -824.963111

157

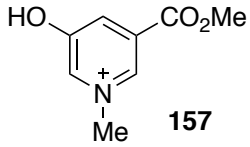

157

N	1.858977	-0.964200	0.000005
C	2.366451	0.283359	-0.000001
C	0.536533	-1.188635	0.000003
C	2.807507	-2.102147	-0.000011
C	-0.343258	-0.115647	-0.000009
C	0.139839	1.184368	-0.000009
C	-1.810796	-0.455558	-0.000006
C	1.524701	1.392538	0.000003
O	2.124052	2.583692	0.000053
O	-2.563580	0.631972	-0.000023
O	-2.197322	-1.595033	0.000011
C	-3.986720	0.393472	0.000014
H	-4.445215	1.378941	0.000392
H	-4.262597	-0.169936	0.892098
H	-4.262733	-0.169299	-0.892432
H	2.240534	-3.030634	0.000149
H	3.426002	-2.043024	0.895961
H	3.425778	-2.043188	-0.896150
H	-0.557356	2.017905	0.000019
H	3.444977	0.391848	-0.000011
H	0.181927	-2.212759	0.000013
H	1.485102	3.313987	-0.000319

0 imaginary frequencies
E = -590.818077
G = -590.674599
E_{solv} = -591.084255
G_{solv} = -590.940777

Cat TS-157

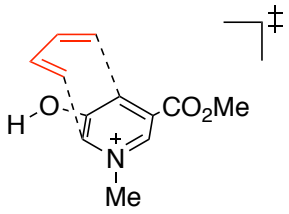

TS-157
endo (4+3)
22.1

N	-0.932284	1.832220	0.171320
C	-1.760292	0.735231	0.508645
C	0.379975	1.641266	-0.075900
C	-1.593771	3.087312	-0.179440
C	1.020969	0.466592	0.226560
C	0.297867	-0.589268	0.853303
C	2.468756	0.374829	-0.092367
C	-1.041823	-0.379789	1.118524
O	-1.745943	-1.291407	1.770685
O	2.956103	-0.833929	0.198686
O	3.105958	1.282488	-0.566841
C	4.360431	-0.998398	-0.059537
C	-2.861898	-1.277973	-0.872764
C	-1.892014	-2.280336	-0.858162
H	4.594536	-2.019074	0.234193
H	4.932633	-0.281536	0.531059
H	4.564515	-0.839252	-1.119403
H	-0.843956	3.873097	-0.263962
H	-2.301207	3.357356	0.607962
H	-2.125884	2.993446	-1.132199
C	-2.518488	0.107843	-0.980599
C	-0.547844	-1.994920	-1.019934
H	0.198967	-2.774218	-0.901398
H	-1.696441	0.317219	-1.668980
H	-3.362704	0.773755	-1.153251
H	-0.214772	-1.100965	-1.533257
H	-3.896489	-1.549396	-0.677232
H	-2.190988	-3.289651	-0.591792
H	0.938521	2.475200	-0.490066
H	0.810961	-1.437486	1.293240
H	-2.627017	1.066413	1.085002
H	-2.654837	-1.002009	1.950618

1 imaginary frequency
E = -746.698985
G = -746.469725
E_{solv} = -747.027554
G_{solv} = -746.798294

3'Me_3NH^+

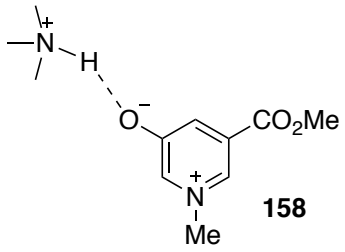

158

N	1.695409	2.314856	-0.000031
C	0.350017	2.304183	-0.000697
C	2.422045	1.187622	0.000271
C	2.377504	3.624458	0.000817
C	1.760916	-0.036059	-0.000145
C	0.380148	-0.092464	-0.000846
C	2.638003	-1.253819	0.000111
C	-0.400830	1.100265	-0.001125
O	-1.674424	1.143992	-0.001796
O	1.933191	-2.382554	-0.000303
O	3.841201	-1.188743	0.000623
C	2.721341	-3.583913	-0.000154
H	2.006245	-4.403351	-0.000592
H	3.350656	-3.615102	0.890522
H	3.351422	-3.614820	-0.890299
H	3.453530	3.463149	-0.001575
H	2.086774	4.173803	0.896647
H	2.083317	4.176721	-0.892066
H	-0.116502	-1.057817	-0.001296
H	-0.151733	3.264333	-0.000915
H	3.501525	1.260736	0.000806
H	-2.649811	0.071524	-0.000778
N	-3.630859	-0.442722	0.000283
C	-4.318590	0.039941	-1.221983
C	-4.313259	0.033931	1.227863
H	-3.761848	-0.298681	-2.096492
H	-4.330949	1.130005	-1.200792
H	-5.337752	-0.353106	-1.250950
H	-3.752989	-0.309312	2.098311
H	-5.332415	-0.358950	1.259155
H	-4.325395	1.124094	1.212232
C	-3.461712	-1.912529	-0.003735
H	-2.910095	-2.205302	-0.898439
H	-4.442704	-2.394353	-0.002882
H	-2.906385	-2.209763	0.887194

0 imaginary frequencies
E = -765.235815
G = -764.979212
E_{solv} = -765.545297
G_{solv} = -765.288694

Cat TS-158

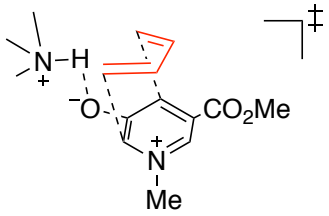

TS-158
exo (4+3)
25.3

N	1.785144	-1.807868	-1.063190
C	0.521510	-2.080272	-0.554933
C	2.295790	-0.575682	-0.885297
C	2.669906	-2.934685	-1.339208
C	1.477524	0.492492	-0.573022
C	0.093476	0.319623	-0.404104
C	2.147719	1.811062	-0.414950
C	-0.447112	-0.983745	-0.481274
O	-1.673265	-1.297101	-0.349527
O	1.284132	2.772801	-0.064571
O	3.331685	1.987544	-0.569885
C	1.871951	4.070633	0.098497
C	0.703431	-2.543685	1.287084
C	1.475184	-1.594521	1.980942
C	0.976734	-0.353636	2.442289
C	-0.288303	0.094897	2.204615
H	-0.580413	1.091687	2.521357
H	-1.078450	-0.558031	1.845673
H	-0.370341	-2.573841	1.476883
H	1.145323	-3.533305	1.185194
H	2.530458	-1.803332	2.138329
H	1.686445	0.321541	2.913904
H	1.054420	4.732272	0.377545
H	2.331990	4.394323	-0.836614
H	2.632736	4.041786	0.880315
H	-0.557917	1.184122	-0.334466
H	3.352415	-0.424724	-1.078268
H	0.101572	-3.021769	-0.900833
H	3.521938	-2.587085	-1.922921
H	2.128313	-3.687899	-1.913361
H	3.027495	-3.376564	-0.401643
H	-2.720010	-0.290842	-0.278065
N	-3.655712	0.305298	-0.295862
C	-3.638455	1.270686	0.826637
C	-4.748481	-0.688020	-0.150620
C	-3.709253	0.985360	-1.611684
H	-2.782478	1.938261	0.710244
H	-3.549535	0.720828	1.764892
H	-4.563039	1.853521	0.824788
H	-4.629781	-1.201253	0.804274
H	-5.715326	-0.180299	-0.188465
H	-4.668922	-1.412046	-0.962148
H	-3.642263	0.230921	-2.396539
H	-4.646628	1.539606	-1.702517
H	-2.864172	1.671125	-1.692166

1 imaginary frequency

E = -921.1256315
G = -920.7839393
E_{solv} = -921.4828464
G_{solv} = -921.1411542

APPENDIX II

^{1}H NMR and ^{13}C NMR Spectra

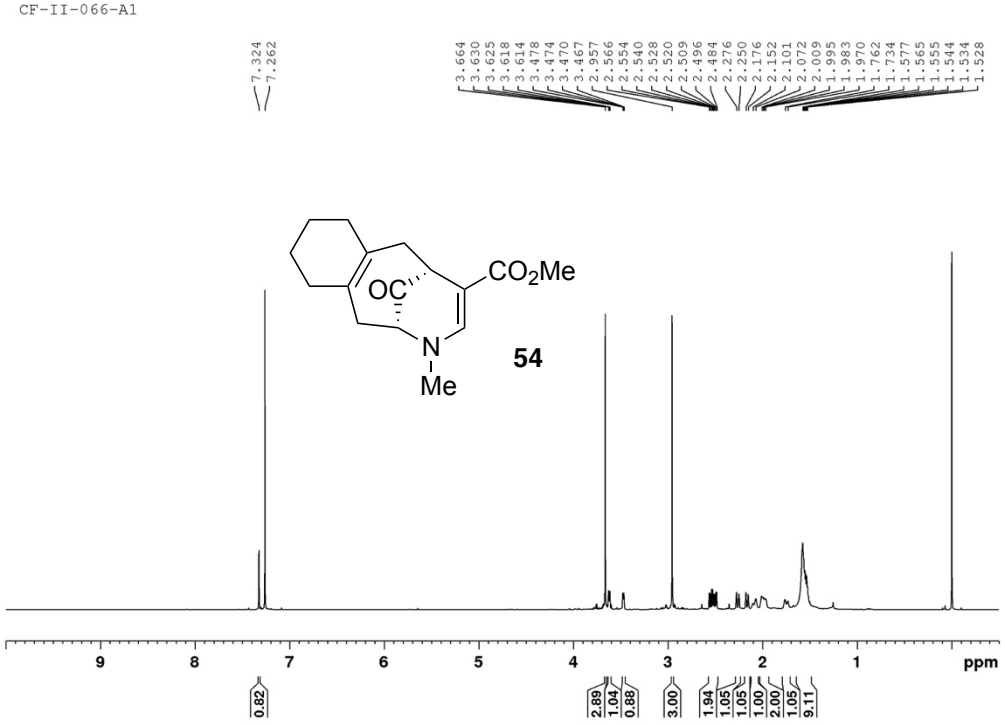
CF-II-066-A1
7.324
7.262
3.664
3.630
3.625
3.618
3.614
3.478
3.474
3.470
3.467
2.957
2.566
2.554
2.540
2.528
2.520
2.509
2.496
2.484
2.276
2.250
2.176
2.152
2.101
2.072
2.009
1.995
1.983
1.970
1.762
1.734
1.577
1.565
1.555
1.544
1.534
1.528
CO2Me
OC
N
Me
54
9
8
7
6
5
4
3
2
1
ppm
0.82
2.89
1.04
0.88
3.00
1.94
1.05
1.05
1.00
2.00
1.05
9.11

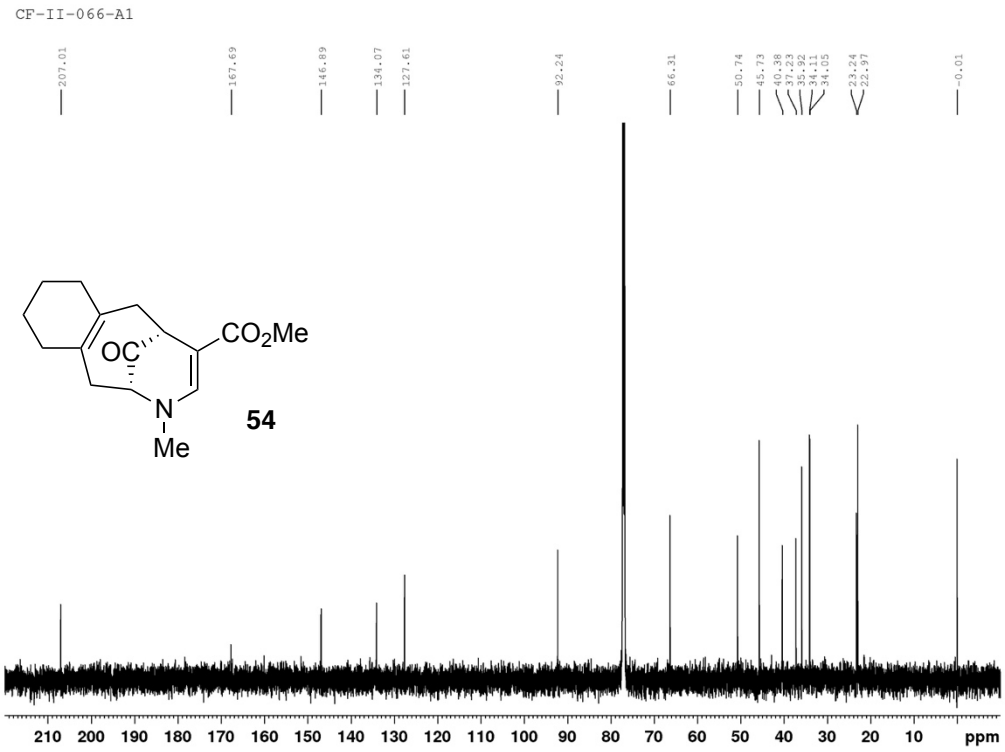
CF-II-066-A1
207.01
167.69
146.89
134.07
127.61
92.24
66.31
50.74
45.73
40.38
37.23
35.92
34.11
34.05
23.24
22.97
-0.01
CO2Me
OC
N
Me
54
210
200
190
180
170
160
150
140
130
120
110
100
90
80
70
60
50
40
30
20
10
ppm

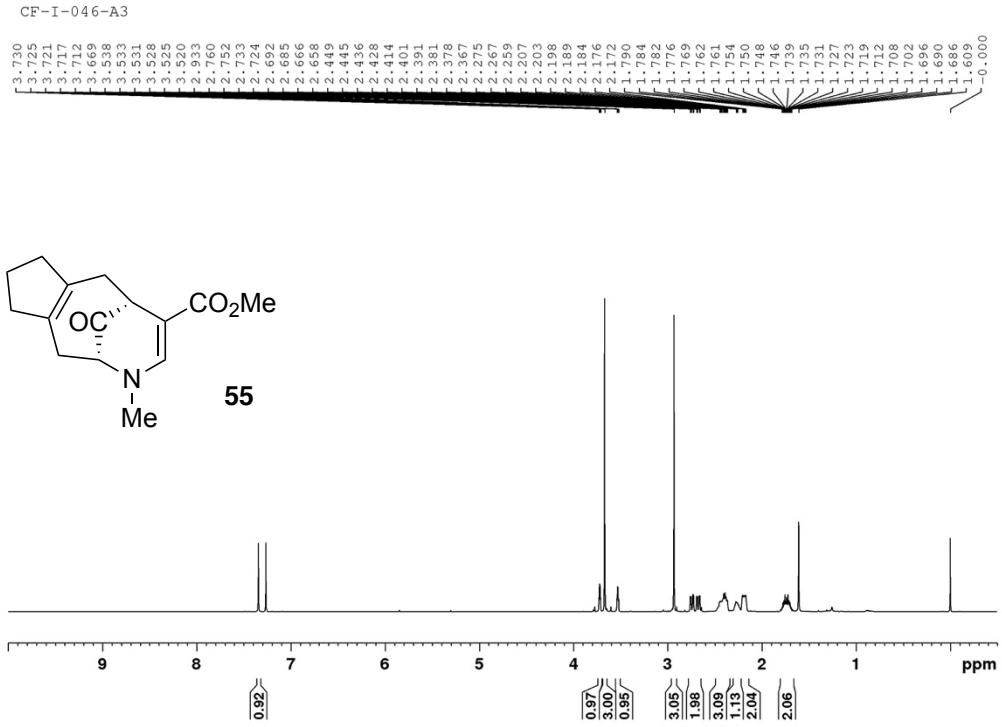
CF-I-046-A3
3.730
3.725
3.721
3.717
3.712
3.669
3.538
3.533
3.531
3.528
3.525
3.520
2.933
2.760
2.752
2.733
2.724
2.692
2.685
2.666
2.658
2.449
2.445
2.436
2.428
2.414
2.401
2.391
2.381
2.378
2.367
2.275
2.267
2.259
2.207
2.203
2.198
2.189
2.184
2.176
2.172
1.790
1.784
1.782
1.776
1.769
1.762
1.761
1.754
1.750
1.748
1.746
1.739
1.735
1.731
1.727
1.723
1.719
1.712
1.708
1.702
1.696
1.690
1.686
1.609
0.000
CO2Me
OC
N
Me
55
9
8
7
6
5
4
3
2
1
ppm
0.92
0.97
3.00
0.95
3.05
1.98
3.09
1.13
2.04
2.06

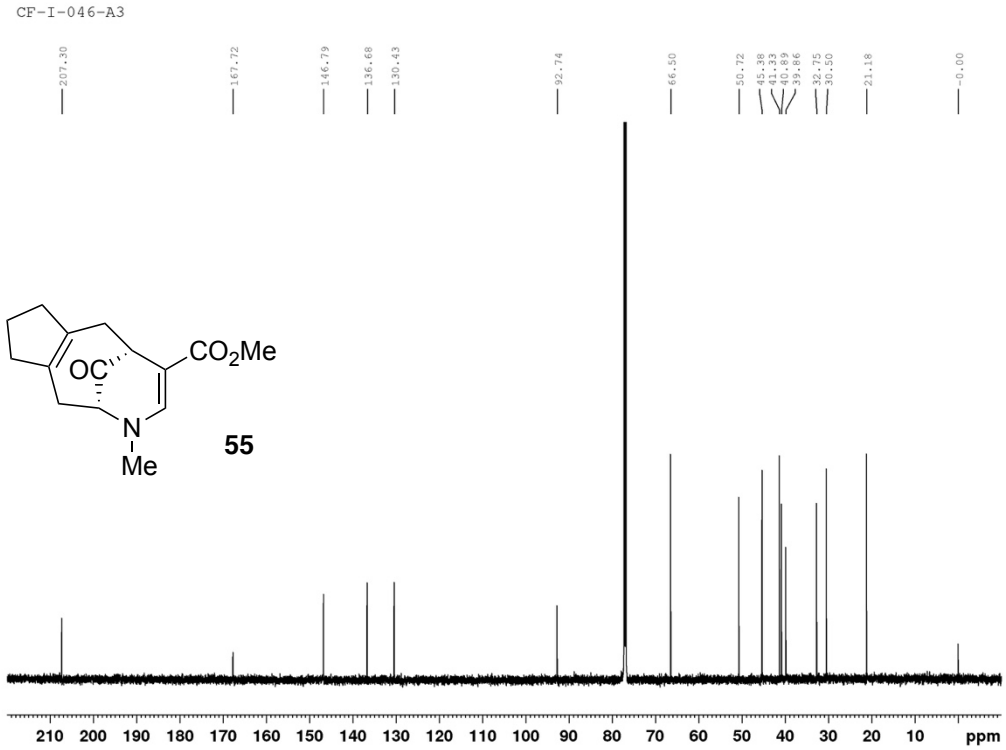
CF-I-046-A3
207.30
167.72
146.79
136.68
130.43
92.74
66.50
50.72
45.38
41.33
40.89
39.66
32.75
30.50
21.18
0.00
CO2Me
OC
N
Me
55
210
200
190
180
170
160
150
140
130
120
110
100
90
80
70
60
50
40
30
20
10
ppm

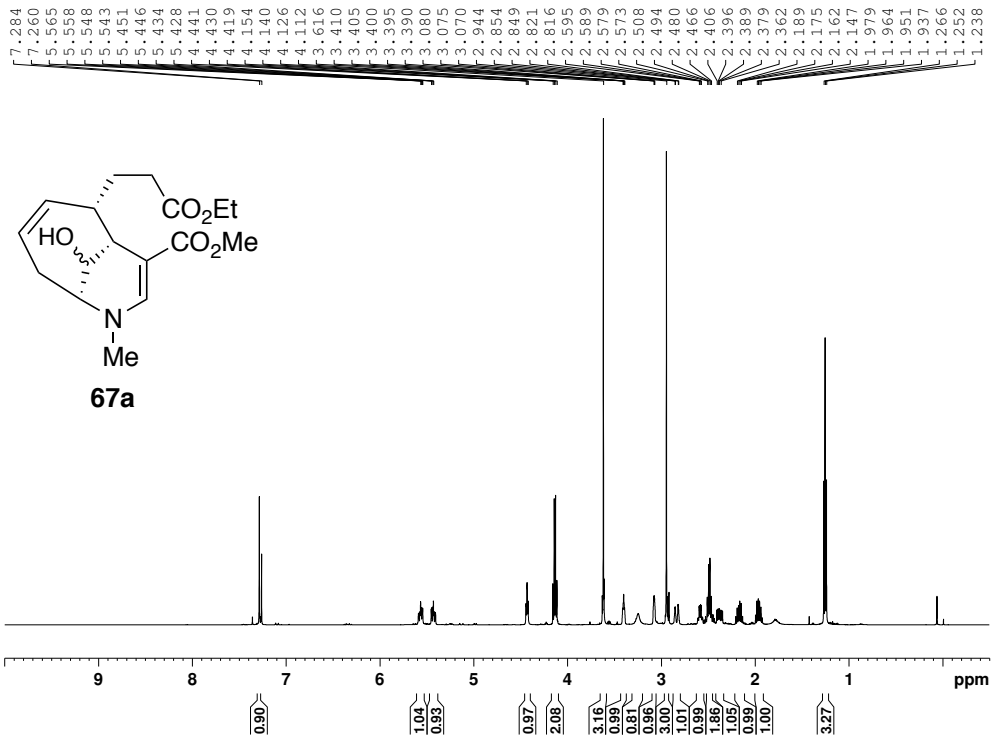
7.284
7.260
5.565
5.558
5.548
5.543
5.451
5.446
5.434
5.428
4.441
4.430
4.419
4.154
4.140
4.126
4.112
3.616
3.410
3.405
3.400
3.395
3.390
3.080
3.075
3.070
2.944
2.854
2.849
2.821
2.816
2.595
2.589
2.579
2.573
2.508
2.494
2.480
2.466
2.406
2.396
2.389
2.379
2.362
2.189
2.175
2.162
2.147
1.979
1.964
1.951
1.937
1.266
1.252
1.238
CO2Et
CO2Me
HO
N
Me
67a
9
8
7
6
5
4
3
2
1
ppm
0.90
1.04
0.93
0.97
2.08
3.16
0.99
0.81
0.96
3.00
1.01
0.99
1.86
1.05
0.99
1.00
3.27

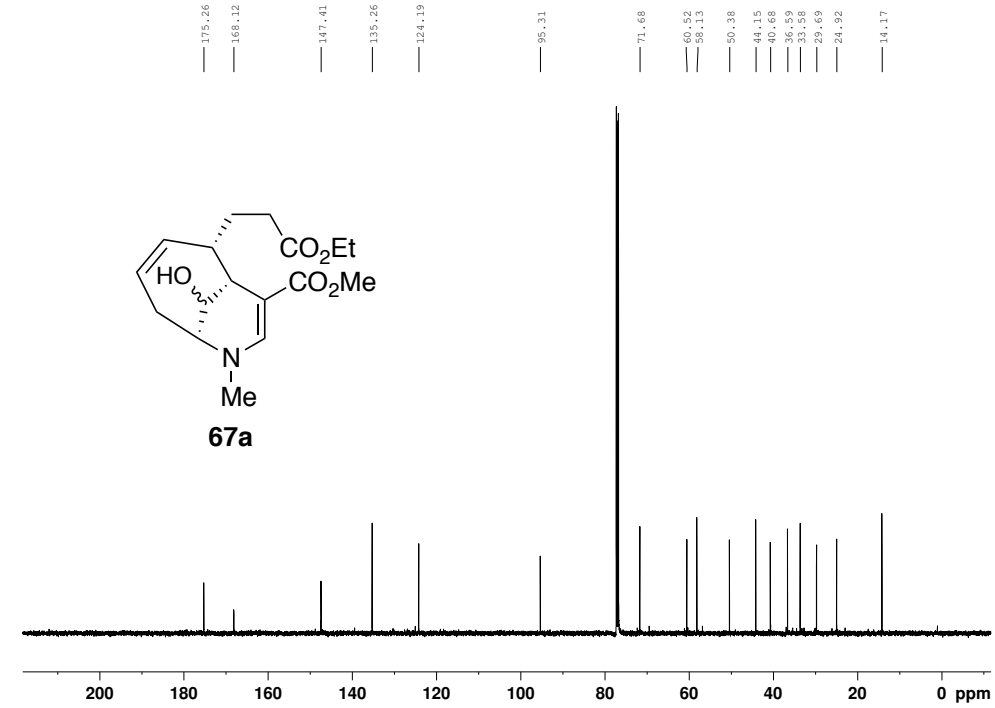
175.26
168.12
147.41
135.26
124.19
95.31
71.68
60.52
58.13
50.38
44.15
40.68
36.59
33.58
29.69
24.92
14.17
CO2Et
CO2Me
HO
N
Me
67a
200
180
160
140
120
100
80
60
40
20
0 ppm

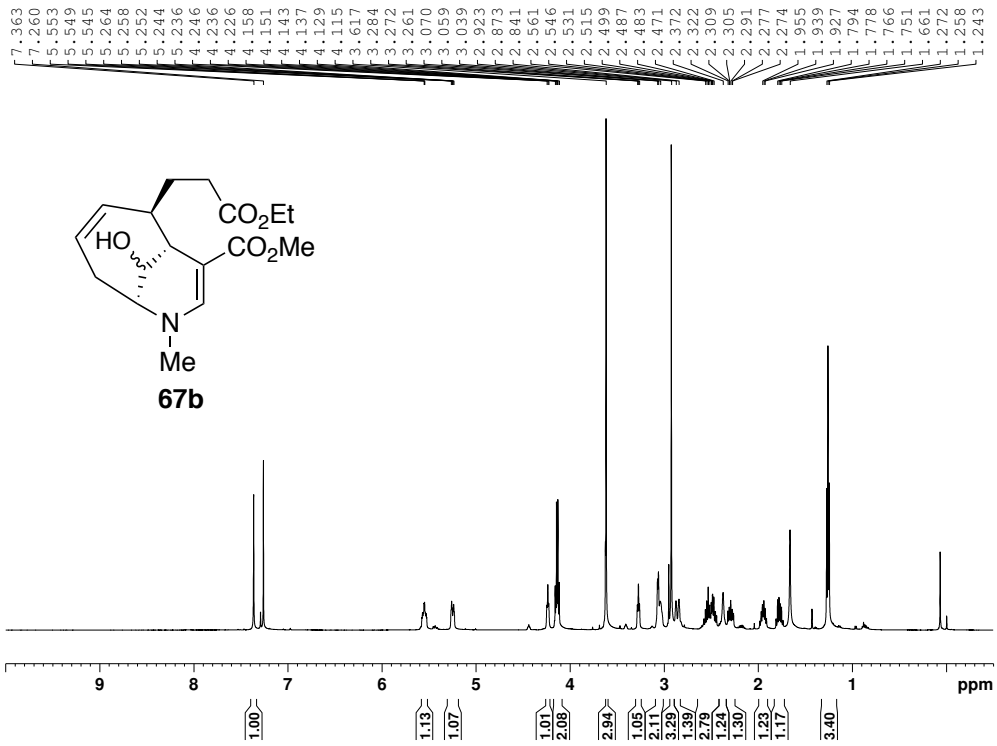
7.363
7.260
5.553
5.549
5.545
5.264
5.258
5.252
5.244
5.236
4.246
4.236
4.226
4.158
4.151
4.143
4.137
4.129
4.115
3.617
3.284
3.272
3.261
3.070
3.059
3.039
2.923
2.873
2.841
2.561
2.546
2.531
2.515
2.499
2.487
2.483
2.471
2.372
2.322
2.309
2.305
2.291
2.277
2.274
1.955
1.939
1.927
1.794
1.778
1.766
1.751
1.661
1.272
1.258
1.243
CO2Et
CO2Me
HO
N
Me
67b
9
8
7
6
5
4
3
2
1
ppm
1.00
1.13
1.07
1.01
2.08
2.94
1.05
2.11
3.29
1.39
2.79
1.24
1.30
1.23
1.17
3.40

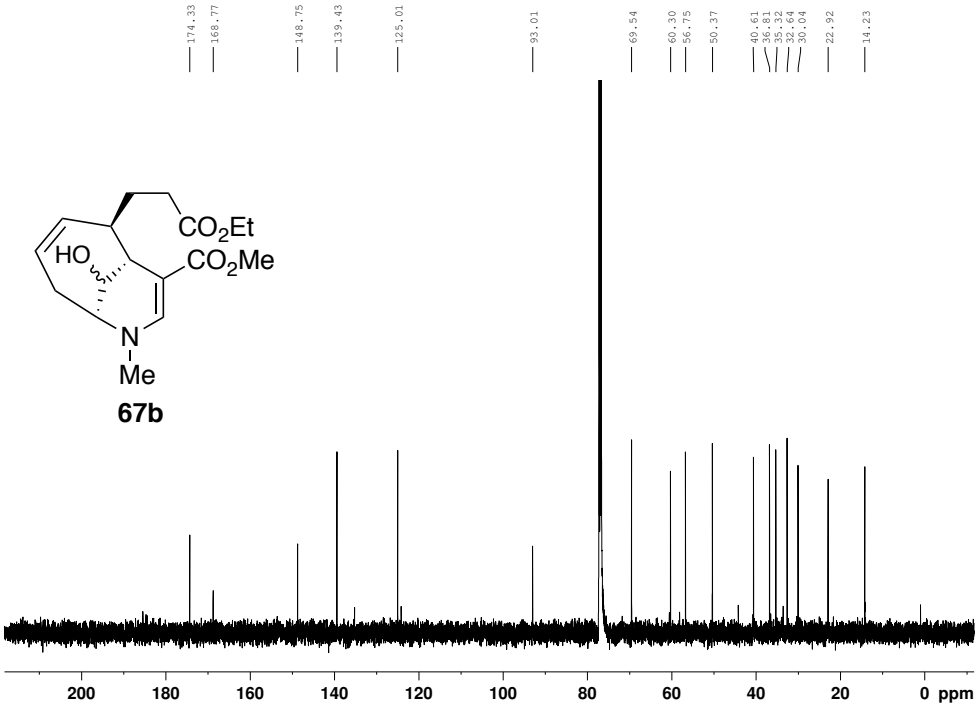
174.33
168.77
148.75
139.43
125.01
93.01
69.54
60.30
56.75
50.37
40.61
36.81
35.32
32.64
30.04
22.92
14.23
CO2Et
CO2Me
HO
N
Me
67b
200
180
160
140
120
100
80
60
40
20
0 ppm

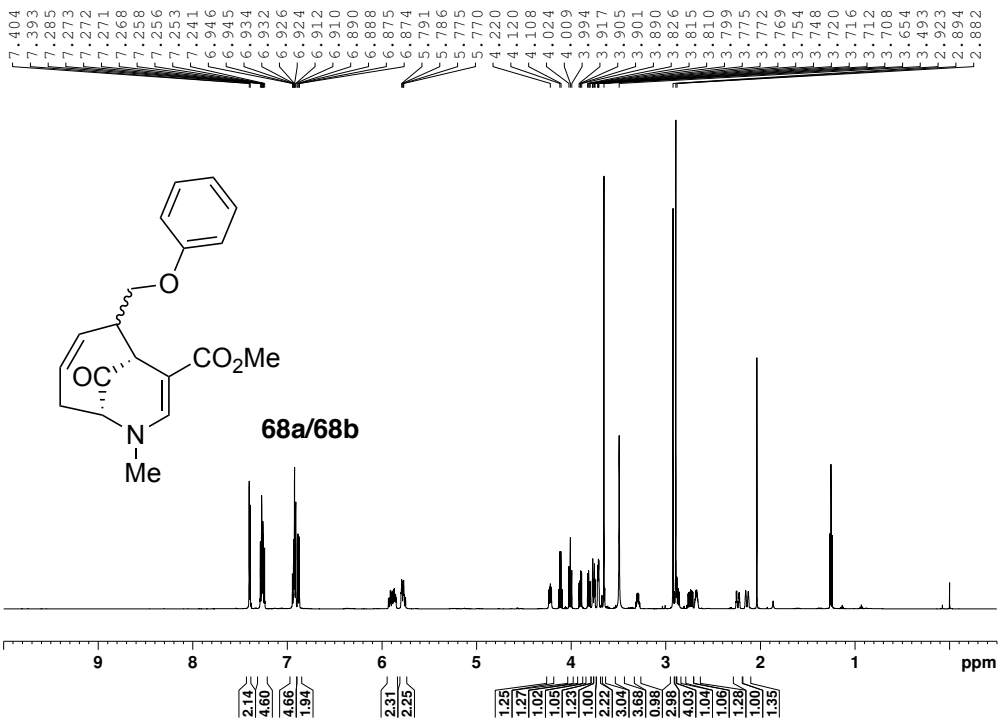
7.404
7.393
7.285
7.273
7.272
7.271
7.268
7.258
7.256
7.253
7.241
6.946
6.945
6.934
6.932
6.926
6.924
6.912
6.910
6.890
6.888
6.875
6.874
5.791
5.786
5.775
5.770
4.220
4.120
4.108
4.024
4.009
3.994
3.917
3.905
3.901
3.890
3.826
3.815
3.810
3.799
3.775
3.772
3.769
3.754
3.748
3.720
3.716
3.712
3.708
3.654
3.493
2.923
2.894
2.882
O
CO2Me
OC
N
Me
68a/68b
9
8
7
6
5
4
3
2
1
ppm
2.14
4.60
4.66
1.94
2.31
2.25
1.25
1.27
1.02
1.05
1.23
1.00
2.22
3.04
3.68
0.98
2.98
4.03
1.04
1.06
1.28
1.00
1.35

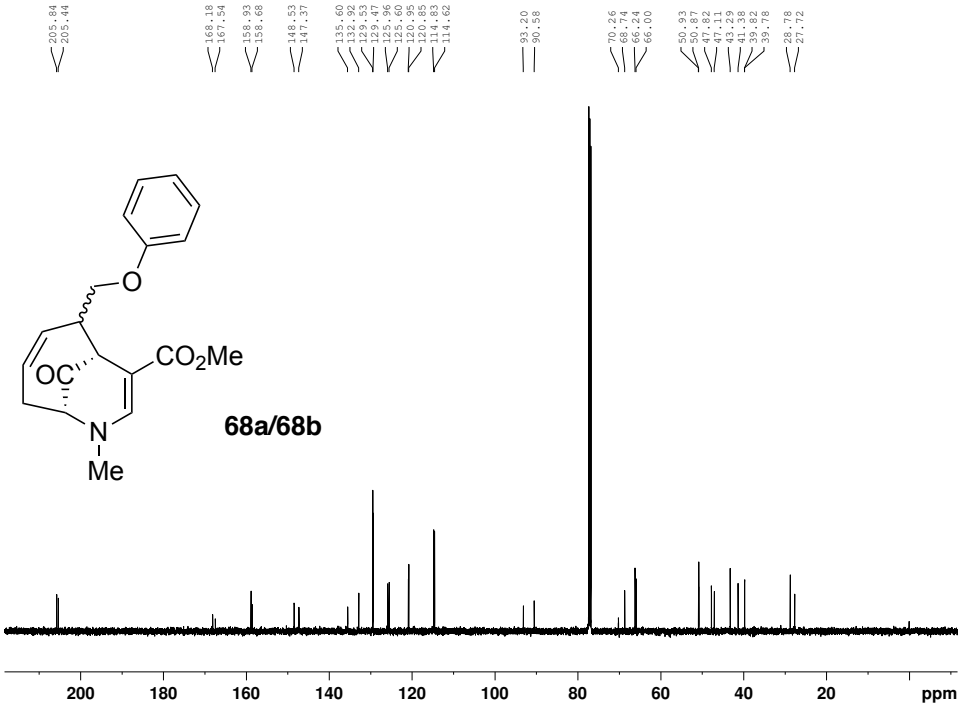
205.84
205.44
168.18
167.54
158.93
158.68
148.53
147.37
135.60
132.92
129.53
129.47
125.96
125.60
120.95
120.85
114.83
114.62
93.20
90.58
70.26
68.74
66.24
66.00
50.93
50.87
47.82
47.11
43.29
41.38
39.82
39.78
28.78
27.72
O
CO2Me
OC
N
Me
68a/68b
200
180
160
140
120
100
80
60
40
20
ppm

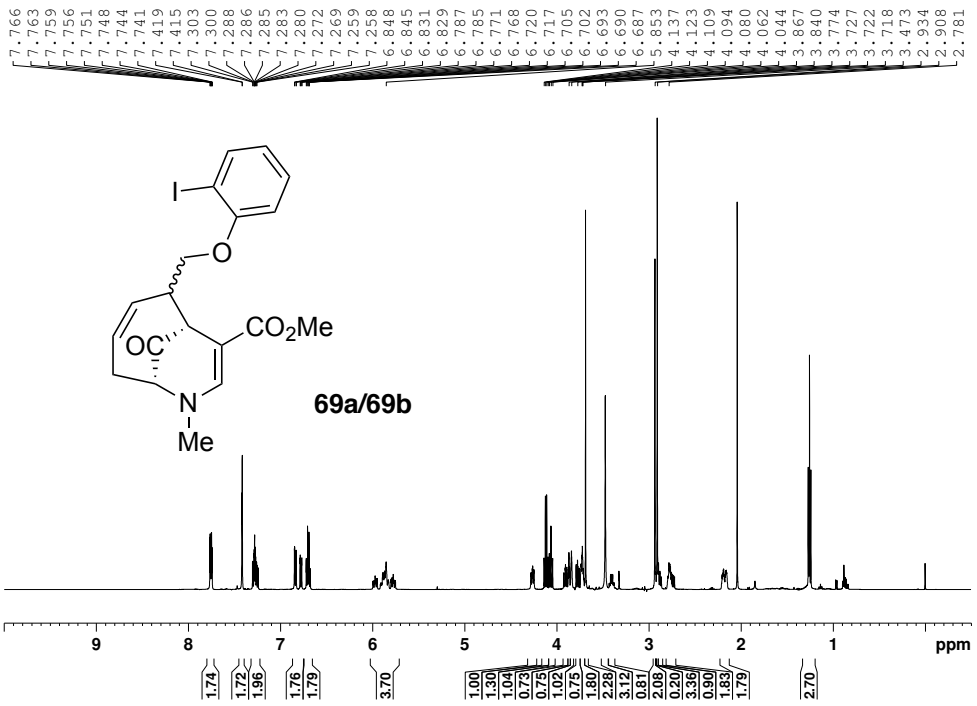
7.766
7.763
7.759
7.756
7.751
7.748
7.744
7.741
7.419
7.415
7.303
7.300
7.288
7.286
7.285
7.283
7.280
7.272
7.269
7.259
7.258
6.848
6.845
6.831
6.829
6.787
6.785
6.771
6.768
6.720
6.717
6.705
6.702
6.693
6.690
6.687
5.853
4.137
4.123
4.109
4.094
4.080
4.062
4.044
3.867
3.840
3.774
3.727
3.722
3.718
3.473
2.934
2.908
2.781
I
O
CO2Me
OC
N
Me
69a/69b
9
8
7
6
5
4
3
2
1
ppm
1.74
1.72
1.96
1.76
1.79
3.70
1.00
1.30
1.04
0.73
0.75
1.02
0.75
1.80
2.28
3.12
0.81
2.08
0.20
3.36
0.90
1.83
1.79
2.70

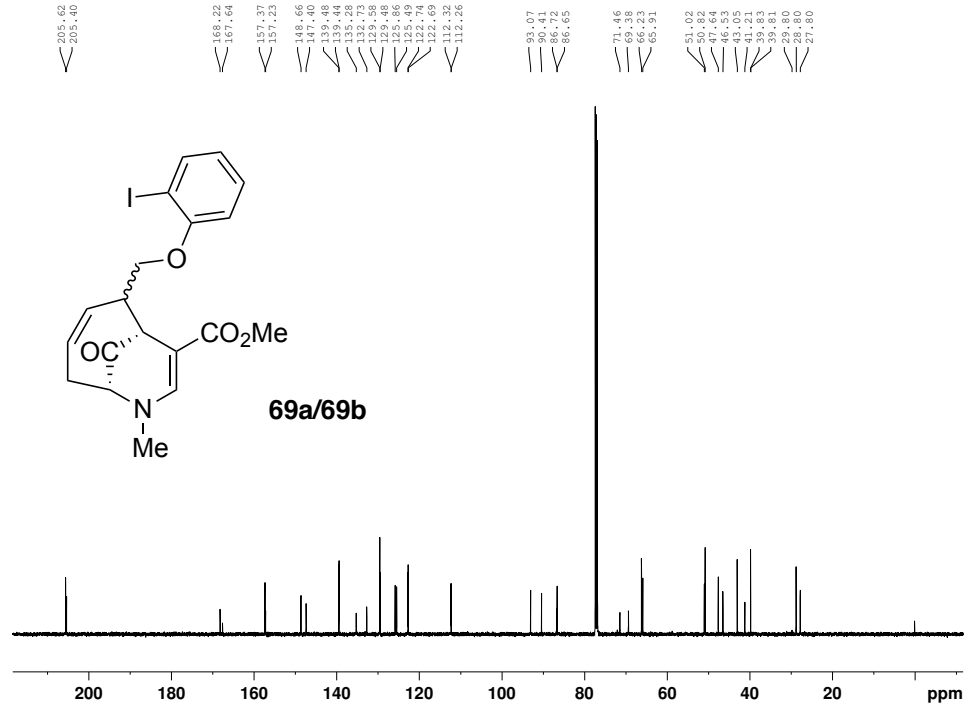
205.62
205.40
168.22
167.64
157.37
157.23
148.66
147.40
139.48
139.44
135.28
132.73
129.98
129.48
125.86
125.49
122.74
122.69
112.32
112.26
93.07
90.41
86.72
86.65
71.46
69.38
66.23
65.91
51.02
50.82
47.64
46.53
43.05
41.21
39.83
39.81
29.80
28.80
27.80
I
O
CO2Me
OC
N
Me
69a/69b
200
180
160
140
120
100
80
60
40
20
ppm

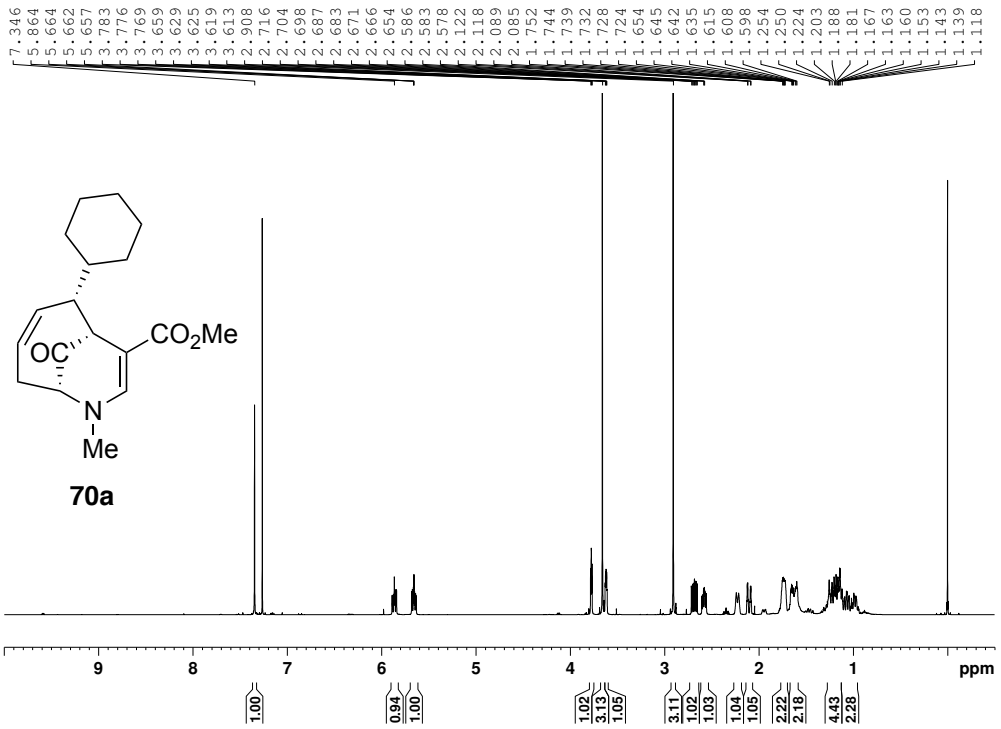
7.346
5.864
5.664
5.662
5.657
3.783
3.776
3.769
3.659
3.629
3.625
3.619
3.613
2.908
2.716
2.704
2.698
2.687
2.683
2.671
2.666
2.654
2.586
2.583
2.578
2.122
2.118
2.089
2.085
1.752
1.744
1.739
1.732
1.728
1.724
1.654
1.645
1.642
1.635
1.615
1.608
1.598
1.254
1.250
1.224
1.203
1.188
1.181
1.167
1.163
1.160
1.153
1.143
1.139
1.118
CO2Me
OC
N
Me
70a
9
8
7
6
5
4
3
2
1
ppm
1.00
0.94
1.00
1.02
3.13
1.05
3.11
1.02
1.03
1.04
1.05
2.22
2.18
4.43
2.28

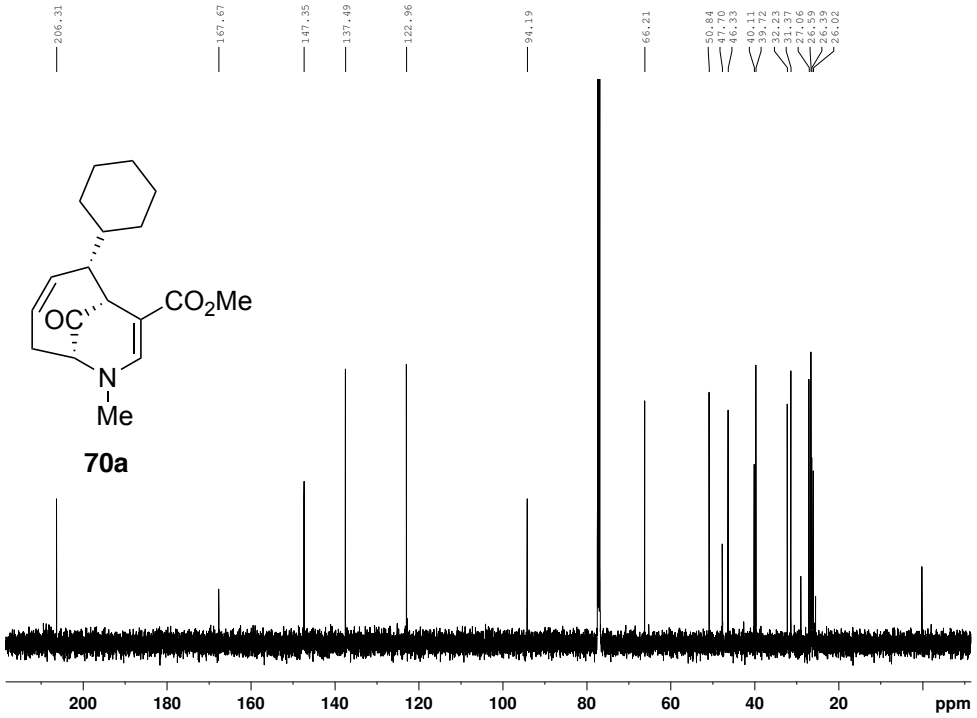
206.31
167.67
147.35
137.49
122.96
94.19
66.21
50.84
47.70
46.33
40.11
39.72
32.23
31.37
27.06
26.59
26.39
26.02
CO2Me
OC
N
Me
70a
200
180
160
140
120
100
80
60
40
20
ppm

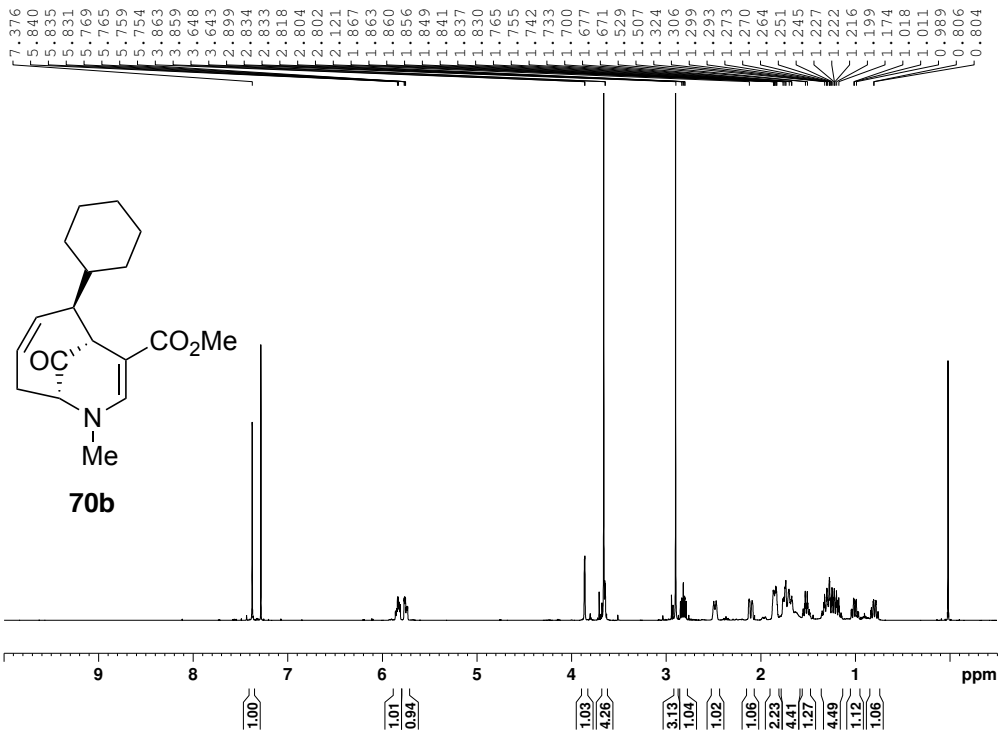
7.376
5.840
5.835
5.831
5.769
5.765
5.759
5.754
3.863
3.859
3.648
3.643
2.899
2.834
2.833
2.818
2.804
2.802
2.121
1.867
1.863
1.860
1.856
1.849
1.841
1.837
1.830
1.765
1.755
1.742
1.733
1.700
1.677
1.671
1.529
1.507
1.324
1.306
1.299
1.293
1.273
1.270
1.264
1.251
1.245
1.227
1.222
1.216
1.199
1.174
1.018
1.011
0.989
0.806
0.804
CO2Me
OC
N
Me
70b
9
8
7
6
5
4
3
2
1
ppm
1.00
1.01
0.94
1.03
4.26
3.13
1.04
1.02
1.06
2.23
4.41
1.27
4.49
1.12
1.06

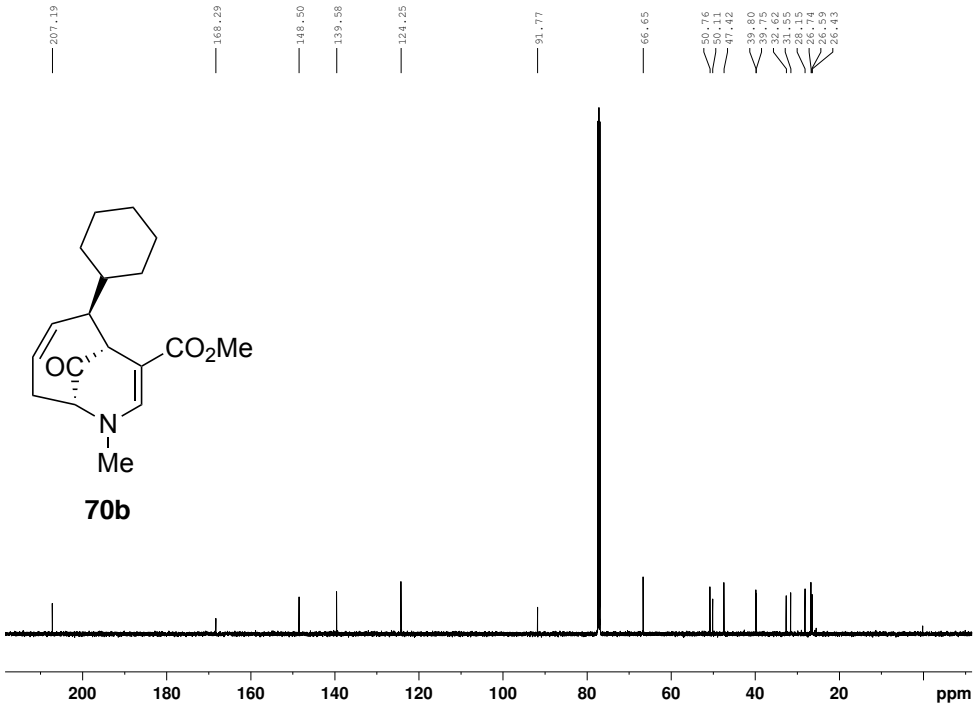
207.19
168.29
148.50
139.58
124.25
91.77
66.65
50.76
50.11
47.42
39.80
39.75
32.62
31.55
28.15
26.74
26.59
26.43
CO2Me
OC
N
Me
70b
200
180
160
140
120
100
80
60
40
20
ppm

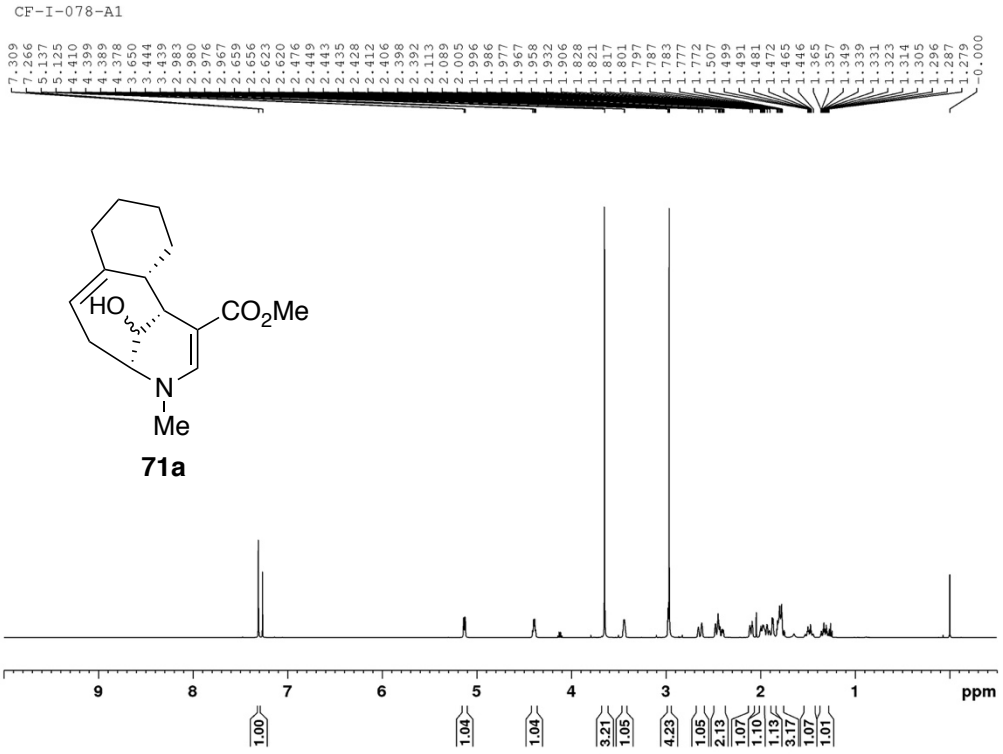
CF-I-078-A1
HO
CO2Me
N
Me
71a
ppm

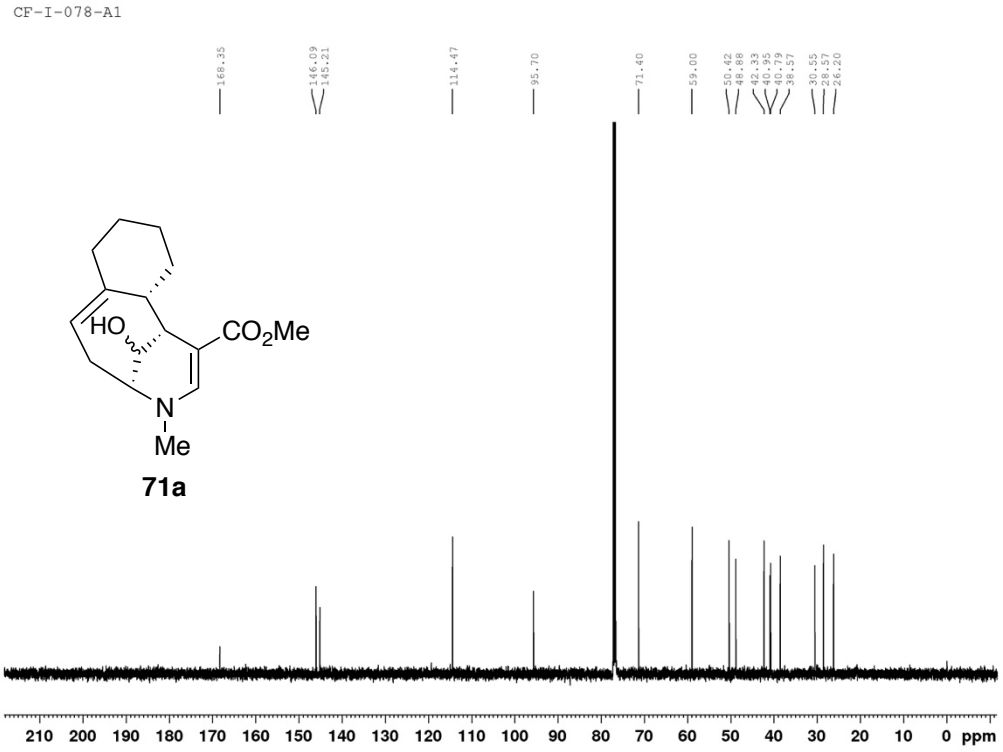
CF-I-078-A1
HO
CO2Me
N
Me
71a
ppm

CF-I-078-A2

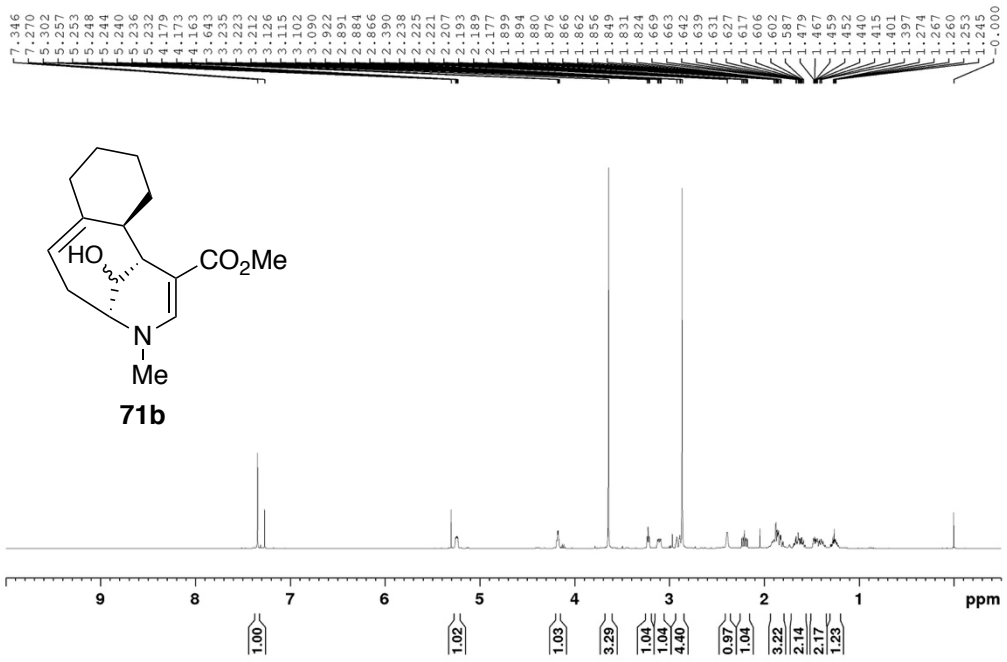

71b

CF-I-078-A2

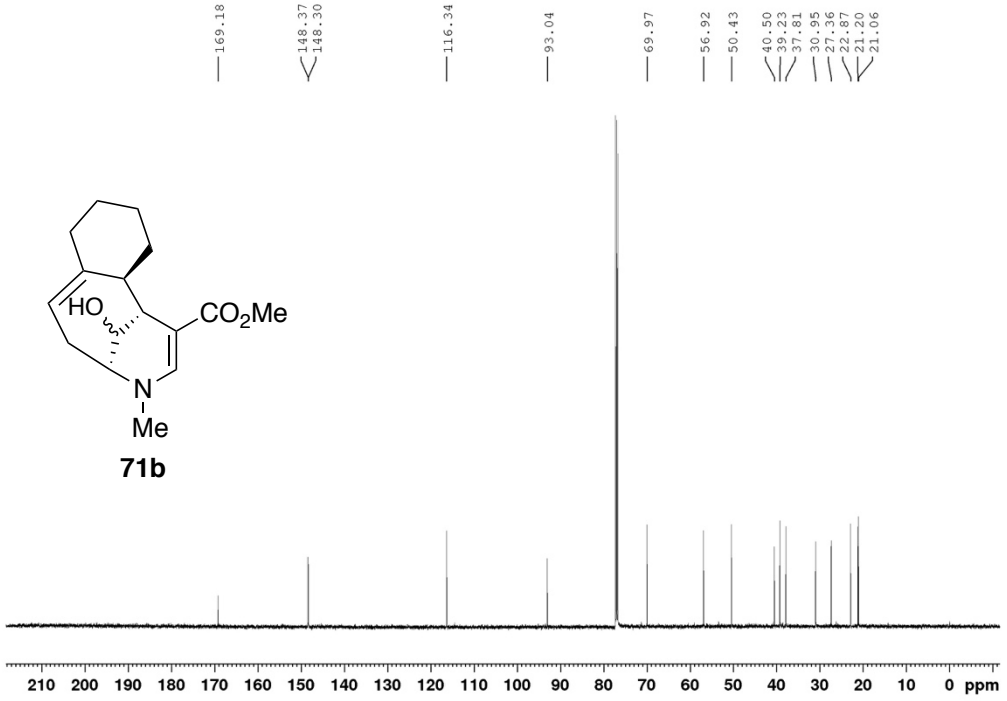

71b

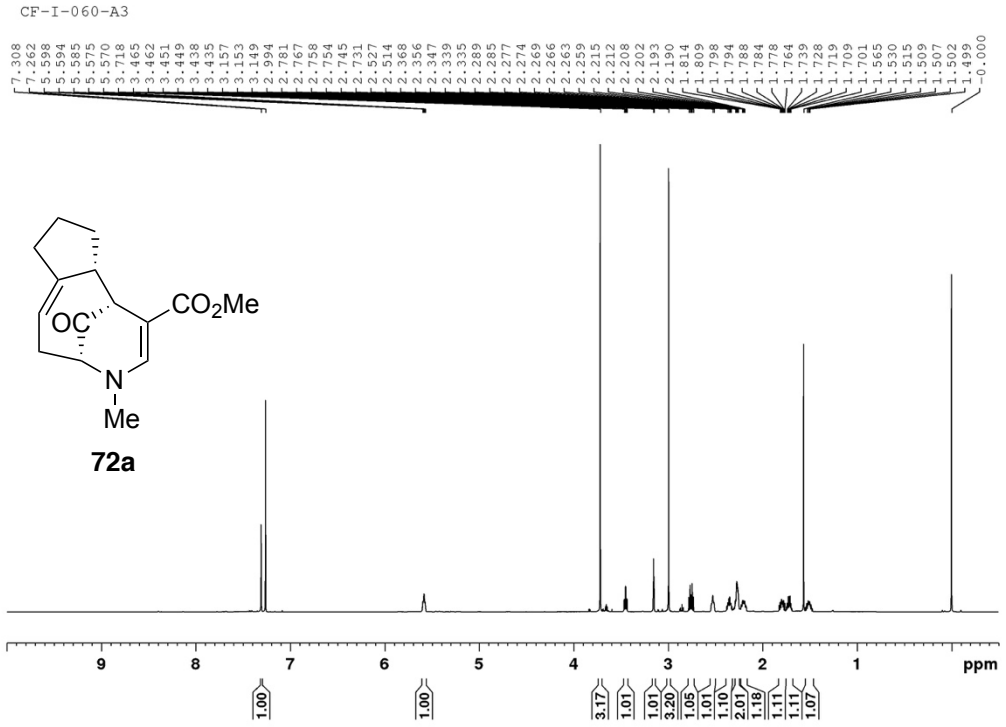
CF-I-060-A3
CO2Me
OC
N
Me
72a
ppm

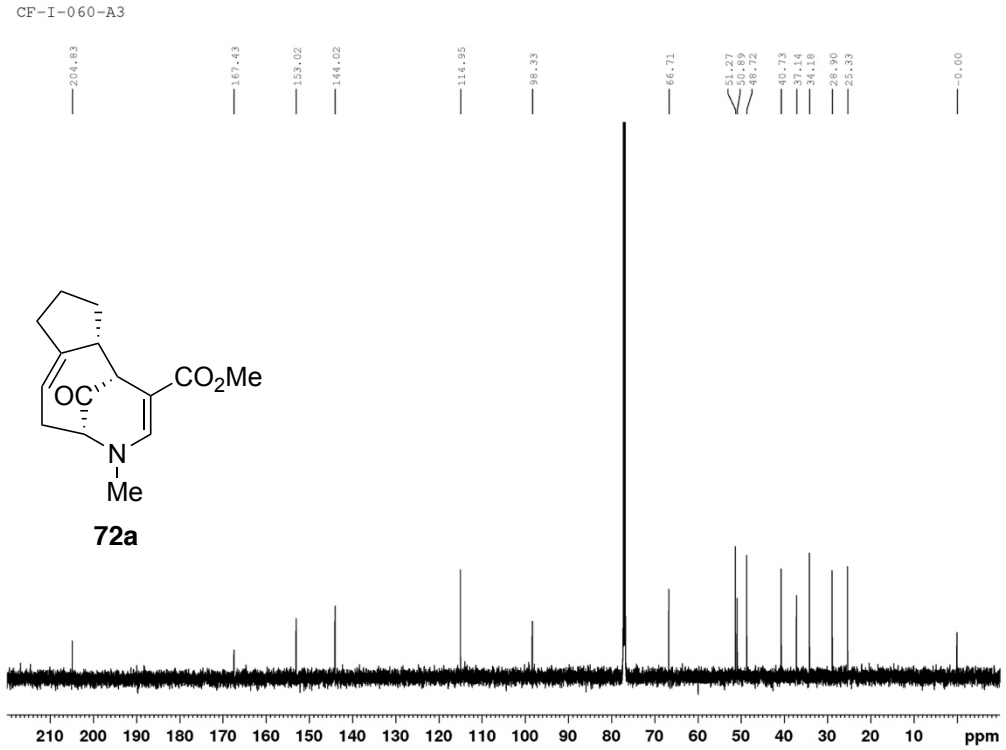
CF-I-060-A3
CO2Me
OC
N
Me
72a
ppm

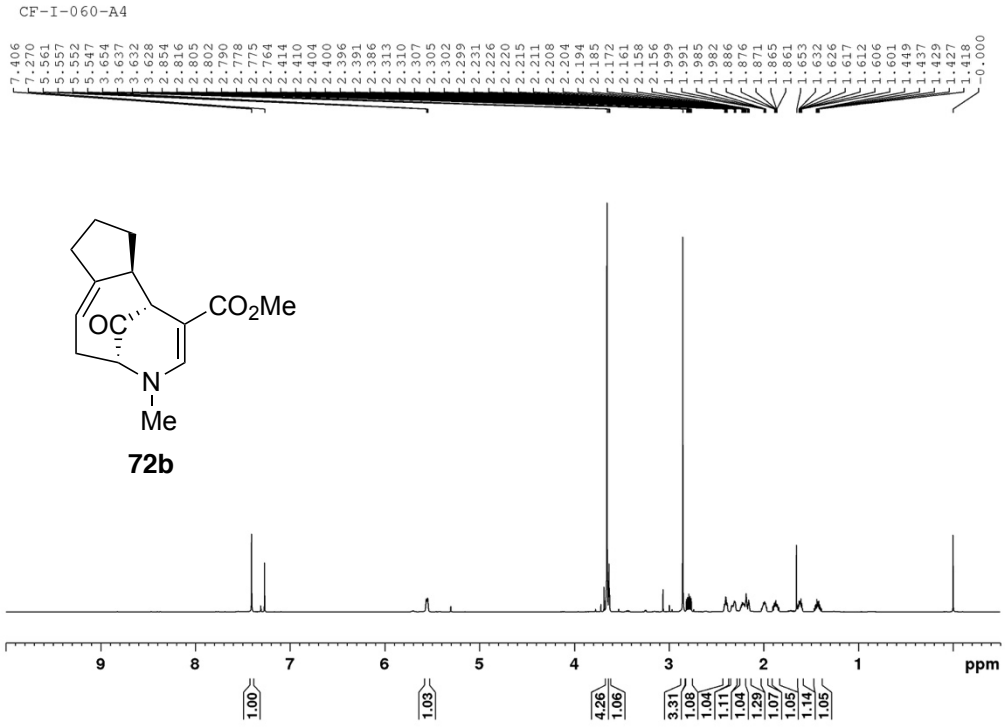
CF-I-060-A4
7.406
7.270
5.561
5.557
5.552
5.547
3.654
3.637
3.632
3.628
2.854
2.816
2.805
2.802
2.790
2.778
2.775
2.764
2.414
2.410
2.404
2.400
2.396
2.391
2.386
2.313
2.310
2.307
2.305
2.302
2.299
2.231
2.226
2.220
2.215
2.211
2.208
2.204
2.194
2.185
2.172
2.161
2.158
2.156
1.999
1.991
1.985
1.982
1.886
1.876
1.871
1.865
1.861
1.653
1.632
1.626
1.617
1.612
1.606
1.601
1.449
1.437
1.429
1.427
1.418
-0.000
CO2Me
OC
N
Me
72b
9
8
7
6
5
4
3
2
1
ppm
1.00
1.03
4.26
1.06
3.31
1.08
1.04
1.11
1.04
1.29
1.07
1.05
1.14
1.05

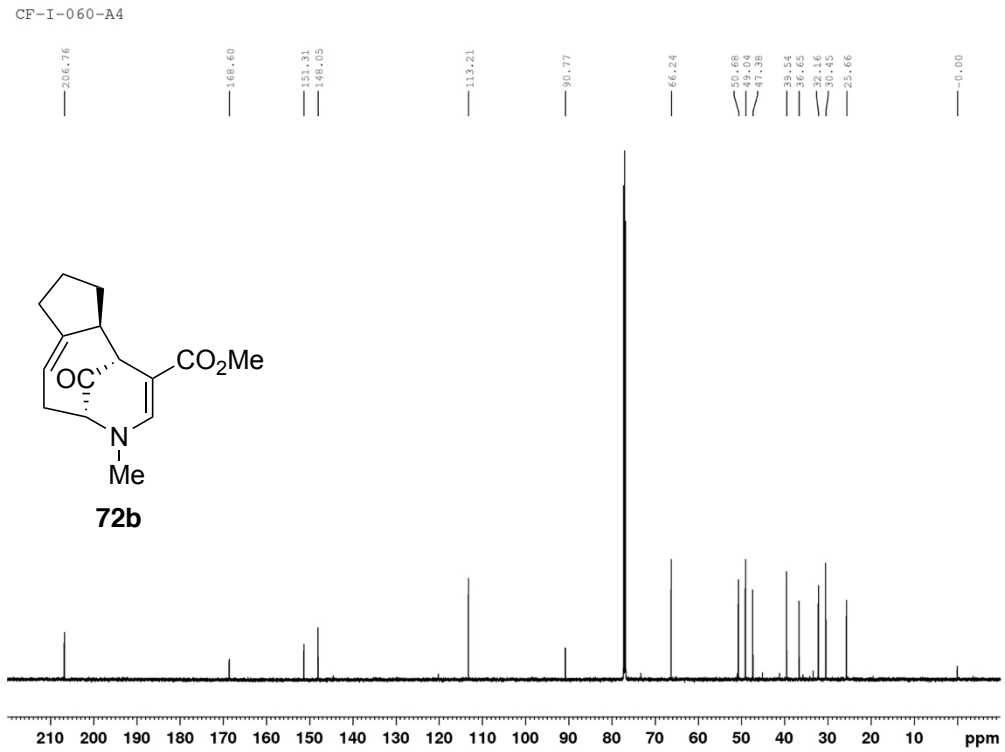
CF-I-060-A4
206.76
168.60
151.31
148.05
113.21
90.77
66.24
50.68
49.04
47.38
39.54
36.65
32.16
30.45
25.66
-0.00
CO2Me
OC
N
Me
72b
210
200
190
180
170
160
150
140
130
120
110
100
90
80
70
60
50
40
30
20
10
ppm

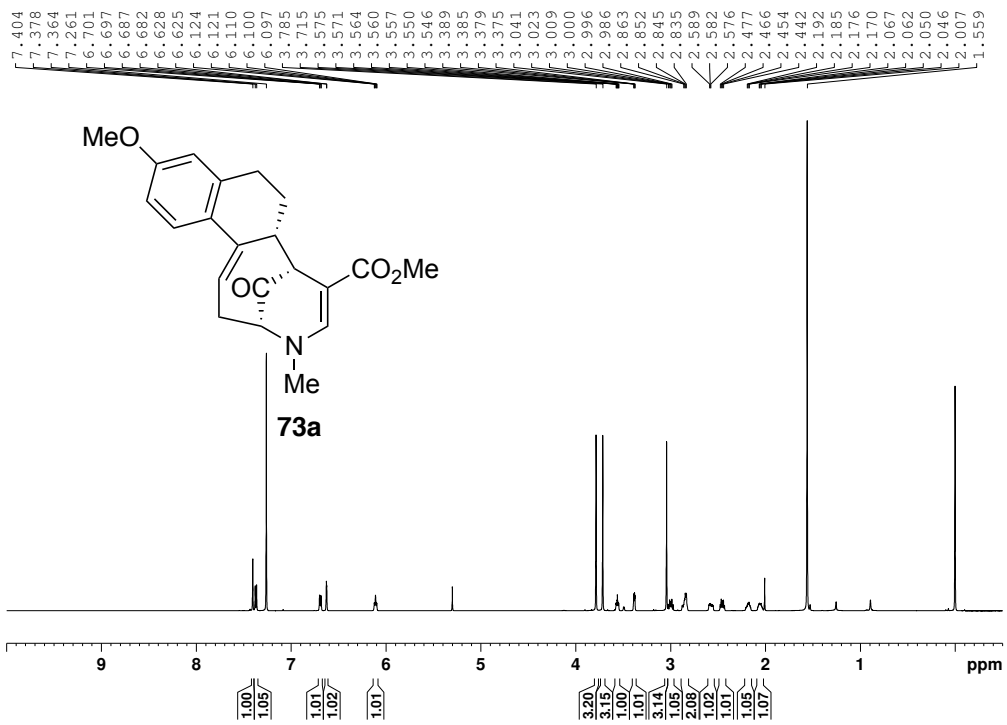
7.404
7.378
7.364
7.261
6.701
6.697
6.687
6.682
6.628
6.625
6.124
6.121
6.110
6.100
6.097
3.785
3.715
3.575
3.571
3.564
3.560
3.557
3.550
3.546
3.389
3.385
3.379
3.375
3.041
3.023
3.009
3.000
2.996
2.986
2.863
2.852
2.845
2.835
2.589
2.582
2.576
2.477
2.466
2.454
2.442
2.192
2.185
2.176
2.170
2.067
2.062
2.050
2.046
2.007
1.559
MeO
CO2Me
OC
N
Me
73a
9
8
7
6
5
4
3
2
1
ppm
1.00
1.05
1.01
1.02
1.01
3.20
3.15
1.00
1.01
3.14
1.05
2.08
1.02
1.01
1.05
1.07

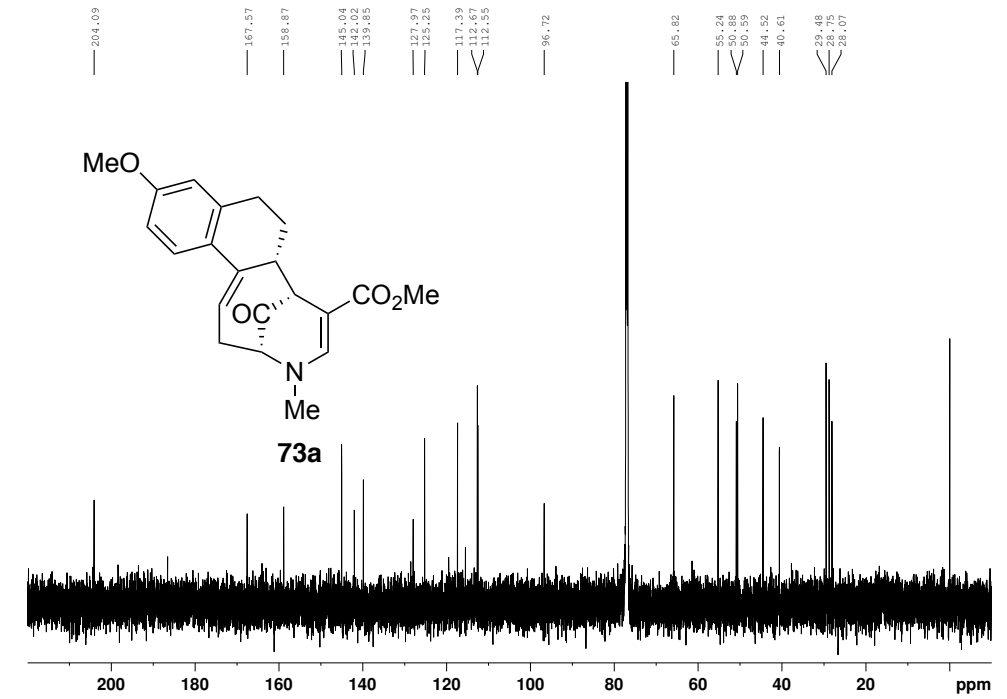
204.09
167.57
158.87
145.04
142.02
139.85
127.97
125.25
117.39
112.67
112.55
96.72
65.82
55.24
50.88
50.59
44.52
40.61
29.48
28.75
28.07
MeO
CO2Me
OC
N
Me
73a
200
180
160
140
120
100
80
60
40
20
ppm

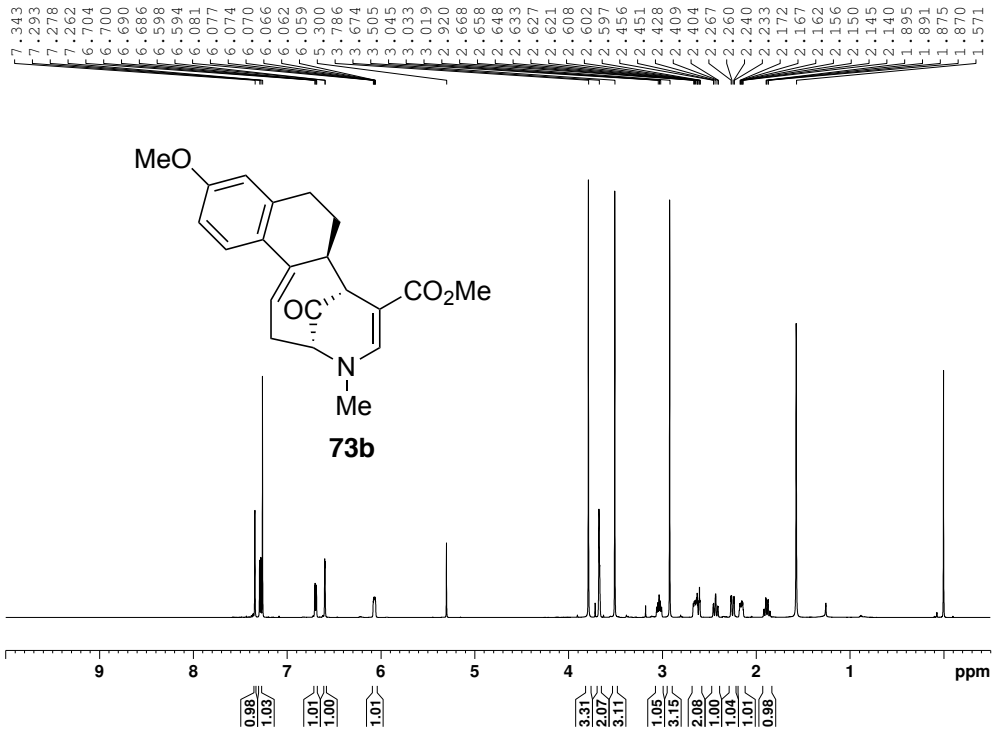
7.343
7.293
7.278
7.262
6.704
6.700
6.690
6.686
6.598
6.594
6.081
6.077
6.074
6.070
6.066
6.062
6.059
5.300
3.786
3.674
3.505
3.045
3.033
3.019
2.920
2.668
2.658
2.648
2.633
2.627
2.621
2.608
2.602
2.597
2.456
2.451
2.428
2.409
2.404
2.267
2.260
2.240
2.233
2.172
2.167
2.162
2.156
2.150
2.145
2.140
1.895
1.891
1.875
1.870
1.571
MeO
CO2Me
OC
N
Me
73b
9
8
7
6
5
4
3
2
1
ppm
0.98
1.03
1.01
1.00
1.01
3.31
2.07
3.11
1.05
3.15
2.08
1.00
1.04
1.01
0.98

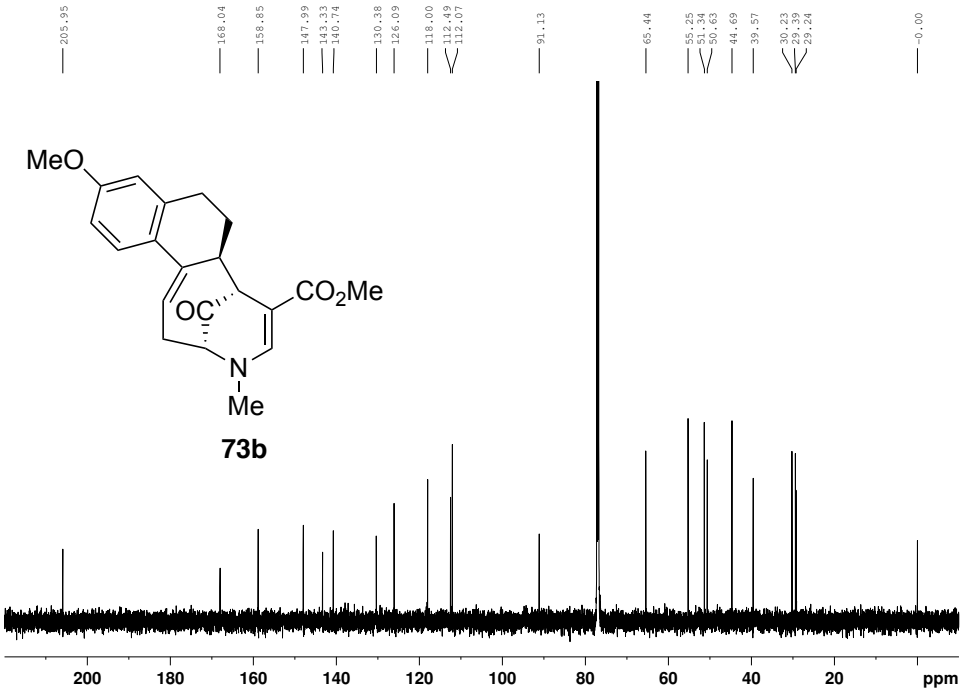
205.95
168.04
158.85
147.99
143.33
140.74
130.38
126.09
118.00
112.49
112.07
91.13
65.44
55.25
51.34
50.63
44.69
39.57
30.23
29.39
29.24
-0.00
MeO
CO2Me
OC
N
Me
73b
200
180
160
140
120
100
80
60
40
20
ppm

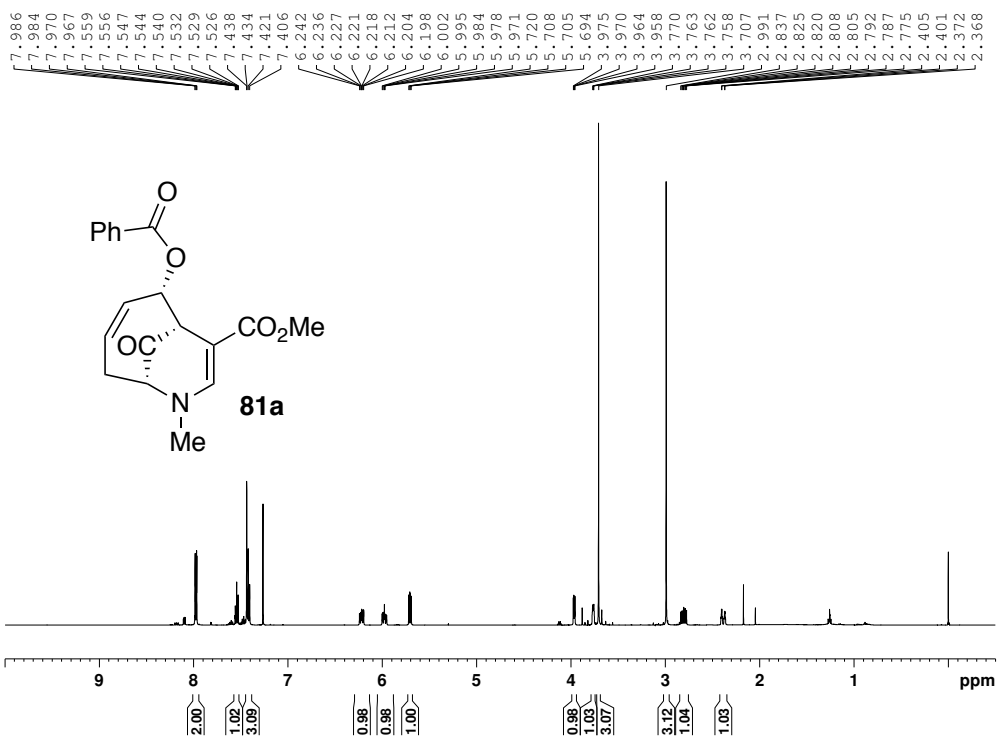
7.986
7.984
7.970
7.967
7.559
7.556
7.547
7.544
7.540
7.532
7.529
7.526
7.438
7.434
7.421
7.406
6.242
6.236
6.227
6.221
6.218
6.212
6.204
6.198
6.002
5.995
5.984
5.978
5.971
5.720
5.708
5.705
5.694
3.975
3.970
3.964
3.958
3.770
3.763
3.762
3.758
3.707
2.991
2.837
2.825
2.820
2.808
2.805
2.792
2.787
2.775
2.405
2.401
2.372
2.368
Ph
O
O
CO2Me
OC
N
Me
81a
9
8
7
6
5
4
3
2
1
ppm
2.00
1.02
3.09
0.98
0.98
1.00
0.98
1.03
3.07
3.12
1.04
1.03

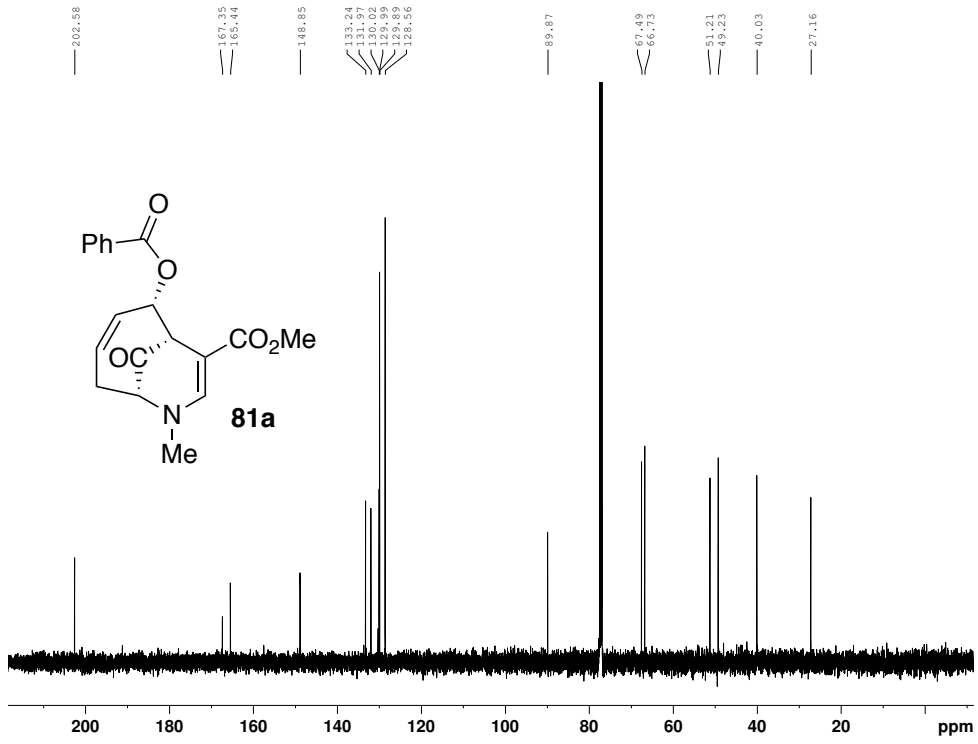
202.58
167.35
165.44
148.85
133.24
131.97
130.02
129.99
129.89
128.56
89.87
67.49
66.73
51.21
49.23
40.03
27.16
Ph
O
O
CO2Me
OC
N
Me
81a
200
180
160
140
120
100
80
60
40
20
ppm

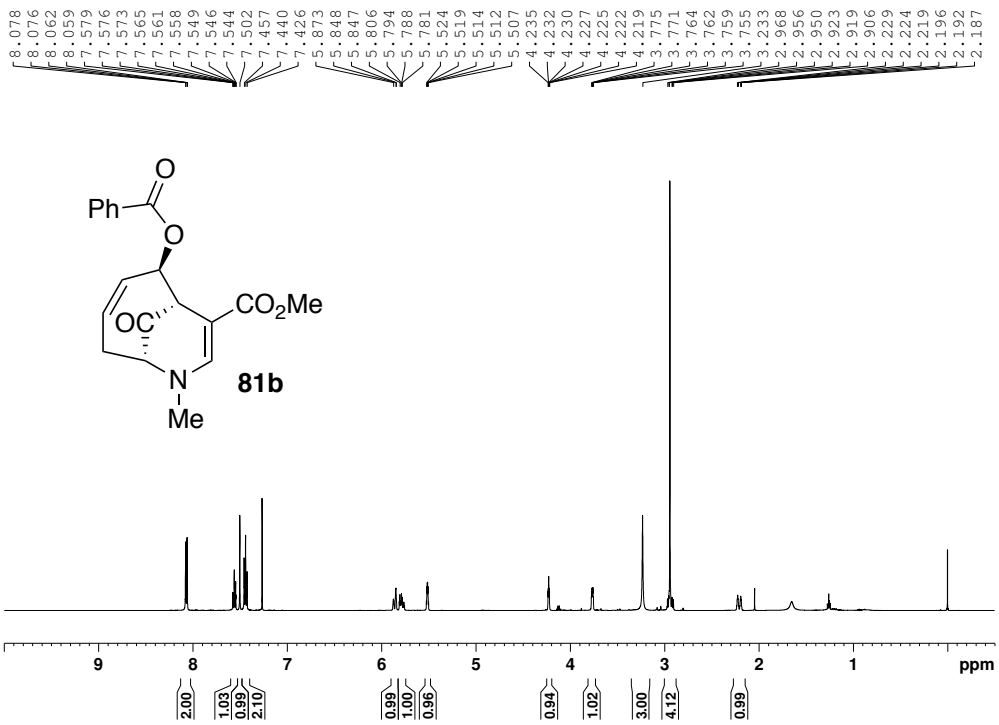
8.078
8.076
8.062
8.059
7.579
7.576
7.573
7.565
7.561
7.558
7.549
7.546
7.544
7.502
7.457
7.440
7.426
5.873
5.848
5.847
5.806
5.794
5.788
5.781
5.524
5.519
5.514
5.512
5.507
4.235
4.232
4.230
4.227
4.225
4.222
4.219
3.775
3.771
3.764
3.762
3.759
3.755
3.233
2.968
2.956
2.950
2.923
2.919
2.906
2.229
2.224
2.219
2.196
2.192
2.187
Ph
O
O
CO2Me
OC
N
Me
81b
9
8
7
6
5
4
3
2
1
ppm
2.00
1.03
0.99
2.10
0.99
1.00
0.96
0.94
1.02
3.00
4.12
0.99

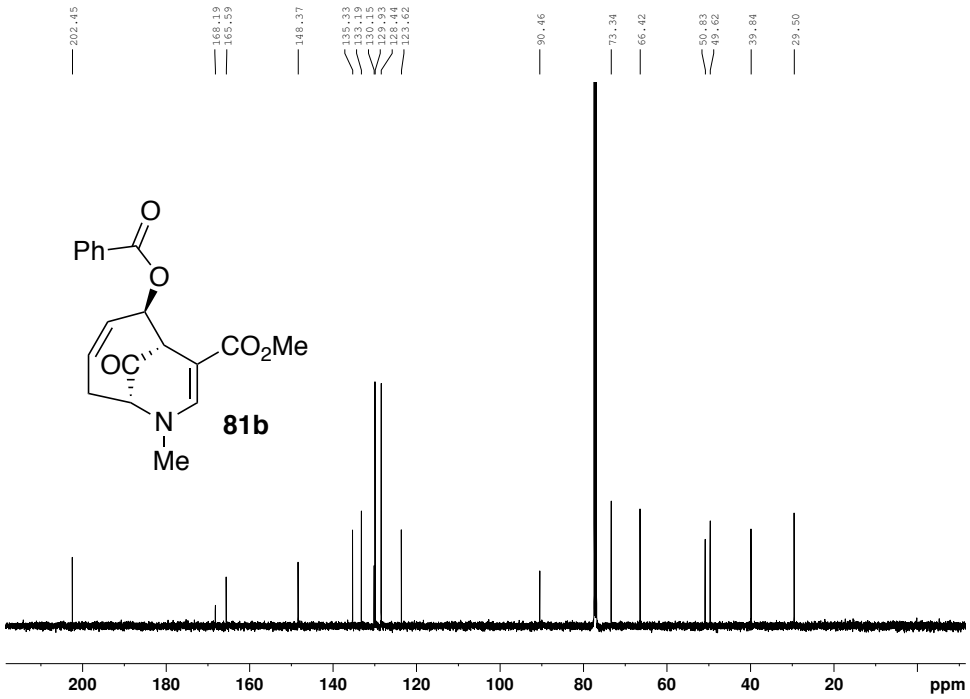
202.45
168.19
165.59
148.37
135.33
133.19
130.15
129.93
128.44
123.62
90.46
73.34
66.42
50.83
49.62
39.84
29.50
Ph
O
O
CO2Me
OC
N
Me
81b
200
180
160
140
120
100
80
60
40
20
ppm

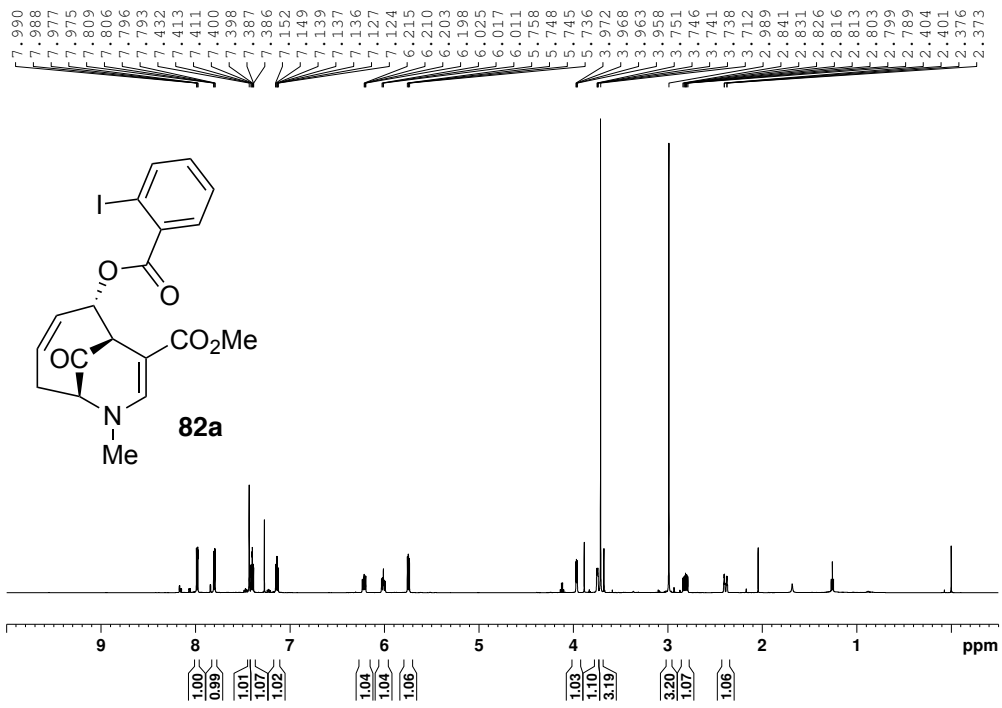
7.990
7.988
7.977
7.975
7.809
7.806
7.796
7.793
7.432
7.413
7.411
7.400
7.398
7.387
7.386
7.152
7.149
7.139
7.137
7.136
7.127
7.124
6.215
6.210
6.203
6.198
6.025
6.017
6.011
5.758
5.748
5.745
5.736
3.972
3.968
3.963
3.958
3.751
3.746
3.741
3.738
3.712
2.989
2.841
2.831
2.826
2.816
2.813
2.803
2.799
2.789
2.404
2.401
2.376
2.373
I
O
O
CO2Me
OC
N
Me
82a
9
8
7
6
5
4
3
2
1
ppm
1.00
0.99
1.01
1.07
1.02
1.04
1.04
1.06
1.03
1.10
3.19
3.20
1.07
1.06

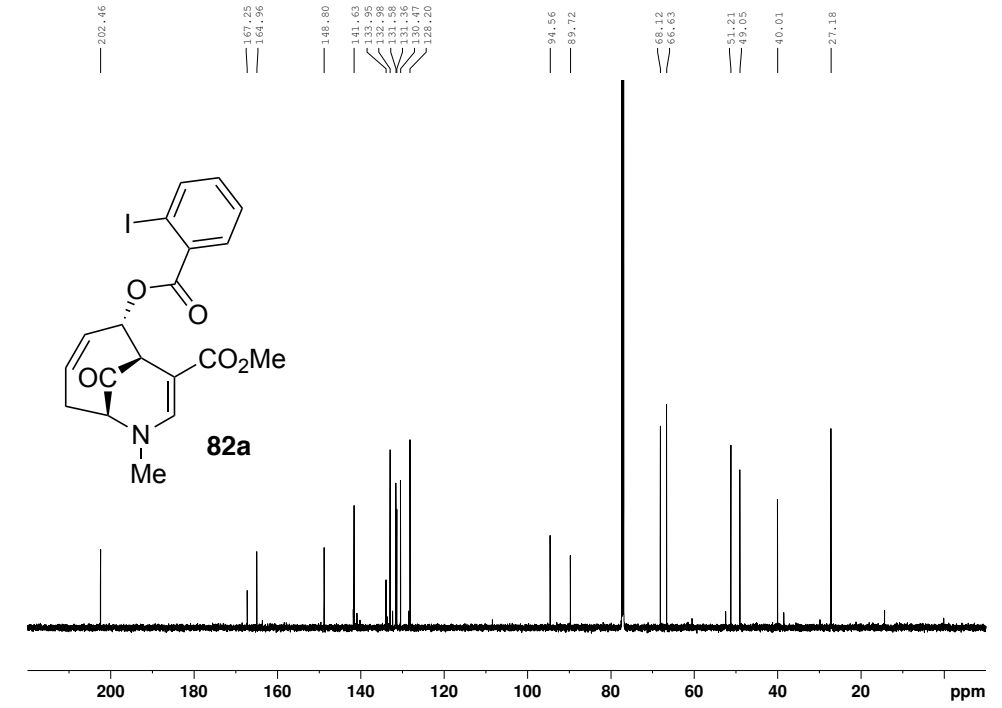
202.46
167.25
164.96
148.80
141.63
133.95
132.98
131.58
131.36
130.47
128.20
94.56
89.72
68.12
66.63
51.21
49.05
40.01
27.18
I
O
O
CO2Me
OC
N
Me
82a
200
180
160
140
120
100
80
60
40
20
ppm

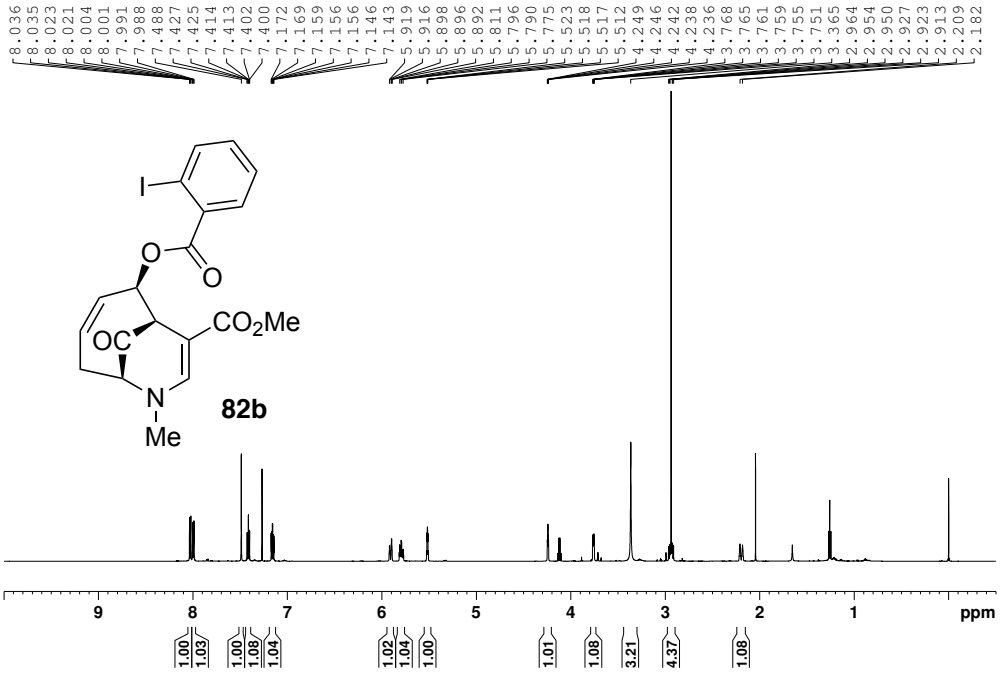
8.036
8.035
8.023
8.021
8.004
8.001
7.991
7.988
7.488
7.427
7.425
7.414
7.413
7.402
7.400
7.172
7.169
7.159
7.156
7.156
7.146
7.143
5.919
5.916
5.898
5.896
5.892
5.811
5.796
5.790
5.775
5.523
5.518
5.517
5.512
4.249
4.246
4.242
4.238
4.236
3.768
3.765
3.761
3.759
3.755
3.751
3.365
2.964
2.954
2.950
2.927
2.923
2.913
2.209
2.182
I
O
O
CO2Me
OC
N
Me
82b
9
8
7
6
5
4
3
2
1
ppm
1.00
1.03
1.00
1.08
1.04
1.02
1.04
1.00
1.01
1.08
3.21
4.37
1.08

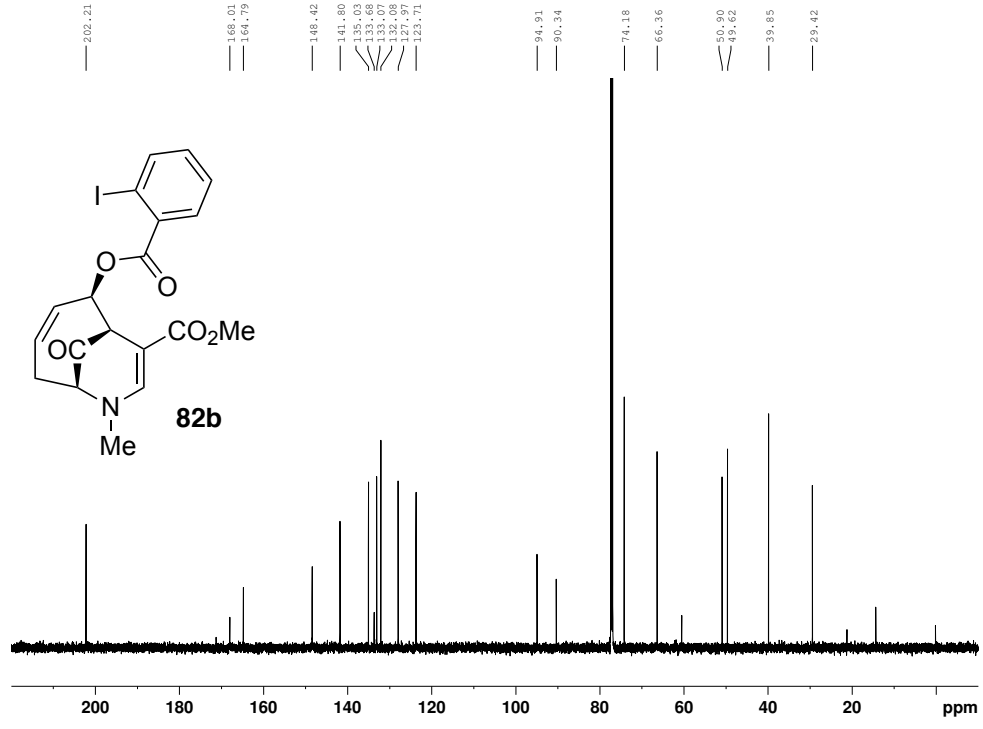
202.21
168.01
164.79
148.42
141.80
135.03
133.68
133.07
132.08
127.97
123.71
94.91
90.34
74.18
66.36
50.90
49.62
39.85
29.42
I
O
O
CO2Me
OC
N
Me
82b
200
180
160
140
120
100
80
60
40
20
ppm

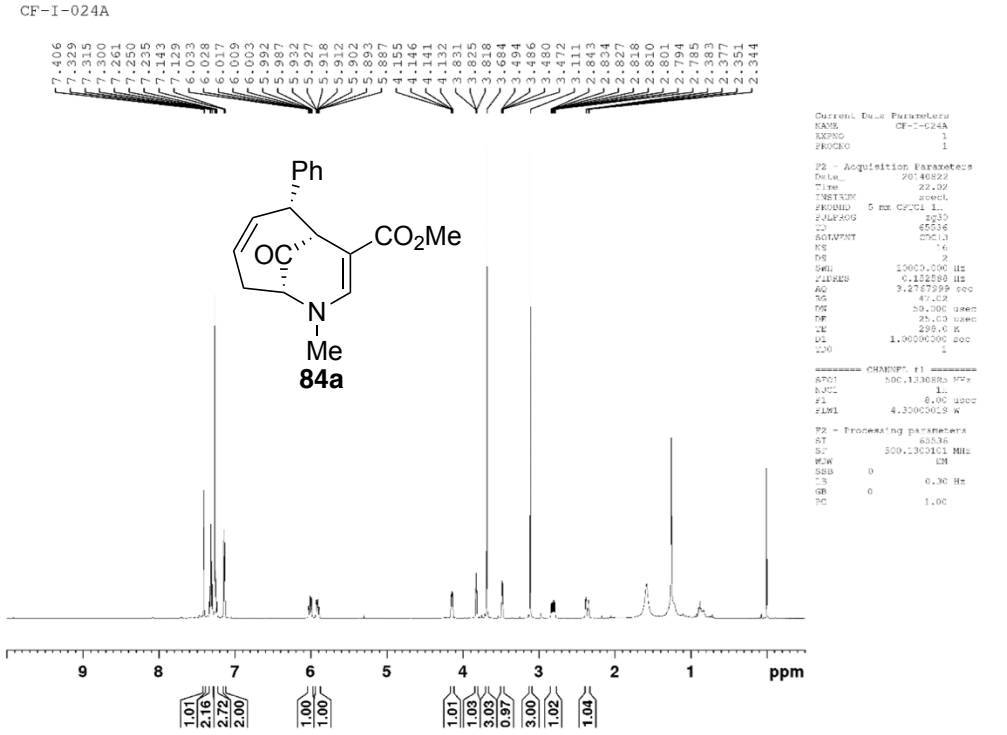
CF-I-024A
Ph
CO2Me
OC
N
Me
84a
ppm

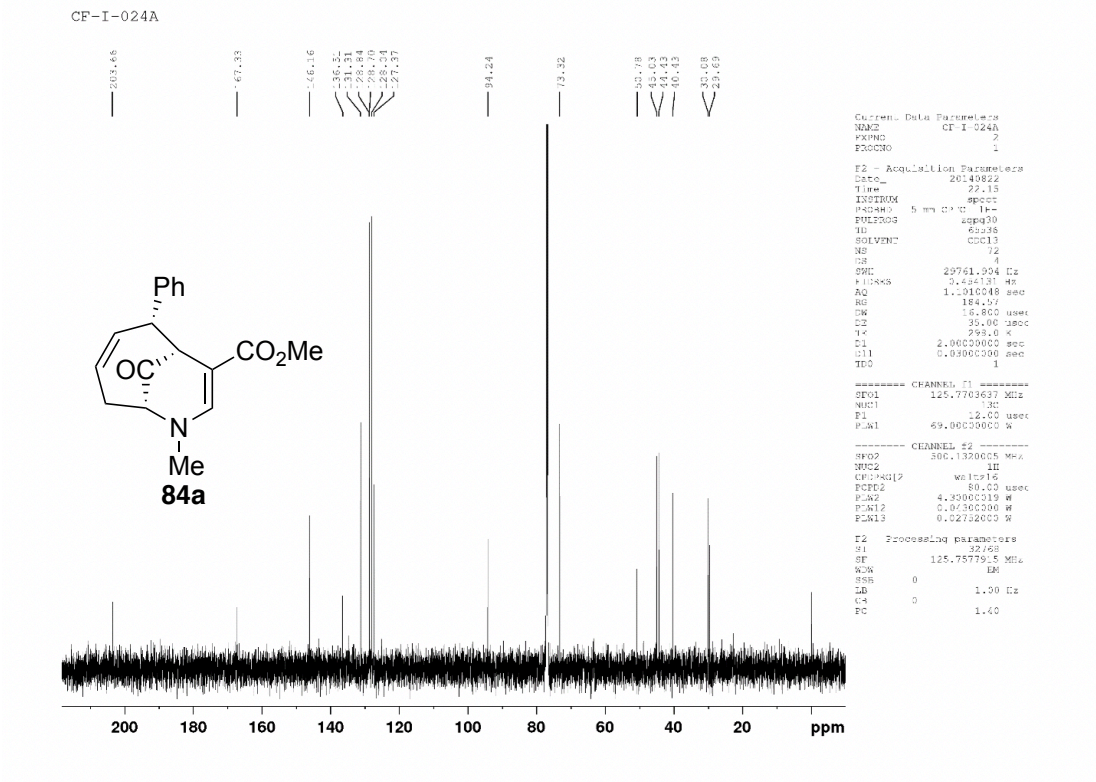
CF-I-024A
Ph
CO2Me
OC
N
Me
84a
ppm

CF-I-024B 2nd

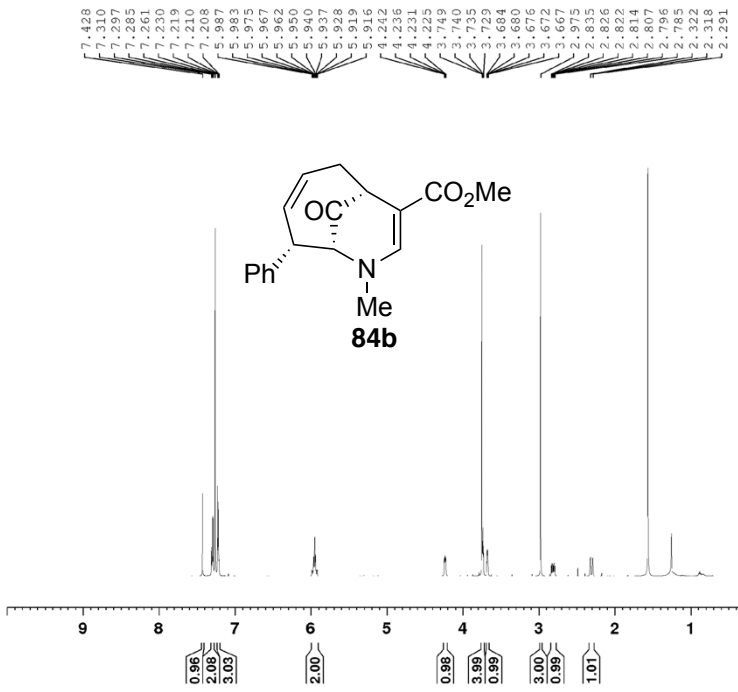


```
Current Data Parameters
NAME                  CF-I-024B
EXPNO                         1
PROCNO                        1

F2 - Acquisition Parameters
Date_                  20140825
Time                      20.51
INSTRUM                   spect
PROBHD    5 mm CPTCI 1H/
PULPROG                   zg30
TD                       65536
SOLVENT                  CDCl3
NS                           16
DS                            2
SWH                  12019.230 Hz
FIDRES                0.183399 Hz
AQ                    2.7262976 sec
RG                        68.88
DW                       41.600 usec
DE                       30.00 usec
TE                       298.0 K
D1                    1.00000000 sec
TD0                           1

======== CHANNEL f1 ========
SFO1                599.6637031 MHz
NUC1                        1H
PL1                       8.00 usec
PLW1                6.30959988 W

F2 - Processing parameters
SI                        65536
SF                599.6600141 MHz
WDW                         EM
SSB                  0
LB                            0.30 Hz
GB                   0
PC                            1.00
```

CF-I-024B

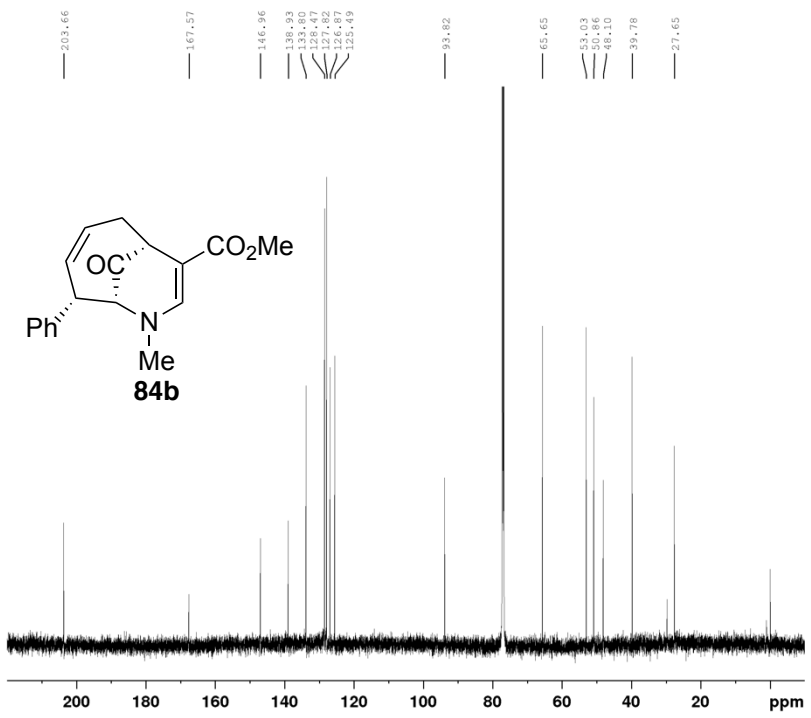


```
Current Data Parameters
NAME                  CF-I-024B
EXPNO                         2
PROCNO                        1

F2 - Acquisition Parameters
Date_                  20140825
Time                      22.19
INSTRUM                   spect
PROBHD    5 mm CPTCI 1H/
PULPROG                 zgpg30
TD                       65536
SOLVENT                  CDCl3
NS                         642
DS                           4
SWH                  42613.637 Hz
FIDRES                0.650232 Hz
AQ                    0.7689557 sec
RG                       188.21
DW                       11.733 usec
DE                       20.00 usec
TE                       298.0 K
D1                    2.00000000 sec
D11                   0.03000000 sec
TD0                           1

======== CHANNEL f1 ========
SFO1                150.8012132 MHz
NUC1                        13C
P1                       12.00 usec
PLW1                94.00000000 W

======== CHANNEL f2 ========
SFO2                599.6623986 MHz
NUC2                        1H
CPDPRG[2                waltz16
PCPD2                    80.00 usec
PLW2                 6.30959988 W
PLW12                0.06309600 W
PLW13                0.04038100 W

F2 - Processing parameters
SI                        32768
SF                150.7846309 MHz
WDW                         EM
SSB                  0
LB                            1.00 Hz
GB                   0
PC                            1.40
```

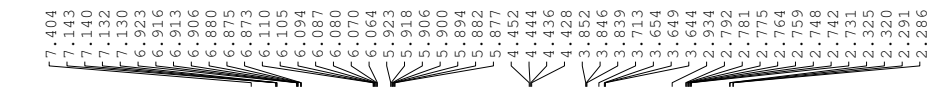
7.404
7.143
7.140
7.132
7.130
6.923
6.916
6.913
6.906
6.880
6.875
6.873
6.110
6.105
6.094
6.087
6.080
6.070
6.064
5.923
5.918
5.906
5.900
5.894
5.882
5.877
4.452
4.444
4.436
4.428
3.852
3.846
3.839
3.713
3.654
3.649
3.644
2.934
2.792
2.781
2.775
2.764
2.759
2.748
2.742
2.731
2.325
2.320
2.291
2.286

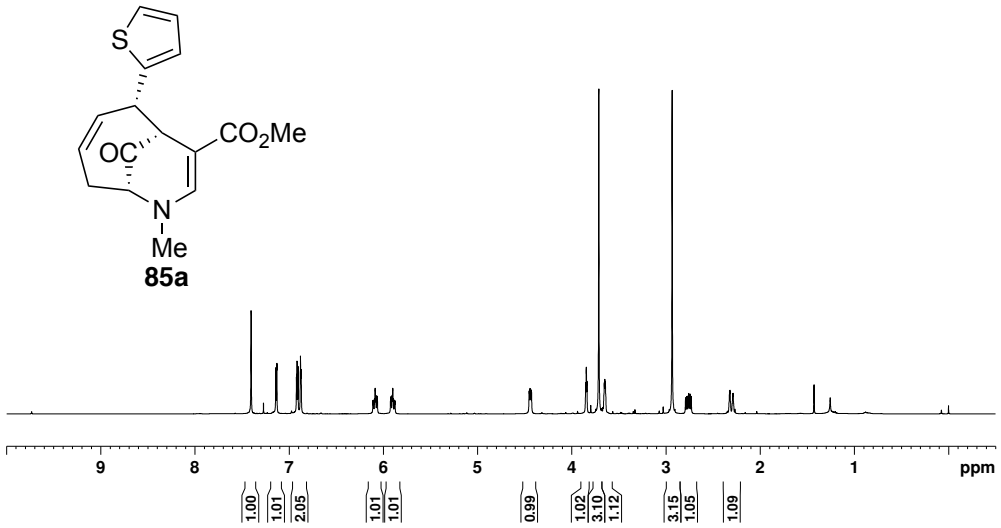
S
CO2Me
OC
N
Me
85a
9
8
7
6
5
4
3
2
1
ppm
1.00
1.01
2.05
1.01
1.01
0.99
1.02
3.10
1.12
3.15
1.05
1.09

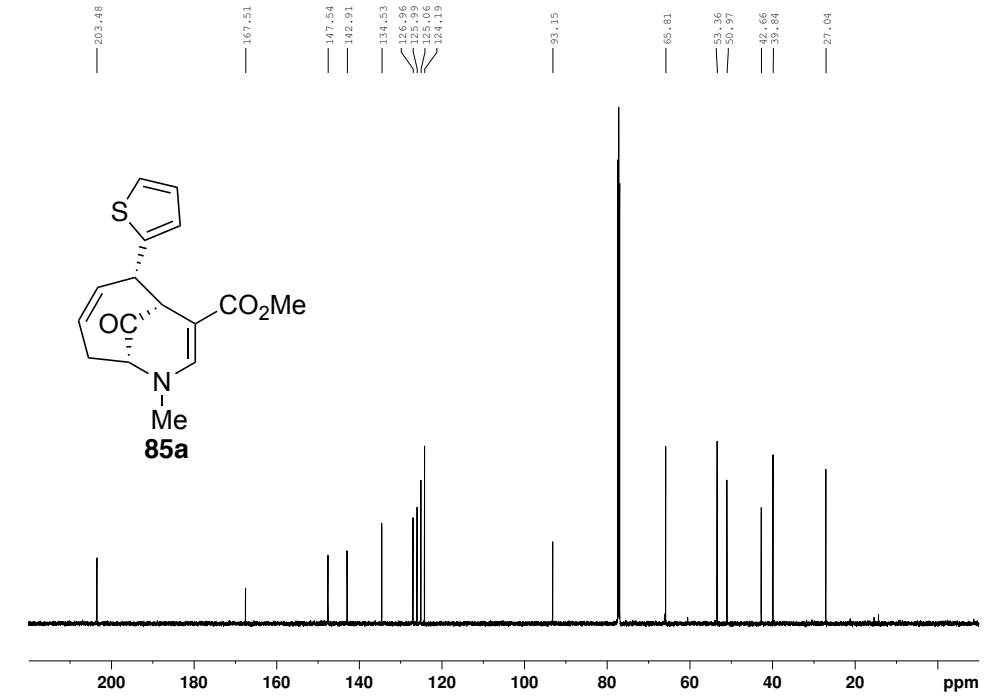
203.48
167.51
147.54
142.91
134.53
126.96
125.99
125.06
124.19
93.15
65.81
53.36
50.97
42.66
39.84
27.04
S
CO2Me
OC
N
Me
85a
200
180
160
140
120
100
80
60
40
20
ppm

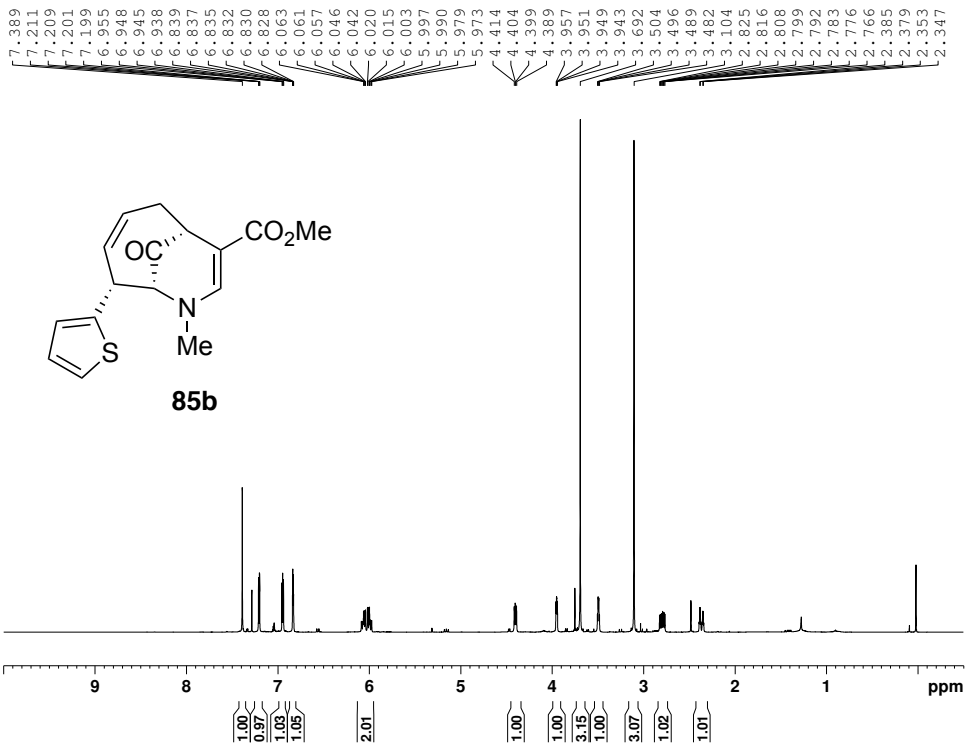
7.389
7.211
7.209
7.201
7.199
6.955
6.948
6.945
6.938
6.839
6.837
6.835
6.832
6.830
6.828
6.063
6.061
6.057
6.046
6.042
6.020
6.015
6.003
5.997
5.990
5.979
5.973
4.414
4.404
4.399
4.389
3.957
3.951
3.949
3.943
3.692
3.504
3.496
3.489
3.482
3.104
2.825
2.816
2.808
2.799
2.792
2.783
2.776
2.766
2.385
2.379
2.353
2.347
CO2Me
OC
N
Me
S
85b
9
8
7
6
5
4
3
2
1
ppm
1.00
0.97
1.03
1.05
2.01
1.00
1.00
3.15
1.00
3.07
1.02
1.01

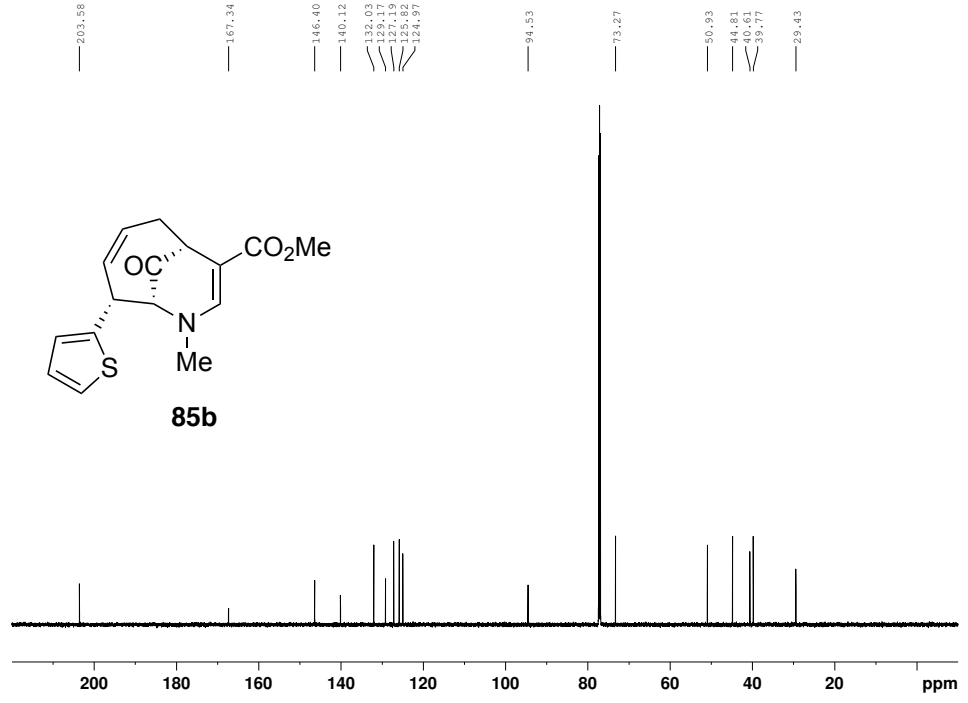
203.58
167.34
146.40
140.12
132.03
129.17
127.19
125.82
124.97
94.53
73.27
50.93
44.81
40.61
39.77
29.43
CO2Me
OC
N
Me
S
85b
200
180
160
140
120
100
80
60
40
20
ppm

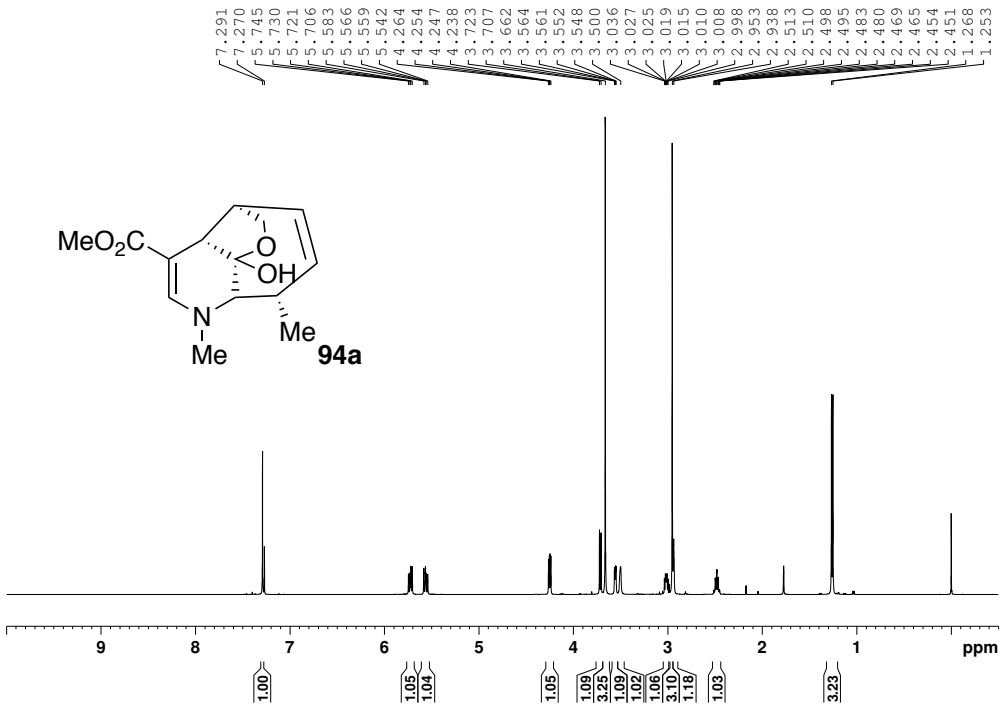
7.291
7.270
5.745
5.730
5.721
5.706
5.583
5.566
5.559
5.542
4.264
4.254
4.247
4.238
3.723
3.707
3.662
3.564
3.561
3.552
3.548
3.500
3.036
3.027
3.025
3.019
3.015
3.010
3.008
2.998
2.953
2.938
2.513
2.510
2.498
2.495
2.483
2.480
2.469
2.465
2.454
2.451
1.268
1.253
MeO2C
O
OH
N
Me
Me
94a
9
8
7
6
5
4
3
2
1
ppm
1.00
1.05
1.04
1.05
1.09
3.25
1.09
1.02
1.06
3.10
1.18
1.03
3.23

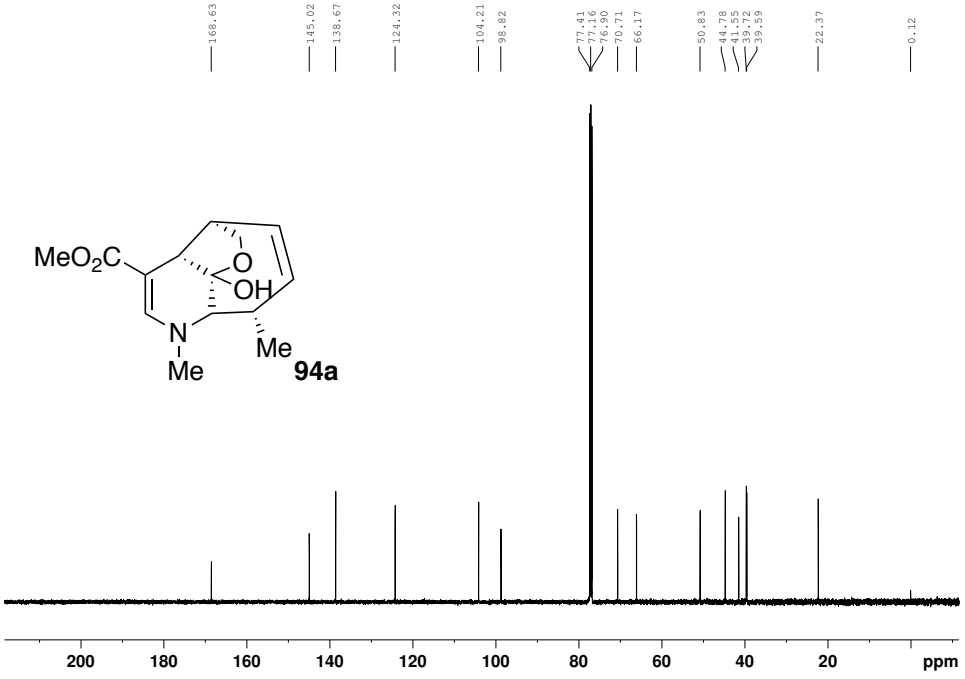
168.63
145.02
138.67
124.32
104.21
98.82
77.41
77.16
76.90
70.71
66.17
50.83
44.78
41.55
39.72
39.59
22.37
0.12
MeO2C
O
OH
N
Me
Me
94a
200
180
160
140
120
100
80
60
40
20
ppm

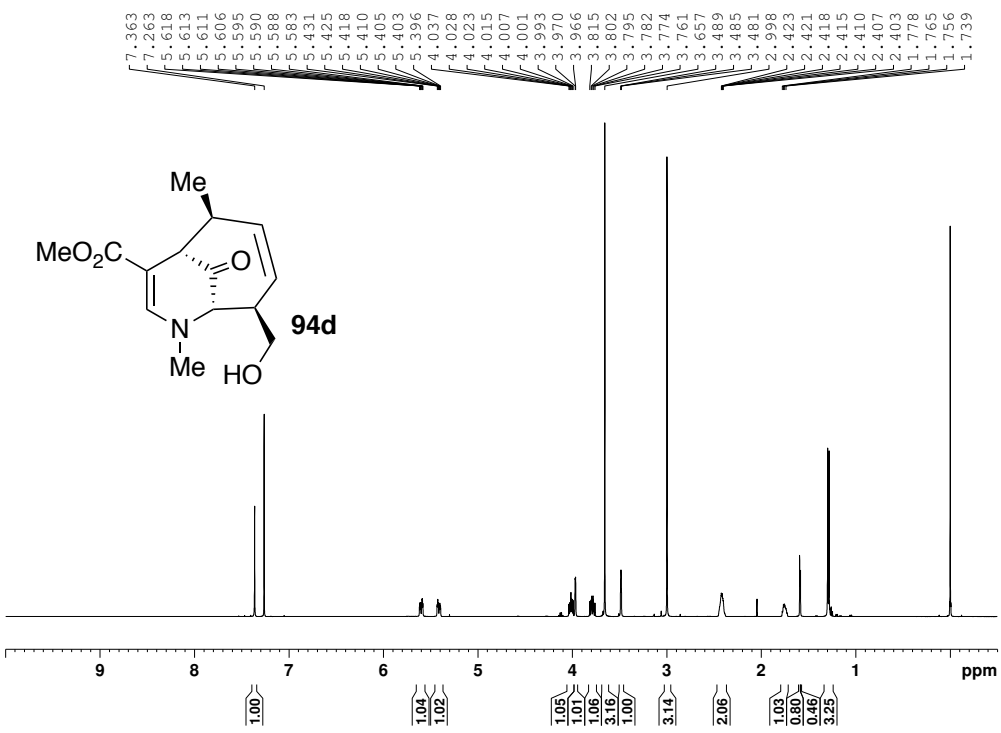
7.363
7.263
5.618
5.613
5.611
5.606
5.595
5.590
5.588
5.583
5.431
5.425
5.418
5.410
5.405
5.403
5.396
4.037
4.028
4.023
4.015
4.007
4.001
3.993
3.970
3.966
3.815
3.802
3.795
3.782
3.774
3.761
3.657
3.489
3.485
3.481
2.998
2.423
2.421
2.418
2.415
2.410
2.407
2.403
1.778
1.765
1.756
1.739
Me
MeO2C
O
N
Me
HO
94d
9
8
7
6
5
4
3
2
1
ppm
1.00
1.04
1.02
1.05
1.01
1.06
3.16
1.00
3.14
2.06
1.03
0.80
0.46
3.25

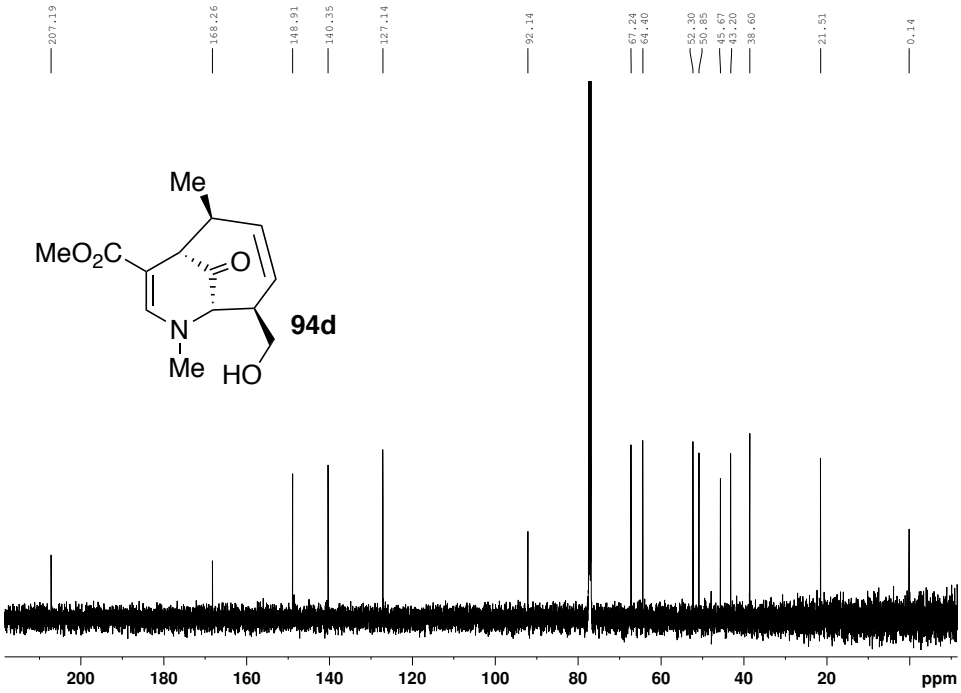
207.19
168.26
148.91
140.35
127.14
92.14
67.24
64.40
52.30
50.85
45.67
43.20
38.60
21.51
0.14
Me
MeO2C
O
N
Me
HO
94d
200
180
160
140
120
100
80
60
40
20
ppm

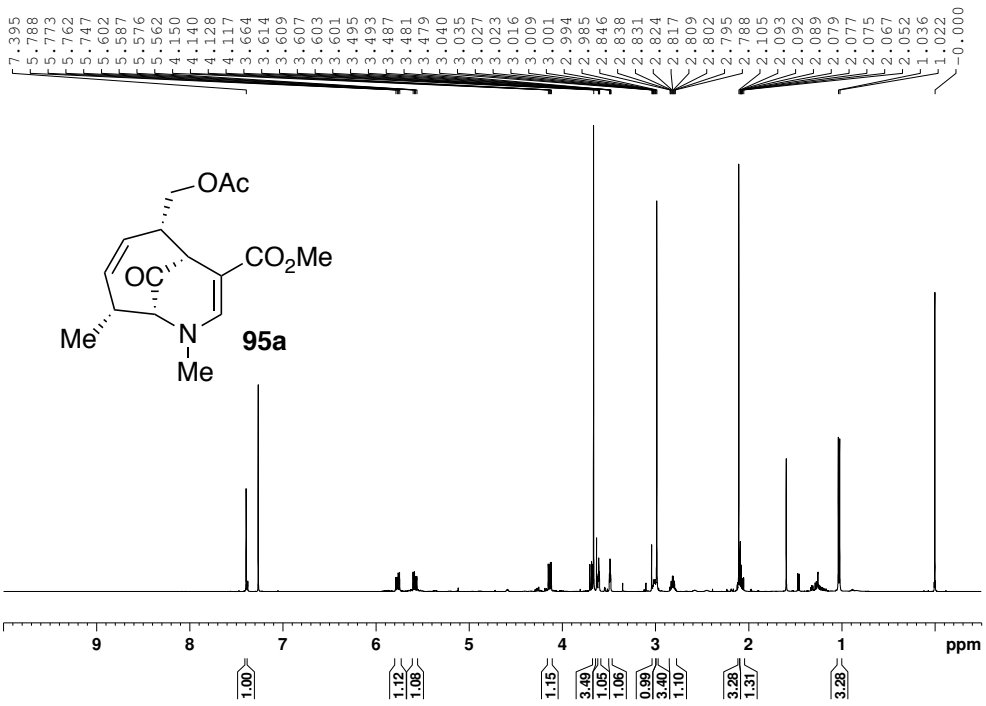
7.395
5.788
5.773
5.762
5.747
5.602
5.587
5.576
5.562
4.150
4.140
4.128
4.117
3.664
3.614
3.609
3.607
3.603
3.601
3.495
3.493
3.487
3.481
3.479
3.040
3.035
3.027
3.023
3.016
3.009
3.001
2.994
2.985
2.846
2.838
2.831
2.824
2.817
2.809
2.802
2.795
2.788
2.105
2.093
2.092
2.089
2.079
2.077
2.075
2.067
2.052
1.036
1.022
-0.000
OAc
CO2Me
OC
Me
N
Me
95a
9
8
7
6
5
4
3
2
1
ppm
1.00
1.12
1.08
1.15
3.49
1.05
1.06
0.99
3.40
1.10
3.28
1.31
3.28

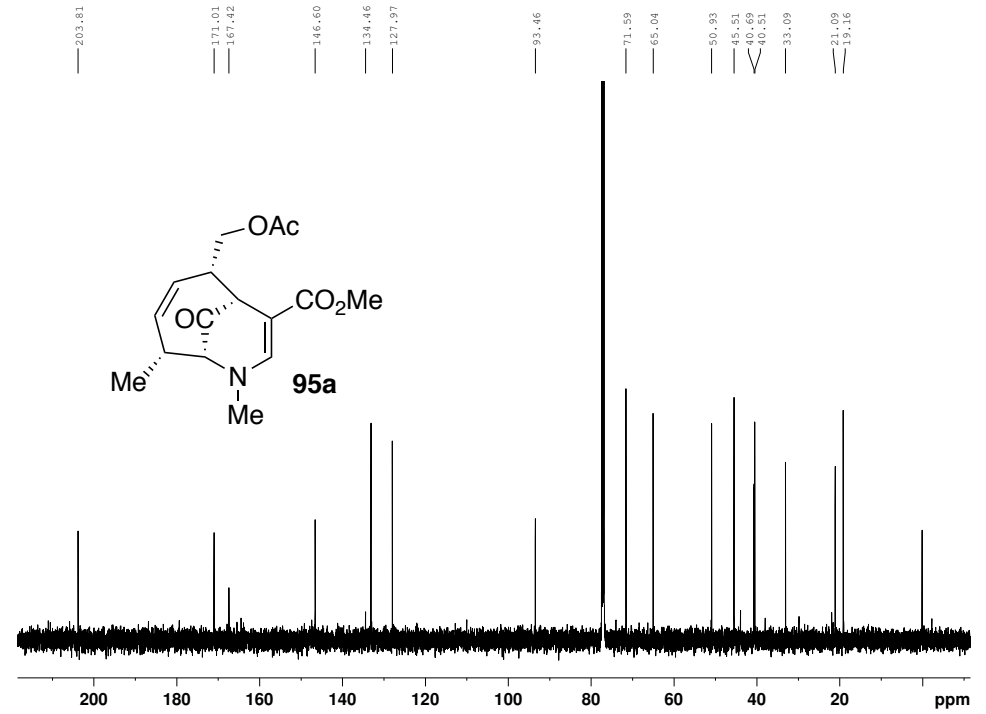
203.81
171.01
167.42
146.60
134.46
127.97
93.46
71.59
65.04
50.93
45.51
40.69
40.51
33.09
21.09
19.16
OAc
CO2Me
OC
Me
N
Me
95a
200
180
160
140
120
100
80
60
40
20
ppm

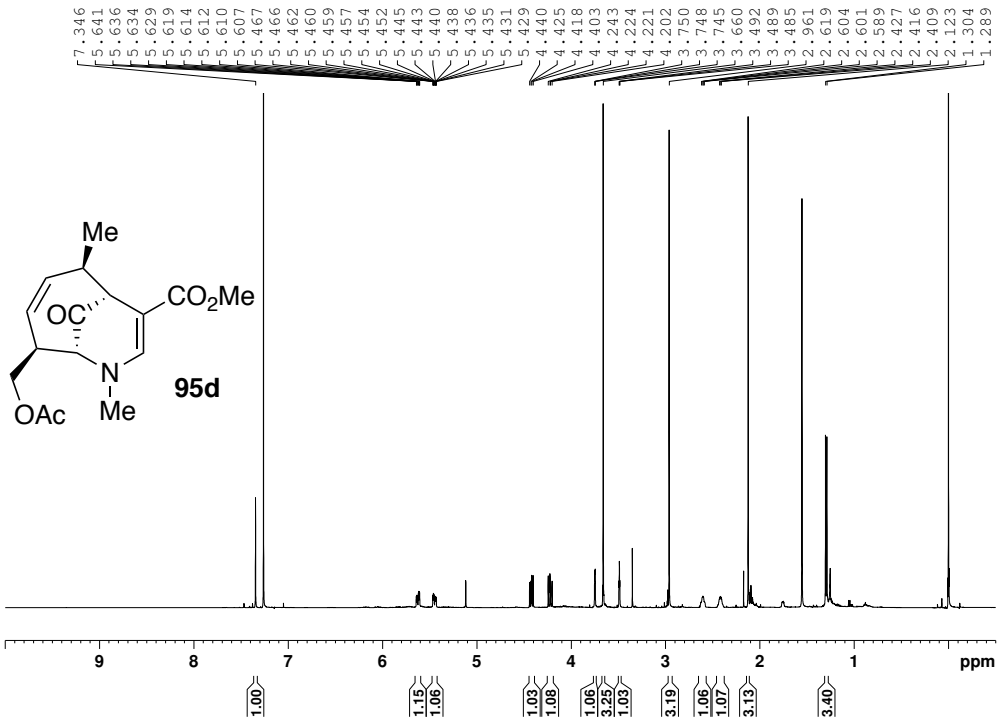
7.346
5.641
5.636
5.634
5.629
5.619
5.614
5.612
5.610
5.607
5.467
5.466
5.462
5.460
5.459
5.457
5.454
5.452
5.445
5.443
5.440
5.438
5.436
5.435
5.431
5.429
4.440
4.425
4.418
4.403
4.243
4.224
4.221
4.202
3.750
3.748
3.745
3.660
3.492
3.489
3.485
2.961
2.619
2.604
2.601
2.589
2.427
2.416
2.409
2.123
1.304
1.289
Me
CO2Me
OC
N
Me
OAc
95d
9
8
7
6
5
4
3
2
1
ppm
1.00
1.15
1.06
1.03
1.08
1.06
3.25
1.03
3.19
1.06
1.07
3.13
3.40

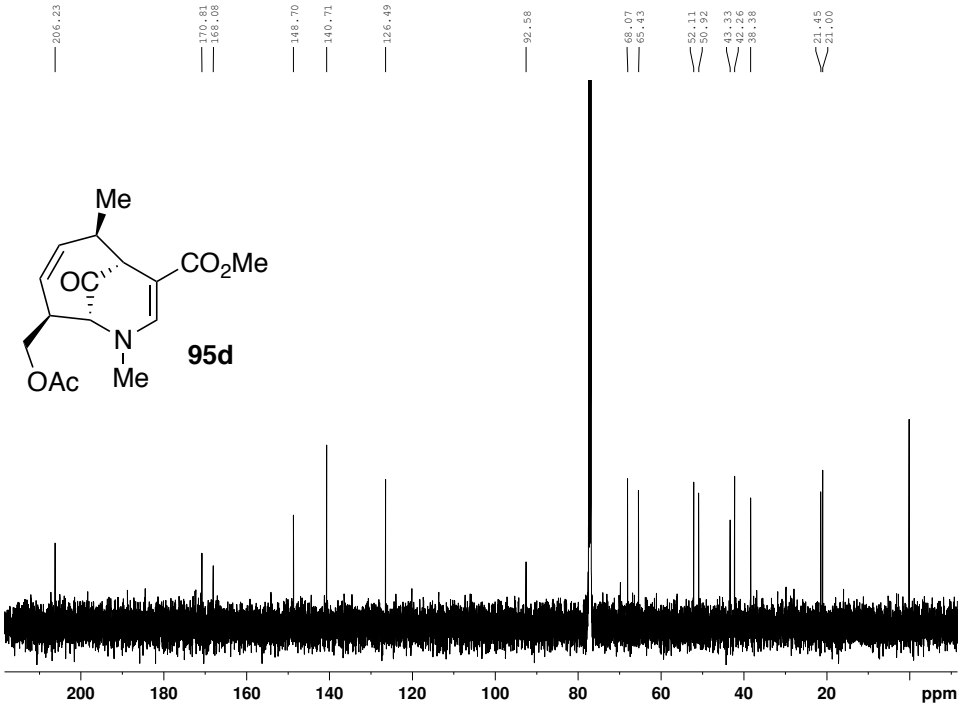
206.23
170.81
168.08
148.70
140.71
126.49
92.58
68.07
65.43
52.11
50.92
43.33
42.26
38.38
21.45
21.00
Me
CO2Me
OC
N
Me
OAc
95d
200
180
160
140
120
100
80
60
40
20
ppm

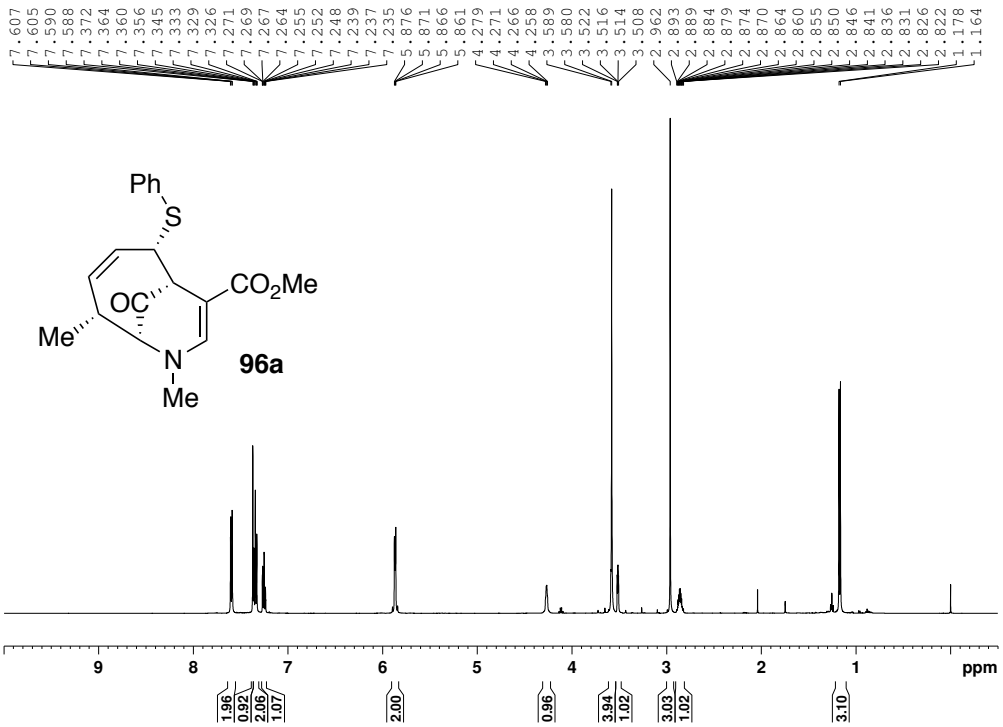
7.607
7.605
7.590
7.588
7.372
7.364
7.360
7.356
7.345
7.333
7.329
7.326
7.271
7.269
7.267
7.264
7.255
7.252
7.248
7.239
7.237
7.235
5.876
5.871
5.866
5.861
4.279
4.271
4.266
4.258
3.589
3.580
3.522
3.516
3.514
3.508
2.962
2.893
2.889
2.884
2.879
2.874
2.870
2.864
2.860
2.855
2.850
2.846
2.841
2.836
2.831
2.826
2.822
1.178
1.164
Ph
S
CO2Me
OC
Me
N
Me
96a
9
8
7
6
5
4
3
2
1
ppm
1.96
0.92
2.06
1.07
2.00
0.96
3.94
1.02
3.03
1.02
3.10

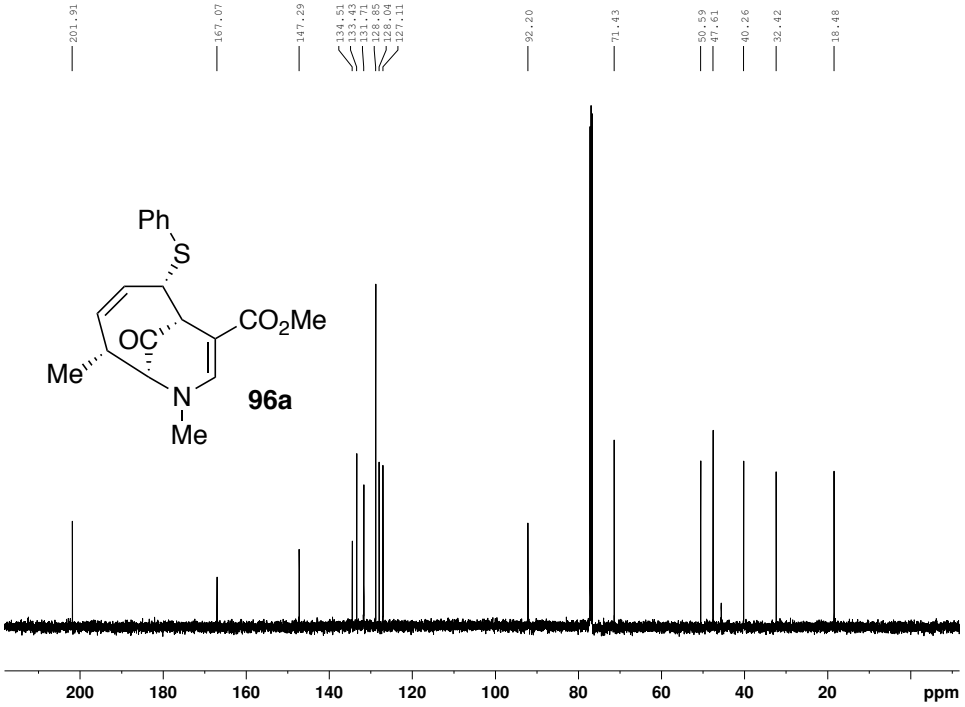
201.91
167.07
147.29
134.51
133.43
131.71
128.85
128.04
127.11
92.20
71.43
50.59
47.61
40.26
32.42
18.48
Ph
S
CO2Me
OC
Me
N
Me
96a
200
180
160
140
120
100
80
60
40
20
ppm

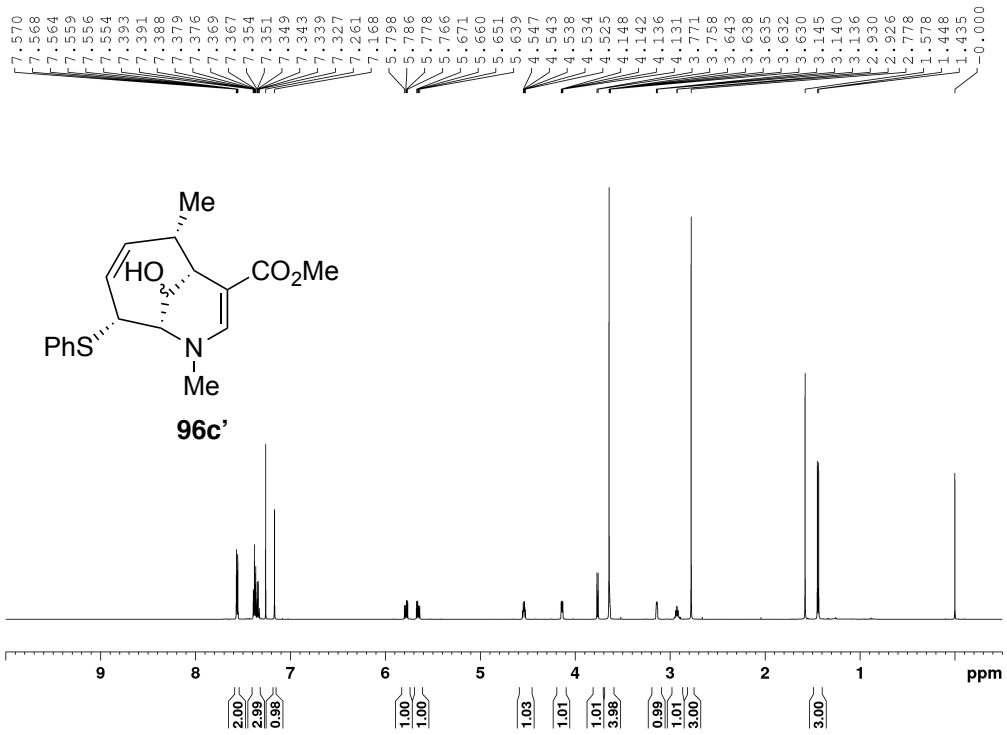
7.570
7.568
7.564
7.559
7.556
7.554
7.393
7.391
7.388
7.379
7.376
7.369
7.367
7.354
7.351
7.349
7.343
7.339
7.327
7.261
7.168
5.798
5.786
5.778
5.766
5.671
5.660
5.651
5.639
4.547
4.543
4.538
4.534
4.525
4.148
4.142
4.136
4.131
3.771
3.758
3.643
3.638
3.635
3.632
3.630
3.145
3.140
3.136
2.930
2.926
2.778
1.578
1.448
1.435
0.000
Me
HO
CO2Me
PhS
N
Me
96c'
9
8
7
6
5
4
3
2
1
ppm
2.00
2.99
0.98
1.00
1.00
1.03
1.01
1.01
3.98
0.99
1.01
3.00
3.00

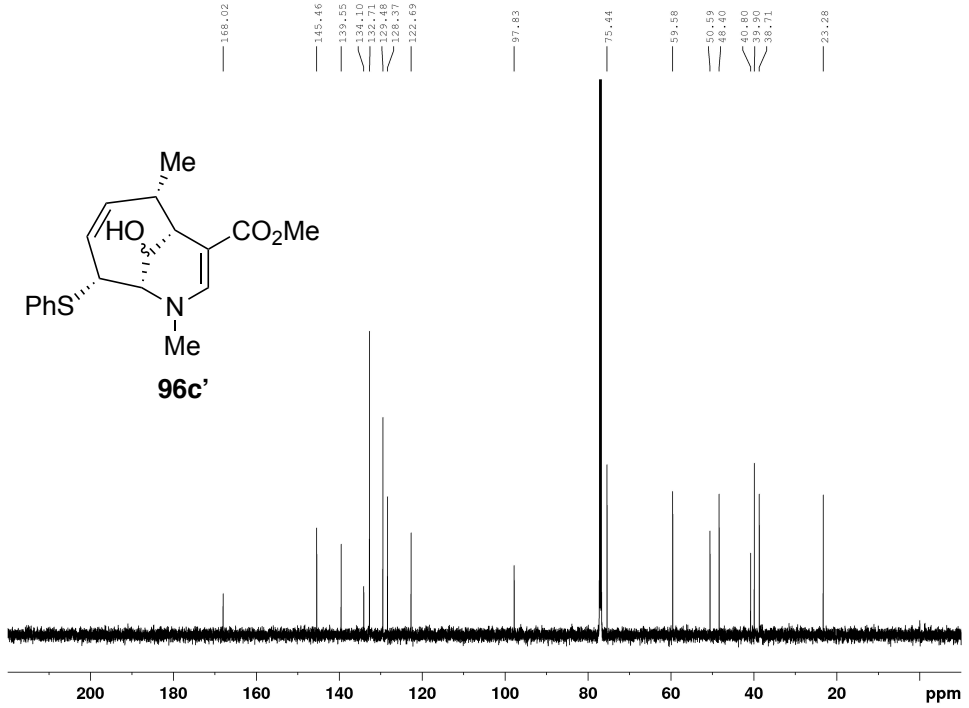
168.02
145.46
139.55
134.10
132.71
132.48
128.37
122.69
97.83
75.44
59.58
50.59
48.40
40.80
39.90
38.71
23.28
Me
HO
CO2Me
PhS
N
Me
96c'
200
180
160
140
120
100
80
60
40
20
ppm

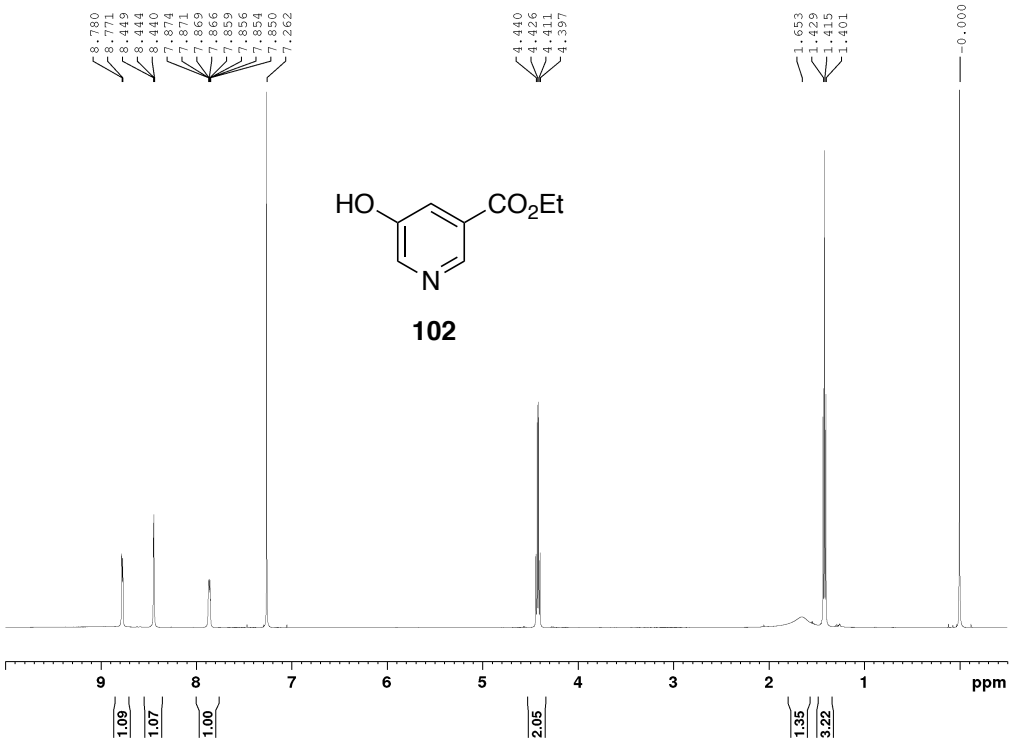
8.780
8.771
8.449
8.444
8.440
7.874
7.871
7.869
7.866
7.859
7.856
7.854
7.850
7.262
4.440
4.426
4.411
4.397
1.653
1.429
1.415
1.401
0.000
HO
CO2Et
N
9
8
7
6
5
4
3
2
1
ppm
1.09
1.07
1.00
2.05
1.35
3.22

102

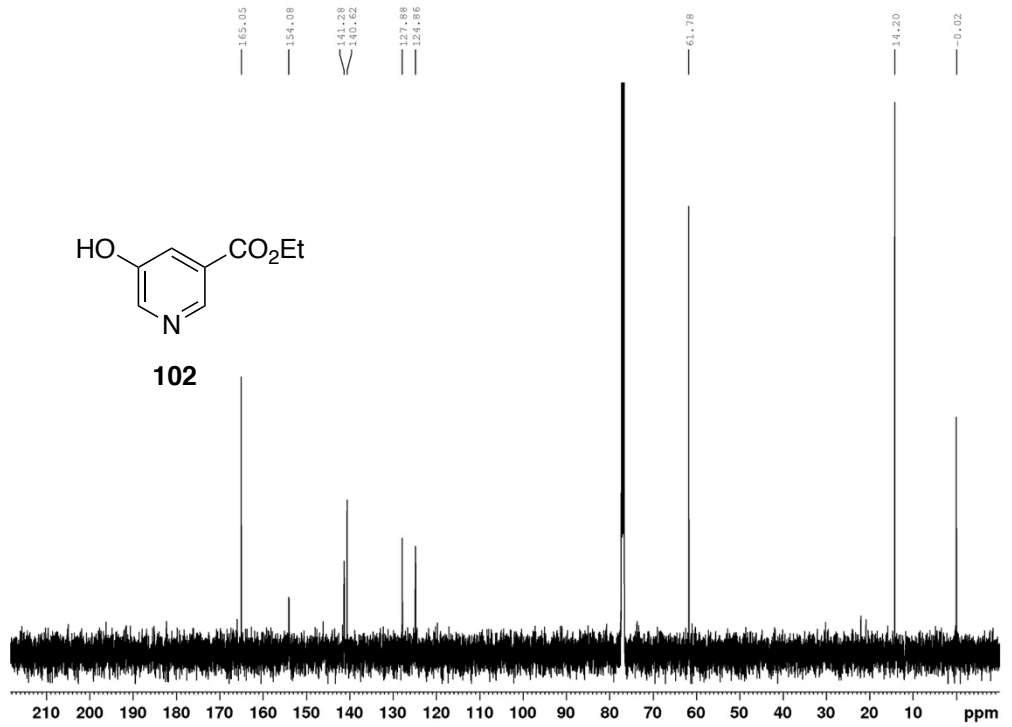
165.05
154.08
141.28
140.62
127.88
124.86
61.78
14.20
0.02
HO
CO2Et
N
210
200
190
180
170
160
150
140
130
120
110
100
90
80
70
60
50
40
30
20
10
ppm

102

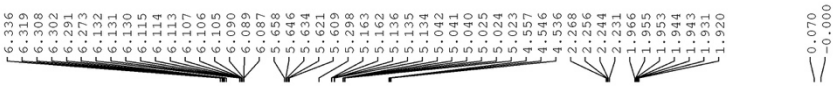
6.336
6.319
6.308
6.302
6.291
6.273
6.132
6.131
6.130
6.115
6.114
6.113
6.107
6.106
6.105
6.090
6.089
6.087
5.658
5.646
5.634
5.621
5.609
5.298
5.163
5.162
5.136
5.135
5.134
5.042
5.041
5.040
5.025
5.024
5.023
4.557
4.546
4.536
2.268
2.256
2.244
2.231
1.966
1.955
1.953
1.944
1.943
1.931
1.920
0.070
-0.000

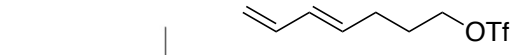
OTf

107

9
8
7
6
5
4
3
2
1
ppm
1.00
1.03
1.00
1.06
1.01
2.23
2.13
2.18
0.43

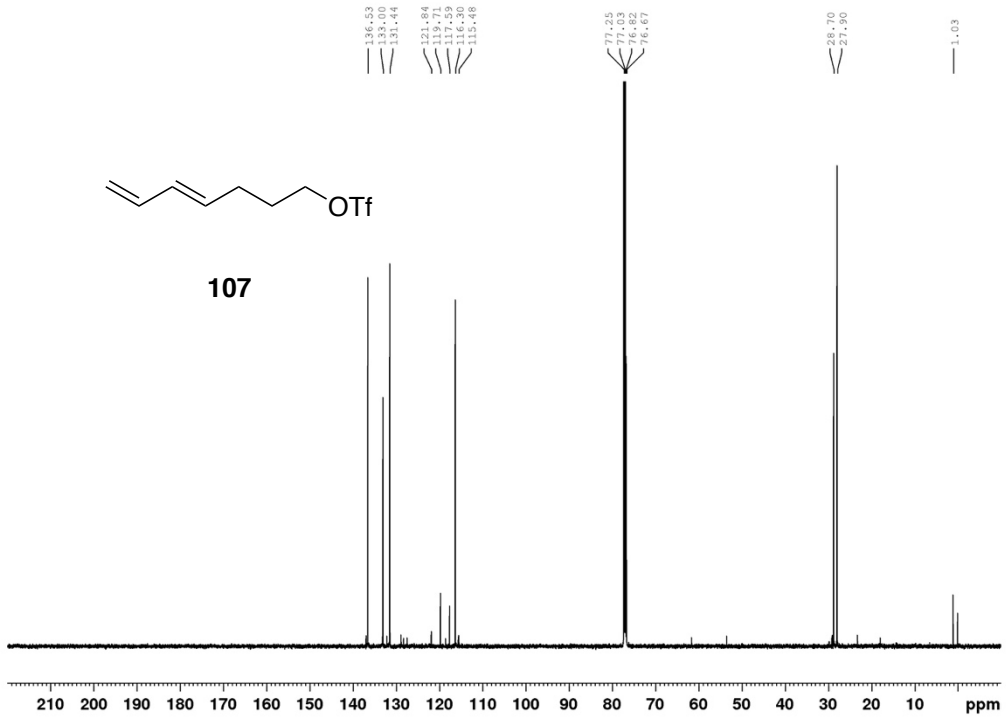
136.53
133.00
131.44
121.84
119.71
117.59
116.30
115.48
77.25
77.03
76.82
76.67
28.70
27.90
1.03
210
200
190
180
170
160
150
140
130
120
110
100
90
80
70
60
50
40
30
20
10
ppm

OTf

107

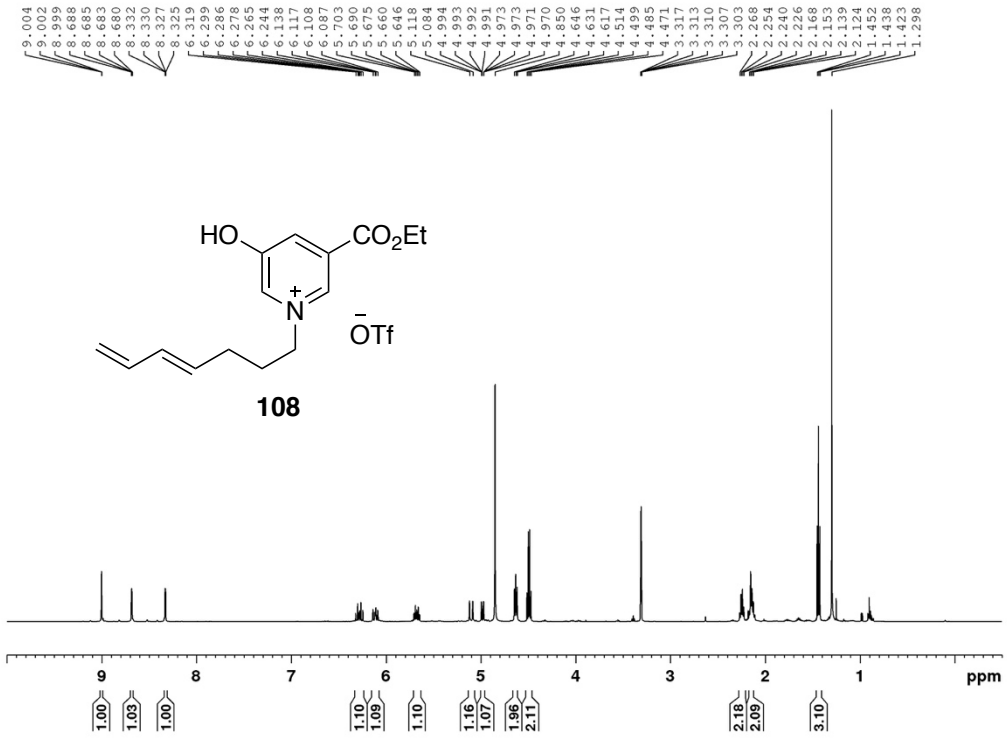
HO
CO2Et
N+
OTf−
108
ppm

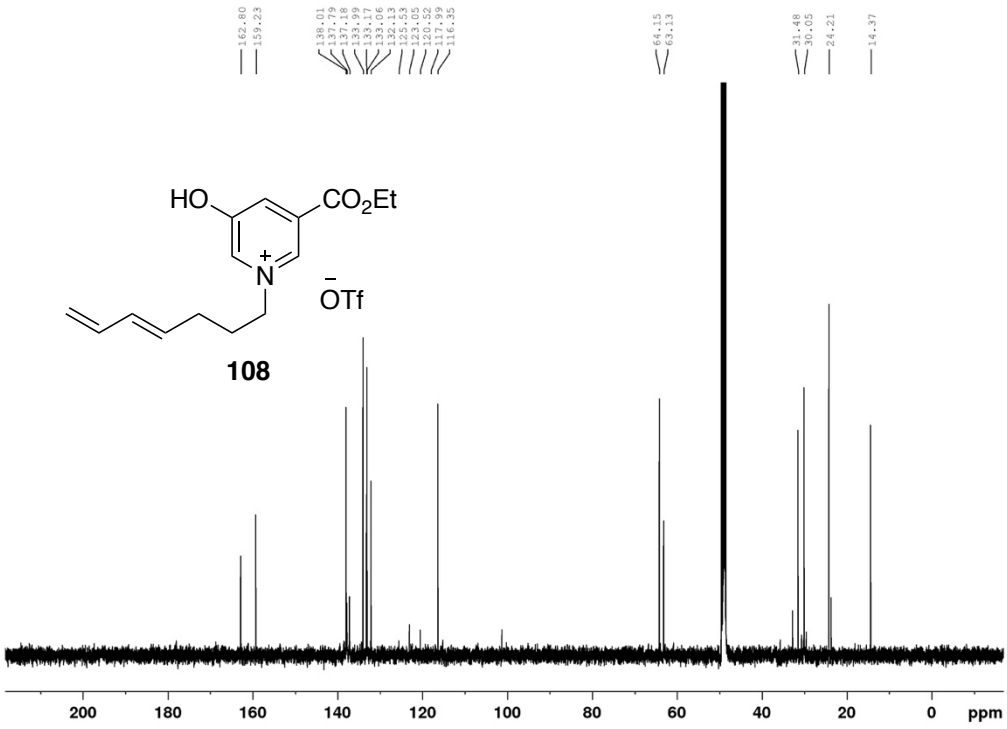
HO
CO2Et
N+
OTf−
108
ppm

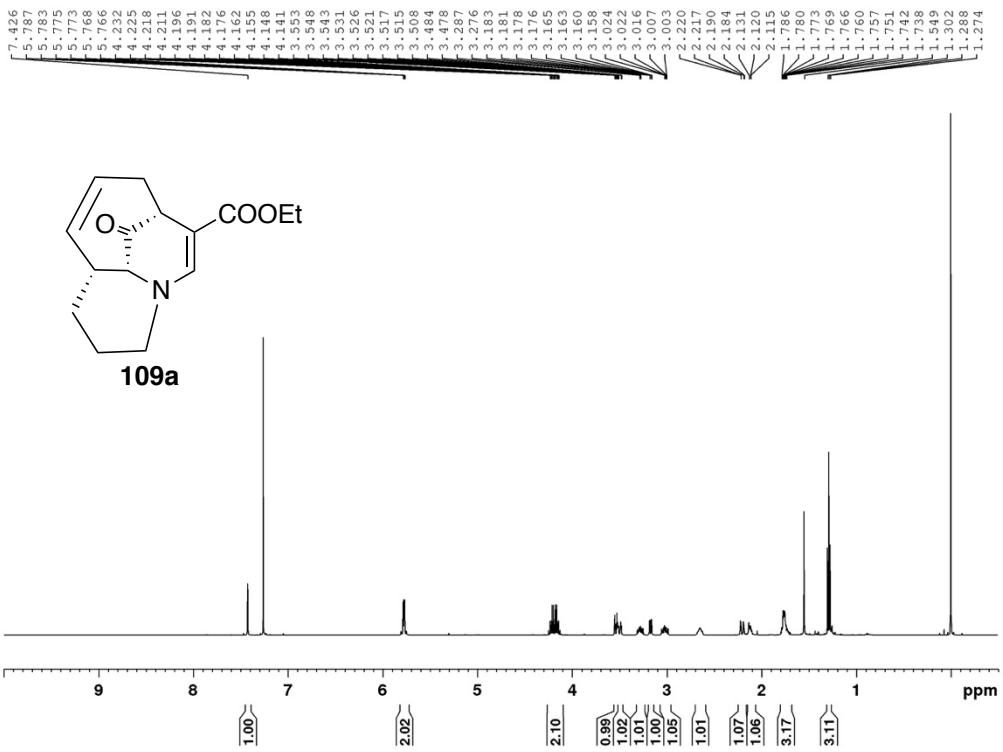
COOEt
O
N
109a
ppm

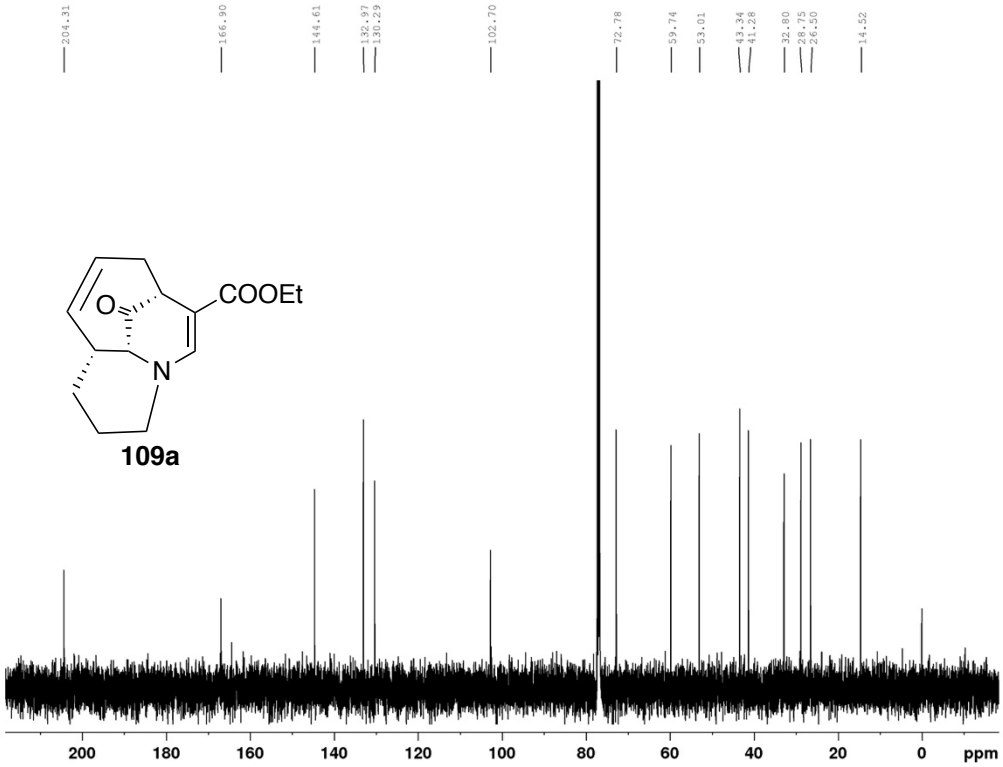
COOEt
O
N
109a
ppm

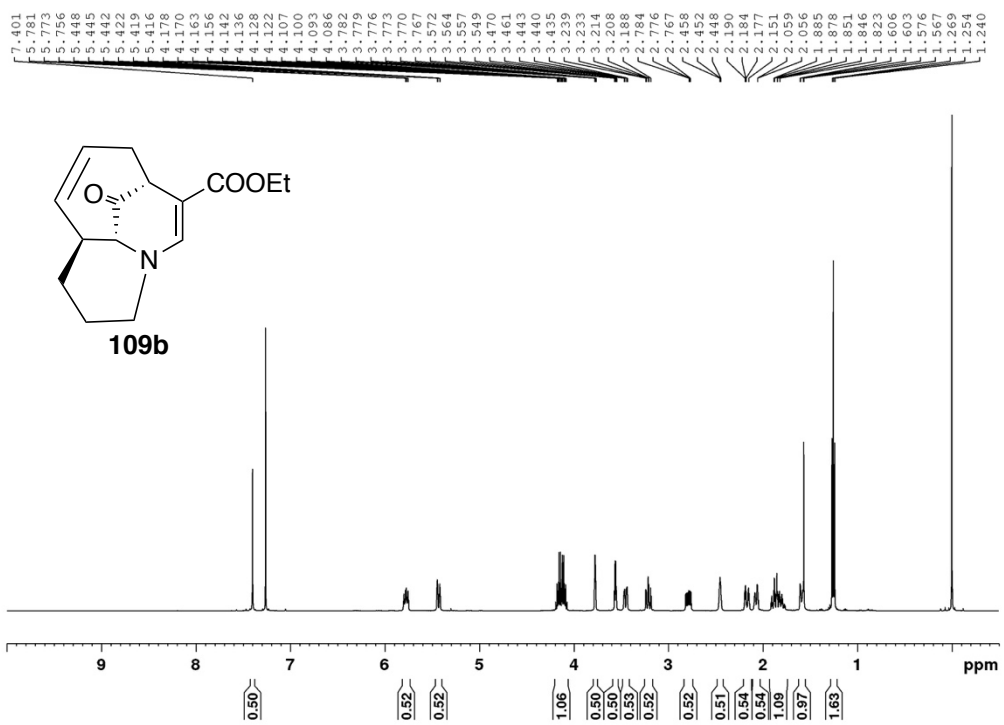
7.401
5.781
5.773
5.756
5.448
5.445
5.442
5.422
5.419
5.416
4.178
4.170
4.163
4.156
4.142
4.136
4.128
4.122
4.107
4.100
4.093
4.086
3.782
3.779
3.776
3.773
3.770
3.767
3.572
3.564
3.557
3.549
3.470
3.461
3.443
3.440
3.435
3.239
3.233
3.214
3.208
3.188
2.784
2.776
2.767
2.458
2.452
2.448
2.190
2.184
2.177
2.151
2.059
2.056
1.885
1.878
1.851
1.846
1.823
1.606
1.603
1.576
1.567
1.269
1.254
1.240
O
N
COOEt
109b
9
8
7
6
5
4
3
2
1
ppm
0.50
0.52
0.52
1.06
0.50
0.50
0.53
0.52
0.52
0.51
0.54
0.54
1.09
0.97
1.63

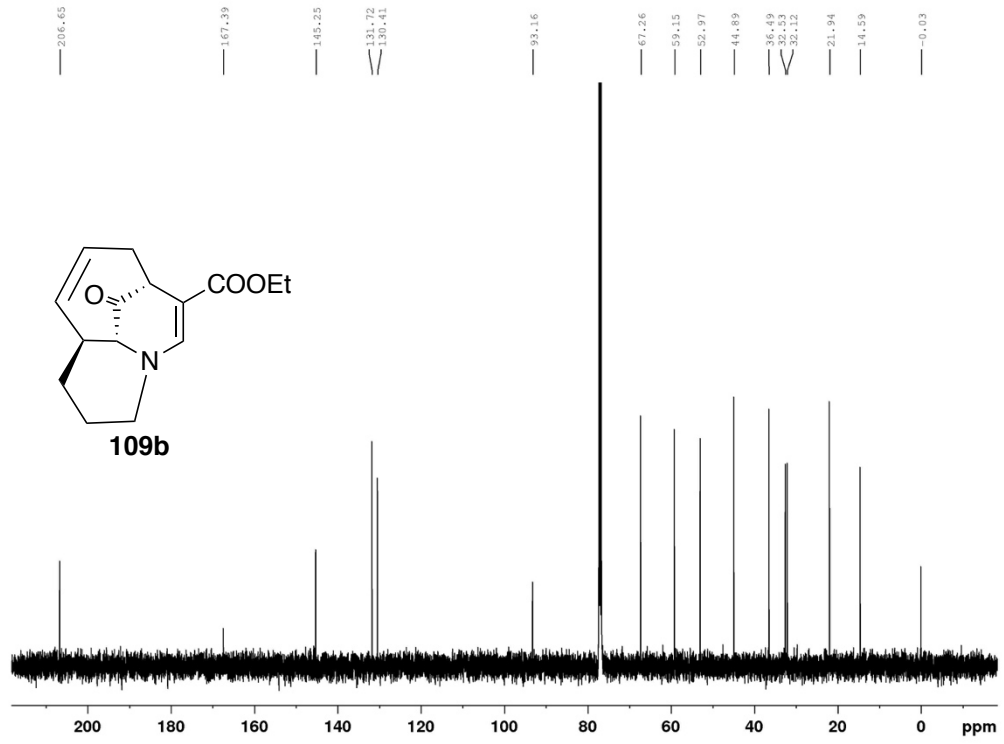
206.65
167.39
145.25
131.72
130.41
93.16
67.26
59.15
52.97
44.89
36.49
32.53
32.12
21.94
14.59
-0.03
O
N
COOEt
109b
200
180
160
140
120
100
80
60
40
20
0
ppm

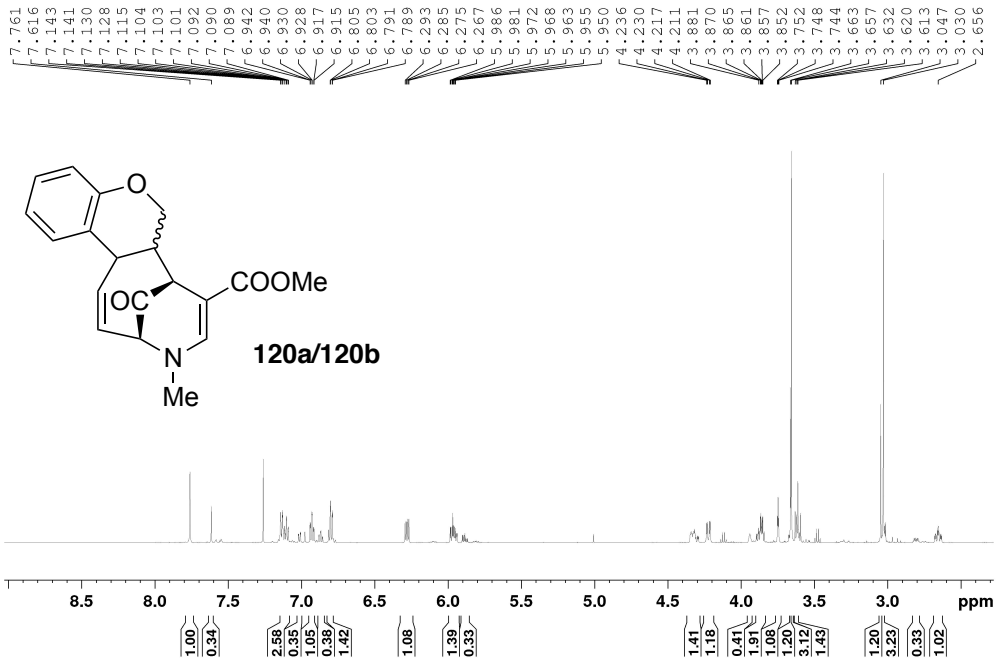
7.761
7.616
7.143
7.141
7.130
7.128
7.115
7.104
7.103
7.101
7.092
7.090
7.089
6.942
6.940
6.930
6.928
6.917
6.915
6.805
6.803
6.791
6.789
6.293
6.285
6.275
6.267
5.986
5.981
5.972
5.968
5.963
5.955
5.950
4.236
4.230
4.217
4.211
3.881
3.870
3.865
3.861
3.857
3.852
3.752
3.748
3.744
3.663
3.657
3.632
3.620
3.613
3.047
3.030
2.656
O
COOMe
OC
N
Me
120a/120b
8.5
8.0
7.5
7.0
6.5
6.0
5.5
5.0
4.5
4.0
3.5
3.0
ppm
1.00
0.34
2.58
0.35
1.05
0.38
1.42
1.08
1.39
0.33
1.41
1.18
0.41
1.91
1.08
1.20
3.12
1.43
1.20
3.23
0.33
1.02

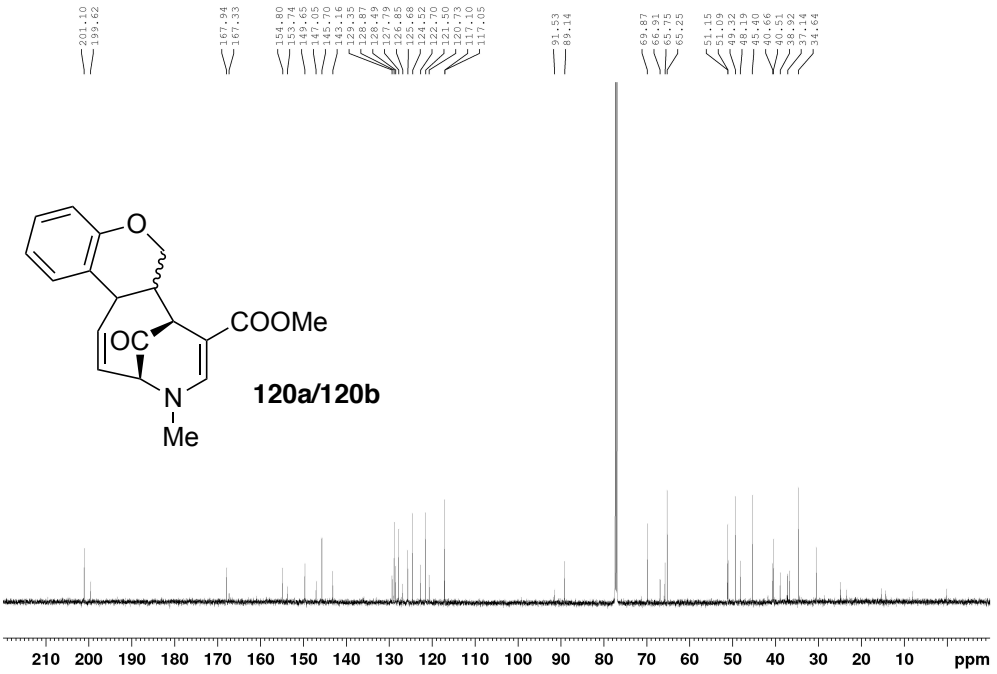
201.10
199.62
167.94
167.33
154.80
153.74
149.65
147.55
145.70
143.16
129.35
128.87
128.49
127.79
126.65
125.68
124.52
122.70
121.50
120.73
117.70
117.05
91.53
89.14
69.87
66.91
65.75
65.25
51.15
51.09
49.32
48.19
45.40
40.66
40.51
38.92
37.14
34.64
O
COOMe
OC
N
Me
120a/120b
210
200
190
180
170
160
150
140
130
120
110
100
90
80
70
60
50
40
30
20
10
ppm

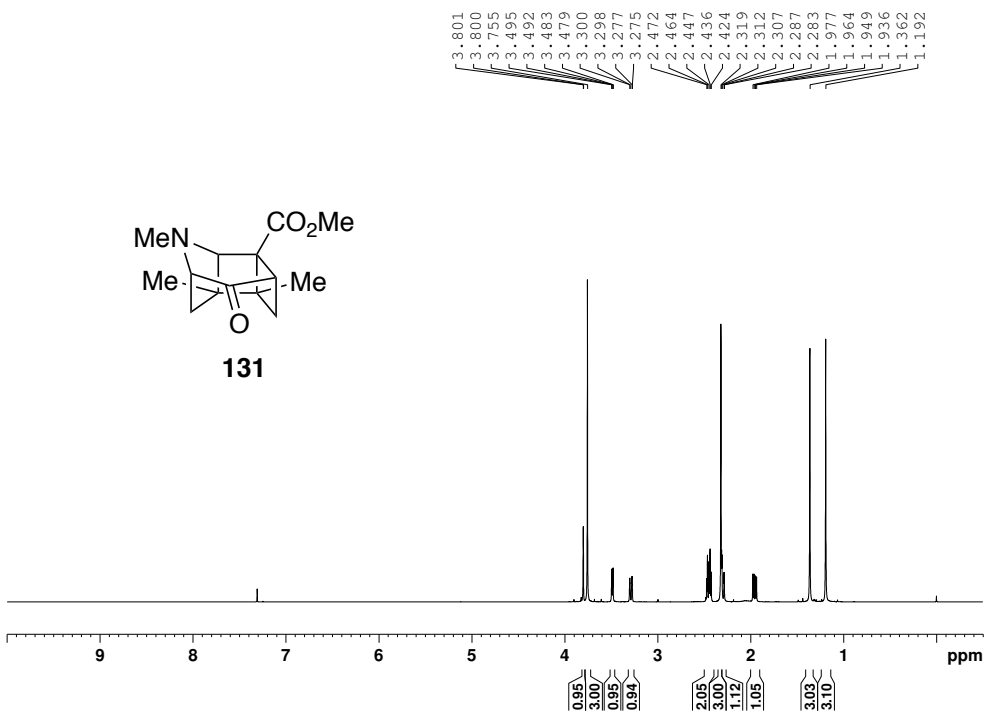
3.801
3.800
3.755
3.495
3.492
3.483
3.479
3.300
3.298
3.277
3.275
2.472
2.464
2.447
2.436
2.424
2.319
2.312
2.307
2.287
2.283
1.977
1.964
1.949
1.936
1.362
1.192
MeN
CO2Me
Me
Me
O
131
9
8
7
6
5
4
3
2
1
ppm
0.95
3.00
0.95
0.94
2.05
3.00
1.12
1.05
3.03
3.10

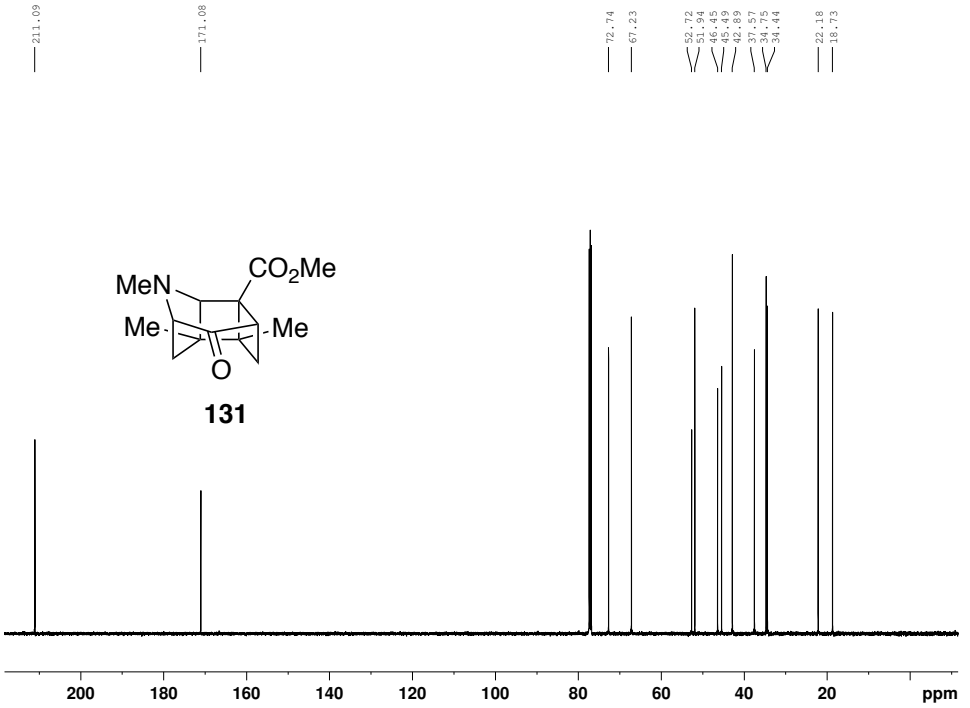
211.09
171.08
72.74
67.23
52.72
51.94
46.45
45.49
42.89
37.57
34.75
34.44
22.18
18.73
MeN
CO2Me
Me
Me
O
131
200
180
160
140
120
100
80
60
40
20
ppm

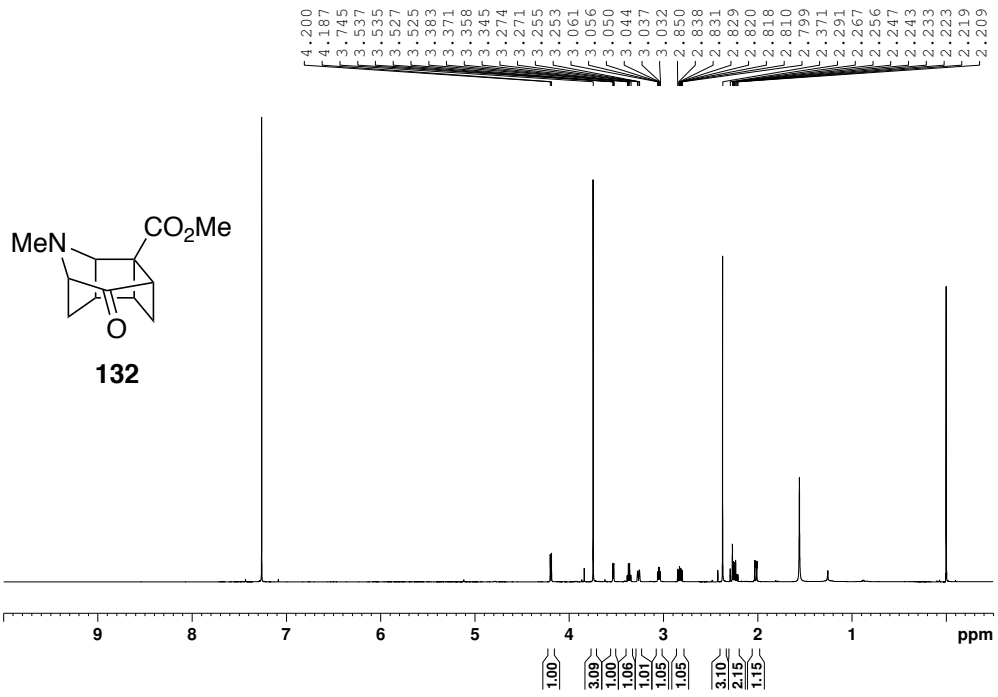
4.200
4.187
3.745
3.537
3.535
3.527
3.525
3.383
3.371
3.358
3.345
3.274
3.271
3.255
3.253
3.061
3.056
3.050
3.044
3.037
3.032
2.850
2.838
2.831
2.829
2.820
2.818
2.810
2.799
2.371
2.291
2.267
2.256
2.247
2.243
2.233
2.223
2.219
2.209
MeN
CO2Me
O
132
9
8
7
6
5
4
3
2
1
ppm
1.00
3.09
1.00
1.06
1.01
1.05
1.05
3.10
2.15
1.15

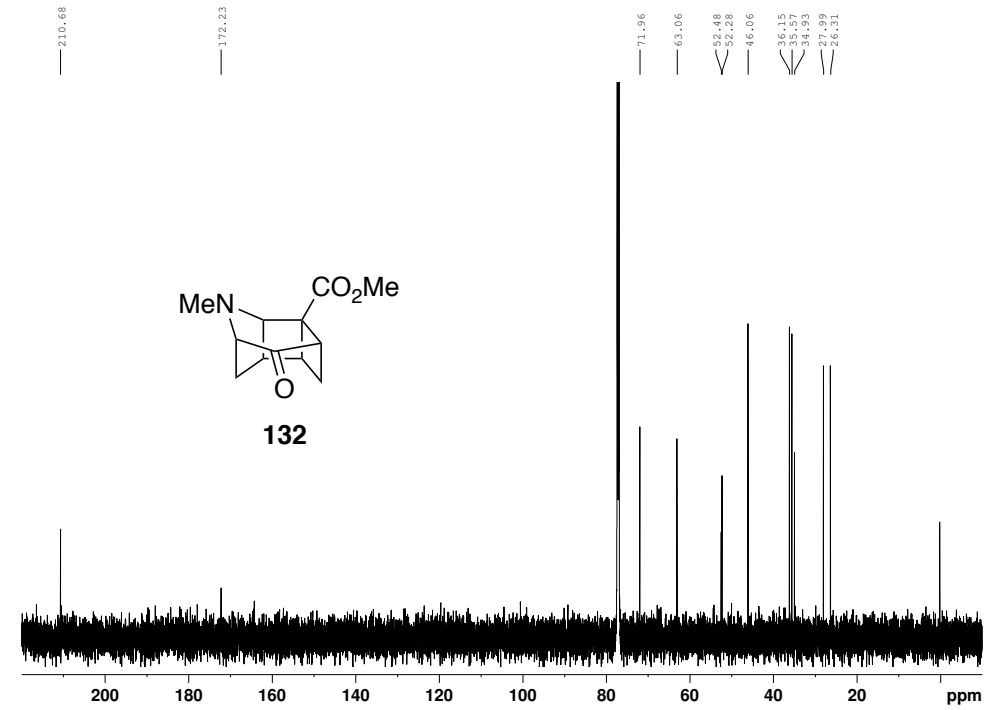
210.68
172.23
71.96
63.06
52.48
52.28
46.06
36.15
35.57
34.83
27.99
26.31
MeN
CO2Me
O
132
200
180
160
140
120
100
80
60
40
20
ppm

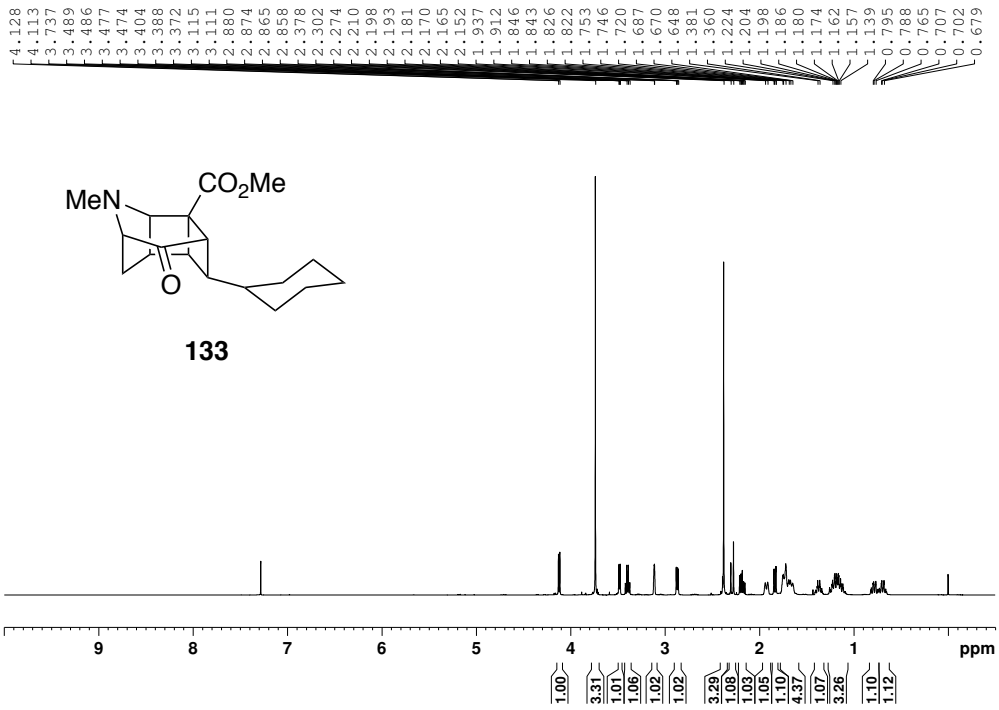
4.128
4.113
3.737
3.489
3.486
3.477
3.474
3.404
3.388
3.372
3.115
3.111
2.880
2.874
2.865
2.858
2.378
2.302
2.274
2.210
2.198
2.193
2.181
2.170
2.165
2.152
1.937
1.912
1.846
1.843
1.826
1.822
1.753
1.746
1.720
1.687
1.670
1.648
1.381
1.360
1.224
1.204
1.198
1.186
1.180
1.174
1.162
1.157
1.139
0.795
0.788
0.765
0.707
0.702
0.679
MeN
CO2Me
O
133
9
8
7
6
5
4
3
2
1
ppm
1.00
3.31
1.01
1.06
1.02
1.02
3.29
1.08
1.03
1.05
1.10
4.37
1.07
3.26
1.10
1.12

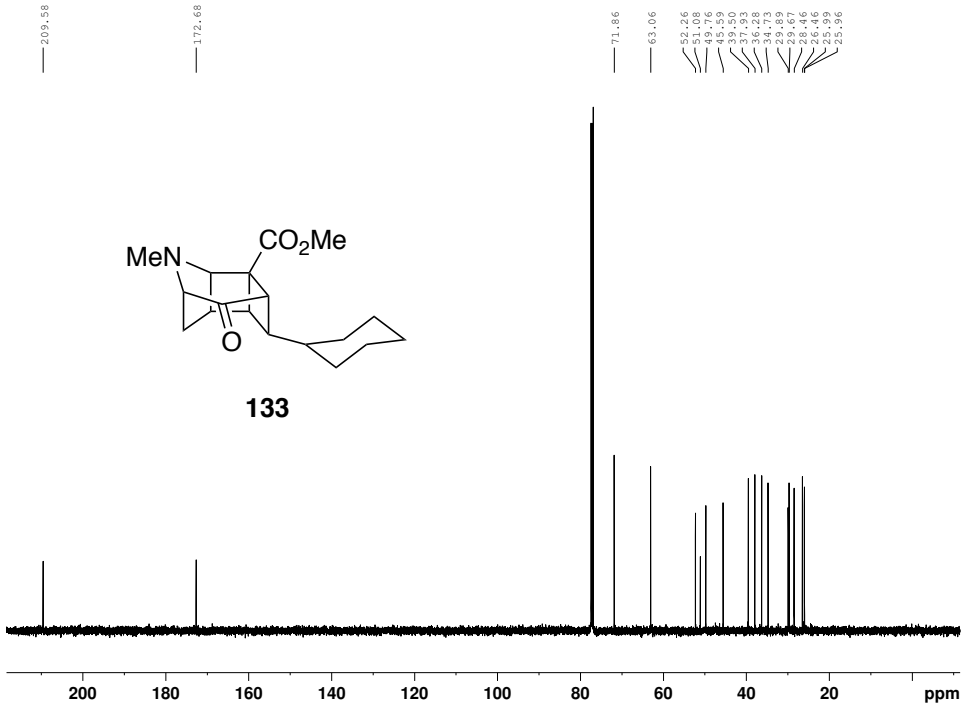
209.58
172.68
71.86
63.06
52.26
51.08
49.76
45.59
45.50
37.93
36.28
34.73
29.89
29.67
28.46
26.46
25.99
25.96
MeN
CO2Me
O
133
200
180
160
140
120
100
80
60
40
20
ppm

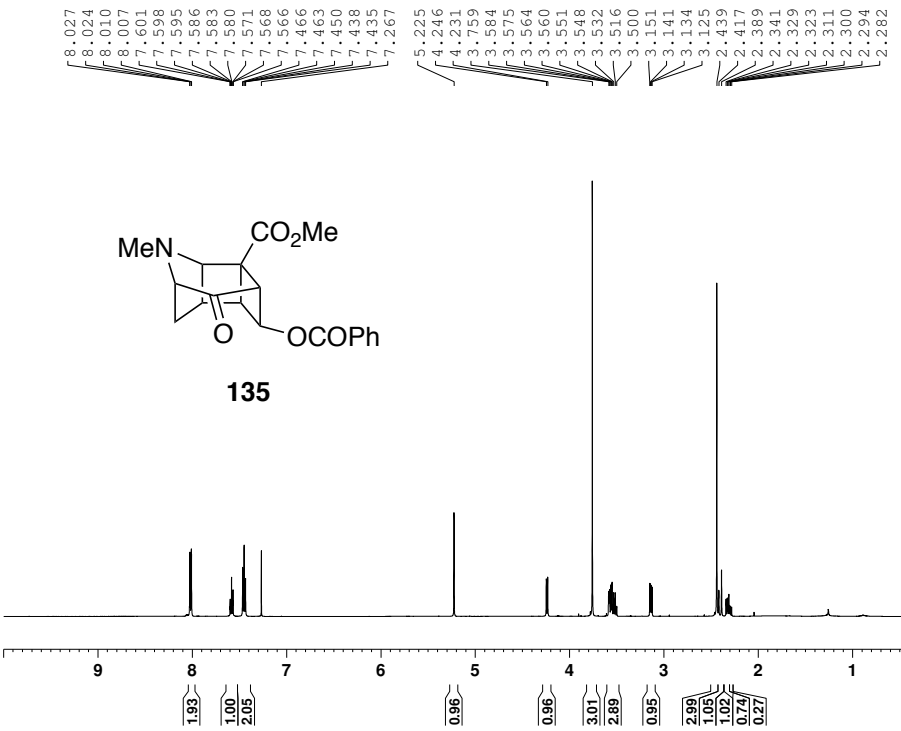
8.027
8.024
8.010
8.007
7.601
7.598
7.595
7.586
7.583
7.580
7.571
7.568
7.566
7.466
7.463
7.450
7.438
7.435
7.267
5.225
4.246
4.231
3.759
3.584
3.575
3.564
3.560
3.551
3.548
3.532
3.516
3.500
3.151
3.141
3.134
3.125
2.439
2.417
2.389
2.341
2.329
2.323
2.311
2.300
2.294
2.282
MeN
CO2Me
O
OCOPh
135
9
8
7
6
5
4
3
2
1
ppm
1.93
1.00
2.05
0.96
0.96
3.01
2.89
0.95
2.99
1.05
1.02
0.74
0.27

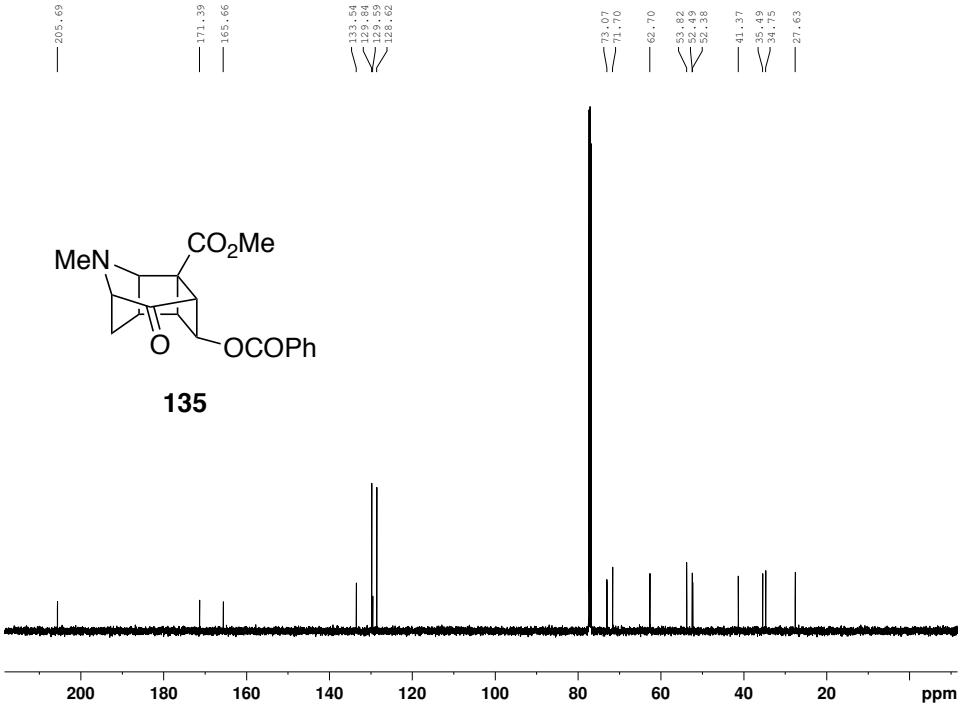
205.69
171.39
165.66
133.54
129.84
129.59
128.62
73.07
71.70
62.70
53.82
52.49
52.38
41.37
35.49
34.75
27.63
MeN
CO2Me
O
OCOPh
135
200
180
160
140
120
100
80
60
40
20
ppm

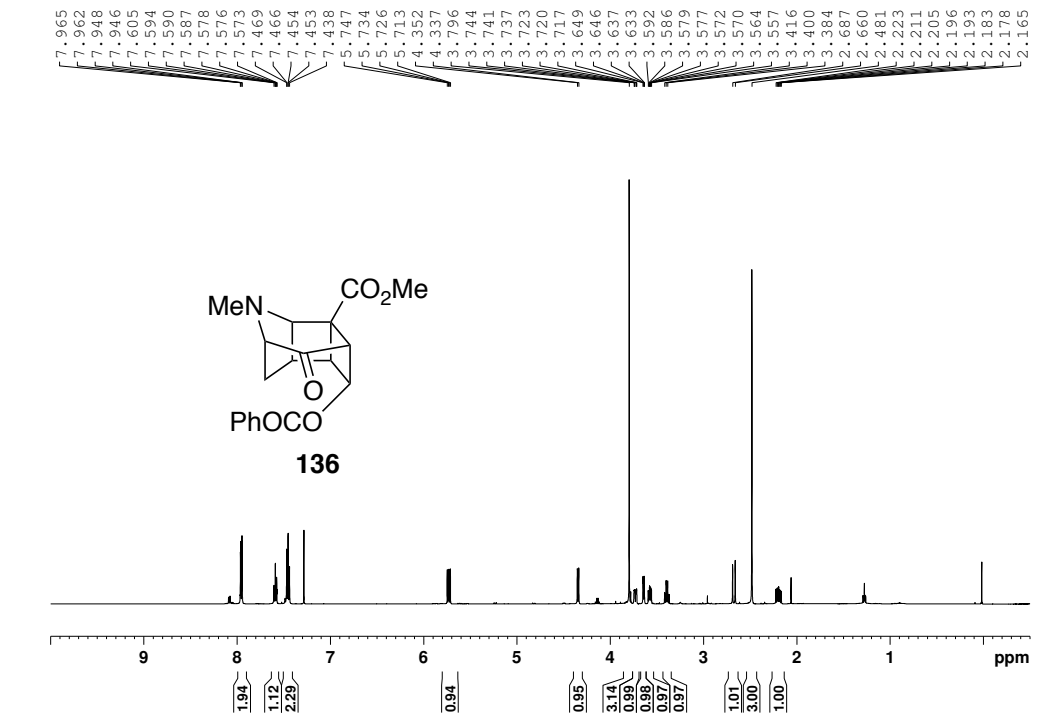
7.965
7.962
7.948
7.946
7.605
7.594
7.590
7.587
7.578
7.576
7.573
7.469
7.466
7.454
7.453
7.438
5.747
5.734
5.726
5.713
4.352
4.337
3.796
3.744
3.741
3.737
3.723
3.720
3.717
3.649
3.646
3.637
3.633
3.592
3.586
3.579
3.577
3.572
3.570
3.564
3.557
3.416
3.400
3.384
2.687
2.660
2.481
2.223
2.211
2.205
2.196
2.193
2.183
2.178
2.165
MeN
CO2Me
O
PhOCO
136
9
8
7
6
5
4
3
2
1
ppm
1.94
1.12
2.29
0.94
0.95
3.14
0.99
0.98
0.97
0.97
1.01
3.00
1.00

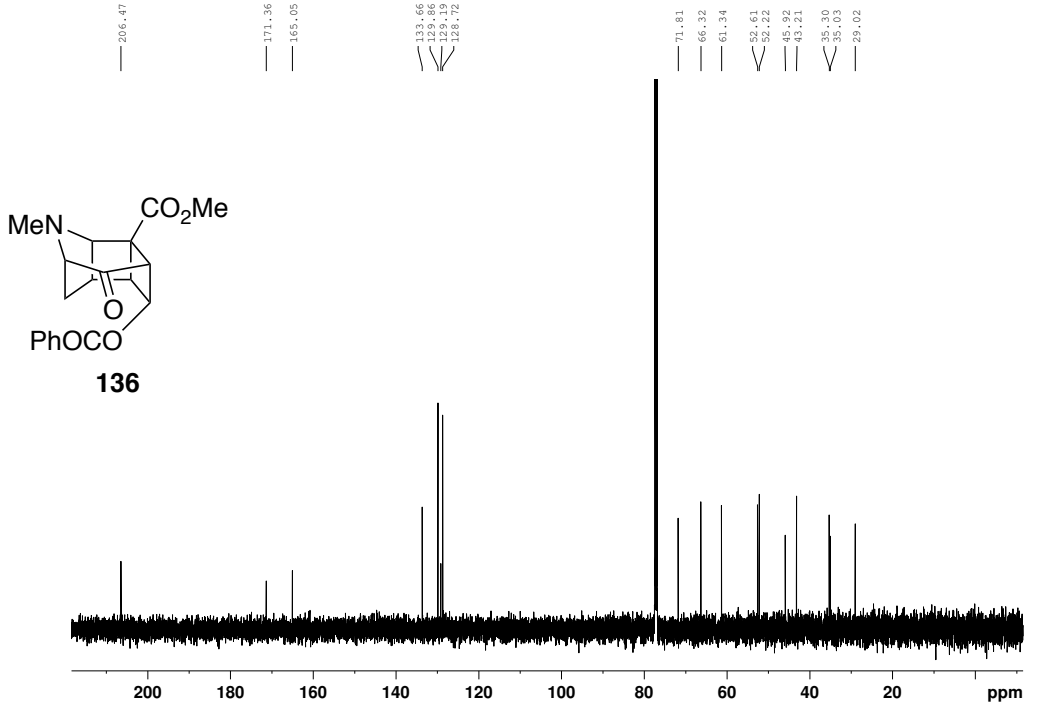
206.47
171.36
165.05
133.66
129.86
129.19
128.72
71.81
66.32
61.34
52.61
52.22
45.92
43.21
35.30
35.03
29.02
MeN
CO2Me
O
PhOCO
136
200
180
160
140
120
100
80
60
40
20
ppm

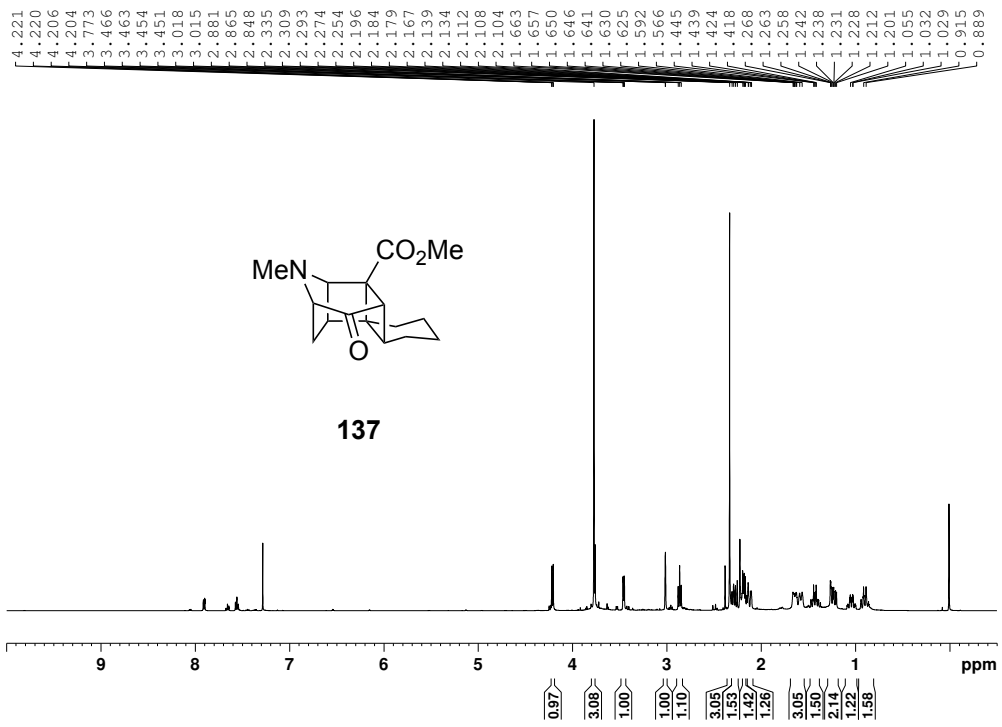
4.221
4.220
4.206
4.204
3.773
3.466
3.463
3.454
3.451
3.018
3.015
2.881
2.865
2.848
2.335
2.309
2.293
2.274
2.254
2.196
2.184
2.179
2.167
2.139
2.134
2.112
2.108
2.104
1.663
1.657
1.650
1.646
1.641
1.630
1.625
1.592
1.566
1.445
1.439
1.424
1.418
1.268
1.263
1.258
1.242
1.238
1.231
1.228
1.212
1.201
1.055
1.032
1.029
0.915
0.889
MeN
CO2Me
O
9
8
7
6
5
4
3
2
1
ppm
0.97
3.08
1.00
1.00
1.10
3.05
1.53
1.42
1.26
3.05
1.50
2.14
1.22
1.58

137

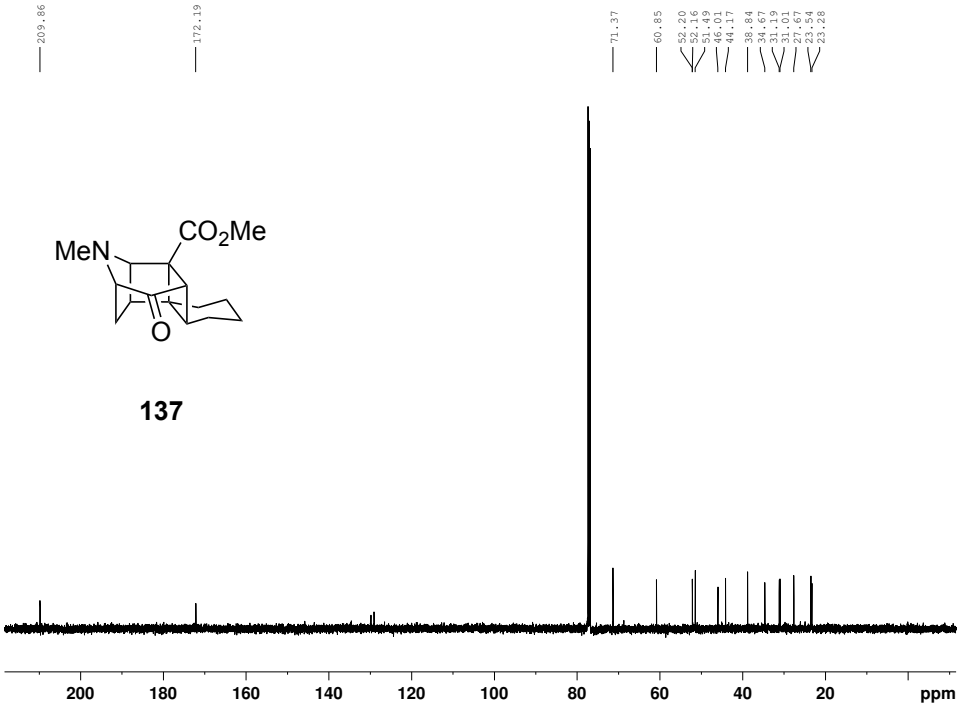
209.86
172.19
71.37
60.85
52.20
52.16
51.49
46.01
44.17
38.84
34.67
31.19
31.01
27.67
23.54
23.28
MeN
CO2Me
O
200
180
160
140
120
100
80
60
40
20
ppm

137

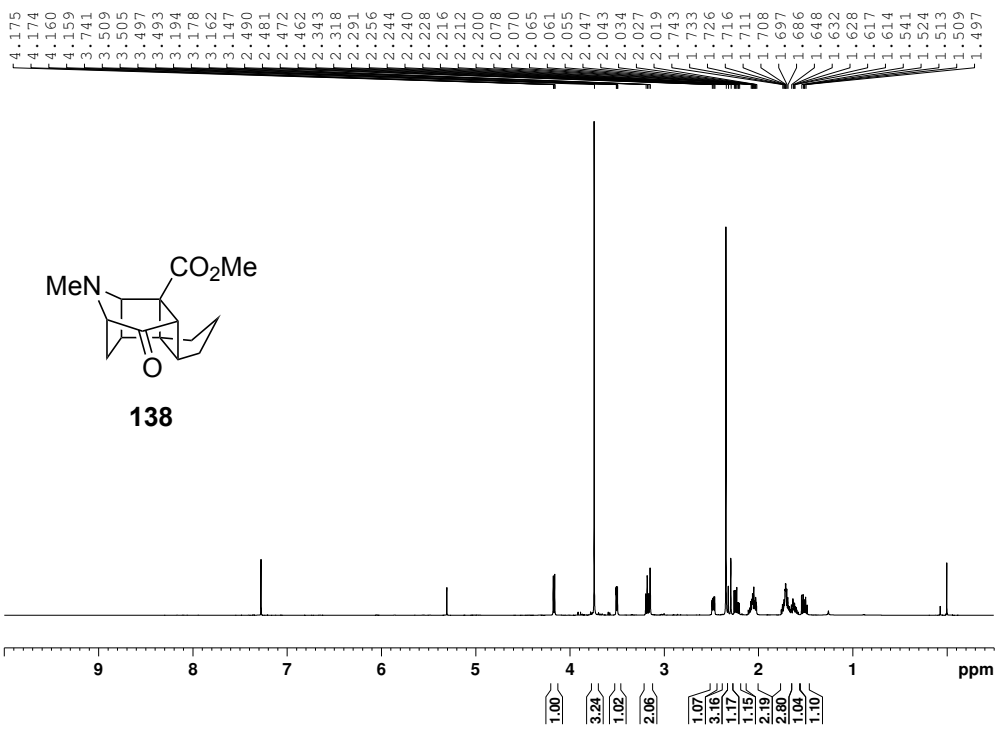
4.175
4.174
4.160
4.159
3.741
3.509
3.505
3.497
3.493
3.194
3.178
3.162
3.147
2.490
2.481
2.472
2.462
2.343
2.318
2.291
2.256
2.244
2.240
2.228
2.216
2.212
2.200
2.078
2.070
2.065
2.061
2.055
2.047
2.043
2.034
2.027
2.019
1.743
1.733
1.726
1.716
1.711
1.708
1.697
1.686
1.648
1.632
1.628
1.617
1.614
1.541
1.524
1.513
1.509
1.497
MeN
CO2Me
O
138
9
8
7
6
5
4
3
2
1
ppm
1.00
3.24
1.02
2.06
1.07
3.16
1.17
1.15
2.19
2.80
1.04
1.10

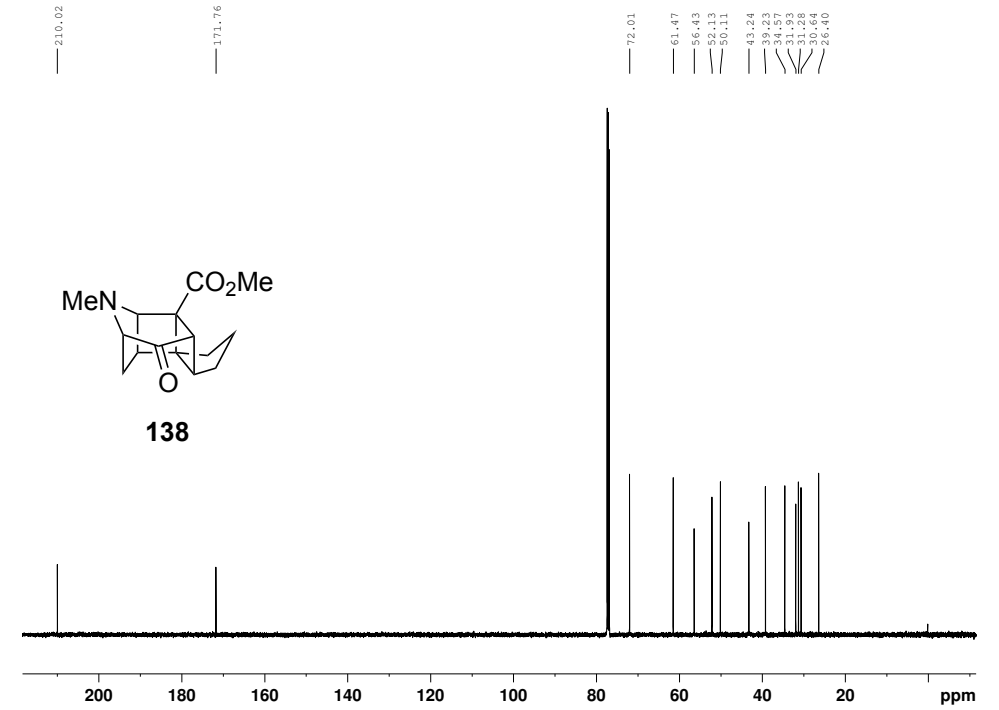
210.02
171.76
72.01
61.47
56.43
52.13
50.11
43.24
39.23
34.57
31.93
31.28
30.64
26.40
MeN
CO2Me
O
138
200
180
160
140
120
100
80
60
40
20
ppm

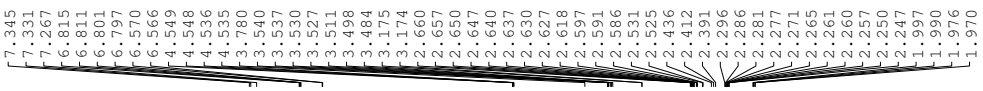
7.345
7.331
7.267
6.815
6.811
6.801
6.797
6.570
6.566
4.549
4.548
4.536
4.535
3.780
3.540
3.537
3.530
3.527
3.511
3.498
3.484
3.175
3.174
2.660
2.657
2.650
2.647
2.640
2.637
2.630
2.627
2.618
2.597
2.591
2.586
2.531
2.525
2.436
2.412
2.391
2.296
2.286
2.281
2.277
2.271
2.265
2.261
2.260
2.257
2.250
2.247
1.997
1.990
1.976
1.970

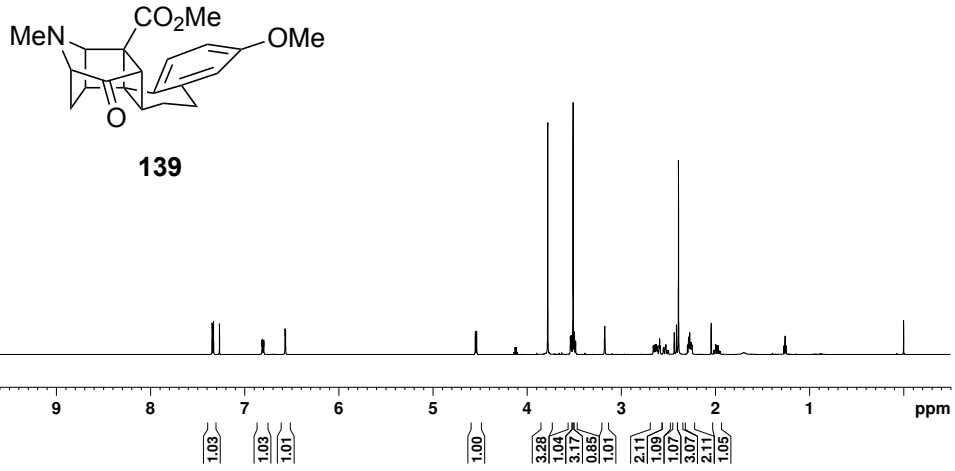
MeN
CO2Me
OMe
O
9
8
7
6
5
4
3
2
1
ppm
1.03
1.03
1.01
1.00
3.28
1.04
3.17
0.85
1.01
2.11
1.09
1.07
3.07
2.11
1.05

139

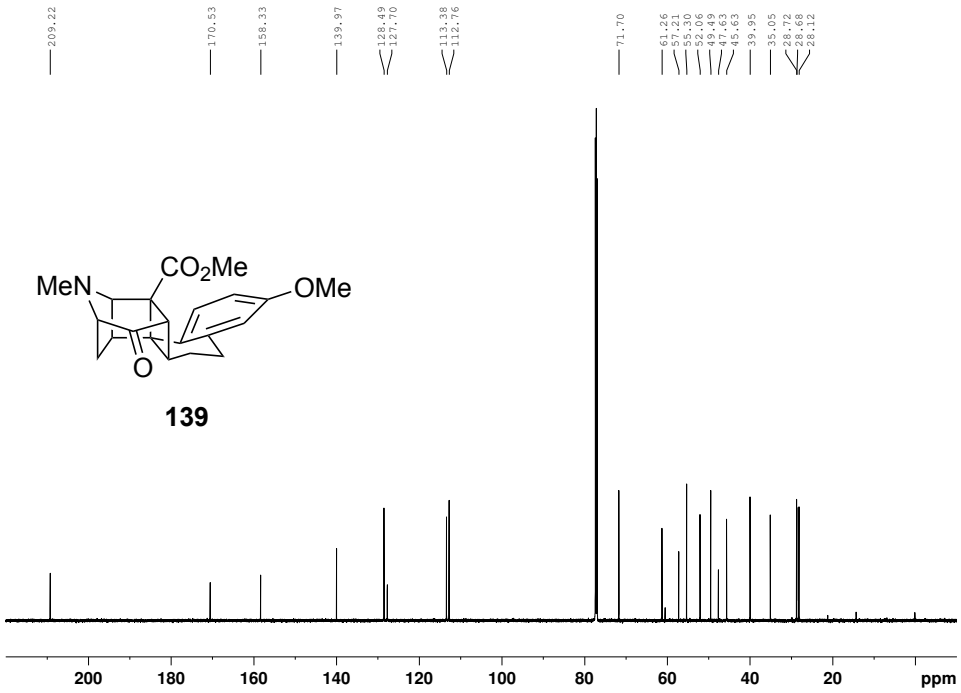
209.22
170.53
158.33
139.97
128.49
127.70
113.38
112.76
71.70
61.26
57.21
55.30
52.06
49.49
47.63
45.63
39.95
35.05
28.72
28.60
28.12
MeN
CO2Me
OMe
O
200
180
160
140
120
100
80
60
40
20
ppm

139

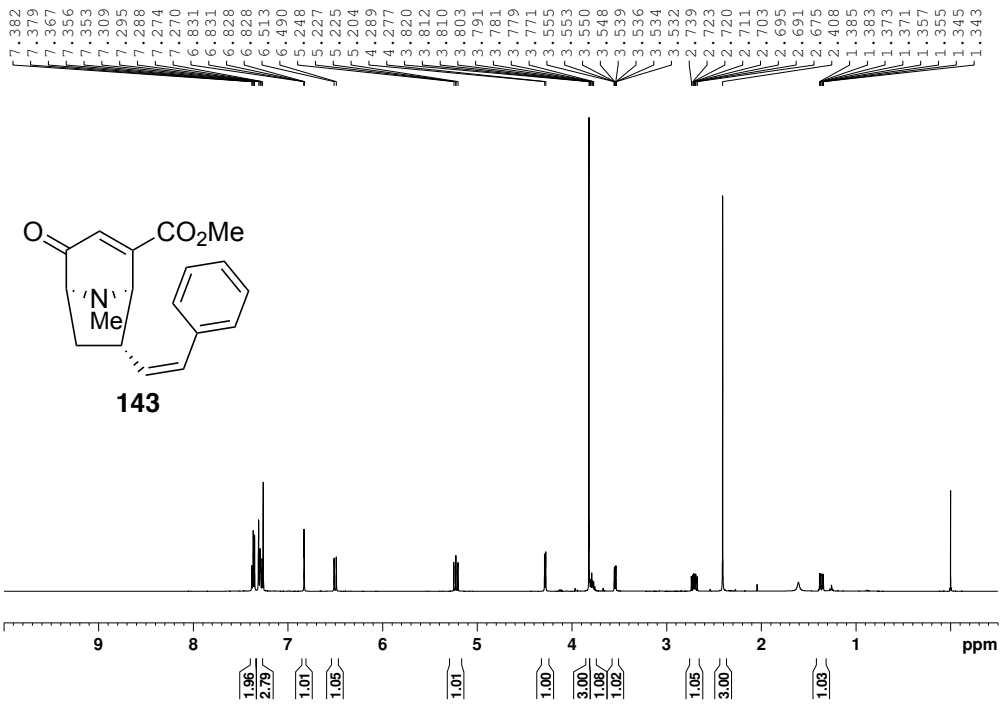
7.382
7.379
7.367
7.356
7.353
7.309
7.295
7.288
7.274
7.270
6.831
6.831
6.828
6.828
6.513
6.490
5.248
5.227
5.225
5.204
4.289
4.277
3.820
3.812
3.810
3.803
3.791
3.781
3.779
3.771
3.555
3.553
3.550
3.548
3.539
3.536
3.534
3.532
2.739
2.723
2.720
2.711
2.703
2.695
2.691
2.675
2.408
1.385
1.383
1.373
1.371
1.357
1.355
1.345
1.343
O
CO2Me
N
Me
143
9
8
7
6
5
4
3
2
1
ppm
1.96
2.79
1.01
1.05
1.01
1.00
3.00
1.08
1.02
1.05
3.00
1.03

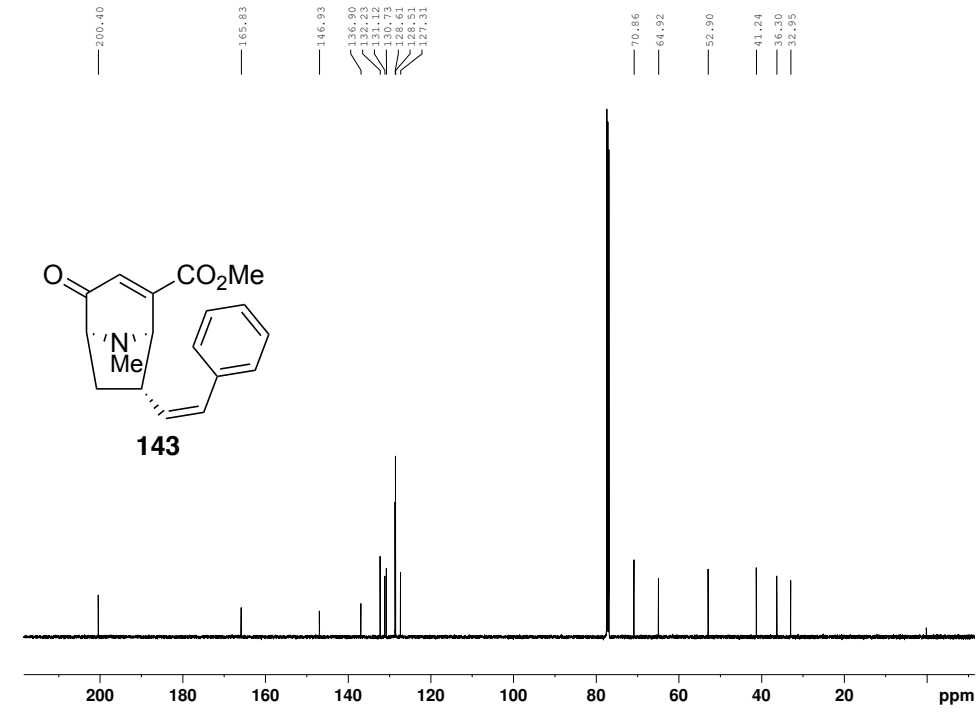
200.40
165.83
146.93
136.90
132.23
131.12
130.73
128.61
128.51
127.31
70.86
64.92
52.90
41.24
36.30
32.95
O
CO2Me
N
Me
143
200
180
160
140
120
100
80
60
40
20
ppm

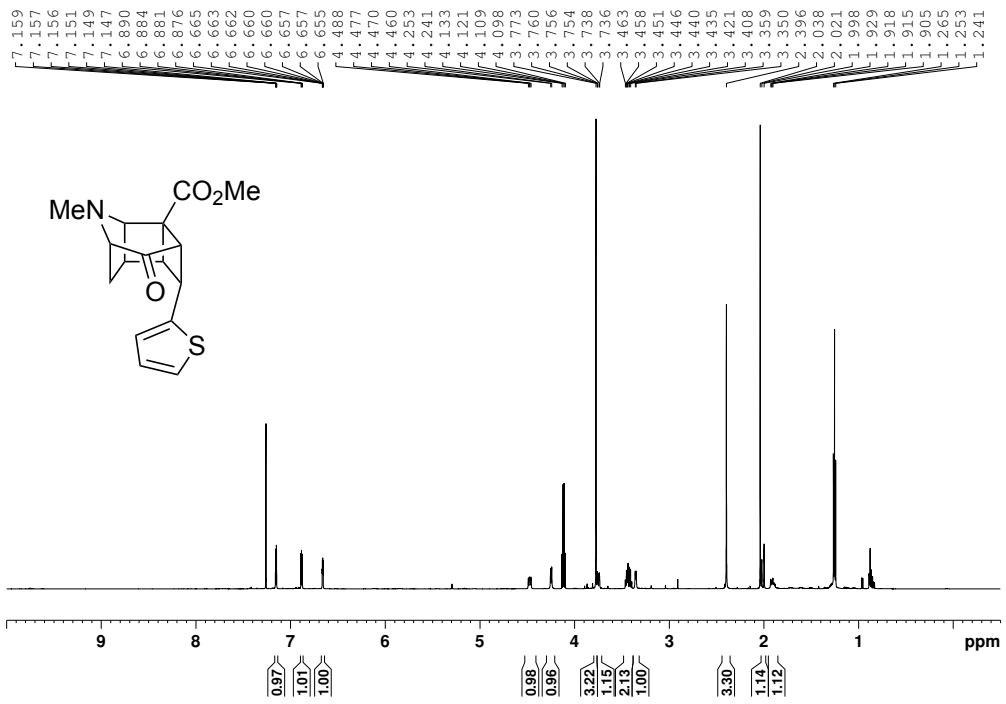
7.159
7.157
7.156
7.151
7.149
7.147
6.890
6.884
6.881
6.876
6.665
6.663
6.662
6.660
6.660
6.657
6.657
6.655
4.488
4.477
4.470
4.460
4.253
4.241
4.133
4.121
4.109
4.098
3.773
3.760
3.756
3.754
3.738
3.736
3.463
3.458
3.451
3.446
3.440
3.435
3.421
3.408
3.359
3.350
2.396
2.038
2.021
1.998
1.929
1.918
1.915
1.905
1.265
1.253
1.241
MeN
CO2Me
O
S
9
8
7
6
5
4
3
2
1
ppm
0.97
1.01
1.00
0.98
0.96
3.22
1.15
2.13
1.00
3.30
1.14
1.12

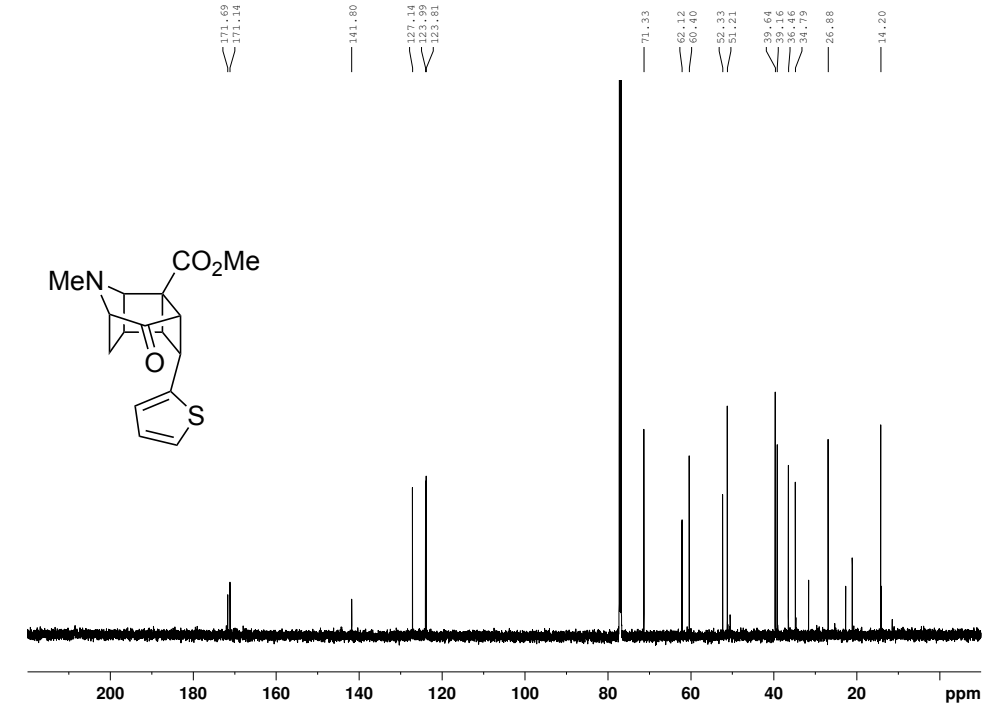
171.69
171.14
141.80
127.14
123.99
123.81
71.33
62.12
60.40
52.33
51.21
39.64
39.16
36.46
34.79
26.88
14.20
MeN
CO2Me
O
S
200
180
160
140
120
100
80
60
40
20
ppm

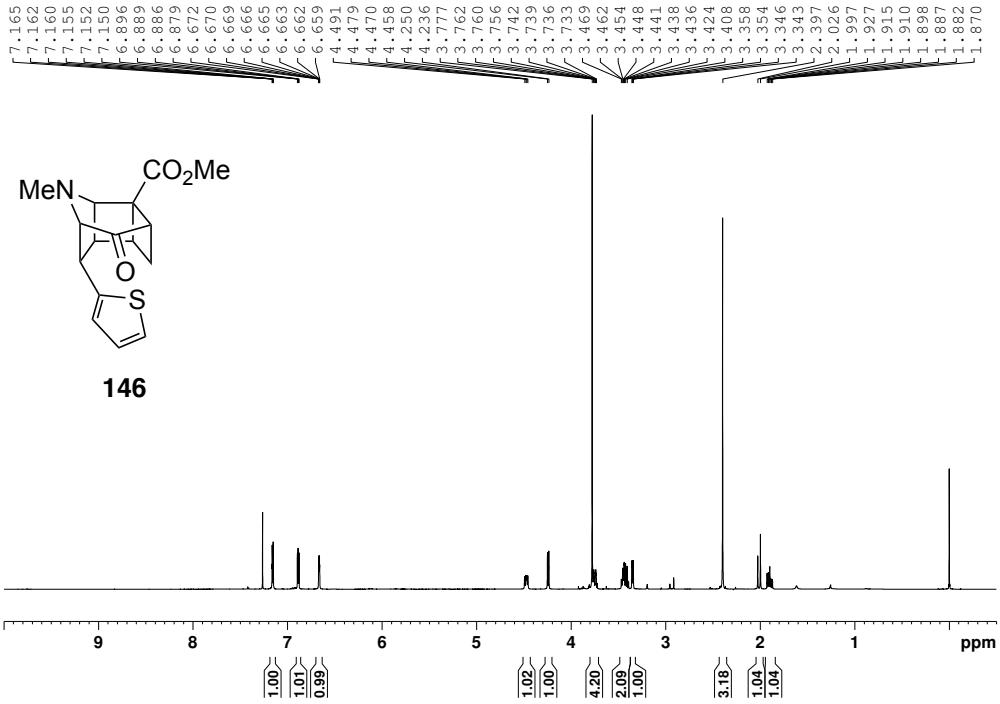
7.165
7.162
7.160
7.155
7.152
7.150
6.896
6.889
6.886
6.879
6.672
6.670
6.669
6.666
6.665
6.663
6.662
6.659
4.491
4.479
4.470
4.458
4.250
4.236
3.777
3.762
3.760
3.756
3.742
3.739
3.736
3.733
3.469
3.462
3.454
3.448
3.441
3.438
3.436
3.424
3.408
3.358
3.354
3.346
3.343
2.397
2.026
1.997
1.927
1.915
1.910
1.898
1.887
1.882
1.870
MeN
CO2Me
O
S
9
8
7
6
5
4
3
2
1
ppm
1.00
1.01
0.99
1.02
1.00
4.20
2.09
1.00
3.18
1.04
1.04

146

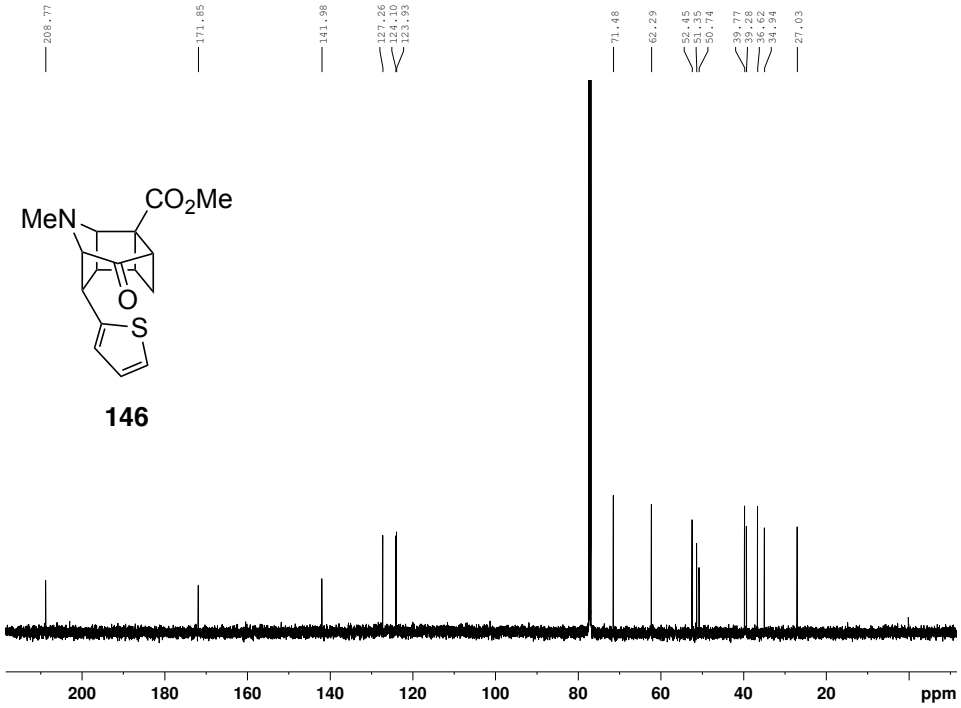
208.77
171.85
141.98
127.26
124.10
123.93
71.48
62.29
52.45
51.35
50.74
39.77
39.28
36.62
34.94
27.03
MeN
CO2Me
O
S
200
180
160
140
120
100
80
60
40
20
ppm

146

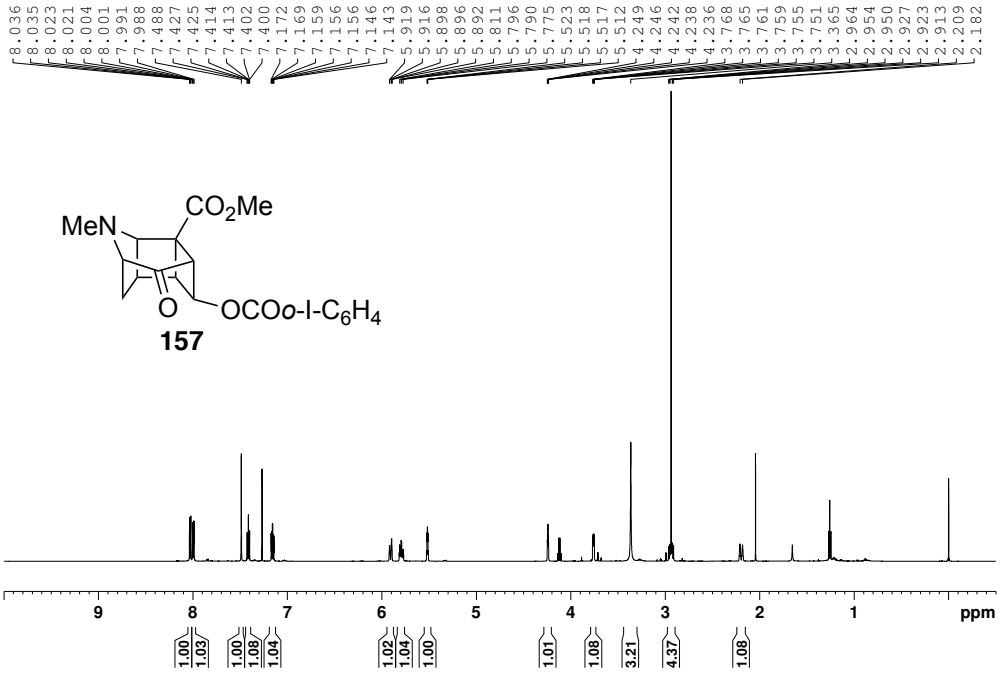
8.036
8.035
8.023
8.021
8.004
8.001
7.991
7.988
7.488
7.427
7.425
7.414
7.413
7.402
7.400
7.172
7.169
7.159
7.156
7.156
7.146
7.143
5.919
5.916
5.898
5.896
5.892
5.811
5.796
5.790
5.775
5.523
5.518
5.517
5.512
4.249
4.246
4.242
4.238
4.236
3.768
3.765
3.761
3.759
3.755
3.751
3.365
2.964
2.954
2.950
2.927
2.923
2.913
2.209
2.182
MeN
CO2Me
O
OCOo-I-C6H4
157
9
8
7
6
5
4
3
2
1
ppm
1.00
1.03
1.00
1.08
1.04
1.02
1.04
1.00
1.01
1.08
3.21
4.37
1.08

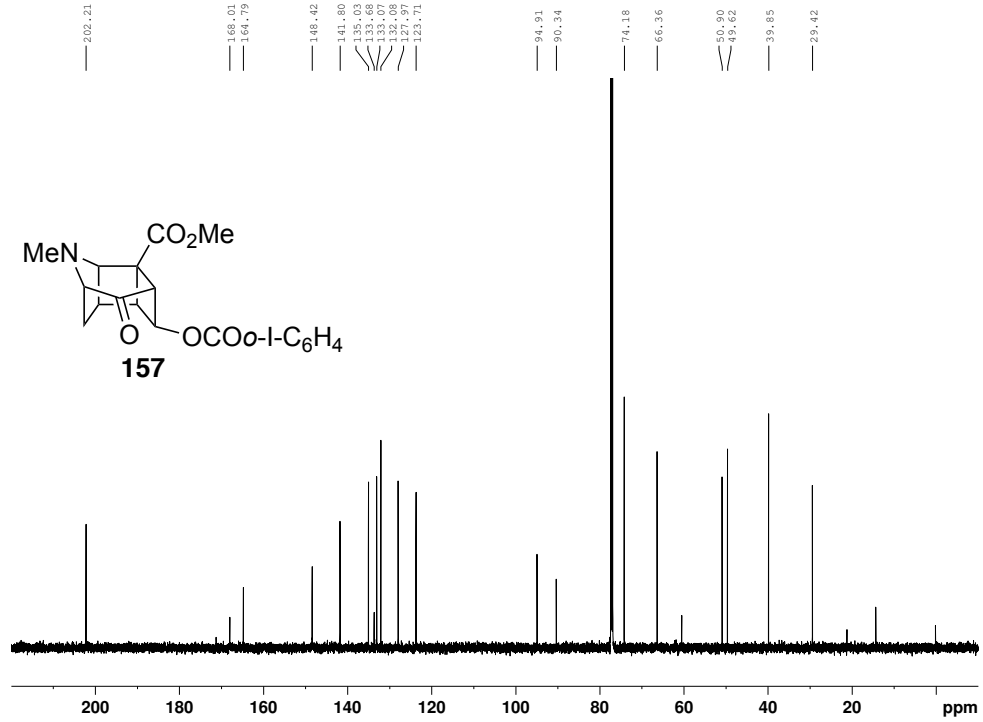
202.21
168.01
164.79
148.42
141.80
135.03
133.68
133.07
132.08
127.97
123.71
94.91
90.34
74.18
66.36
50.90
49.62
39.85
29.42
MeN
CO2Me
O
OCOo-I-C6H4
157
200
180
160
140
120
100
80
60
40
20
ppm

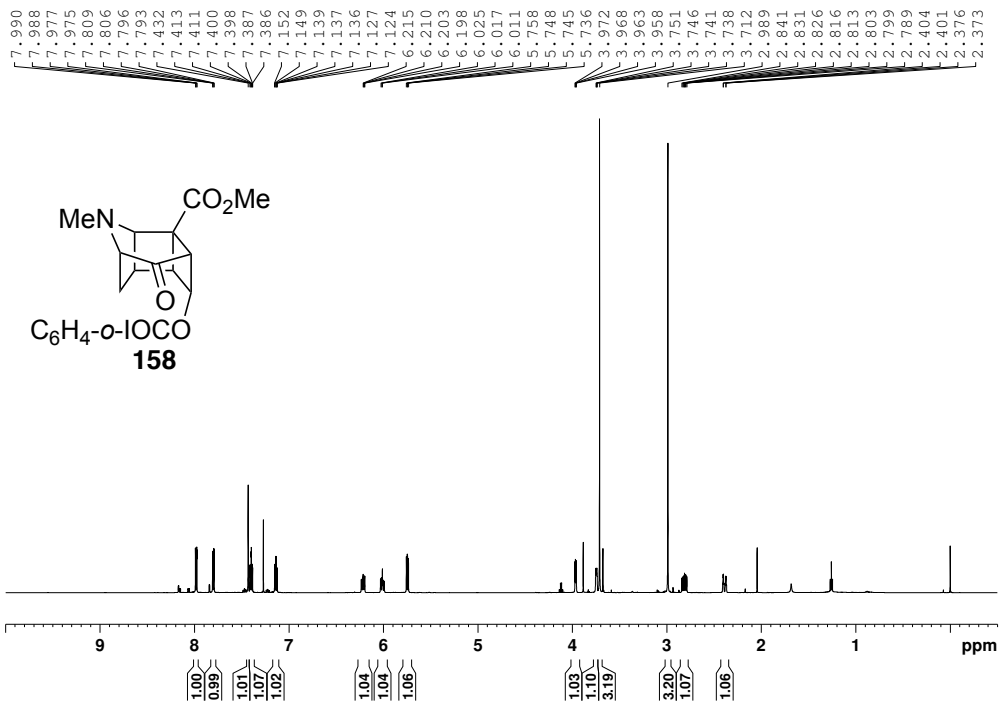
7.990
7.988
7.977
7.975
7.809
7.806
7.796
7.793
7.432
7.413
7.411
7.400
7.398
7.387
7.386
7.152
7.149
7.139
7.137
7.136
7.127
7.124
6.215
6.210
6.203
6.198
6.025
6.017
6.011
5.758
5.748
5.745
5.736
3.972
3.968
3.963
3.958
3.751
3.746
3.741
3.738
3.712
2.989
2.841
2.831
2.826
2.816
2.813
2.803
2.799
2.789
2.404
2.401
2.376
2.373
MeN
CO2Me
O
C6H4-o-IOCO
158
9
8
7
6
5
4
3
2
1
ppm
1.00
0.99
1.01
1.07
1.02
1.04
1.04
1.06
1.03
1.10
3.19
3.20
1.07
1.06

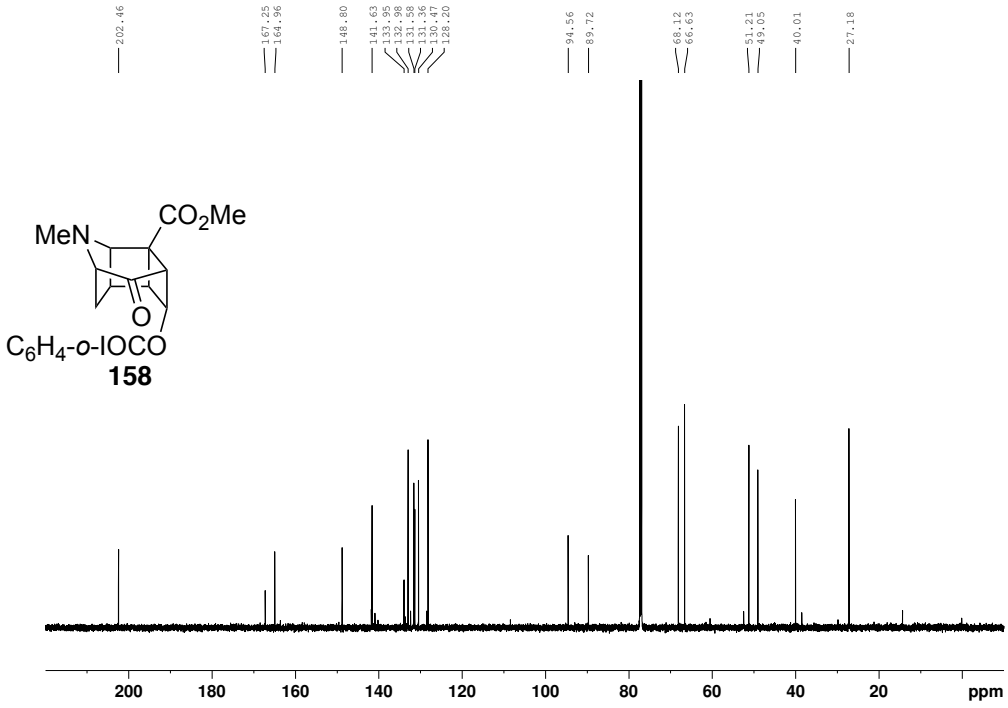
202.46
167.25
164.96
148.80
141.63
133.95
132.98
131.58
131.36
130.47
128.20
94.56
89.72
68.12
66.63
51.21
49.05
40.01
27.18
MeN
CO2Me
O
C6H4-o-IOCO
158
200
180
160
140
120
100
80
60
40
20
ppm

APPENDIX III: X-RAY CRYSTAL STRUCTURE

X-ray data for 67b:

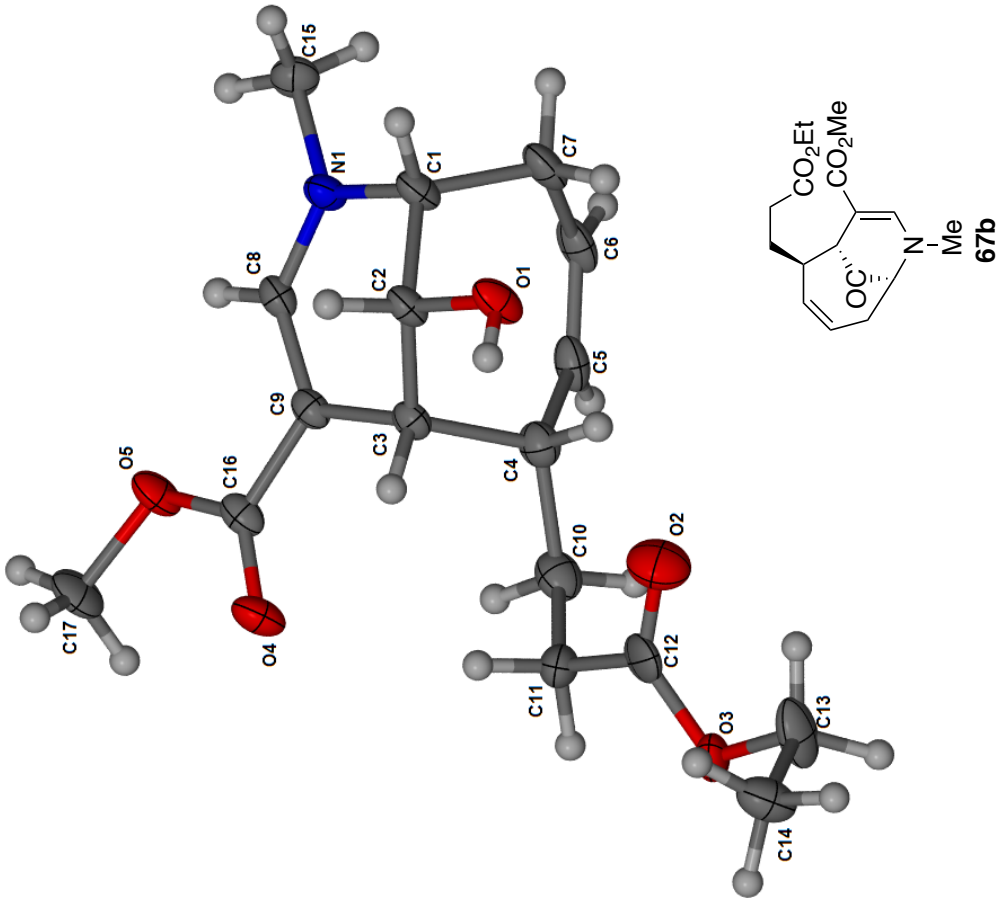

Table 1. Crystal data and structure refinement for CF-I-125-A2.

Identification code	CF-I-125-A2	
Empirical formula	C17 H25 N O5	
Formula weight	323.38	
Temperature	100(2) K	
Wavelength	0.71073 Å	
Crystal system	Triclinic	
Space group	P-1	
Unit cell dimensions	a = 7.7227(18) Å	a= 94.751(3)°.
	b = 10.036(2) Å	b= 109.316(3)°.
	c = 11.323(3) Å	g = 101.122(3)°.
Volume	802.4(3) $Å^3$	
Z	2	
Density (calculated)	1.338 Mg/m^3	
Absorption coefficient	0.098 mm^{-1}	
F(000)	348	
Crystal size	0.500 x 0.150 x 0.100 mm^3	
Theta range for data collection	1.930 to 28.243°.	
Index ranges	-10<=h<=10, -13<=k<=13, -15<=l<=15	
Reflections collected	11502	
Independent reflections	3965 [R(int) = 0.0325]	
Completeness to theta = 25.242°	100.0 %	
Absorption correction	Semi-empirical from equivalents	
Max. and min. transmission	0.99 and 0.92	
Refinement method	Full-matrix least-squares on F^2	
Data / restraints / parameters	3965 / 2 / 243	
Goodness-of-fit on F^2	1.018	
Final R indices [I>2sigma(I)]	R1 = 0.0604, wR2 = 0.1428	
R indices (all data)	R1 = 0.0960, wR2 = 0.1604	
Extinction coefficient	n/a	
Largest diff. peak and hole	0.848 and -0.304 $e.Å^{-3}$	

X-ray data for 70b:

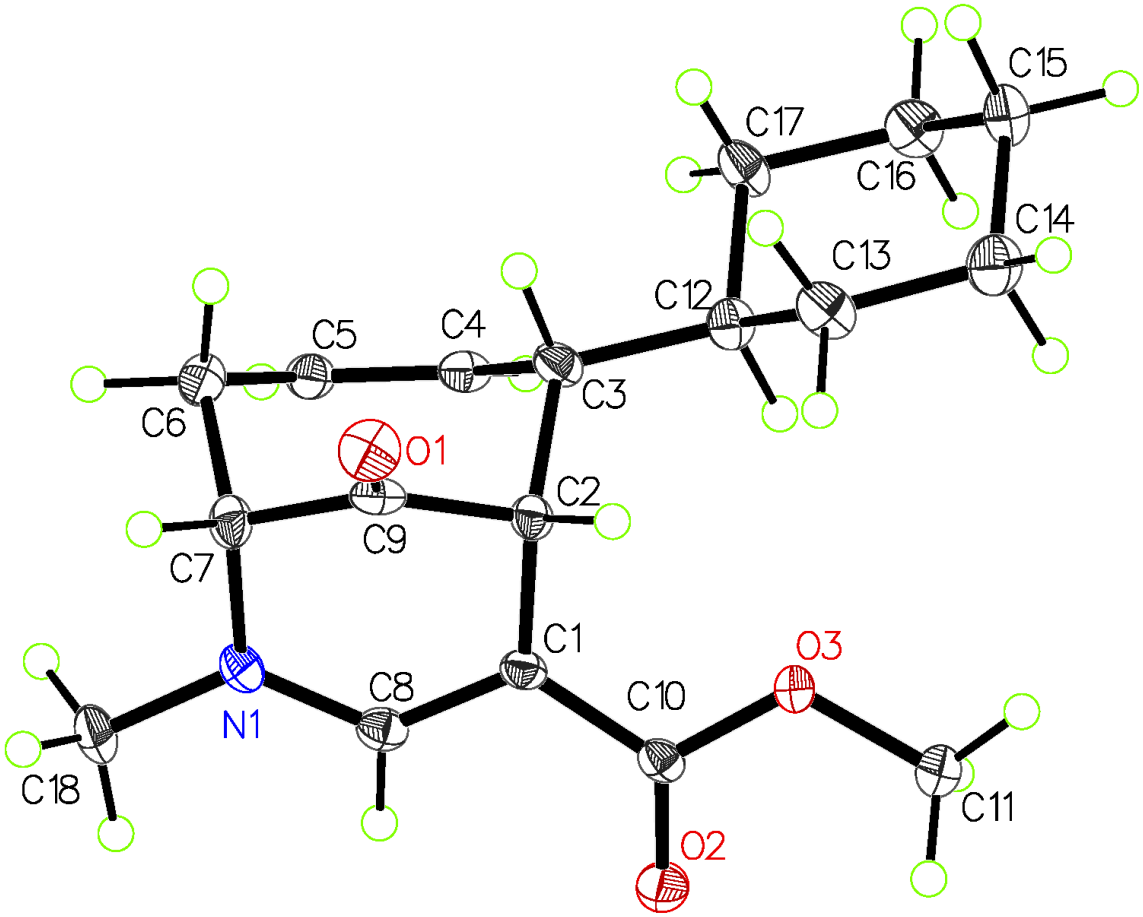

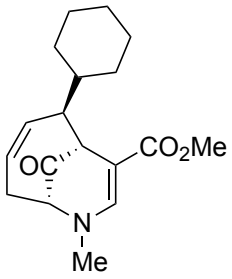

70b

Table 1. Crystal data and structure refinement for CF-VI-092-A3.

Identification code	s1	
Empirical formula	C18 H25 N O3	
Formula weight	303.39	
Temperature	100 K	
Wavelength	0.71073 Å	
Crystal system	Triclinic	
Space group	P-1	
Unit cell dimensions	a = 8.6858(12) Å	a= 83.416(2)°.
	b = 10.2567(14) Å	b= 66.417(2)°.
	c = 10.4459(15) Å	g = 65.627(2)°.
Volume	775.45(19) $Å^3$	
Z	2	
Density (calculated)	1.299 Mg/m^3	
Absorption coefficient	0.088 mm^{-1}	
F(000)	328	
Crystal size	0.08 x 0.03 x 0.01 mm^3	
Theta range for data collection	2.131 to 28.041°.	
Index ranges	-11<=h<=11, -13<=k<=13, -13<=l<=13	
Reflections collected	15291	
Independent reflections	3744 [R(int) = 0.0847]	
Completeness to theta = 25.242°	100.0 %	
Absorption correction	Semi-empirical from equivalents	
Max. and min. transmission	0.7456 and 0.6714	
Refinement method	Full-matrix least-squares on F^2	
Data / restraints / parameters	3744 / 0 / 275	
Goodness-of-fit on F^2	1.015	
Final R indices [I>2sigma(I)]	R1 = 0.0608, wR2 = 0.1068	
R indices (all data)	R1 = 0.1244, wR2 = 0.1258	
Extinction coefficient	n/a	
Largest diff. peak and hole	0.477 and -0.329 $e.Å^{-3}$	

X-ray data for 71a':

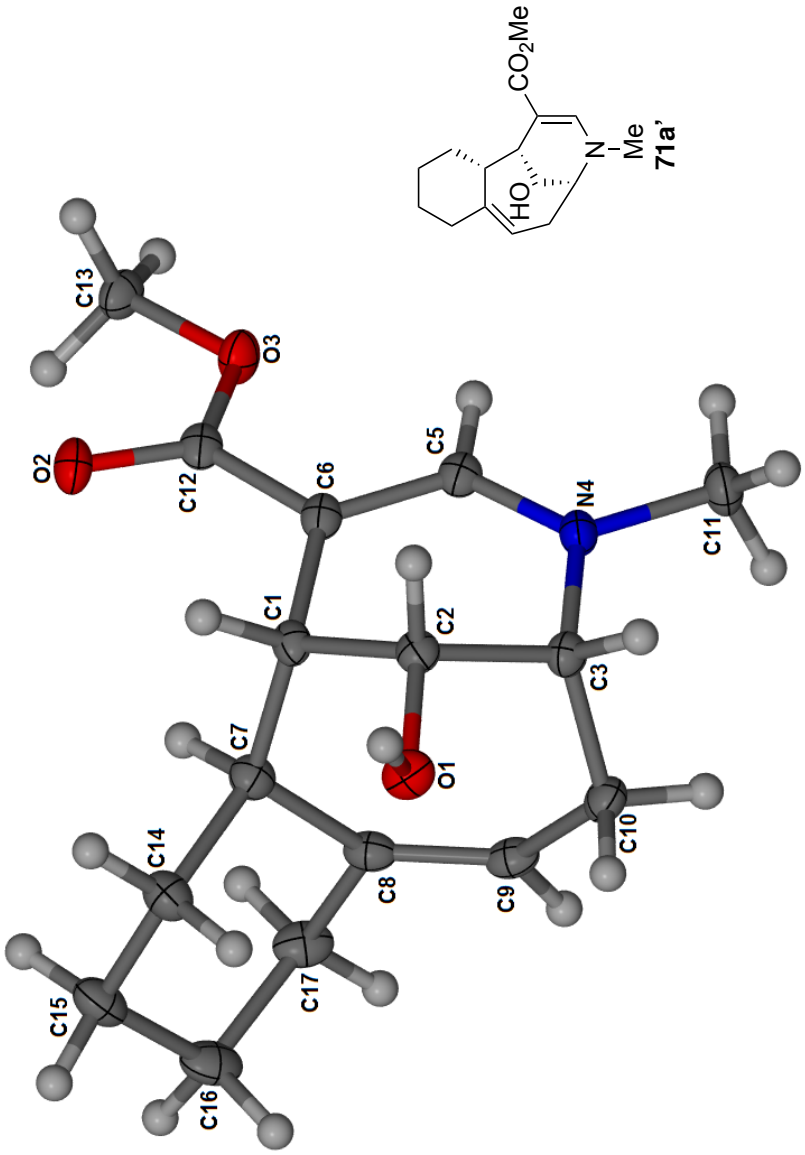

Table 1. Crystal data and structure refinement for cfii086a3.

Identification code	CF-II-086-A3	
Empirical formula	C16 H23 N O3	
Formula weight	277.35	
Temperature	100(2) K	
Wavelength	1.54178 Å	
Crystal system	Orthorhombic	
Space group	P b c a	
Unit cell dimensions	a = 14.9970(4) Å	a= 90°.
	b = 12.0136(3) Å	b= 90°.
	c = 15.4429(4) Å	g = 90°.
Volume	2782.32(12) $Å^3$	
Z	8	
Density (calculated)	1.324 Mg/m^3	
Absorption coefficient	0.730 mm^{-1}	
F(000)	1200	
Crystal size	0.250 x 0.250 x 0.150 mm^3	
Theta range for data collection	5.520 to 72.119°.	
Index ranges	-17<=h<=18, -14<=k<=14, -18<=l<=18	
Reflections collected	34108	
Independent reflections	2737 [R(int) = 0.0226]	
Completeness to theta = 67.679°	100.0 %	
Absorption correction	Semi-empirical from equivalents	
Max. and min. transmission	0.90 and 0.85	
Refinement method	Full-matrix least-squares on F^2	
Data / restraints / parameters	2737 / 0 / 187	
Goodness-of-fit on F^2	1.061	
Final R indices [I>2sigma(I)]	R1 = 0.0410, wR2 = 0.1079	
R indices (all data)	R1 = 0.0411, wR2 = 0.1080	
Extinction coefficient	n/a	
Largest diff. peak and hole	0.416 and -0.356 $e.Å^{-3}$	

X-ray data for 72b:

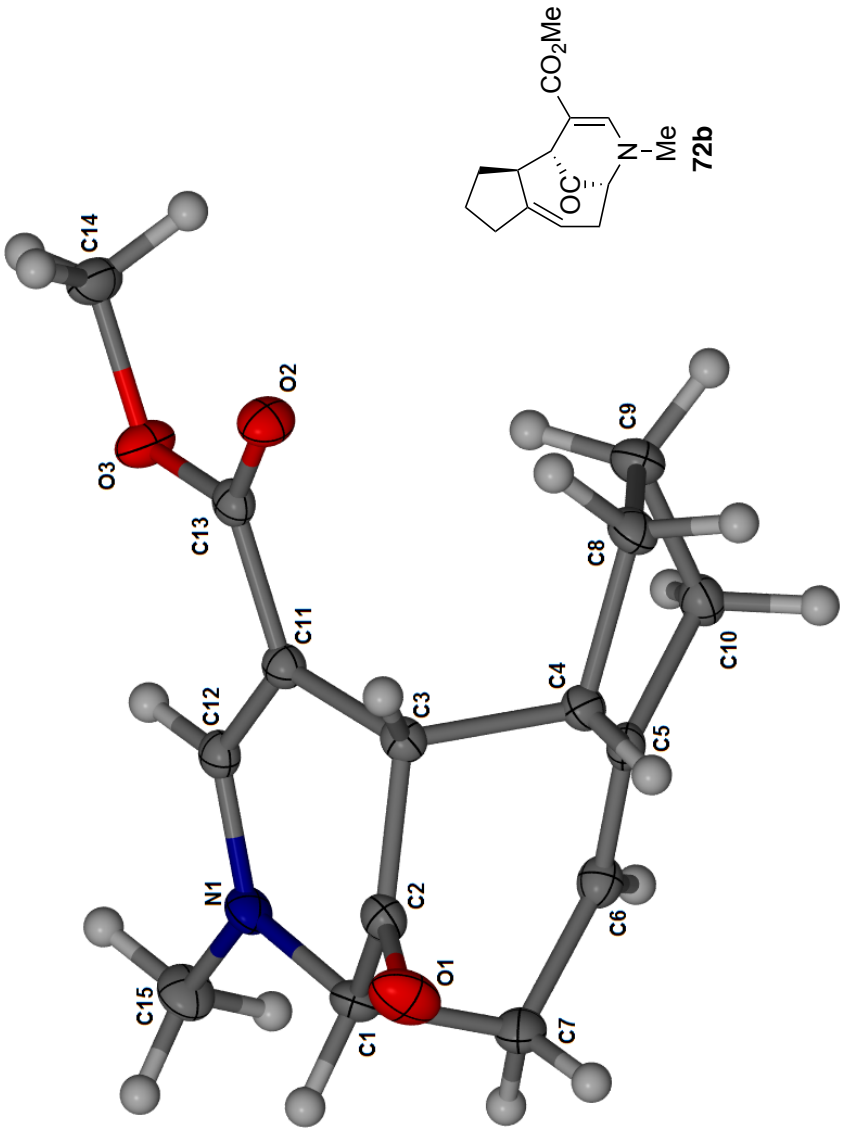

Table 1. Crystal data and structure refinement for cf-i-061-a4.

Identification code	CF-I-061-A4	
Empirical formula	C60 H76 N4 O12	
Formula weight	1045.24	
Temperature	150(2) K	
Wavelength	0.71073 Å	
Crystal system	Monoclinic	
Space group	$P2_1/n$	
Unit cell dimensions	a = 7.3751(3) Å	a= 90°.
	b = 13.3424(6) Å	b= 99.1440(10)°.
	c = 13.1177(6) Å	g = 90°.
Volume	1274.40(10) $Å^3$	
Z	1	
Density (calculated)	1.362 Mg/m^3	
Absorption coefficient	0.095 mm^{-1}	
F(000)	560	
Crystal size	0.400 x 0.300 x 0.200 mm^3	
Theta range for data collection	2.984 to 28.329°.	
Index ranges	-9<=h<=9, -17<=k<=17, -17<=l<=16	
Reflections collected	15256	
Independent reflections	3170 [R(int) = 0.0349]	
Completeness to theta = 25.242°	99.9 %	
Absorption correction	Semi-empirical from equivalents	
Max. and min. transmission	0.98 and 0.89	
Refinement method	Full-matrix least-squares on F^2	
Data / restraints / parameters	3170 / 0 / 174	
Goodness-of-fit on F^2	1.027	
Final R indices [I>2sigma(I)]	R1 = 0.0444, wR2 = 0.1029	
R indices (all data)	R1 = 0.0589, wR2 = 0.1097	
Extinction coefficient	n/a	
Largest diff. peak and hole	0.344 and -0.304 $e.Å^{-3}$	

X-ray data for 73a:

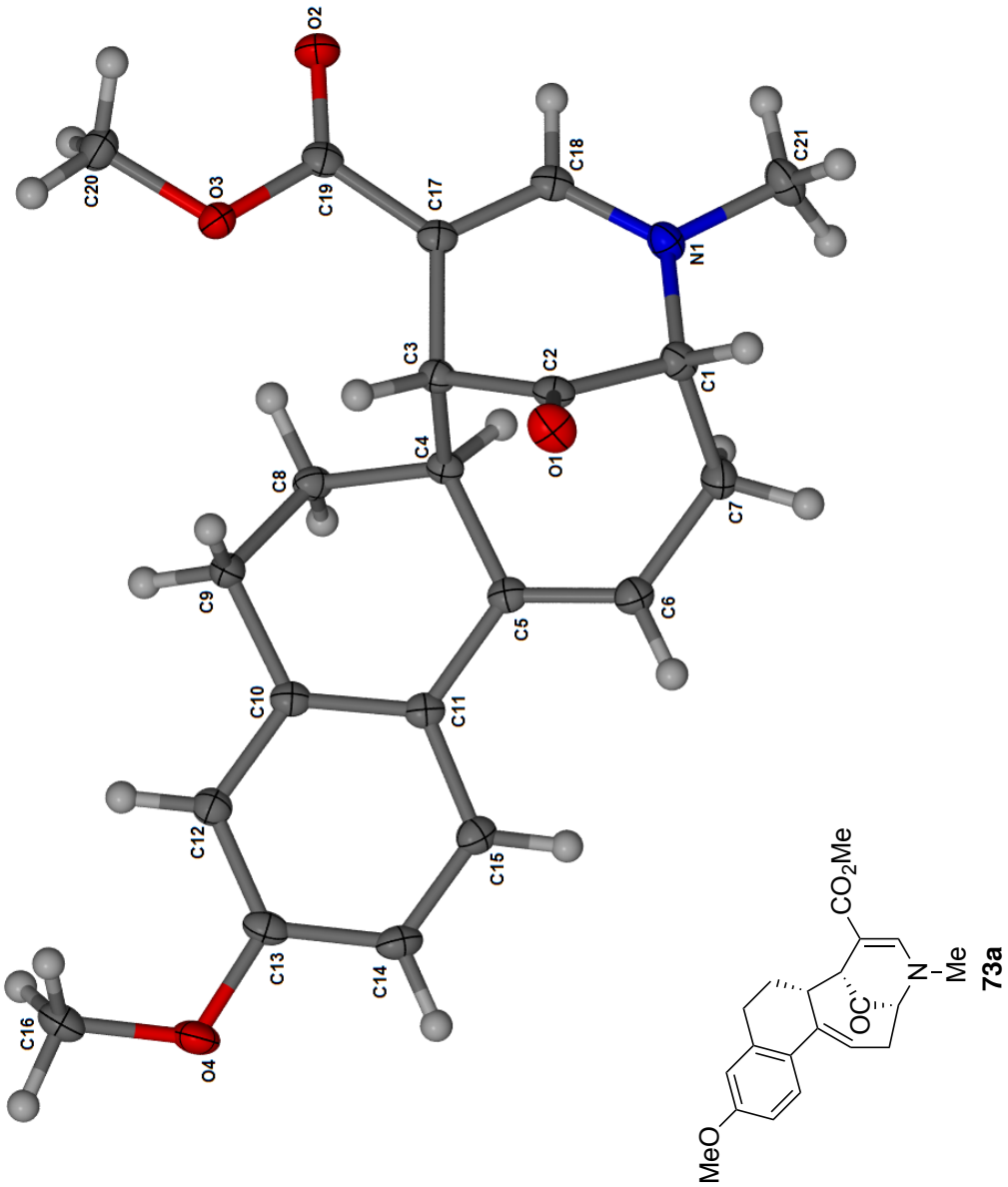

Table 1. Crystal data and structure refinement for cf-i-071-a3.

Identification code	CF-I-071-A3	
Empirical formula	C21 H23 N O4	
Formula weight	353.40	
Temperature	100(2) K	
Wavelength	1.54178 Å	
Crystal system	Monoclinic	
Space group	$P2_1/n$	
Unit cell dimensions	a = 9.8077(4) Å	a= 90°.
	b = 14.0882(6) Å	b= 99.728(2)°.
	c = 12.6344(5) Å	g = 90°.
Volume	1720.63(12) $Å^3$	
Z	4	
Density (calculated)	1.364 Mg/m^3	
Absorption coefficient	0.765 mm^{-1}	
F(000)	752	
Crystal size	0.200 x 0.200 x 0.050 mm^3	
Theta range for data collection	4.739 to 72.253°.	
Index ranges	-12<=h<=12, -17<=k<=17, -15<=l<=15	
Reflections collected	35491	
Independent reflections	3371 [R(int) = 0.0249]	
Completeness to theta = 67.679°	99.5 %	
Absorption correction	Semi-empirical from equivalents	
Max. and min. transmission	0.96 and 0.84	
Refinement method	Full-matrix least-squares on F^2	
Data / restraints / parameters	3371 / 0 / 239	
Goodness-of-fit on F^2	1.043	
Final R indices [I>2sigma(I)]	R1 = 0.0323, wR2 = 0.0823	
R indices (all data)	R1 = 0.0338, wR2 = 0.0835	
Extinction coefficient	0.0018(2)	
Largest diff. peak and hole	0.324 and -0.207 $e.Å^{-3}$	

X-ray data for 73b:

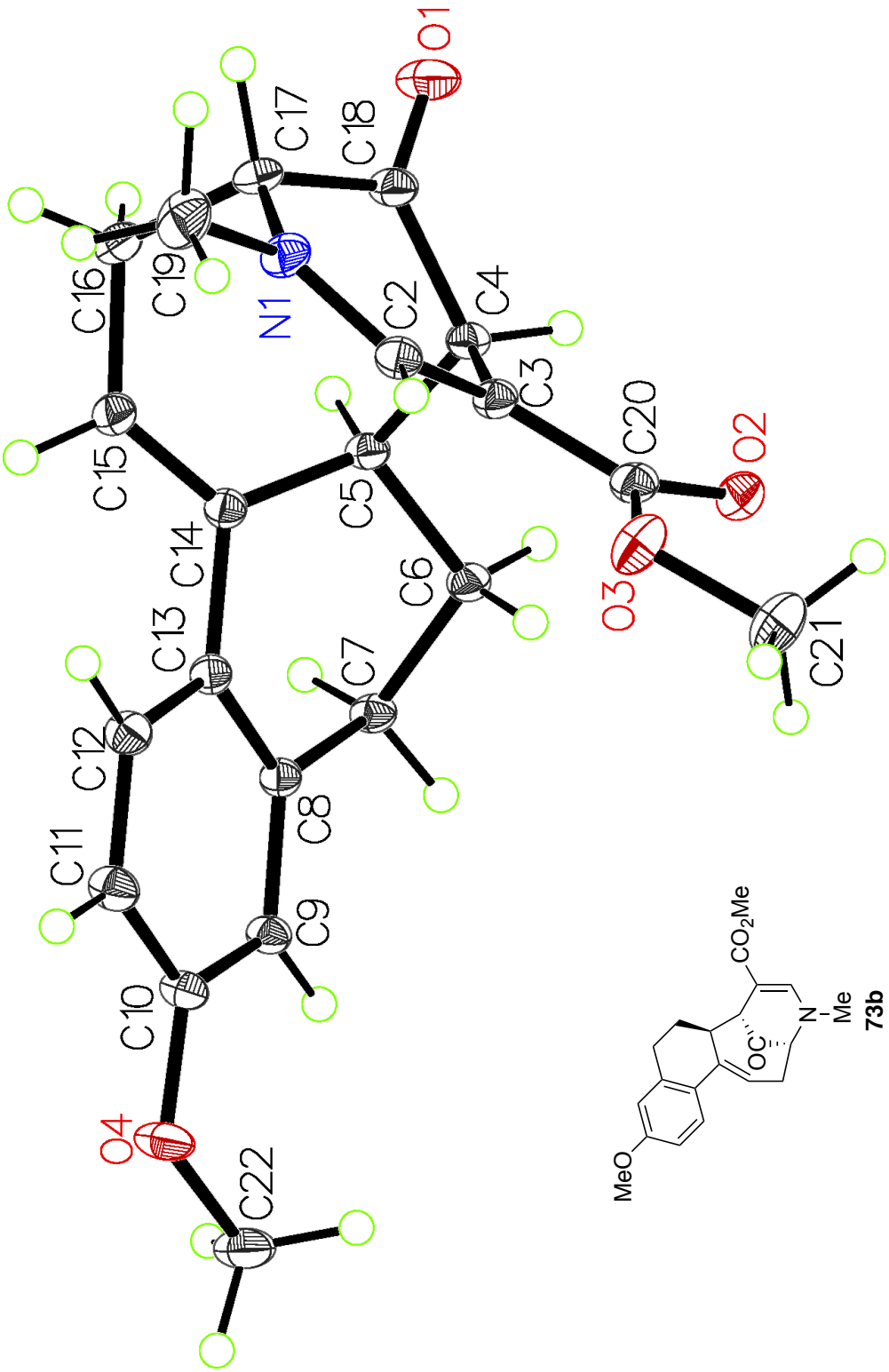

Table 1. Crystal data and structure refinement for CF-II-101-A52.

Identification code	s1	
Empirical formula	C21 H23 N O4	
Formula weight	353.40	
Temperature	100 K	
Wavelength	0.71073 Å	
Crystal system	Monoclinic	
Space group	P 1 21/n 1	
Unit cell dimensions	a = 11.2459(3) Å	a= 90°.
	b = 13.1564(3) Å	b= 95.2977(13)°.
	c = 12.2108(3) Å	g = 90°.
Volume	1798.94(8) $Å^3$	
Z	4	
Density (calculated)	1.305 Mg/m^3	
Absorption coefficient	0.090 mm^{-1}	
F(000)	752	
Crystal size	0.54 x 0.38 x 0.24 mm^3	
Theta range for data collection	2.281 to 31.869°.	
Index ranges	-16<=h<=16, -19<=k<=19, -18<=l<=18	
Reflections collected	78150	
Independent reflections	6186 [R(int) = 0.0425]	
Completeness to theta = 25.242°	100.0 %	
Absorption correction	Semi-empirical from equivalents	
Max. and min. transmission	0.7463 and 0.6693	
Refinement method	Full-matrix least-squares on F^2	
Data / restraints / parameters	6186 / 0 / 304	
Goodness-of-fit on F^2	1.061	
Final R indices [I>2sigma(I)]	R1 = 0.0405, wR2 = 0.1071	
R indices (all data)	R1 = 0.0546, wR2 = 0.1177	
Extinction coefficient	n/a	
Largest diff. peak and hole	0.542 and -0.211 $e.Å^{-3}$	

X-ray data for 81a:

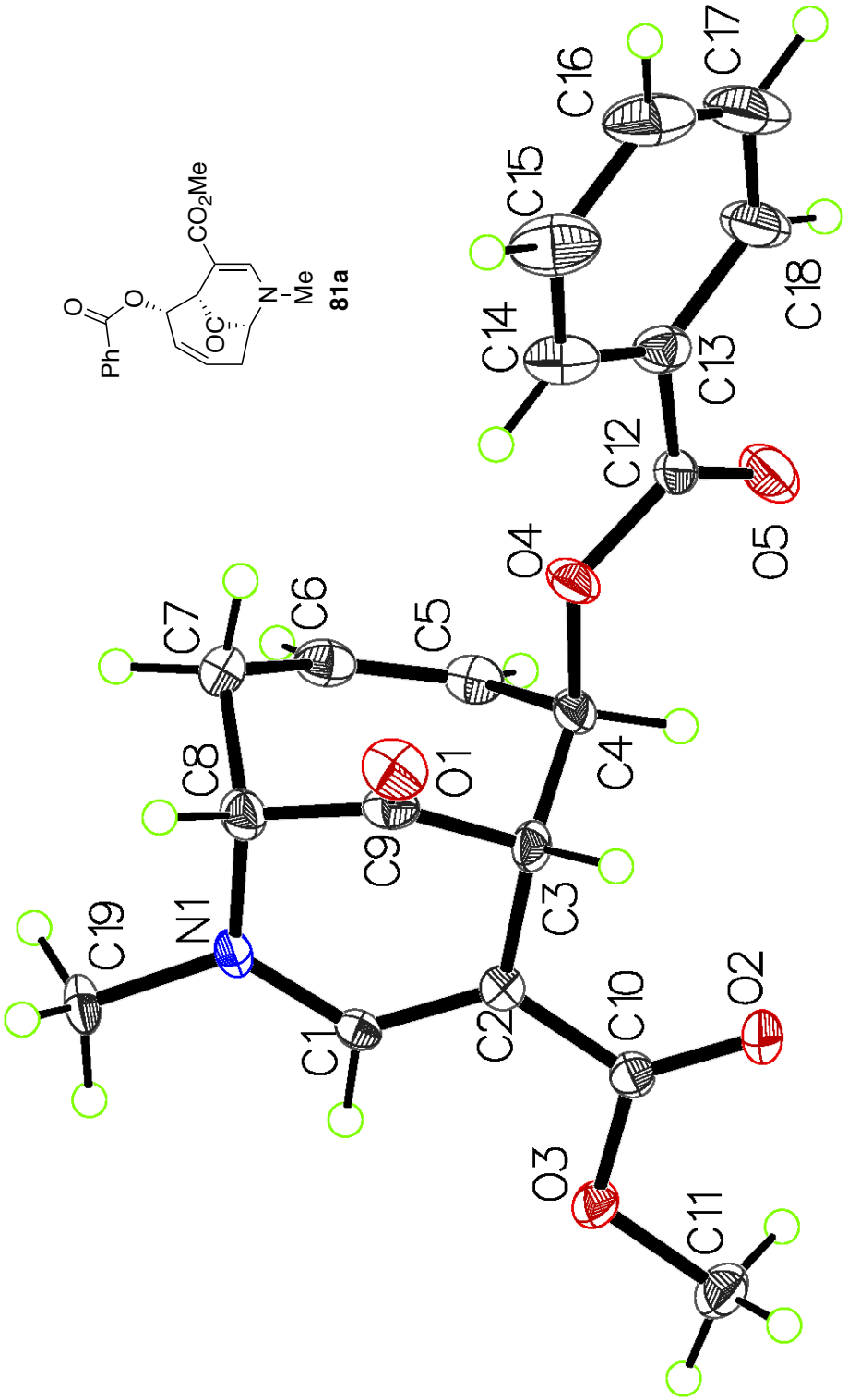

Table 1. Crystal data and structure refinement for CF-VI-050-A3.

Identification code	s1_a	
Empirical formula	C19 H19 N O5	
Formula weight	341.35	
Temperature	100.15 K	
Wavelength	0.71073 Å	
Crystal system	Orthorhombic	
Space group	$P2_12_12_1$	
Unit cell dimensions	a = 7.4180(4) Å	a= 90°.
	b = 8.3999(5) Å	b= 90°.
	c = 27.5589(13) Å	g = 90°.
Volume	1717.21(16) $Å^3$	
Z	4	
Density (calculated)	1.320 Mg/m^3	
Absorption coefficient	0.096 mm^{-1}	
F(000)	720	
Crystal size	0.30 x 0.25 x 0.05 mm^3	
Theta range for data collection	2.535 to 26.427°.	
Index ranges	-9<=h<=9, -10<=k<=10, -34<=l<=34	
Reflections collected	26001	
Independent reflections	3533 [R(int) = 0.0600]	
Completeness to theta = 25.242°	99.9 %	
Absorption correction	Semi-empirical from equivalents	
Max. and min. transmission	0.7454 and 0.6883	
Refinement method	Full-matrix least-squares on F^2	
Data / restraints / parameters	3533 / 0 / 228	
Goodness-of-fit on F^2	1.137	
Final R indices [I>2sigma(I)]	R1 = 0.0475, wR2 = 0.1136	
R indices (all data)	R1 = 0.0553, wR2 = 0.1163	
Absolute structure parameter	0.5	
Extinction coefficient	n/a	
Largest diff. peak and hole	0.309 and -0.240 $e.Å^{-3}$	

X-ray data for 81b:

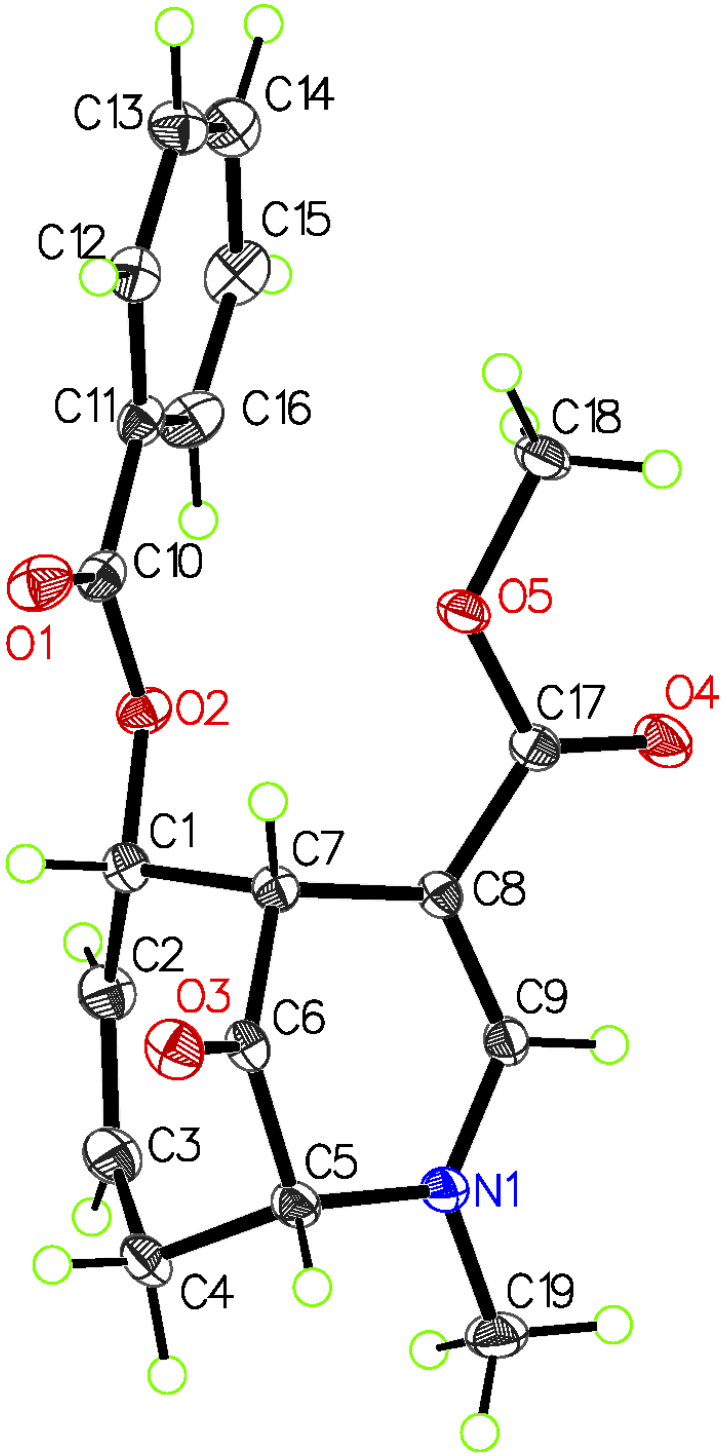

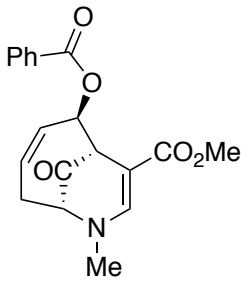

81b

Table 1. Crystal data and structure refinement for CF-VI-050-A4.

Identification code	s1	
Empirical formula	C19 H19 N O5	
Formula weight	341.35	
Temperature	100 K	
Wavelength	0.71073 Å	
Crystal system	Monoclinic	
Space group	P 1 21/n 1	
Unit cell dimensions	a = 9.2136(6) Å	a= 90°.
	b = 10.4625(7) Å	b= 92.593(2)°.
	c = 17.0024(11) Å	g = 90°.
Volume	1637.31(19) $Å^3$	
Z	4	
Density (calculated)	1.385 Mg/m^3	
Absorption coefficient	0.101 mm^{-1}	
F(000)	720	
Crystal size	0.47 x 0.22 x 0.14 mm^3	
Theta range for data collection	2.286 to 30.109°.	
Index ranges	-12<=h<=12, -14<=k<=14, -23<=l<=23	
Reflections collected	43820	
Independent reflections	4812 [R(int) = 0.0548]	
Completeness to theta = 25.242°	99.8 %	
Absorption correction	Semi-empirical from equivalents	
Max. and min. transmission	0.7460 and 0.6567	
Refinement method	Full-matrix least-squares on F^2	
Data / restraints / parameters	4812 / 0 / 275	
Goodness-of-fit on F^2	1.053	
Final R indices [I>2sigma(I)]	R1 = 0.0468, wR2 = 0.1081	
R indices (all data)	R1 = 0.0638, wR2 = 0.1174	
Extinction coefficient	n/a	
Largest diff. peak and hole	0.457 and -0.254 $e.Å^{-3}$	

X-ray data for 82b:

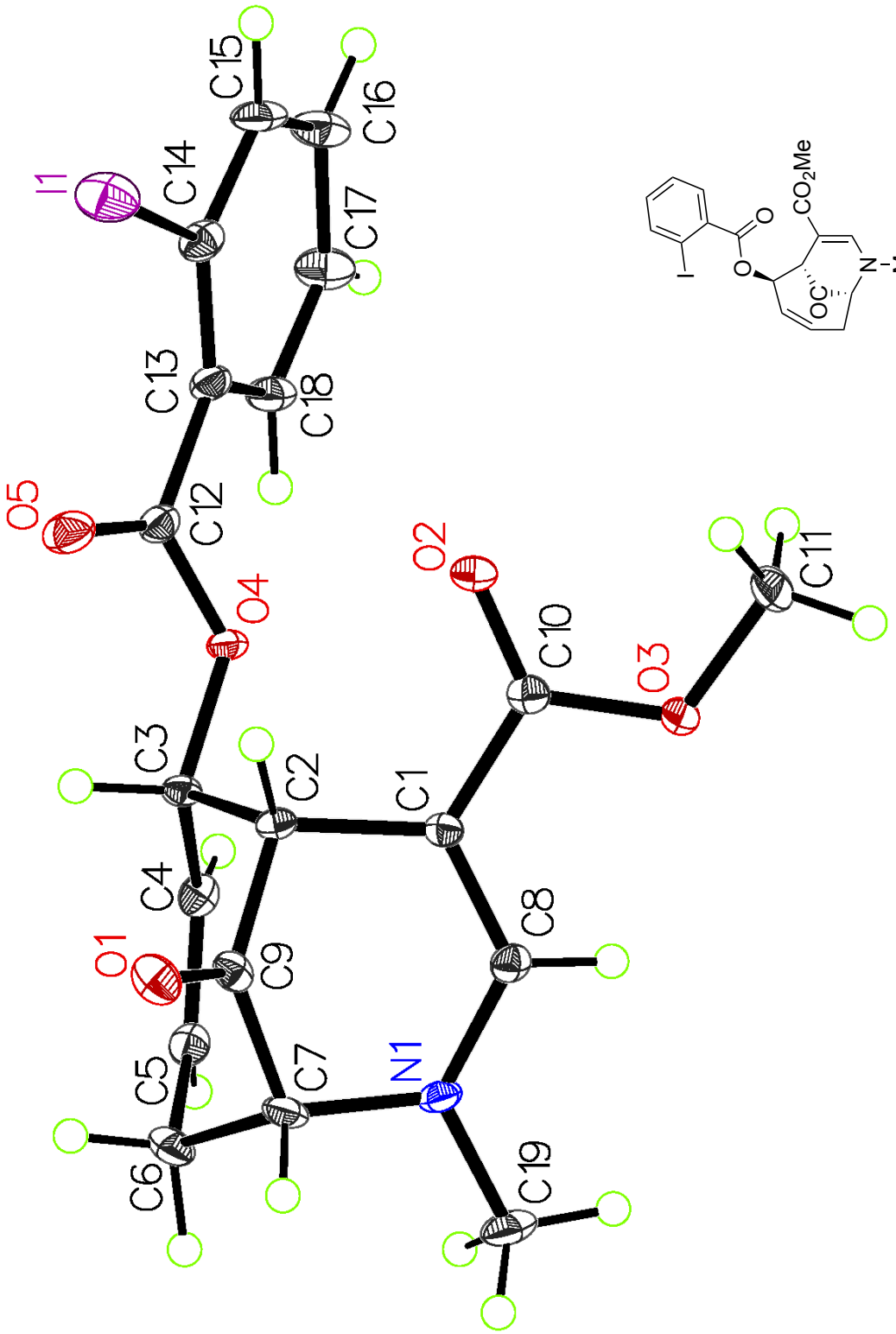

Table 1. Crystal data and structure refinement for CF-VII-092-A3.

Identification code	s1_a	
Empirical formula	C19 H18 I N O5	
Formula weight	467.24	
Temperature	100 K	
Wavelength	0.71073 Å	
Crystal system	Triclinic	
Space group	P-1	
Unit cell dimensions	a = 7.5210(5) Å	a= 108.918(2)°.
	b = 9.4854(6) Å	b= 93.794(2)°.
	c = 13.6083(9) Å	g = 95.881(2)°.
Volume	908.43(10) $Å^3$	
Z	2	
Density (calculated)	1.708 Mg/m^3	
Absorption coefficient	1.793 mm^{-1}	
F(000)	464	
Crystal size	0.26 x 0.05 x 0.02 mm^3	
Theta range for data collection	3.018 to 27.157°.	
Index ranges	-8<=h<=9, -12<=k<=12, -17<=l<=17	
Reflections collected	27144	
Independent reflections	4004 [R(int) = 0.0401]	
Completeness to theta = 25.242°	99.5 %	
Absorption correction	Semi-empirical from equivalents	
Max. and min. transmission	0.7455 and 0.6252	
Refinement method	Full-matrix least-squares on F^2	
Data / restraints / parameters	4004 / 0 / 237	
Goodness-of-fit on F^2	1.079	
Final R indices [I>2sigma(I)]	R1 = 0.0302, wR2 = 0.0637	
R indices (all data)	R1 = 0.0364, wR2 = 0.0662	
Extinction coefficient	n/a	
Largest diff. peak and hole	0.827 and -1.239 $e.Å^{-3}$	

X-ray data for 86a:

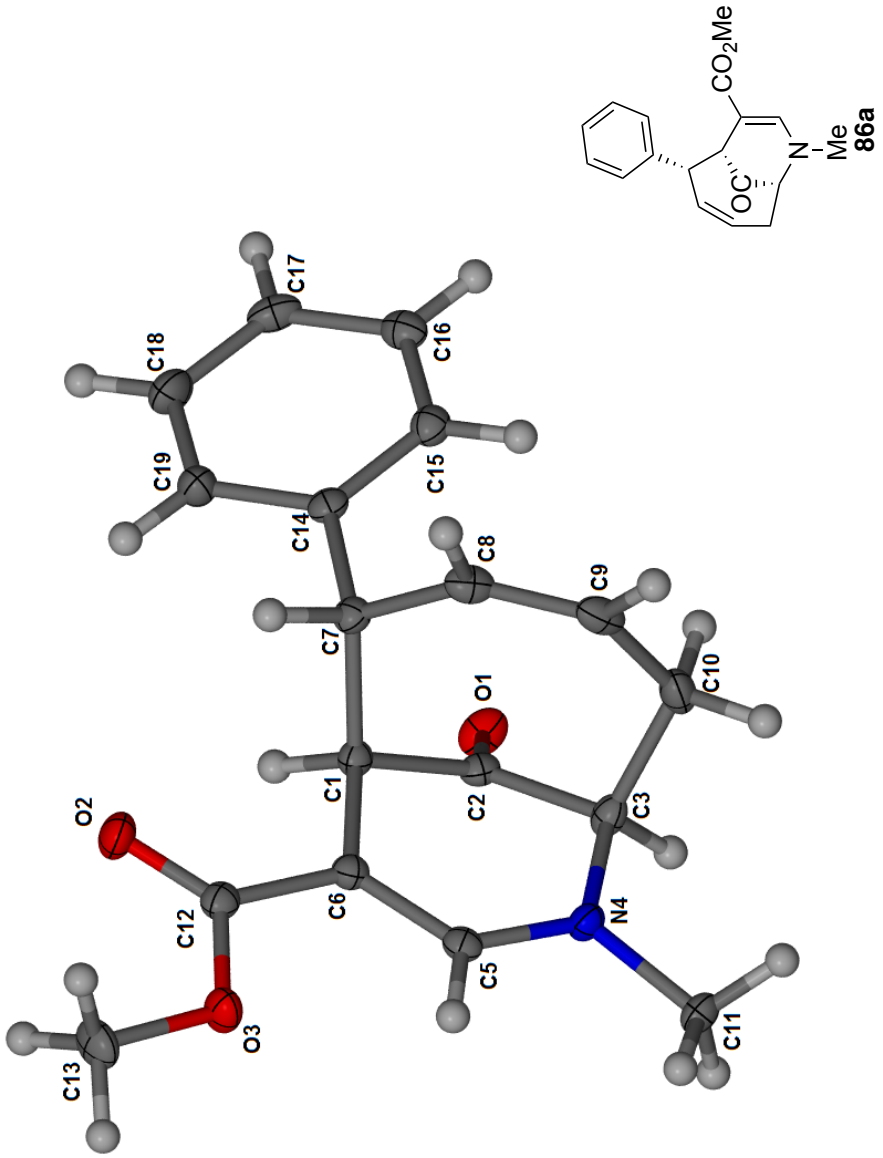

X-ray data for 86b:

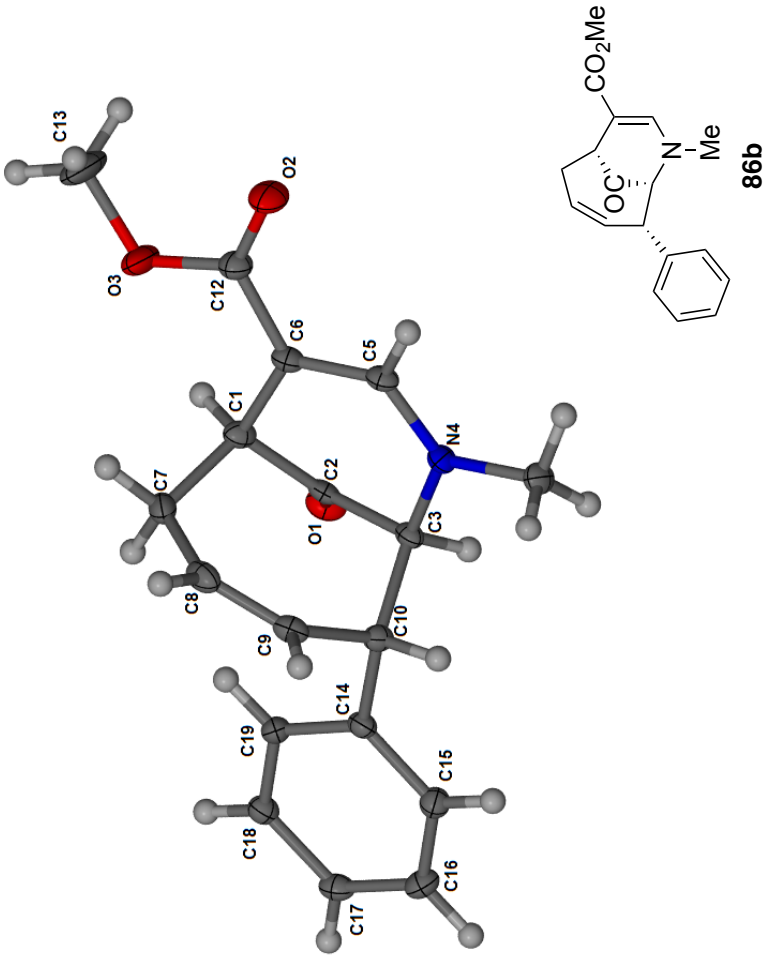

Table 1. Crystal data and structure refinement for CF-IV-27-A2.

Identification code	CF-IV-27-A2	
Empirical formula	C18 H19 N O3	
Formula weight	297.34	
Temperature	100(2) K	
Wavelength	0.71073 Å	
Crystal system	Orthorhombic	
Space group	$P2_12_12_1$	
Unit cell dimensions	a = 7.0211(7) Å	a= 90°.
	b = 11.7262(12) Å	b= 90°.
	c = 18.3049(19) Å	g = 90°.
Volume	1507.1(3) $Å^3$	
Z	4	
Density (calculated)	1.310 Mg/m^3	
Absorption coefficient	0.089 mm^{-1}	
F(000)	632	
Crystal size	0.350 x 0.250 x 0.250 mm^3	
Theta range for data collection	2.225 to 28.327°.	
Index ranges	-9<=h<=9, -15<=k<=15, -23<=l<=24	
Reflections collected	12132	
Independent reflections	3769 [R(int) = 0.0290]	
Completeness to theta = 25.242°	99.9 %	
Absorption correction	Semi-empirical from equivalents	
Max. and min. transmission	0.98 and 0.90	
Refinement method	Full-matrix least-squares on F^2	
Data / restraints / parameters	3769 / 0 / 201	
Goodness-of-fit on F^2	1.026	
Final R indices [I>2sigma(I)]	R1 = 0.0362, wR2 = 0.0863	
R indices (all data)	R1 = 0.0423, wR2 = 0.0899	
Absolute structure parameter	0.1(4)	
Extinction coefficient	n/a	
Largest diff. peak and hole	0.220 and -0.221 e.$Å^{-3}$	

X-ray data for 87a:

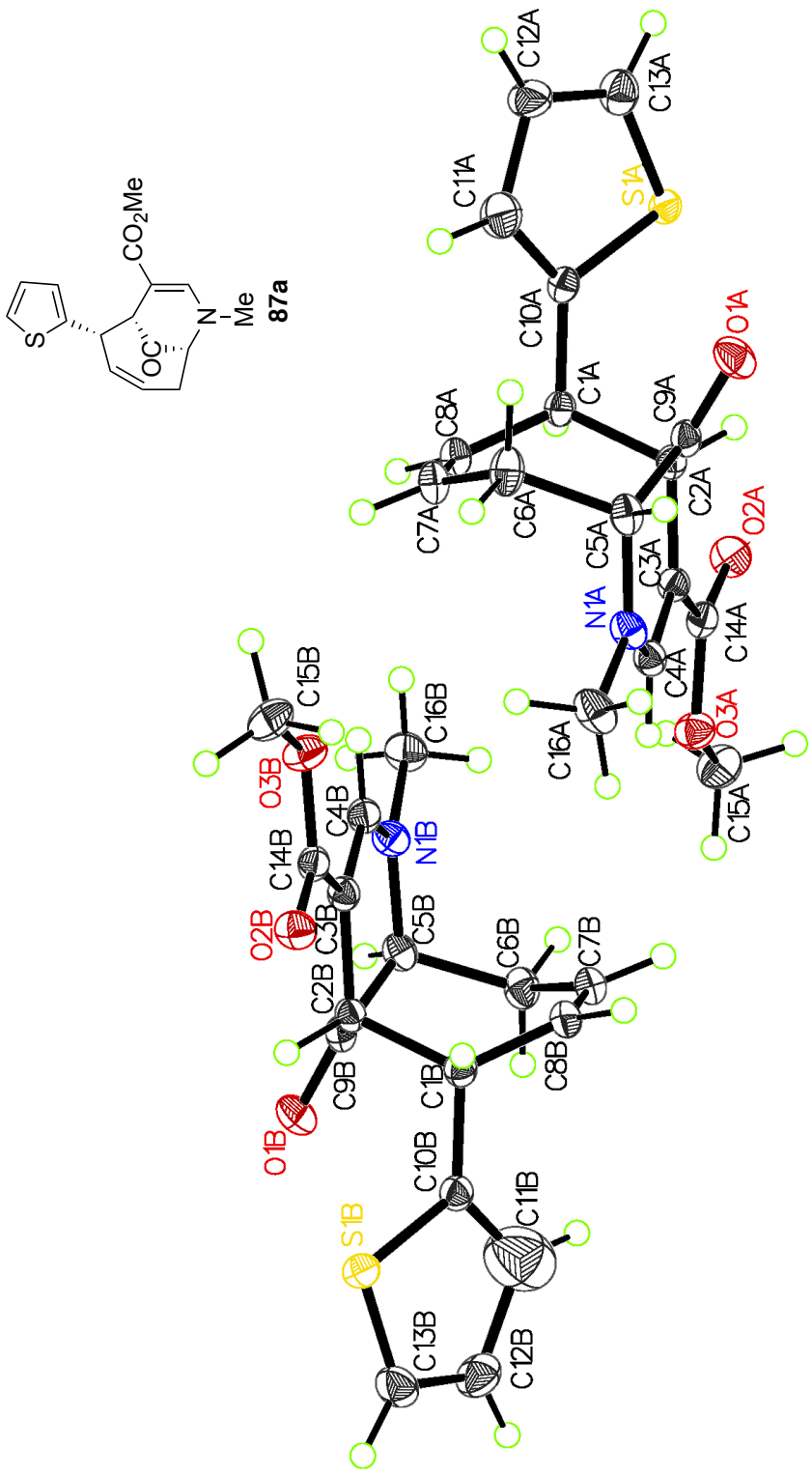

Table 1. Crystal data and structure refinement for CF-VII-028-A3.

Identification code	s1_a	
Empirical formula	C16 H17 N O3 S	
Formula weight	303.36	
Temperature	100.15 K	
Wavelength	0.71073 Å	
Crystal system	Monoclinic	
Space group	P 1 21/c 1	
Unit cell dimensions	a = 14.2147(5) Å	a= 90°.
	b = 10.3942(4) Å	b= 94.456(2)°.
	c = 19.5232(7) Å	g = 90°.
Volume	2875.84(18) $Å^3$	
Z	8	
Density (calculated)	1.401 Mg/m^3	
Absorption coefficient	0.235 mm^{-1}	
F(000)	1280	
Crystal size	0.53 x 0.24 x 0.13 mm^3	
Theta range for data collection	1.437 to 35.822°.	
Index ranges	-23<=h<=23, -17<=k<=17, -32<=l<=32	
Reflections collected	189237	
Independent reflections	13431 [R(int) = 0.0345]	
Completeness to theta = 25.242°	100.0 %	
Absorption correction	Semi-empirical from equivalents	
Max. and min. transmission	0.7470 and 0.7055	
Refinement method	Full-matrix least-squares on F^2	
Data / restraints / parameters	13431 / 3 / 419	
Goodness-of-fit on F^2	1.063	
Final R indices [I>2sigma(I)]	R1 = 0.0404, wR2 = 0.1046	
R indices (all data)	R1 = 0.0574, wR2 = 0.1174	
Extinction coefficient	n/a	
Largest diff. peak and hole	0.556 and -0.415 $e.Å^{-3}$	

X-ray data for 87b:

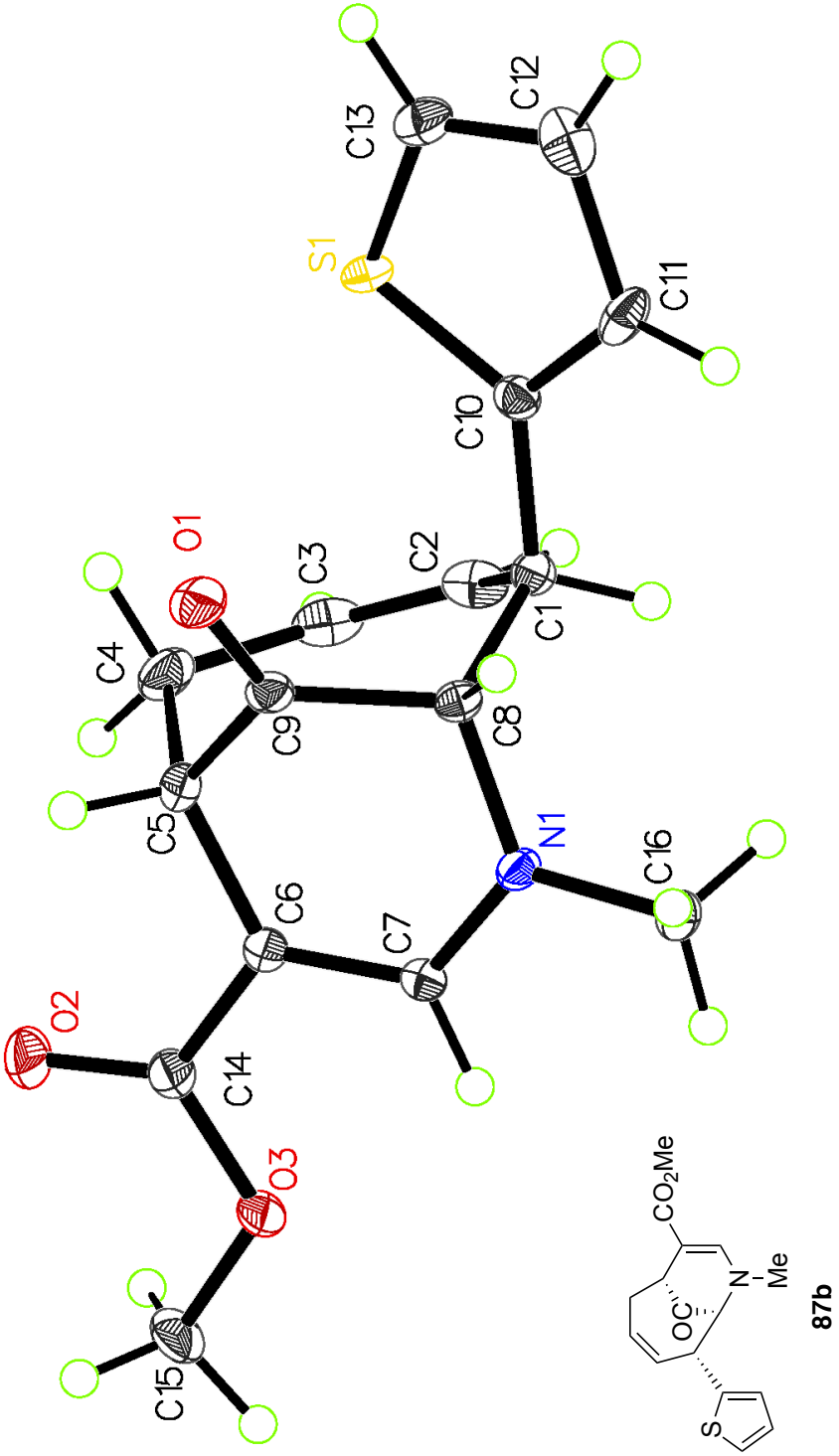

Table 1. Crystal data and structure refinement for CF-VII-028-A2.

Identification code	s1	
Empirical formula	C16 H17 N O3 S	
Formula weight	303.36	
Temperature	100 K	
Wavelength	0.71073 Å	
Crystal system	Triclinic	
Space group	P-1	
Unit cell dimensions	a = 8.8532(2) Å	a= 61.8743(9)°.
	b = 9.8929(3) Å	b= 80.4870(10)°.
	c = 10.1731(3) Å	g = 64.3812(9)°.
Volume	707.70(3) $Å^3$	
Z	2	
Density (calculated)	1.424 Mg/m^3	
Absorption coefficient	0.238 mm^{-1}	
F(000)	320	
Crystal size	0.21 x 0.14 x 0.08 mm^3	
Theta range for data collection	2.545 to 31.136°.	
Index ranges	-12<=h<=12, -14<=k<=14, -14<=l<=14	
Reflections collected	37134	
Independent reflections	4547 [R(int) = 0.0631]	
Completeness to theta = 25.242°	99.9 %	
Absorption correction	Semi-empirical from equivalents	
Max. and min. transmission	0.7462 and 0.7134	
Refinement method	Full-matrix least-squares on F^2	
Data / restraints / parameters	4547 / 0 / 250	
Goodness-of-fit on F^2	1.050	
Final R indices [I>2sigma(I)]	R1 = 0.0478, wR2 = 0.0958	
R indices (all data)	R1 = 0.0791, wR2 = 0.1085	
Extinction coefficient	n/a	
Largest diff. peak and hole	0.442 and -0.395 $e.Å^{-3}$	

X-ray data for 94a:

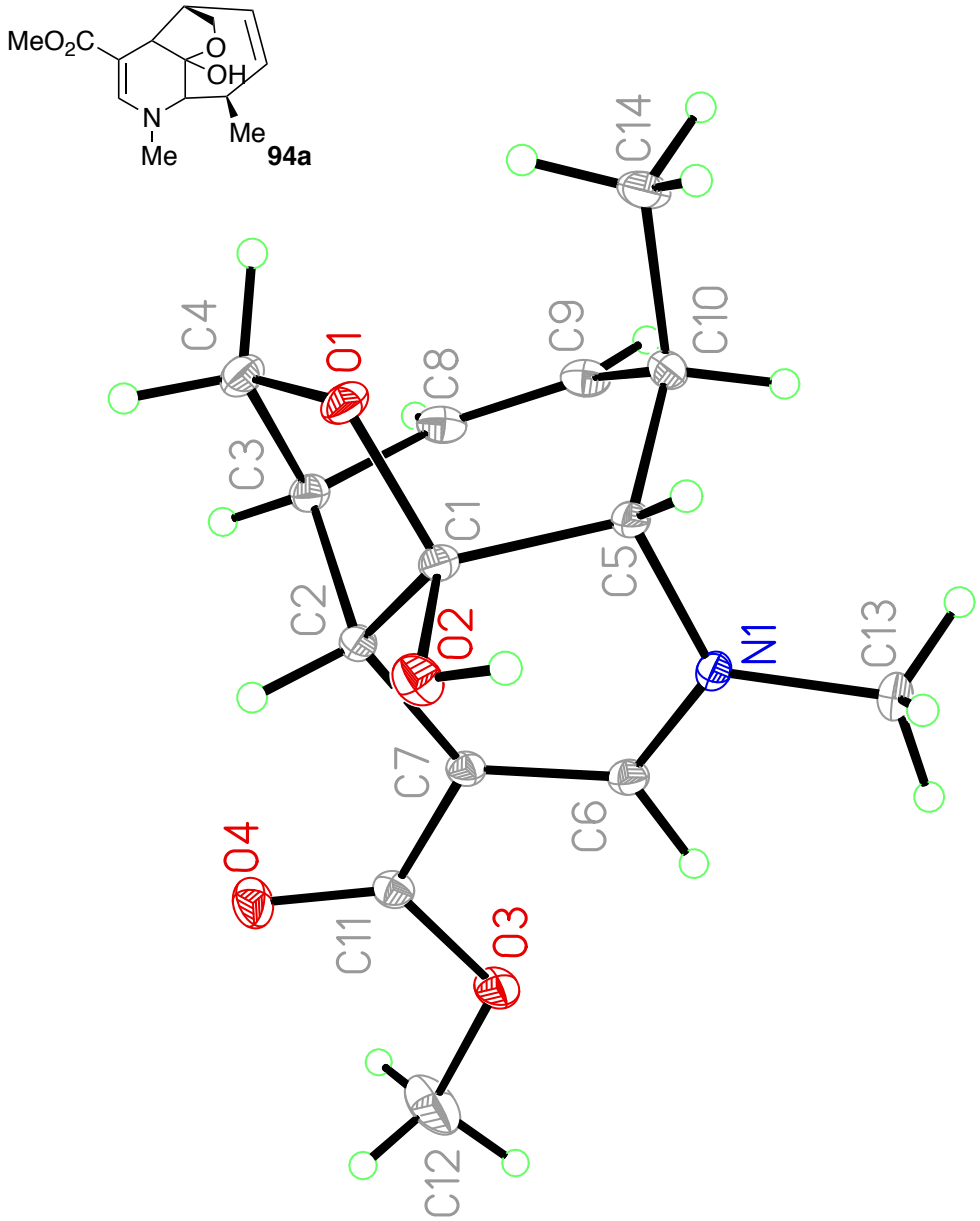

Table 1. Crystal data and structure refinement for CF-IV-095-A3-2.

Identification code	s1_a	
Empirical formula	C14 H19 N O4	
Formula weight	265.30	
Temperature	100(2) K	
Wavelength	0.71073 Å	
Crystal system	Monoclinic	
Space group	$P2_1/n$	
Unit cell dimensions	a = 10.0281(4) Å	a= 90°.
	b = 8.8101(4) Å	b= 107.184(2)°.
	c = 15.1125(7) Å	g = 90°.
Volume	1275.57(10) $Å^3$	
Z	4	
Density (calculated)	1.381 Mg/m^3	
Absorption coefficient	0.101 mm^{-1}	
F(000)	568	
Crystal size	0.290 x 0.240 x 0.140 mm^3	
Theta range for data collection	2.708 to 30.535°.	
Index ranges	-14<=h<=14, -12<=k<=12, -21<=l<=21	
Reflections collected	29415	
Independent reflections	3885 [R(int) = 0.0410]	
Completeness to theta = 25.242°	99.5 %	
Absorption correction	Semi-empirical from equivalents	
Max. and min. transmission	0.7461 and 0.6943	
Refinement method	Full-matrix least-squares on F^2	
Data / restraints / parameters	3885 / 0 / 229	
Goodness-of-fit on F^2	1.048	
Final R indices [I>2sigma(I)]	R1 = 0.0395, wR2 = 0.0982	
R indices (all data)	R1 = 0.0501, wR2 = 0.1048	
Extinction coefficient	n/a	
Largest diff. peak and hole	0.422 and -0.233 $e.Å^{-3}$	

X-ray data for 94d:

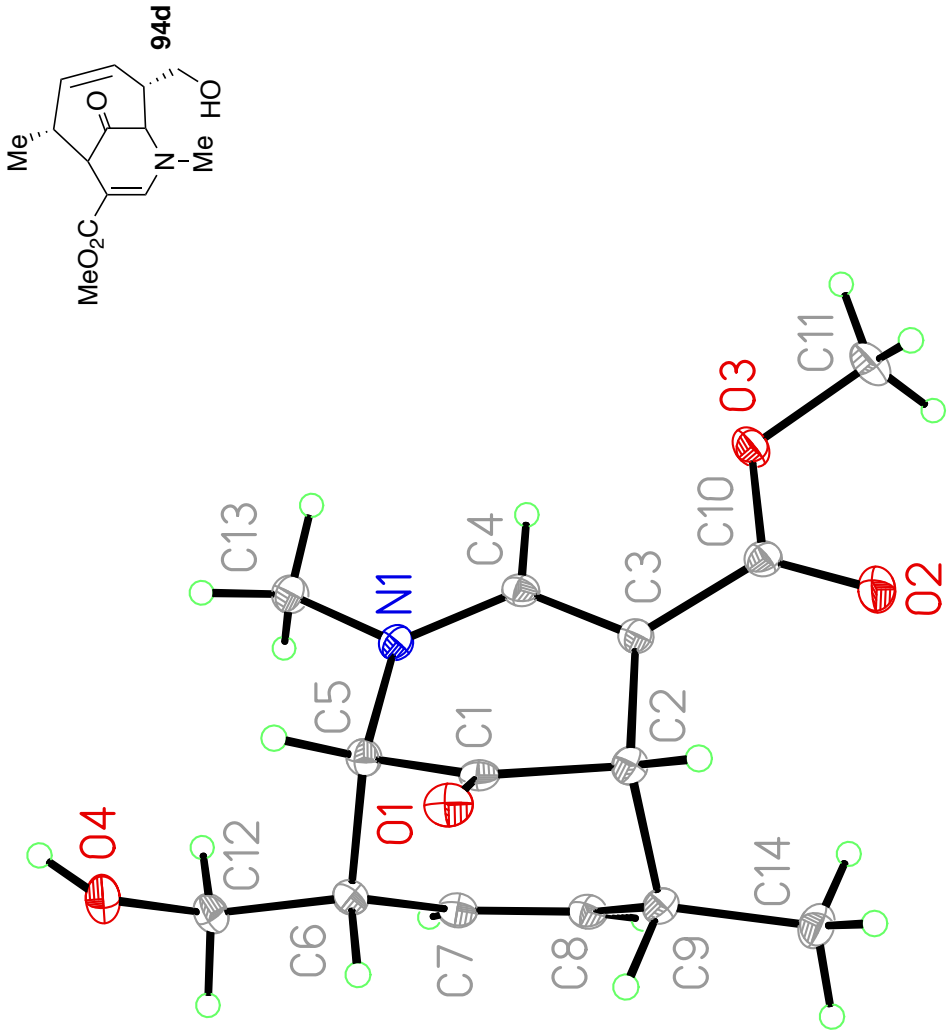

Table 1. Crystal data and structure refinement for CF-IV-095-A3-1.

Identification code	s2	
Empirical formula	C14 H19 N O4	
Formula weight	265.30	
Temperature	100(2) K	
Wavelength	0.71073 Å	
Crystal system	Triclinic	
Space group	P-1	
Unit cell dimensions	a = 7.5321(5) Å	a= 112.047(2)°.
	b = 9.5317(7) Å	b= 95.653(2)°.
	c = 9.6535(7) Å	g = 90.158(2)°.
Volume	638.66(8) $Å^3$	
Z	2	
Density (calculated)	1.380 Mg/m^3	
Absorption coefficient	0.101 mm^{-1}	
F(000)	284	
Crystal size	0.360 x 0.360 x 0.250 mm^3	
Theta range for data collection	2.289 to 30.374°.	
Index ranges	-10<=h<=10, -13<=k<=13, -13<=l<=13	
Reflections collected	24735	
Independent reflections	3840 [R(int) = 0.0489]	
Completeness to theta = 25.242°	99.5 %	
Absorption correction	Semi-empirical from equivalents	
Max. and min. transmission	0.7460 and 0.6979	
Refinement method	Full-matrix least-squares on F^2	
Data / restraints / parameters	3840 / 0 / 226	
Goodness-of-fit on F^2	1.020	
Final R indices [I>2sigma(I)]	R1 = 0.0480, wR2 = 0.1102	
R indices (all data)	R1 = 0.0694, wR2 = 0.1219	
Extinction coefficient	n/a	
Largest diff. peak and hole	0.455 and -0.253 $e.Å^{-3}$	

X-ray data for 95a:

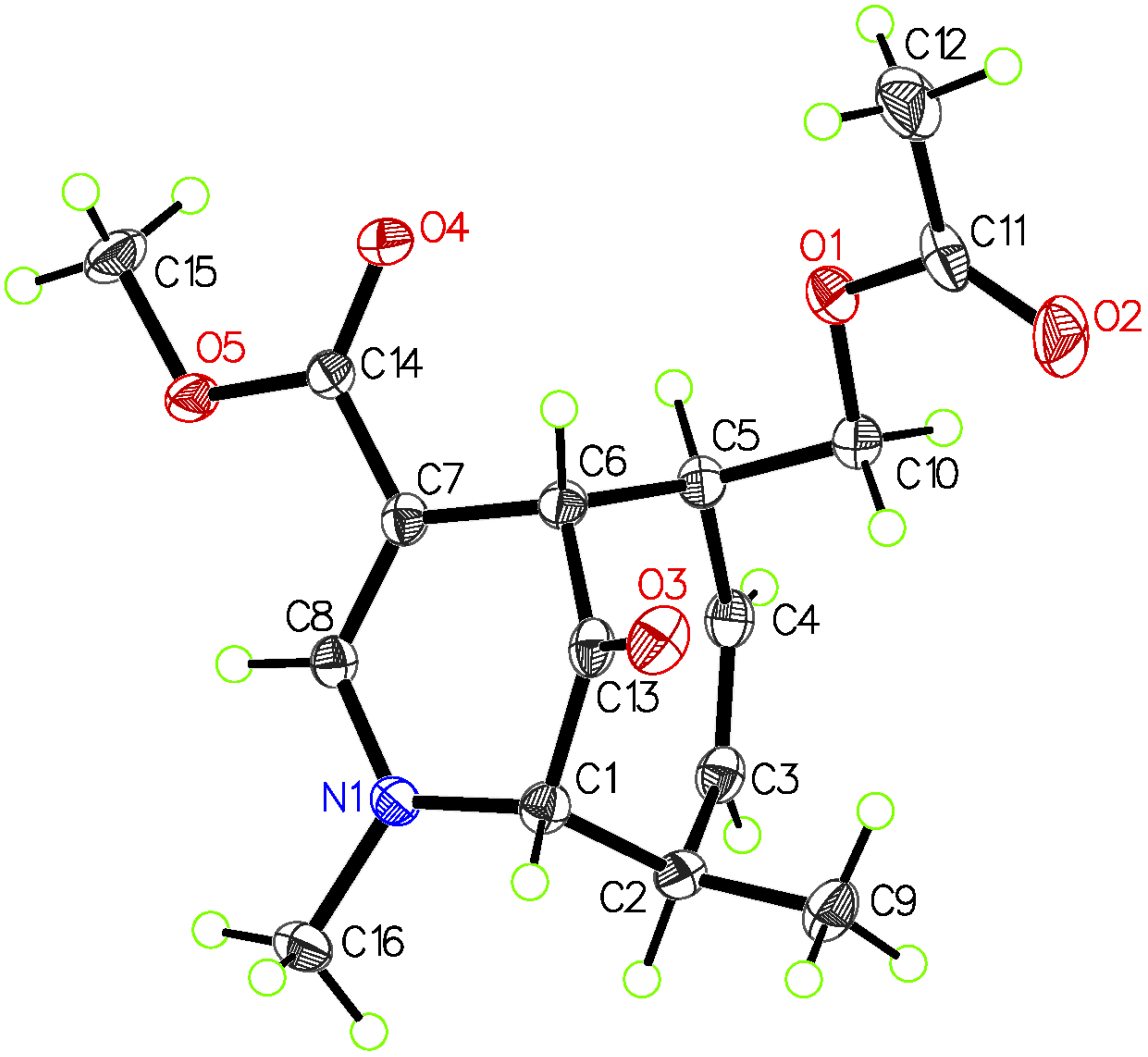

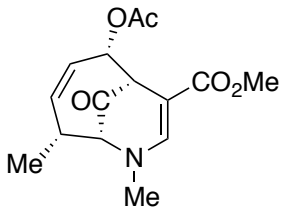

95a

Table 1. Crystal data and structure refinement for CF-V-030-A4.

Identification code	s1_a	
Empirical formula	C16 H21 N O5	
Formula weight	307.34	
Temperature	100 K	
Wavelength	0.71073 Å	
Crystal system	Orthorhombic	
Space group	$Pna2_1$	
Unit cell dimensions	a = 10.3686(5) Å	a= 90°.
	b = 17.7636(8) Å	b= 90°.
	c = 8.7645(4) Å	g = 90°.
Volume	1614.28(13) $Å^3$	
Z	4	
Density (calculated)	1.265 Mg/m^3	
Absorption coefficient	0.094 mm^{-1}	
F(000)	656	
Crystal size	0.3 x 0.26 x 0.15 mm^3	
Theta range for data collection	3.020 to 26.393°.	
Index ranges	-12<=h<=12, -22<=k<=21, -10<=l<=10	
Reflections collected	23881	
Independent reflections	3261 [R(int) = 0.0352]	
Completeness to theta = 25.242°	98.5 %	
Absorption correction	Semi-empirical from equivalents	
Max. and min. transmission	0.7454 and 0.6751	
Refinement method	Full-matrix least-squares on F^2	
Data / restraints / parameters	3261 / 1 / 203	
Goodness-of-fit on F^2	1.045	
Final R indices [I>2sigma(I)]	R1 = 0.0301, wR2 = 0.0803	
R indices (all data)	R1 = 0.0312, wR2 = 0.0812	
Absolute structure parameter	-0.3(2)	
Extinction coefficient	n/a	
Largest diff. peak and hole	0.172 and -0.158 $e.Å^{-3}$	

X-ray data for 96a:

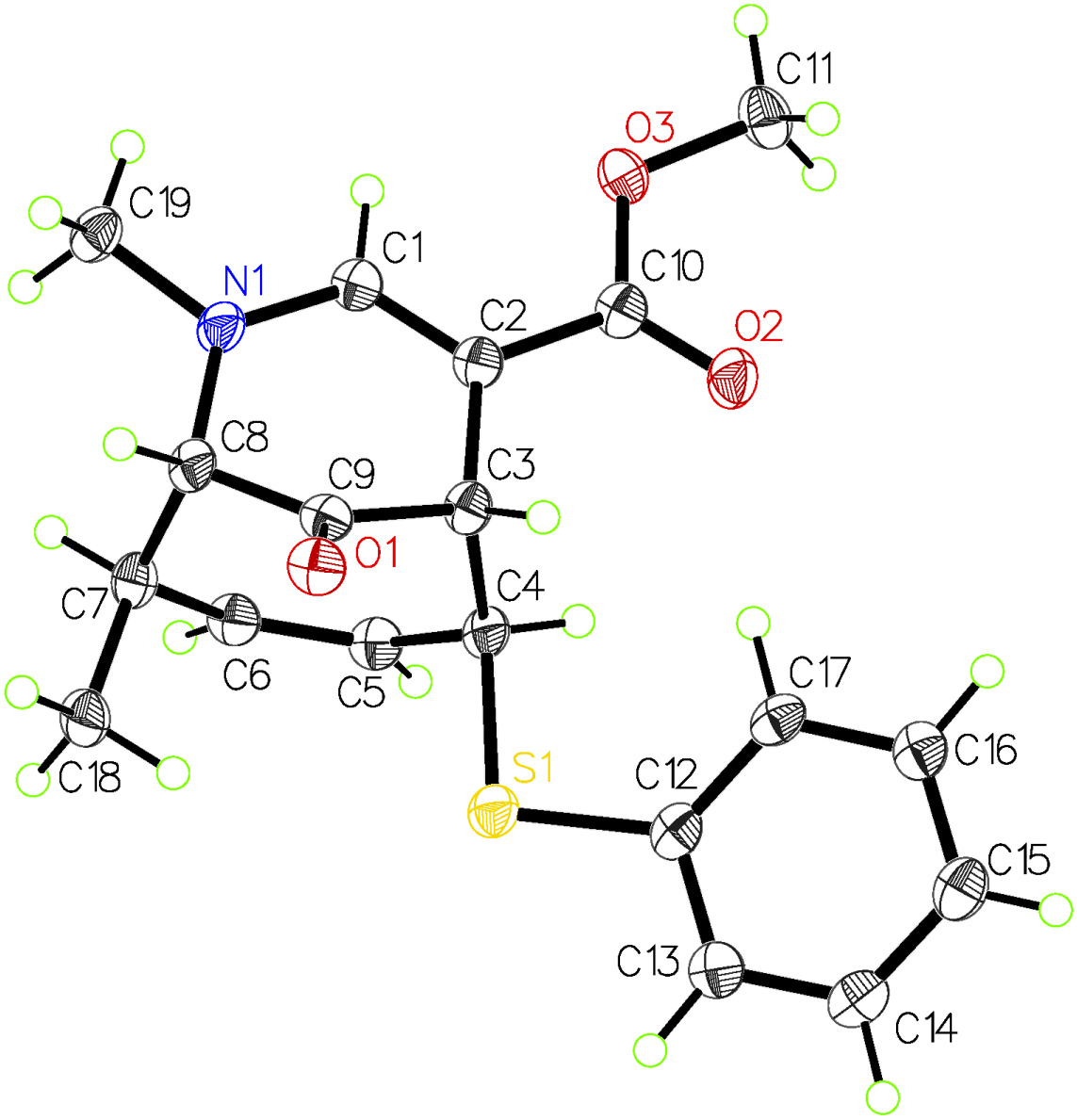

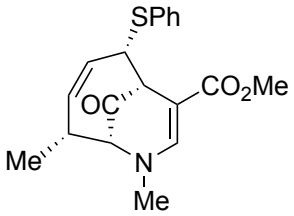

96a

Table 1. Crystal data and structure refinement for CF-VII-028-A3.

Identification code	s1_a	
Empirical formula	C16 H17 N O3 S	
Formula weight	303.36	
Temperature	100.15 K	
Wavelength	0.71073 Å	
Crystal system	Monoclinic	
Space group	P 1 21/c 1	
Unit cell dimensions	a = 14.2147(5) Å	a= 90°.
	b = 10.3942(4) Å	b= 94.456(2)°.
	c = 19.5232(7) Å	g = 90°.
Volume	2875.84(18) $Å^3$	
Z	8	
Density (calculated)	1.401 Mg/m^3	
Absorption coefficient	0.235 mm^{-1}	
F(000)	1280	
Crystal size	0.53 x 0.24 x 0.13 mm^3	
Theta range for data collection	1.437 to 35.822°.	
Index ranges	-23<=h<=23, -17<=k<=17, -32<=l<=32	
Reflections collected	189237	
Independent reflections	13431 [R(int) = 0.0345]	
Completeness to theta = 25.242°	100.0 %	
Absorption correction	Semi-empirical from equivalents	
Max. and min. transmission	0.7470 and 0.7055	
Refinement method	Full-matrix least-squares on F^2	
Data / restraints / parameters	13431 / 3 / 419	
Goodness-of-fit on F^2	1.063	
Final R indices [I>2sigma(I)]	R1 = 0.0404, wR2 = 0.1046	
R indices (all data)	R1 = 0.0574, wR2 = 0.1174	
Extinction coefficient	n/a	
Largest diff. peak and hole	0.556 and -0.415 $e.Å^{-3}$	

X-ray data for 96c':

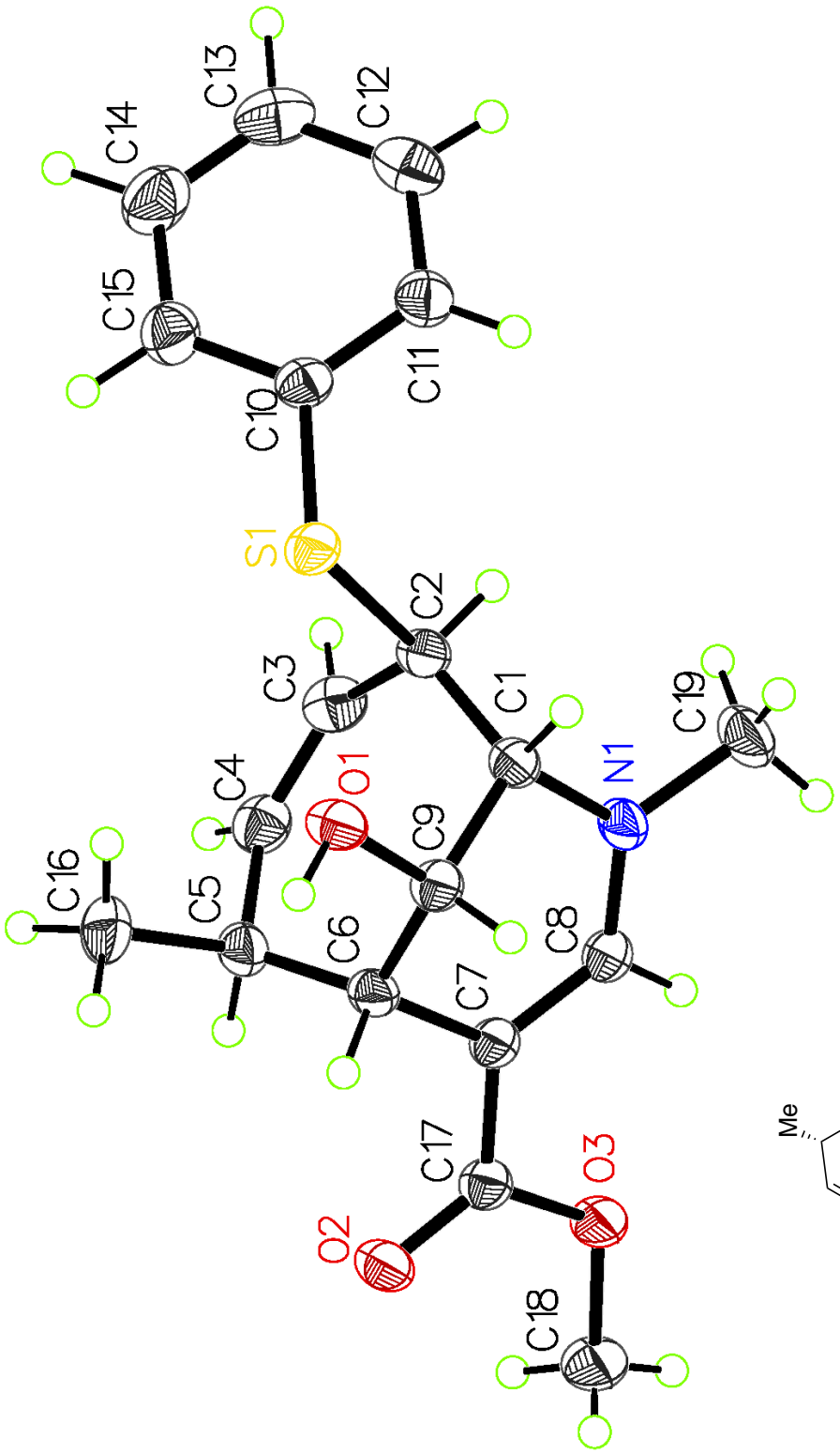

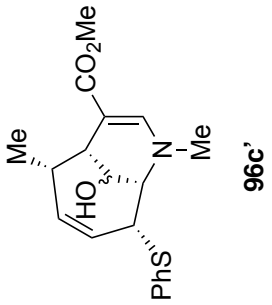

96c'

Table 1. Crystal data and structure refinement for CF-VII-074-A4.

Identification code	s1	
Empirical formula	C19 H23 N O3 S	
Formula weight	345.44	
Temperature	100 K	
Wavelength	1.54178 Å	
Crystal system	Triclinic	
Space group	P-1	
Unit cell dimensions	a = 8.5069(3) Å	a= 91.6157(19)°.
	b = 10.1751(4) Å	b= 99.4635(18)°.
	c = 10.6767(4) Å	g = 93.2822(18)°.
Volume	909.42(6) $Å^3$	
Z	2	
Density (calculated)	1.262 Mg/m^3	
Absorption coefficient	1.711 mm^{-1}	
F(000)	368	
Crystal size	0.3 x 0.15 x 0.1 mm^3	
Theta range for data collection	4.201 to 74.041°.	
Index ranges	-10<=h<=10, -12<=k<=11, -13<=l<=13	
Reflections collected	29176	
Independent reflections	3561 [R(int) = 0.0292]	
Completeness to theta = 67.679°	97.6 %	
Absorption correction	Semi-empirical from equivalents	
Max. and min. transmission	0.7538 and 0.6644	
Refinement method	Full-matrix least-squares on F^2	
Data / restraints / parameters	3561 / 0 / 283	
Goodness-of-fit on F^2	1.051	
Final R indices [I>2sigma(I)]	R1 = 0.0328, wR2 = 0.0856	
R indices (all data)	R1 = 0.0342, wR2 = 0.0867	
Extinction coefficient	n/a	
Largest diff. peak and hole	0.306 and -0.189 $e.Å^{-3}$	

X-ray data for 109a:

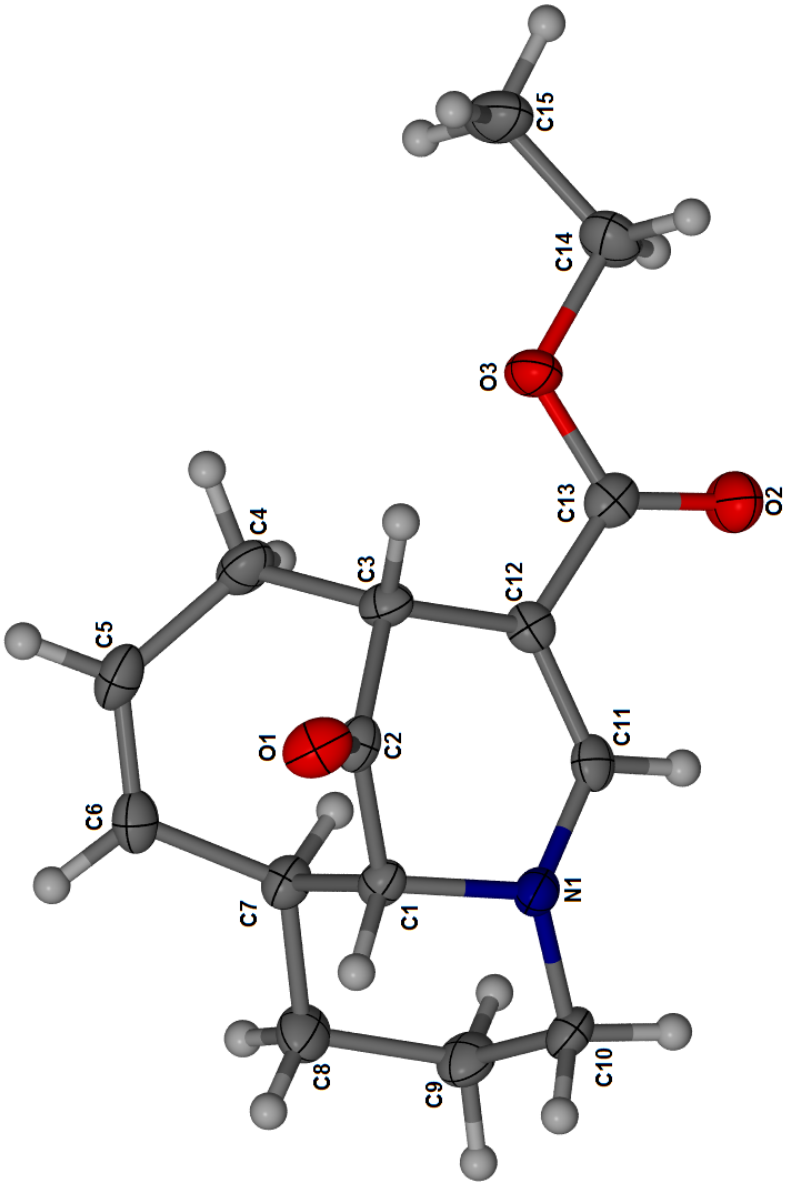

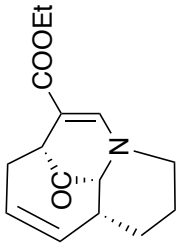

109a

Table 1. Crystal data and structure refinement for cf-ii-122-a1.

Identification code	CF-II-122-A1	
Empirical formula	C60 H76 N4 O12	
Formula weight	1045.24	
Temperature	150(2) K	
Wavelength	0.71073 Å	
Crystal system	Orthorhombic	
Space group	$P2_12_12_1$	
Unit cell dimensions	a = 7.1832(3) Å	a= 90°.
	b = 10.5514(6) Å	b= 90°.
	c = 17.9398(9) Å	g = 90°.
Volume	1359.71(12) $Å^3$	
Z	1	
Density (calculated)	1.277 Mg/m^3	
Absorption coefficient	0.089 mm^{-1}	
F(000)	560	
Crystal size	0.250 x 0.250 x 0.080 mm^3	
Theta range for data collection	2.239 to 28.289°.	
Index ranges	-8<=h<=9, -12<=k<=14, -17<=l<=23	
Reflections collected	7337	
Independent reflections	3274 [R(int) = 0.0403]	
Completeness to theta = 25.242°	99.9 %	
Absorption correction	Semi-empirical from equivalents	
Max. and min. transmission	0.99 and 0.87	
Refinement method	Full-matrix least-squares on F^2	
Data / restraints / parameters	3274 / 0 / 173	
Goodness-of-fit on F^2	1.072	
Final R indices [I>2sigma(I)]	R1 = 0.0527, wR2 = 0.0906	
R indices (all data)	R1 = 0.0875, wR2 = 0.1015	
Absolute structure parameter	0.4(7)	
Extinction coefficient	n/a	
Largest diff. peak and hole	0.243 and -0.246 $e.Å^{-3}$	

X-ray data for 139:

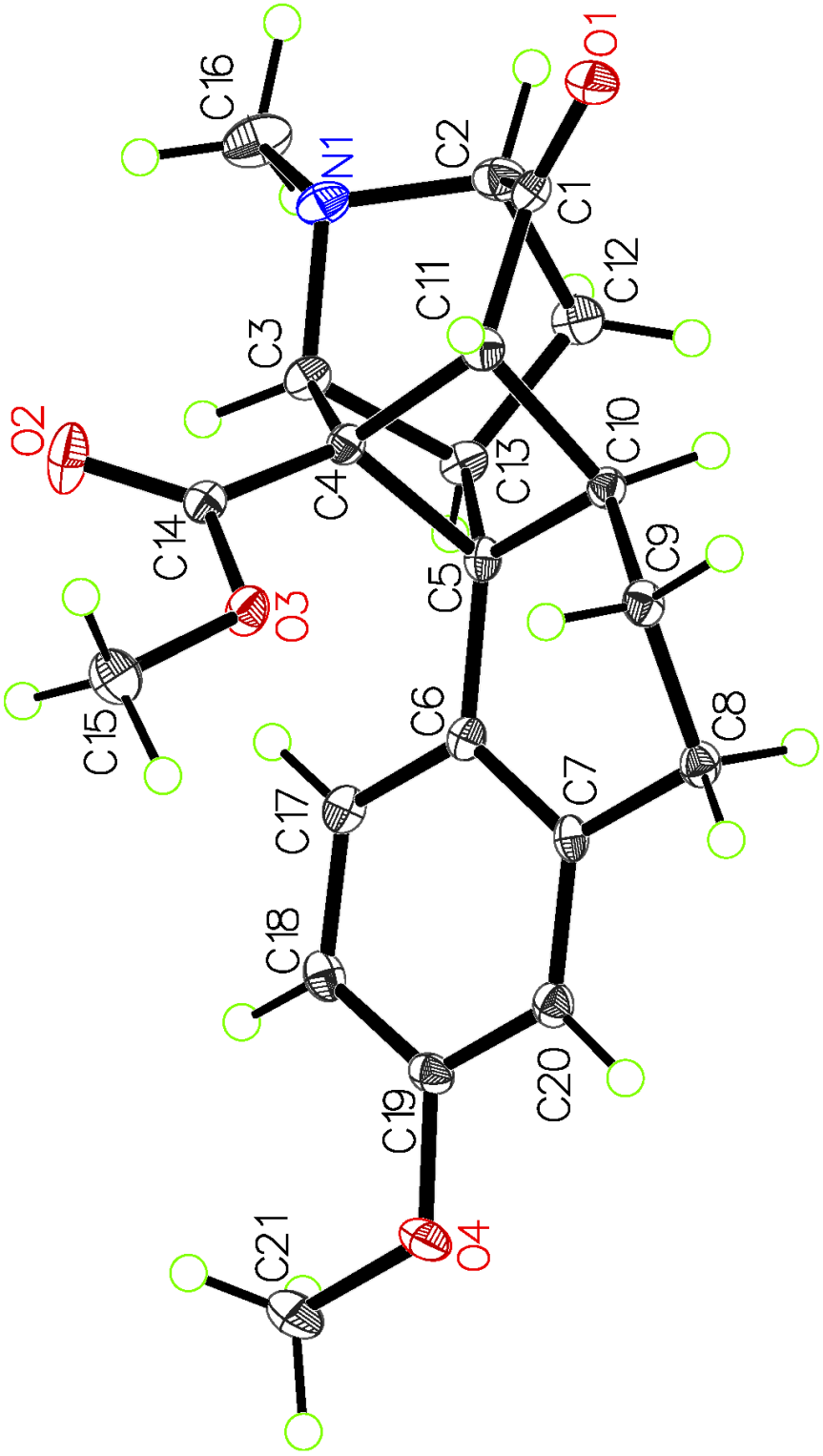

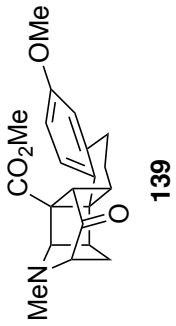

139

Table 1. Crystal data and structure refinement for CF-VI-071-A3.

Identification code	s1	
Empirical formula	C21 H23 N O4	
Formula weight	353.40	
Temperature	100 K	
Wavelength	0.71073 Å	
Crystal system	Monoclinic	
Space group	P 1 21/n 1	
Unit cell dimensions	a = 11.6167(5) Å	a= 90°.
	b = 7.4454(3) Å	b= 91.0667(16)°.
	c = 19.8963(8) Å	g = 90°.
Volume	1720.55(12) $Å^3$	
Z	4	
Density (calculated)	1.364 Mg/m^3	
Absorption coefficient	0.094 mm^{-1}	
F(000)	752	
Crystal size	0.8 x 0.15 x 0.05 mm^3	
Theta range for data collection	2.921 to 27.711°.	
Index ranges	-15<=h<=15, -9<=k<=9, -26<=l<=26	
Reflections collected	39589	
Independent reflections	4022 [R(int) = 0.0589]	
Completeness to theta = 25.242°	99.9 %	
Absorption correction	Semi-empirical from equivalents	
Max. and min. transmission	0.7456 and 0.6929	
Refinement method	Full-matrix least-squares on F^2	
Data / restraints / parameters	4022 / 0 / 295	
Goodness-of-fit on F^2	1.058	
Final R indices [I>2sigma(I)]	R1 = 0.0431, wR2 = 0.0958	
R indices (all data)	R1 = 0.0569, wR2 = 0.1024	
Extinction coefficient	n/a	
Largest diff. peak and hole	0.285 and -0.241 $e.Å^{-3}$	

X-ray data for 139:

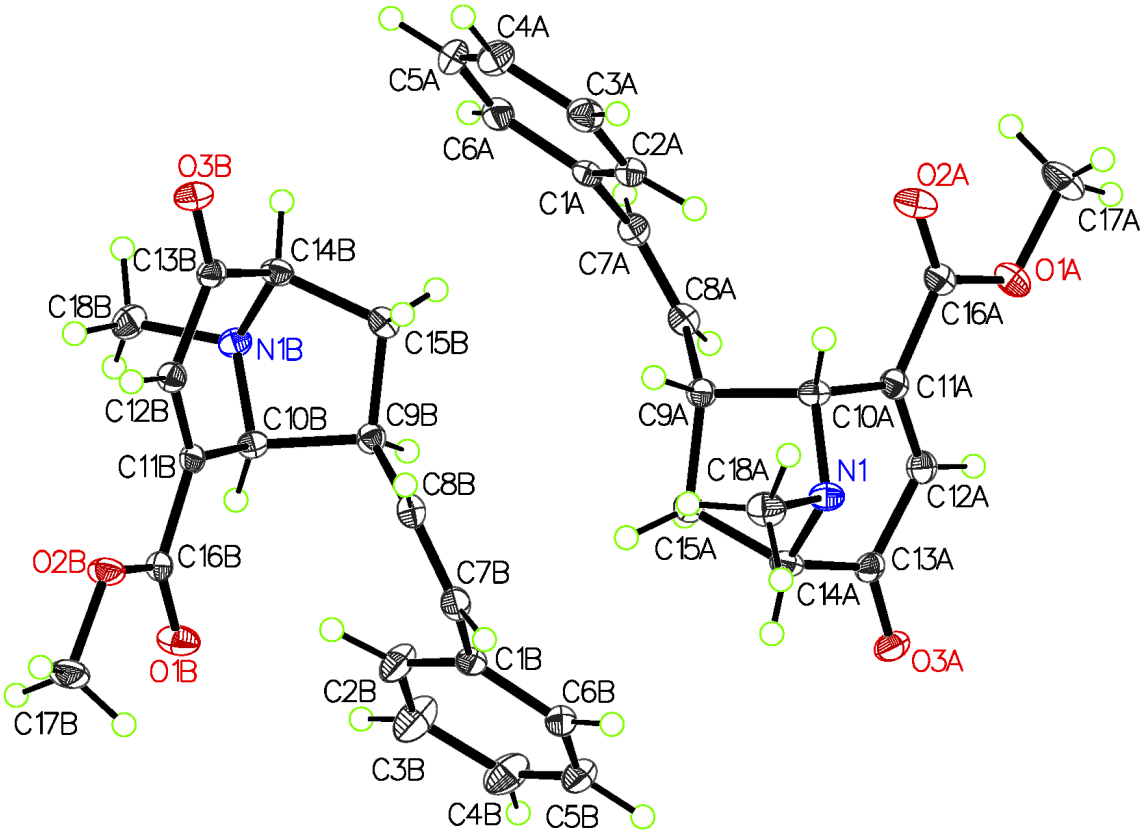

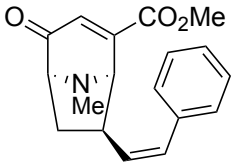

143

Table 1. Crystal data and structure refinement for CF-V-109-A3.

Identification code	s1	
Empirical formula	C18 H19 N O3	
Formula weight	297.34	
Temperature	100 K	
Wavelength	1.54178 Å	
Crystal system	Triclinic	
Space group	P-1	
Unit cell dimensions	a = 11.2163(2) Å	a= 105.1470(10)°.
	b = 12.4848(2) Å	b= 113.0720(10)°.
	c = 12.9993(3) Å	g = 99.3610(10)°.
Volume	1542.87(5) $Å^3$	
Z	4	
Density (calculated)	1.280 Mg/m^3	
Absorption coefficient	0.704 mm^{-1}	
F(000)	632	
Crystal size	0.37 x 0.25 x 0.05 mm^3	
Theta range for data collection	3.843 to 72.403°.	
Index ranges	-13<=h<=13, -15<=k<=15, -16<=l<=16	
Reflections collected	57486	
Independent reflections	5936 [R(int) = 0.0387]	
Completeness to theta = 67.679°	97.9 %	
Absorption correction	Semi-empirical from equivalents	
Max. and min. transmission	0.7536 and 0.6921	
Refinement method	Full-matrix least-squares on F^2	
Data / restraints / parameters	5936 / 0 / 511	
Goodness-of-fit on F^2	1.040	
Final R indices [I>2sigma(I)]	R1 = 0.0342, wR2 = 0.0800	
R indices (all data)	R1 = 0.0432, wR2 = 0.0852	
Extinction coefficient	n/a	
Largest diff. peak and hole	0.238 and -0.223 $e.Å^{-3}$	

REFERENCES

1. Cheng, H. M.; Tian, W.; Peixoto, P. A.; Dhudshia, B.; Chen, D. Y.-K., Synthesis of ent-Nanolobatolide. *Angewandte Chemie International Edition* **2011,** *50* (18), 4165-4168.

2. Jørgensen, L.; McKerrall, S. J.; Kuttruff, C. A.; Ungeheuer, F.; Felding, J.; Baran, P. S., 14-Step Synthesis of (+)-Ingenol from (+)-3-Carene. *Science* **2013,** *341* (6148), 878-882.

3. Schwartz, B. D.; Denton, J. R.; Lian, Y.; Davies, H. M. L.; Williams, C. M., Asymmetric [4 + 3] Cycloadditions between Vinylcarbenoids and Dienes: Application to the Total Synthesis of the Natural Product (−)-5-epi-Vibsanin E. *J Am Chem Soc* **2009,** *131* (23), 8329-8332.

4. Trost, B. M.; Dong, L.; Schroeder, G. M., Total Synthesis of (+)-Allocyathin B2. *J Am Chem Soc* **2005,** *127* (9), 2844-2845.

5. Allinger, N. L.; Tribble, M. T.; Miller, M. A.; Wertz, D. H., Conformational analysis. LXIX. Improved force field for the calculation of the structures and energies of hydrocarbons. *J Am Chem Soc* **1971,** *93* (7), 1637-1648.

6. Illuminati, G.; Mandolini, L., Ring closure reactions of bifunctional chain molecules. *Accounts of Chemical Research* **1981,** *14* (4), 95-102.

7. Woodward, R. B.; Hoffmann, R., The Conservation of Orbital Symmetry. *Angewandte Chemie International Edition in English* **1969,** *8* (11), 781-853.

8. Harmata, M., Exploration of Fundamental and Synthetic Aspects of the Intramolecular 4 + 3 Cycloaddition Reaction†. *Accounts of Chemical Research* **2001,** *34* (7), 595-605.

9. Hoffmann, H. M. R., The Cycloaddition of Allyl Cations to 1,3-Dienes: General Method for the Synthesis of Seven-Membered Carbocycles. New Synthetic Methods (40). *Angewandte Chemie International Edition in English* **1984,** *23* (1), 1-19.

10. Cramer, C. J.; Barrows, S. E., Quantum chemical characterization of cycloaddition reactions between the hydroxyallyl cation and dienes of varying nucleophilicity. *The Journal of organic chemistry* **1998,** *63* (16), 5523-5532.

11. Cramer, C. J.; Barrows, S. E., Quantum chemical characterization of cycloaddition reactions between 1, 3‐butadiene and oxyallyl cations of varying electrophilicity. *J Phys Org Chem* **2000,** *13* (3), 176-186.

12. Fort, A. W., Capture of a Favorskii Intermediate by Furan. *J Am Chem Soc* **1962,** *84* (24), 4979-4981.

13. Hill, A.; Hoffmann, H., One stage synthesis of bicyclo [3.2. 2] nona-6, 8-dien-3-ones. Silver trifluoroacetate induced reaction of 2-methoxyallyl bromide with arenes. *J Am Chem Soc* **1974,** *96* (14), 4597-4603.

14. Ernst, H.; Hoffmann, H. M. R., Synthese von Norbornen-Derivaten aus Cyclopentadien und Allylalkoholen in einem sauren Zweiphasensystem. *Angewandte Chemie* **1980,** *92* (10), 861-863.

15. Giguere, R. J.; Hoffmann, H. M. R.; Hursthouse, M. B.; Trotter, J., Cycloadditions of allyl cations. 24. Sterically crowded ring systems. Preparation and x-ray crystal structure of 9,10,11,11,13,13-hexamethyl-12-oxo-9,10-propanoanthracene. *The Journal of Organic Chemistry* **1981,** *46* (14), 2868-2871.

16. Schmid, R.; Schmid, H., Silberioneninduzierte Reaktion von 3-Chlor-2-pyrrolidinocyclohexen mit 1,3-Dienen. Vorläufige Mitteilung. *Helv Chim Acta* **1974,** *57* (6), 1883-1886.

17. Rigby, J. H.; Pigge, F. C., [4 + 3] Cycloaddition Reactions. In *Organic Reactions*, John Wiley & Sons, Inc.: 1997; p 351.

18. Katritzky, A. R.; Dennis, N., Cycloaddition reactions of heteroaromatic six-membered rings. *Chem Rev* **1989,** *89* (4), 827-861.

19. Dennis, N.; Ibrahim, B.; Katritzky, A. R., 1,3-Dipolar character of six-membered aromatic rings. Part XXI. Thermal cycloadditions of 1-(5-nitro-2-pyridyl)- and 1-(4,6-dimethylpyrimidin-2-yl)-3-oxidopyridinium with 2, 4, and 6 [small pi]-electron components. *Journal of the Chemical Society, Perkin Transactions 1* **1976,** (21), 2307-2328.

20. Katritzky, A. R.; Rahimi-Rastgoo, S.; Sabongi, G. J.; Fischer, G. W., 1,3-Dipolar character of six-membered aromatic rings. Part 51. Cycloadditions of 1-([small beta]-benzoylvinyl)-3-

oxidopyridiniums and subsequent transformations. *Journal of the Chemical Society, Perkin Transactions 1* **1980,** (0), 362-371.

21. Dennis, N.; Katritzky, A. R.; Rittner, R., 1,3-Dipolar character of six-membered aromatic rings. Part XXV. 5-Aryl-1-methyl-3-oxidopyridiniums. *Journal of the Chemical Society, Perkin Transactions 1* **1976,** (21), 2329-2334.

22. Mok, K.-L.; Nye, M. J., 1,3-Cycloaddition of heterocyclic zwitterions to dienes. *Journal of the Chemical Society, Chemical Communications* **1974,** (15), 608-610.

23. Sammes, P. G.; Street, L. J., The preparation and some reactions of 3-oxidopyrylium. *Journal of the Chemical Society, Perkin Transactions 1* **1983,** (0), 1261-1265.

24. Peese, K. M.; Gin, D. Y., Efficient synthetic access to the hetisine C-20-diterpenoid alkaloids. A concise synthesis of nominine via oxidoisoquinolinium-1,3-dipolar and dienamine-Diels-Alder cycloadditions. *J Am Chem Soc* **2006,** *128* (27), 8734-8735.

25. Gao, L. M.; Wei, X. M.; Yang, L., A new diterpenoid alkaloid from a Tibetan medicinal herb Aconitum naviculare Stapf. *J Chem Res-S* **2004,** (4), 307-308.

26. Ikeda, S.; Shibuya, M.; Kanoh, N.; Iwabuchi, Y., Synthetic Studies on Daphnicyclidin A: Enantiocontrolled Construction of the BCD Ring System. *Org Lett* **2009,** *11* (8), 1833-1836.

27. Liang, S.; He, C.-Y.; Szabó, L. F.; Feng, Y.; Lin, X.; Wang, Y., Gelsochalotine, a novel indole ring-degraded monoterpenoid indole alkaloid from Gelsemium elegans. *Tetrahedron Letters* **2013,** *54* (8), 887-890.

28. Bennasar, M. L.; Zulaica, E.; Solé, D.; Alonso, S., Rapid Synthesis of the Ervitsine Alkaloid Skeleton by a Sequential RCM-Heck Cyclization Approach. *Synlett* **2008,** *2008* (5), 667-670.

29. Sung, M. J.; Lee, H. I.; Chong, Y.; Cha, J. K., Synthetic studies on [4+3] cycloadditions of oxyallyls. Part 11 - Facile synthesis of the tricyclic core of sarain A. 3-oxidopyridinium betaine cycloaddition approach. *Org Lett* **1999,** *1* (12), 2017-2019.

30. Zhao, Y.; Truhlar, D. G., The M06 suite of density functionals for main group thermochemistry, thermochemical kinetics, noncovalent interactions, excited states, and

transition elements: two new functionals and systematic testing of four M06-class functionals and 12 other functionals. *Theoretical Chemistry Accounts* **2008,** *120* (1), 215-241.

31. Marenich, A. V.; Cramer, C. J.; Truhlar, D. G., Universal Solvation Model Based on Solute Electron Density and on a Continuum Model of the Solvent Defined by the Bulk Dielectric Constant and Atomic Surface Tensions. *The Journal of Physical Chemistry B* **2009,** *113* (18), 6378-6396.

32. Kotha, S.; Chavan, A. S.; Goyal, D., Diversity-Oriented Approaches to Polycyclics and Bioinspired Molecules via the Diels–Alder Strategy: Green Chemistry, Synthetic Economy, and Beyond. *ACS Combinatorial Science* **2015,** *17* (5), 253-302.

33. Comer, E.; Duvall, J. R.; IV, M. d. L., Utilizing diversity-oriented synthesis in antimicrobial drug discovery. *Future Medicinal Chemistry* **2014,** *6* (17), 1927-1942.

34. Serba, C.; Winssinger, N., Following the Lead from Nature: Divergent Pathways in Natural Product Synthesis and Diversity-Oriented Synthesis. *Eur J Org Chem* **2013,** *2013* (20), 4195-4214.

35. Burke, M. D.; Schreiber, S. L., A Planning Strategy for Diversity-Oriented Synthesis. *Angewandte Chemie International Edition* **2004,** *43* (1), 46-58.

36. Schreiber, S. L., Target-Oriented and Diversity-Oriented Organic Synthesis in Drug Discovery. *Science* **2000,** *287* (5460), 1964-1969.

37. Book, C. L(+)-Tartaric acid. https://www.chemicalbook.com/ChemicalProductProperty_EN_CB8212874.htm.

38. Book, C. Succinic acid. https://www.chemicalbook.com/ProductList_en.aspx?kwd=succinic%20acid.

39. Book, C. Salicylic acid. https://www.chemicalbook.com/ProductList_En.aspx?kwd=2-hydroxybenzoic%20acid.

40. Perrin, D. D., *Dissociation constants of organic bases in aqueous solution: supplement 1972*. Butterworths: 1972.

41. Book, C. 3,5-Di(trifluoromethyl)benzoic acid(725-89-3). https://www.chemicalbook.com/ProductMSDSDetailCB0255912_EN.htm.

42. Book, C. Diphenic acid. https://www.chemicalbook.com/ChemicalProductProperty_EN_CB6425276.htm.

43. Huang, J.; Hsung, R. P., Chiral Lewis acid-catalyzed highly enantioselective [4+ 3] cycloaddition reactions of nitrogen-stabilized oxyallyl cations derived from allenamides. *J Am Chem Soc* **2005,** *127* (1), 50-51.

44. Harmata, M.; Ghosh, S. K.; Hong, X.; Wacharasindhu, S.; Kirchhoefer, P., Asymmetric Organocatalysis of 4 + 3 Cycloaddition Reactions. *J Am Chem Soc* **2003,** *125* (8), 2058-2059.

45. Nishikawa, Y.; Shindo, T.; Ishii, K.; Nakamura, H.; Kon, T.; Uno, H., Acrylamide derivatives as antiallergic agents. 2. Synthesis and structure activity relationships of N-[4-[4-(diphenylmethyl)-1-piperazinyl] butyl]-3-(3-pyridyl) acrylamides. *Journal of medicinal chemistry* **1989,** *32* (3), 583-593.

46. NOTHEISZ, F.; FELFOLDI, K.; BARTOK, M.; KARPATI, E., PREPARATION AND PHARMACOLOGY OF ESTERS OF HYDROXYMETHYLPYRIDINES. *ACTA PHYSICA ET CHEMICA* **1980,** *26* (3-4), 185-191.

47. Kyba, E. P.; Liu, S. T.; Chockalingam, K.; Reddy, B. R., A general synthesis of substituted fluorenones and azafluorenones. *The Journal of Organic Chemistry* **1988,** *53* (15), 3513-3521.

48. Sunami, S.; Nishimura, T.; Nishimura, I.; Ito, S.; Arakawa, H.; Ohkubo, M., Synthesis and biological activities of topoisomerase I inhibitors, 6-arylmethylamino analogues of edotecarin. *J. Med. Chem* **2009,** *52* (10), 3225-3237.

49. Zhang, J.; Jiang, Z.; Zhao, D.; He, G.; Zhou, S.; Han, S., Transition-Metal-Free TEMPO Catalyzed Aerobic Oxidation of Alcohols to Carbonyls Using an Efficient Br2 Equivalent under Mild Conditions. *Chinese Journal of Chemistry* **2013,** *31* (6), 794-798.

50. Mori, S.; Takubo, M.; Makida, K.; Yanase, T.; Aoyagi, S.; Maegawa, T.; Monguchi, Y.; Sajiki, H., A simple and efficient oxidation of alcohols with ruthenium on carbon. *Chem Commun* **2009,** (34), 5159-5161.

51. Morisawa, Y.; Kataoka, M.; Watanabe, T.; Kitano, N.; Matsuzawa, T., Modification at the 5-Position of 4-Deoxypyridoxol and α4-Norpyridoxol. *Agricultural and Biological Chemistry* **1975,** *39* (6), 1275-1281.

52. Rekharsky, M. V.; Inoue, Y., Complexation Thermodynamics of Cyclodextrins. *Chem Rev* **1998,** *98* (5), 1875-1918.

53. Bender, M. L., M. Komiyama Cyclodextrin Chemistry. Springer Verlag, Berlin (D): 1978.

54. Hallén, D.; Schön, A.; Shehatta, I.; Wadsö, I., Microcalorimetric titration of α-cyclodextrin with some straight-chain alkan-1-ols at 288.15, 298.15 and 308.15 K. *Journal of the Chemical Society, Faraday Transactions* **1992,** *88* (19), 2859-2863.

55. Rekharsky, M. V.; Mayhew, M. P.; Goldberg, R. N.; Ross, P. D.; Yamashoji, Y.; Inoue, Y., Thermodynamic and nuclear magnetic resonance study of the reactions of α-and β-cyclodextrin with acids, aliphatic amines, and cyclic alcohols. *The Journal of Physical Chemistry B* **1997,** *101* (1), 87-100.

56. Li, J.; Loh, X. J., Cyclodextrin-based supramolecular architectures: Syntheses, structures, and applications for drug and gene delivery. *Advanced Drug Delivery Reviews* **2008,** *60* (9), 1000-1017.

57. Li, S.; Purdy, W. C., Cyclodextrins and their applications in analytical chemistry. *Chem Rev* **1992,** *92* (6), 1457-1470.

58. Rideout, D. C.; Breslow, R., Hydrophobic acceleration of Diels-Alder reactions. *J Am Chem Soc* **1980,** *102* (26), 7816-7817.

59. Loftsson, T.; Stefánsdóttir, Ó.; Friðriksdóttir, H.; Guðmundsson, Ö., Interactions between preservatives and 2-hydroxypropyl-β-cyclodextrin. *Drug Development and Industrial Pharmacy* **1992,** *18* (13), 1477-1484.

60. Assaf, K. I.; Suckova, O.; Al Danaf, N.; von Glasenapp, V.; Gabel, D.; Nau, W. M., Dodecaborate-Functionalized Anchor Dyes for Cyclodextrin-Based Indicator Displacement Applications. *Org Lett* **2016,** *18* (5), 932-935.

61. Silverman, R. B.; Wang, H.-Y.; Qin, Y.; Zou, F.; Kang, S. S.; Jing, Q., Mammalian and Bacterial Nitric Oxide Synthase Inhibitors. Google Patents: 2017.

62. Jolly, P. I.; Fleary-Roberts, N.; O'Sullivan, S.; Doni, E.; Zhou, S.; Murphy, J. A., Reactions of triflate esters and triflamides with an organic neutral super-electron-donor. *Org Biomol Chem* **2012,** *10* (30), 5807-5810.

63. Nunez, A.; Abarca, B.; Cuadro, A. M.; Alvarez-Builla, J.; Vaquero, J. J., Ring-closing metathesis reactions on azinium salts: straightforward access to quinolizinium cations and their dihydro derivatives. *The Journal of organic chemistry* **2009,** *74* (11), 4166-4176.

64. Meijere, A. d.; Meyer, F. E., Fine Feathers Make Fine Birds: The Heck Reaction in Modern Garb. *Angewandte Chemie International Edition in English* **1995,** *33* (23‐24), 2379-2411.

65. Woodcock, S. R.; Branchaud, B. P., Effect of ether versus ester tethering on Heck cyclizations. *Tetrahedron Letters* **2005,** *46* (42), 7213-7215.

66. Maruyama, K.; Nagai, N.; Naruta, Y., Lewis acid-mediated Claisen-type rearrangement of aryl dienyl ethers. *The Journal of Organic Chemistry* **1986,** *51* (26), 5083-5092.

67. Kukula-Koch, W. A.; Widelski, J., Chapter 9 - Alkaloids. In *Pharmacognosy*, Badal, S.; Delgoda, R., Eds. Academic Press: Boston, 2017; pp 163-198.

68. Grynkiewicz, G.; Gadzikowska, M., Tropane alkaloids as medicinally useful natural products and their synthetic derivatives as new drugs. *Pharmacol Rep* **2008,** *60* (4), 439-463.

69. Willstätter, R.; Bruce, J., Zur Kenntnis der Cyclobutanreihe. *Berichte der deutschen chemischen Gesellschaft* **1907,** *40* (4), 3979-3999.

70. Aldoshin, S.; Kozina, O.; Gutsev, G.; Atovmyan, E.; Atovmyan, L.; Nedvetskii, V., Izvestia Akademii Nauk SSSR Seriya Khimicheskaya. **1988**.

71. Eaton, P. E.; Cole, T. W., The Cubane System. *J Am Chem Soc* **1964,** *86* (5), 962-964.

72. Lledo, A.; Benet-Buchholz, J.; Sole, A.; Olivella, S.; Verdaguer, X.; Riera, A., Photochemical Rearrangements of norbornadiene Pauson-Khand cycloadducts. *Angew Chem Int Edit* **2007,** *46* (31), 5943-5946.

73. Winkler, J. D.; Axten, J.; Hammach, A. H.; Kwak, Y.-S.; Lengweiler, U.; Lucero, M. J.; Houk, K. N., Stereoselective synthesis of the tetracyclic core of manzamine via the vinylogous amide photocycloaddition cascade. *Tetrahedron* **1998,** *54* (25), 7045-7056.

74. Winkler, J. D.; Muller, C. L.; Scott, R. D., A new method for the formation of nitrogen-containing ring systems via the intramolecular photocycloaddition of vinylogous amides. A synthesis of mesembrine. *J Am Chem Soc* **1988,** *110* (14), 4831-4832.

75. Winkler, J. D.; Scott, R. D.; Williard, P. G., Asymmetric induction in the vinylogous amide photocycloaddition reaction. A formal synthesis of vindorosine. *J Am Chem Soc* **1990,** *112* (24), 8971-8975.

76. Winkler, J. D.; Axten, J. M., The first total syntheses of ircinol A, ircinal A, and manzamines A and D. *J Am Chem Soc* **1998,** *120* (25), 6425-6426.

77. Soldermann, N.; Velker, J.; Neels, A.; Stoeckli-Evans, H.; Neier, R., The high stereoselectivity of the tandem sequence Diels-Alder reaction/Ireland-Claisen rearrangement starting from substituted O-(E)-Buta-1,3-dienyl ketene acetals and cyclic dienophiles. *Synthesis-Stuttgart* **2007,** (15), 2379-2387.

78. Boja, J.; Cadet, J.; Kopajtic, T.; Lever, J.; Seltzman, H.; Wyrick, C.; Lewin, A.; Abraham, P.; Carroll, F., Selective labeling of the dopamine transporter by the high affinity ligand 3 beta-(4-[125I] iodophenyl) tropane-2 beta-carboxylic acid isopropyl ester. *Molecular pharmacology* **1995,** *47* (4), 779-786.

VITA

Chencheng Fu was born April 4th, 1990 in Chongqing, China. She graduated from Bashu High School in June of 2009. Later that fall, she began her undergraduate education at West China School of Pharmacy in Sichuan University in China. She graduated from Sichuan University in June of 2013. She then began graduate studies at the University of Missouri-Columbia, joining Dr. Harmata's research group in August 2013. She took part in researches about (4+3)-cycloaddition reactions of oxidopyridinium ions and related work during her tenure and graduated with her Ph.D. from University of Missouri-Columbia in July 2019 under Dr. Harmata's guidance. In August 2019, she will join YaoPharma Co., Ltd., a subsidiary of Shanghai Fosun Pharmaceutical Development Co., Ltd. as a research and development chemist.